PERFORMANCE INVESTIGATION & OPTIMISATION OF CO_2 REFRIGERATION SYSTEMS IN RETAIL FOOD STORES

A thesis submitted for the degree of
Doctor of Philosophy

By
Konstantinos M. Tsamos

Department of Mechanical, Aerospace and Civil Engineering
College of Engineering, Design and Physical Science
Brunel University London

September 2016

ABSTRACT

Natural refrigerants are recognized as the most promising working fluids to replace conventional HFCs in food refrigeration systems. Due to its negligible GWP, zero ODP and attractive thermophysical properties, the CO_2 working fluid has grown in popularity over the last decade, especially in supermarket refrigeration systems. Accelerated tax relief schemes for new investments in environmental friendly and energy efficient technologies such as CO_2 refrigerant solution in supermarkets are available across the Europe and rest of the world.

The first part of this work presents an experimental investigation into the performance of CO_2 finned-tube gas coolers/condensers with different designs in a CO_2 booster system. The heat exchangers were mounted in a specially designed test facility that allowed the control of different test conditions and parameters, including air-on temperatures and flow rates, approach temperatures and CO_2 operation pressures. The integrated refrigeration system can provide specified CO_2 fluid parameters at the heat exchanger inlet, through which the system efficiency can be calculated. Subsequently, extensive measurements were recorded from this test rig, with insightful indications into system performance and the most influential parameters for system optimisation. These include heat exchanger designs, air on temperatures and flow rates, supercritical and subcritical pressure controls and cooling capacity controls, which are analysed in this work.

The second part of this work includes simulation model of a transcritical booster CO_2 refrigeration system which has been developed to investigate and evaluate the system performance. The model includes a detailed gas cooler model which can predict accurately the temperature, pressure, air and refrigerant heat transfer coefficient profiles across the heat exchanger. The component and system models were verified using test results from the experimental CO_2 test rig built at Brunel University London.

Mathematical models were also developed to investigate different refrigeration system applications in supermarkets. The control parameters for the systems with CO_2 at the high pressure side were derived from the experimental work of this study. The models compared the system performance, annual consumption and TEWI at ambient conditions of London and Athens. The proposed natural refrigerant systems show good improvements compared to the HFC counterparts in terms of power consumption and annual electricity cost. In particular, the CO_2 refrigeration systems show 20% to 50% reduction in terms of TEWI in case of London and 9% to 35% in case of Athens comparing to cascade R134A and R404A refrigeration system respectively.

PUBLICATIONS

Published Journal Papers

1) EXPERIMENTAL INVESTIGATION OF GAS COOLER/CONDENSER DESIGNS AND EFFECTS ON A CO_2 BOOSTER SYSTEM. K. TSAMOS, Y.GE, ID. SANTOSA, S. TASSOU. APPLIED ENERGY 186 (2017) 470-479.

2) DESIGN OPTIMISATION OF CO_2 GAS COOLER/CONDENSER IN A REFRIGERATION SYSTEM. Y.T. GE, S.A. TASSOU, I. DEWA SANTOSA, K. TSAMOS. APPLIED ENERGY 160 (2015), 973-981

3) INVESTIGATION OF AIR AND REFRIGERANT SIDE HEAT TRANSFER COEFFICIENT OF FINNED-TUBE CO_2 GAS COOLERS USING COMPUTATIONAL FLUID DYNAMICS (CFD). IDEWA M.C. SANTOSA, BABOO L. GOWREESUNKER, SAVVAS A. TASSOU, KONSTANTINOS M. TSAMOS, YUNTING GE. INTERNATIONAL JOURNAL OF HEAT AND MASS TRANSFER, 107 (2017), 168-180

Published Conference Papers

1) EXPERIMENTAL INVESTIGATION OF GAS COOLER/CONDENSER DESIGNS IN A CO_2 BOOSTER SYSTEM. KONSTANTINOS M. TSAMOS, Y.T. GE, ID.M.C. SANTOSA, S.A. TASSOU. (SUSTEM, 2015)

2) EXPERIMENTAL INVESTIGATION OF CO_2 GAS COOLER/CONDENSER IN A REFRIGERATION SYSTEM. KONSTANTINOS M. TSAMOS, YUNTING GE, IDEWA SANTOSA, SAVVAS TASSOU. (SET 2015)

3) EXPERIMENTAL AND NUMERICAL STUDY ON THE PERFORMANCE OF CO_2 REFRIGERATION FOR SUPERMARKET APPLICATIONS. KONSTANTINOS M. TSAMOS, YUNTING GE, I DEWA SANTOSA, SAVVAS A. TASSOU. (29TH EFFOST INTERNATIONAL CONFERENCE)

4) INVESTIGATION OF REFRIGERANT SIDE-HEAT TRANSFER COEFFICIENT OF FINNED-TUBE CO_2 GAS COOLERS USING COMPUTATIONAL FLUID DYNAMICS (CFD) MODEL. IDEWA M.C. SANTOSA, BABOO L. GOWREESUNKER, SAVVAS A. TASSOU, KONSTANTINOS M. TSAMOS, YUNTING GE (SUSTEM, 2015)

5) DESIGN AND INTEGRATION OF CO_2 GAS COOLER/CONDENSER IN A REFRIGERATION SYSTEM. Y.T. GE, S.A. TASSOU , I DEWA SANTOSA, K. TSAMOS, S. JONES, N.ATKINS (3RD IIR INTERNATIONAL CONFERENCE ON SUSTAINABILITY AND THE COLD CHAIN, LONDON, UK, 2014)

6) EXPERIMENTAL INVESTIGATION OF THE PERFORMANCE OF FINNED TUBE CO_2 REFRIGERATION GAS COOLERS. ID.M.C. SANTOSA, K.M.TSAMOS, S.A. TASSOU, Y.T. GE, S. JONES, N. ATKINS (3RD IIR INTERNATIONAL CONFERENCE ON SUSTAINABILITY AND THE COLD CHAIN, LONDON, UK, 2014)

7) EFFECT OF GEOMETRY ON THE PERFORMANCE OF CO_2 GAS COOLER/CONDENSER AND ITS ASSOCIATED REFRIGERATION SYSTEM. YUNTING GE, SAVVAS TASSOU , KONSTANTINOS TSAMOS, I DEWA SANTOSA (24TH IIR INTERNATIONAL CONGRESS OF REFRIGERATION)

8) MODELLING AND ANALYSIS OF CO_2 GAS COOLERS FOR COMMERCIAL REFRIGERATION APPLICATIONS. ID.M.C. SANTOSA, IN. SUAMIR, Y.T. GE, K. TSAMOS, S.A. TASSOU. (2ND IIR PARIS, 2013)

9) DESIGN OPTIMISATION OF CO_2 GAS COOLER/CONDENSER IN A REFRIGERATION SYSTEM. Y.T. GE, S.A. TASSOU, I D. SANTOSA K. TSAMOS. (6TH INTERNATIONAL CONFERENCE ON APPLIED ENERGY – ICAE2014)

Presented Material

1) DESIGN CONSIDERATIONS ON A SMALL SCALE SUPERCRITICAL CO2 POWER SYSTEM FOR INDUSTRIAL HIGH TEMPERATURE WASTE HEAT POWER RECOVERY APPLICATIONS. G. BIANCHI, S. TASSOU, Y. GE, H. JOUHARA, K. TSAMOS, A. LEROUX, M. MIOL. (1^{ST} EUROPEAN SEMINAR ON SUPERCRITICAL CO2 POWER SYSTEMS, 2016)

Awards

BEST STUDENT POSTER PRIZE: INVESTIGATE APPLICATION AND OPTIMISATION OF THE PERFORMANCE OF CO_2 REFRIGERATION SYSTEMS IN RETAIL FOOD STORES. (6TH ANNUAL STUDENT RESEARCH CONFERENCE 2013)

CONTENTS

LIST OF FIGURES

LIST OF TABLES

ACKNOWLEDGEMETS

First, my deepest gratitude is to both of my supervisors Dr. Yunting Ge and Professor Savvas Tassou for their endless support. I was very lucky to have their support and encouragement during my PhD studies. Their understanding and personal guidance has provided a good basis for the present thesis.

I am grateful to the CSEF Brunel University, GEA – Searle and Research Councils UK (RCUK) and especially Professor Savva Tassou and Dr. Yunting Ge, for the scholarship which helped me for the PhD studies. Also, for the opportunity that I had to involve in a number of different research projects which helped me to extend my knowledge and experience in refrigeration field.

I would also like to thank CSEF Brunel University members Dewa Santosa, Costa Xantho, INyoman Suamir, Carlos Amaris, Lesh Gowreesunker, Zoi Mylona, Amir Raisei and Dimitri Parpa for the stimulating discussions, support and advise we have had over those years.

Special thanks to a special person, Ms. Apinporn Wongratchatasawee and her family, for their endless support during those years.

Last but not least, I would like to thank my beloved family, my parents Michalis and Olga Tsamos, my brothers Dimitrios and Anastasios, my grandmother Eleni and my grandfather Anastasio Papanikolaou for their great and never-ending support companying with me all the way.

I praise God, for providing me this opportunity and the power to finish these academic years successfully.

NOMENCLATURE

a	Heat transfer coefficient (W/m^2 K)
AT	Approach temperature (°C)
$bulk$	Bulk Temperature (°C)
C	System relief valve sizing
C	Heat Capacity Rate (W/K)
$c1 – c6$	Coefficient (-)
c_p	specific heat (kJ/kg K)
d	Diameter (m)
D_c	Fin collar outside dimeter (m.)
E	Power consumption (kW)
f	Friction Factor (-)
F_s	Fin spacing (m.)
G	Mass Velocity (kg/s.m^2)
h	Enthalpy (kJ/kg)
ID	Internal Diameter (m)
$LMTD$	Logarithmic mean temperature difference (°C)
$\dot{m}$	Mass flow rate (kg/s)
m	Refrigerant charge (kg)
n	Operating lifetime of the refrigeration systems (years)
N	Number of fins
Nu	Nusslet Number (-)
P	pressure (bar)

Pr	Prandtl number (-)
Q	Cooling Capacity (kW)
q	Heat transferred (W)
Q_{PRV}	Minimum required discharge capacity of the pressure relief valve (kg/h)
r	Radius (m)
r_o	Outer pipe radius (m.)
R	Thermal resistance (K/W)
Re	Reynolds Number (-)
R_{eq}	Equivalent Radius for circular fin (mm)
RH	Relative humidity (%)
Rp	Pressure ratio (-)
Sat	Saturation Temperature (°C)
S_h	Height of fin slit (m.)
S_s	Breadth of slit in the direction of airflow (m.)
T	Temperature (°C)
U	Overall heat transfer coefficient ($W/m^2.K$)
u	Speed (m/s)
UA	Overall heat transfer coefficient (W/K)
V	Air volume flow rate (l/s)
v_{brine}	Specific volume of brine (m^3/kg)
V_{swept}	Compressor Swept Volume (m^3/h)
W	compressor power consumption (kW)
$wall$	Wall Temperature (°C)
x	Mass flow rate fractions(%) / Vapour quality (-)
X_L	Geometric Parameter (m)

X_M	Geometric Parameter (m)

Greek Symbols

β	Indirect emission factor ($kgCO_2/kWh$)
γ	Gamma factor (-)
δ	Fin thickness (m)
Δh	enthalpy difference (kJ/kg)
ΔT	temperature difference (°C)
ε	Effectiveness (-)
η_f	Fin efficiency (%)
η_o	Overall efficiency (%)
k	Thermal Conductivity (W/m.K)
μ	Viscosity (kg/m-s)
ξ	Brine mass fraction (-)
ρ	density (kg/m^3)
φ	F Factor – Air side heat transfer coefficient (-)

Subscripts

a	air
AL	additional load
ave	average
cd	condenser
comp	compressor
dis	discharge
e	electrical

ev	evaporator
f	fin
gc	gas cooler
GC	Gas Cooler
i, j, k	Coordinators
in	inlet
interm	Intermediate
is	isentropic
LT	Low temperature
m	mechanical
MT	Medium Temperature
on	Inlet
opt	Optimum
out	outlet
pseud	pseudocritical
rec	receiver
Rec	Receiver
ref	refrigerant
sat	Saturation Temperature
sub	subcritical
suc	suction
swept	Swept volume
trans	transcritical
v or vol	volumetric

ABBREVIATION AND GLOSSARY

AAC	Additional Air Cooler
AB	Alkyl benzene
AHU	Air Handling Unit
AKV	Electrically operated
AL	Additional Load
BWM	Box-and-Whisher
C/GC	Condenser / Gas Cooler
CCA	Climate Change Act
CCM	Gas by pass control valve – Same as ICM
CFC	Chloro-fluoro-carbon
COP	Coefficients of performance
D	Depth (m)
DX	Direct expansion
DX	Direct expansion
EES	Engineering Equation Solver
GHG	Greenhouse Gas emissions
GWP	Global Warming Potential
H	Height (m)
HC	Hydrocarbon
HCFC	Hydro-chloro-fluoro-carbon
HFC	Hydrofluorocarbons

HP	High pressure
HT	High temperature
ICM	Gas by pass control valve
ICMT	High pressure side control valve
IR	Infrared thermography
IXE	Internal heat exchanger
L	Length (m)
LP	Low Pressure
LT	Low temperature
MMI	Man Machine Interface
MT	Medium temperature refrigerated display cabinet
MT	Medium temperature
ODP	Ozone Depletion Potential
PAG	Polyalkyl glycol
PFC	Perfluorocarbons
PID	Proportional–integral–derivative controller
POE	Polyol ester
PRV	Pressure relief valve
PS	Maximum allowable pressure
PTC-1000	Resistance thermometers
SF6	Sulphur hexafluoride
SRC	Specific refrigerant charge
TEWI	Total equivalent warming impact
Tps	Pseudocritical point
VLT	Power Inverter

1. INTRODUCTION

Greenhouse Gas (GHG) emissions from food refrigeration systems can be divided into two main categories: direct and indirect emissions. The first are due to leakages of refrigerants with high global warming potentials (GWPs), such as R404A. Indirect emissions are produced from the energy required to operate refrigeration systems. Approximately 63% of direct emissions from the food chain result from the food retail sector, in particular from supermarket refrigeration systems (UK NIR 2014). On the other hand, the total electrical energy consumption of supermarket refrigeration systems in the UK represents approximately 3.5% of the nation's total electrical energy consumption (Tassou, 2007). Therefore it is highly important to utilise high efficiency supermarket refrigeration systems with environmentally friendly natural refrigerants such as CO_2. CO_2 is a natural working fluid with zero Ozone Depletion Potential (ODP) and negligible Global Warming Potential (GWP=1). Alongside its excellent environmental characteristics, CO_2 has favourable thermo-physical properties in terms of higher density, specific heat, volumetric cooling capacity, latent heat, thermal conductivity and also is non-toxic and non-flammable. Consequently, the CO_2 refrigerant has been recommended as a satisfactory substitute in supermarket refrigeration systems by both national and international organisations (SKM Enviros, 2011). Through using the natural refrigerant CO_2, opportunities may be found in eliminating direct GHG emissions to the atmosphere and potentially diminishing indirect effects by optimising the system designs and operations.

A number of different CO_2 refrigeration system designs and operating conditions can be adopted in food retail applications; these fall into three categories: indirect, cascade and all CO_2 transcritical systems. For an indirect CO_2 refrigeration system, CO_2 is commonly used as a two-phase secondary coolant while a HFC refrigerant such as R404A is conventionally charged in the primary side (Hinde et al., 2009, Yoon et al., 2014). Due to the excellent thermodynamic properties of CO_2, the system and components can be designed and manufactured to be more compact. In a cascade layout, the system constitutes of two single stage sub-systems, integrated by a cascade heat exchanger. CO_2 is applied into the low cascade side while a working fluid such as R404A, NH_3, hydrocarbon or even CO_2 operates in the high cascade side (Dopazo et al.,

2009, Lee et al., 2006). The cascade system is more flexible since two different working fluids can be utilised in two cascade sides. In an all CO_2 system, it can be a single stage heat pump or air conditioning system (Tao et al., 2010) or a two stage booster system. A booster configuration is commonly employed where CO_2 is the only charged refrigerant. The main advantages of the CO_2 booster system over others include its simpler design requirements, zero direct environmental impact and smaller installation cost. Such a design is suitable for application in supermarket refrigeration as it can produce refrigeration at both medium and low temperatures. However, further enhancement of operation efficiency for such a system is required. One method of improving the seasonal performance of an all CO_2 system would be applying optimised control strategies for the system, with particular focus on high pressures to ensure that it will operate efficiently at all ambient temperature conditions. The optimal discharge pressure controls are affected by the system layout and specifications of associated components. For a CO_2 refrigeration system, by means of mathematical refrigeration models, the optimised refrigerant discharge pressures were correlated to increase lineally with higher ambient temperatures (Kauf, 1999). The correlation can be correctly applied when the types and structures of system components such as heat exchangers and compressors are known. In addition, low pressure side operating conditions such as pressure and superheat also need be specified. Nevertheless, this method does provide a useful guideline in predicting optimised discharge pressures at different operating conditions and various CO_2 transcritical systems. For a CO_2 heat pump system, to maximise the total system COP (heating and cooling), optimal refrigerant discharge pressures were correlated as a function of refrigerant temperatures at gas cooler outlet and evaporation (Sarkar, 2014). The optimised pressures increased with higher gas cooler outlet temperatures but decreased with higher evaporating temperatures. This correlation is also applicable for a particular system when the system component designs such as compressors are specified. Similarly, an optimal CO_2 transcritical COP was modelled as a function of water and ambient air temperatures for an air-water CO_2 heat pump by using dedicated control strategies and integrating them into a system simulation (Hu et al., 2015). In addition, based on thermodynamic analysis, the authors also identified effective parameters on the COP of transcritical CO_2 cycles and generalised a correction to quantify the effects and optimal supercritical pressures for a CO_2 booster system (Ge and Tassou, 2011). Subsequently, the effect of optimal controls of the high-side pressure on the performance of a CO_2 booster system in supermarket

refrigeration systems was analysed and evaluated. This would impart useful information on the impact of system optimal control on system operation (Ge and Tassou, 2009). However, the experimental investigation to validate the theoretical predictions on optimal compressor discharge pressures of different CO_2 systems is still required. Since the CO_2 working fluid has a low critical temperature of 31.1°C and a very high critical pressure of 73.8 bar, its booster system operates mostly at higher pressures compared to other refrigerants. In cases where the ambient temperature is higher than the critical temperature, CO_2 will not condensate in the high pressure-side of the system. Thus, the high pressure CO_2 heat exchanger can act as either a condenser or gas cooler depending on ambient conditions. In such circumstances, the CO_2 gas cooler/condenser must be well designed and controlled to match the cooling capacity requirement of the system at minimal cost and, at the same time, improve system performance. To understand the performance of a CO_2 air cooled gas cooler, a series of tests were conducted at different operating conditions using a purposely designed test facility (Hwang, 2005). The effects of air and refrigerant side flow parameters on the heat exchanger heat transfer and hydraulic behaviours were examined. In addition, the temperature profiles along the heat exchanger circuit pipes were measured. Apart from the investigations into the overall performance of the CO_2 gas coolers, the in-tube cooling processes of CO_2 supercritical flow were extensively tested and correlated [Srinivas et al., 2002, Son and Park, 2006) in order to understand the CO_2 heat transfer and hydraulic behaviours in the heat exchangers. Although the performances of CO_2 finned-tube gas coolers or condensers have been extensively investigated using both experimental and theoretical methods, experimental research on the effect of their integrations with associated systems is still limited (Chang and Kim, 2007). To some extent, this could potentially lead to inaccurate design and mismatching of the heat exchanger size and control when applied into a real system.

Furthermore in terms of supermarket applications, Girotto et al. (2004) presents a comparison between a CO_2 refrigeration system and a direct expansion solution using R404A in terms of annual energy consumption and cost. The author proposed to decrease the approach temperature of the gas cooler by using two-stage compression for the MT circuit. The experimental work by Qureshi and Zubair (2013) proves that a subcooling loop can improve both the cooling capacity and exergetic efficiency of the basic CO_2 cycle. The potential subcooling cycle for both convectional CO_2 system and

CO_2 with double-stage compression and intercooling were presented by Llopis (2015). Minetto et al. (2014) showed that the system with parallel compressor can attain a large energy saving in comparison with the convectional booster system.

1.1.1. LEGISLATION – POLICY -TARGETS

The uncontrolled use of chemical compounds the last four decades increase the limit of average global temperature and resulting a climate change. Climate change is a really complex problem, which has consequences for all spheres of existence on our planet. After 1987, countries joined together to create an international and national treaties consisting by the number of action to protect the ozone layer. The main objectives of those international treaties are to phasing out the production and consumption of a number of chemical substances including substances used in refrigeration technology. The use of natural refrigerants such as CO_2 is a real alternative solution.

1.1.2. MONTREAL PROTOCOL AND THE KYOTO PROTOCOL

Montreal and Kyoto Protocols are two global environmental agreements with common objectives to protect the Earth's atmosphere from the unfriendly human actions. First the Montreal Protocol (1989) targets to phase-out the use of ozone depleting substances including Hydro-chloro-fluoro-carbon (HCFC) and Chloro-fluoro-carbon (CFC) used in a commercial refrigeration applications. On the other hand, Kyoto Protocol is the first international agreement singed from developed and developing countries to reduce the greenhouse gas emissions produced from the industrialised world applications and equipment. The main target of Kyoto Protocol is to reduce the greenhouse gas emissions by 2050 in order to prevent the global raise of temperature for 2°C. Kyoto Protocol focused to reduce the production and use of fluorinated gases which are really common in industrialised world. The link between Kyoto and Montreal Protocols is to phase out the substances with high ozone depletion potential. As an example, the immediate phase-out of HCFCs decided in Montreal in 2007 helps to reduce the production of HCFC by 7.7m tonnes. This HCFC reduction is equivalent with 26 gig tonnes of CO_2 emissions. After this successful target the reduction of HCFC and CFC became a major target (GTZ Proklima, 2008).

1.1.3. F-GAS REGULATION

F-gases regulation was developed after 1990s as a part of Montreal Protocol to control the use fluorinated greenhouse gases such as hydrofluorocarbons (HFCs), perfluorocarbons (PFCs) and sulphur hexafluoride (SF6). The new F-gas regulation

published and come into force on the beginning of 2015, place restrictions on the use of HFCs refrigerants. The main objective is the ban of HFCs refrigerants with GWP higher than 2500 such the R404A in new stationary refrigeration applications (EPEE, 2014).

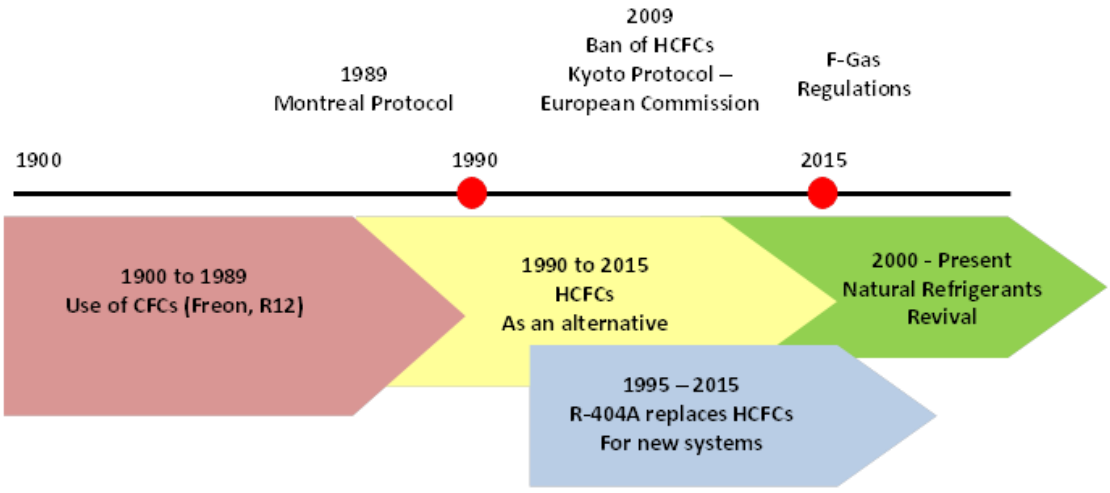

Figure 1.1 Refrigerants & Environmental Agreements

(Wallace, 2013)

1.2.GHG EMISSIONS FROM REFRIGERATION SYSTEMS

The GHG emissions from the refrigeration applications can be split it into two main categories, the "direct" and "indirect". The direct emissions are created by the refrigerant leakage from the system. Refrigerant leakage can be during manufacture process of the refrigeration equipment, charging, normal operation, and repair or recovery process. The extensive pipe-work, the huge number of pipe joints and the poor maintenance in refrigeration plants increase the possibilities for refrigerant losses in the existing refrigeration systems.

The indirect emissions are proportional from the electricity consumption used to operate the refrigeration systems. The indirect emissions from refrigeration system have been reported to be around 8% from the total UK GHG emissions. In the UK, food retail is responsible for approximately 40% of the indirect GHG emissions.

Refrigeration technology, which is important in the processing, transportation and preservation of the food, is potentially responsible for the significant GHG emissions.

Total GHG emissions from food chain refrigeration in UK are 13,720 kT CO_2, where the 35% are created from the direct emissions and 65% from indirect emissions. Table

1.1 illustrate the overall emission from each sector of the food chain process (SKM, 2011).

Table 1.1 Overall Emissions by sector of the food chain

Sector	Total Emissions Direct + Indirect kT CO_2	% of the Total Emissions
Retail	6,530	47%
Food & drink manufacture	2,550	19%
Food service	2,440	18%
Transport	1,430	10%
Cold Storage	510	4%
Agriculture	260	2%
Total	13,720	100%

In the UK, the targets are 60% reduction in GHG emissions by 2030 and 80% by 2050 comparing with 1990 levels (CCC, 2010). The split between direct and indirect emission in food retail sector shows that the direct emission are responsible for 3,000 kT CO_2 from the total of 6,530 kT CO_2. Moreover, the direct emission from the food retail sector is responsible for the 63% of the total direct emission as shown in Fig 1.2.

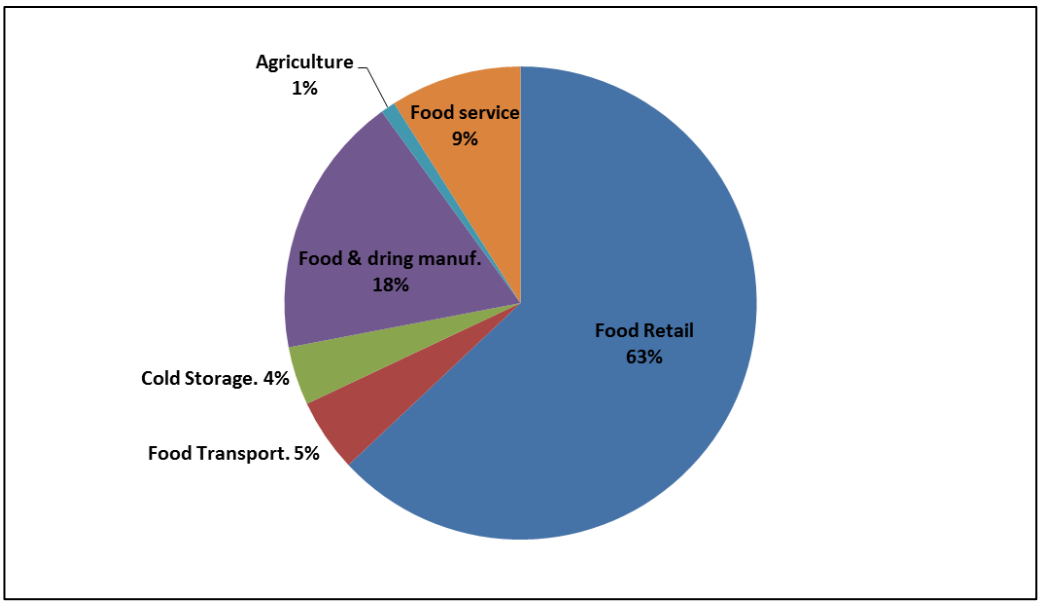

Figure 1.2 Food sector direct GHG emissions

The environmental impact from the refrigerant leakage depends on the type of the refrigerant, amount of charge and leak tightness of the system. The split of direct emission in food retail sector shows that the HFCs refrigerants are responsible for 74% of total direct emission and the 26% created by HCFCs (SKM, 2011).

Typical values for specific refrigerant charge (SRC) are reported in MTP (2008). The SRC values for centralised supermarket system with HFC and HCFC are between 2 to 5 kg per kW refrigerant capacity. The SRC for integral units and split/condensing units are 1.05 and 0.55 kg per kW. The author also report the estimation of refrigerant leakage from centralised supermarket refrigeration systems, integral units and split/condensing units which are 10-25%, 1% and 10-20% respectively MTP (2008). The MTP report also summarised the refrigerant leak rates from more applications. Detailed specific refrigerant charge values and percentage of refrigerant leakage for the different types and applications are illustrated in Appendix A.

The United Nations Environment Programme published the annual emissions for small and large supermarkets which varies 15-25% and 20-30% respectively (UNEP, 2010). The environmental and financial cost from the refrigerant leakage has been reported from Cowan et el. (2010). The author report that the refrigerant leakage from the system affecting on the indirect emissions as well, since the low charge reduces sub-cooling and increasing the superheating degree, resulting the lower system performance.

1.3.EMISSION REDUCTION OPPURTINITIES

In general, there are two types of circumstances that must take into account. The first one is divided into the new and existing system and the second on the large and small applications (SKM Enviros, 2011). As described in the preceding section the direct emissions from the refrigerant leakage are responsible for the environmental impact. Reducing the GHG emissions to the environment become an important objective the last two decades. The Retail Roadmap (IOR-BRA-CT, 2010) and Real Zero Project (IOR, 2009) provide useful information on direct emission techniques for the existing systems. For the new system, specialist studies reported the solution of more alternative refrigerants such as CO_2 (SKM Enviros, 2010 – Rhiemeir et al., 2009). The direct emission opportunities can be divided into various categories which are shown in Table 1.2.

The first category describe the regularly maintenance of the system and individual equipment. This category focuses on the leak test and repair for all plants containing more than 3 kg of HFC or HCFC refrigerants. Moreover, the responsible persons for the leak and repair maintenance are required to hold the F Gas qualification.

Table 1.2 Direct emission opportunities

Category	Type
1	Maintenance
2	Component replace
3	Replace refrigerant existing plane
4	New plant – Low leakage
5	New plant – Alternative refrigerant

The regular leak tests can help companies cut the 25% of the total direct emissions. On the other hand secure the refrigerant amount needed from the system for higher performance and reduction in indirect emissions (SKM Enviros, 2011). The regularly maintenance from qualified person can detect source of regular leaking from the refrigeration system. By replacing the damage component with the new one and sorting out the problem of regularly leakage can reduce the direct emissions by further 25%.

As discussed in this section, the HFC are responsible from 74% of the total direct emissions. The category 3 focuses on the HFC such as R404A which commonly used in supermarket refrigeration plants and are responsible for the 80% of the total HFCs emissions. R407A and R407F have much lower GWP (2,107 and 1,825) and can be replaced the existing R404A which has a very high GWP of 3,992. This led in high reduction of direct emissions. Both of the alternatives refrigerants are efficient in many types of existing system which can reduce the indirect emission by cutting the running costs (SKM Enviros, 2011). Category four describes the way to design and install new plants with the existing HFCs refrigerants. This required better quality components such as valves, joints and sight glasses. Moreover, the pipework needs to be designed in order to avoid high frequency vibrations which led to damage the pipe connection in long term operation. Category four can be related with category three by using the replacement refrigerants of R404A. The most efficient way to reduce the direct

emission is the use alternative refrigerants with very low GWP. The choice of suitable refrigerant should be based on the size of the plant. For example, ammonia is more suitable for large scale plants and hydrocarbon (HC) for really small integral systems of refrigerated cabinets where the refrigerant charge is lower than 1 kg (SKM Enviros, 2011). Currently the CO_2 is gaining a substantial part of the medium centralised supermarket refrigeration system and applied in many countries.

1.4.RESEARCH AIM & OBJECTIVES

The aim of the research in this thesis is to investigate and improve the performance of the CO_2 refrigeration system for supermarket applications. The performance of the existing CO_2 test facility was investigated under different control strategies and system settings. The effects of those control parameters are clearly identified. Moreover, the effect of the condenser/gas cooler designs on the CO_2 booster system has been experimentally and numerically investigated. The control strategies adapted from the experimental results used as an input on further investigation for different CO_2 refrigeration system arrangements. The main objectives of the project are presented below.

- Build a CO_2 refrigeration test facility capable to test different system configuration and control settings.
- Build a unique test facility in order to test a number of condenser/gas cooler heat exchangers designs under controlled conditions based on the air inlet temperature, air volume flow rate and refrigerant conditions.
- Carry out extensive experiments and analyse the condenser/gas cooler performance and how this effect on the system COP.
- Use EES software to simulate the existing CO_2 system and any further modifications on the system arrangement. The validated model used to investigate other control parameters such as pressure and temperature across the system.
- Build a 3-D model in EES software to detail investigate the gas cooler performance under different test conditions and pipe design and arrangement.

- Use the equations derived from the experimental work as control parameters for CO_2 systems and compared those with different refrigeration system arrangements.
- Compare in terms of performance, annual consumption and TEWI eight different refrigeration systems applicable for supermarket solutions.

1.5.STRUCTURE OF THE THESIS

The thesis comprises of nine chapters. Chapter summaries are presented below.

Chapter 1

Chapter 1 provides an introduction of the work in this thesis. Also the legislation-policy-targets for the refrigeration industry are clearly identified. Emissions and reductions opportunities were discussed also. Finally the research aim and objectives were explained.

Chapter 2

Chapter 2 presents a comparison of CO_2 as a refrigerant in terms of thermos-physical properties. EES software was used as a tool to compare with other refrigerants. Safety group, plant recommendations, CO_2 applications and lubricants were also discussed. The comparison between CO_2 and other given refrigerants also extend to terms of price.

Chapter 3

Chapter 3 presents very detailed information for CO_2 applications designed for supermarket applications. All the three different system categories were clearly identified. Advantages and disadvantages of those systems have been discussed in terms of installation and maintenance cost and efficiency. Novelties and different case studies were discussed at the end of this chapter.

Chapter 4

Chapter 4 is clearly describes the computer simulation procedure followed in order to theoretical investigate the performance of the existing system. In this stage the performance of the condenser/gas cooler was calculated based on the thermodynamic properties. Latter this was integrated with the detailed gas cooler model which is presented on the following Chapters.

Chapter 5

The design-construction-modification of the experimental test facilities presented in Chapter 5. Early design criteria, installation and modification details are clearly presented. This chapter presents clearly all the component selections was used to assembly and test the CO_2 test rig.

Chapter 6

Chapter 6 presents the procedure followed to curry out the experimental part of this work. The data analysis procedure is discussed also. Furthermore, the experimental results for both subcritical and transcritical operation cycle are clearly discussed. The difference in terms of operating pressures, temperatures and performance between those two were analysed in terms of ambient conditions and power consumption. In additional, the model validation and further investigation are presented in this chapter. Finally, results from the test rig modifications are presented.

Chapter 7

Chapter 7 illustrates the detailed model of the gas cooler heat exchanger. Both 3-row and 2-row gas coolers were divided into a small segments. The refrigerant and air side heat transfer equations were applied to each small segment. Temperature and pressure across the pipes can be calculated. The results from the model were compared with the experimental results. After the model validated, is integrated to the model described in Chapter 4. Therefore, the results in terms of cooling performance were compared and validated.

Chapter 8

The control strategies in high pressure side of the CO_2 system have been clearly identified from the experimental results. Those control parameters have been used in order to compare different refrigeration system arrangements for supermarket applications. Eight different cases have been investigated in terms of performance, annual power consumption and total equivalent warming impacts. The convectional CO_2 booster system and CO_2/CO_2 cascade system have been improved in terms of power consumption and COP. Other systems including cascade with HFCs and HC were investigated also. Two different climate conditions used in order to identify the difference in terms of power consumptions and TEWI.

Chapter 9

Chapter 9 presents the overall conclusions for this experimental and numerical study. Also, further investigation challenges have been clearly discussed.

2. CO_2 REFRIGERANT

Carbon dioxide was one of the first refrigerants used since the very early stages of refrigeration technology to provide cooling in a vapour compression cycle applications, especially those which required huge amounts of refrigerants such a ship transportation of frozen meat in Gulf of Mexico. The CO_2 as a refrigerant was relatively cheap and readily available for the costumers. Between 1850s and 1920s the carbon dioxide was the most favour refrigerant used in various applications for the time been. It fell out of favour at the early stage of 1930s, when the new synthetic refrigerants were introduced for the small commercial applications and the use of ammonia replaced the carbon dioxide in industrial applications. The very high critical pressure and its low critical temperature of 31° were the main reasons for the phasing-out of CO_2. In case the ambient temperature is higher than the critical temperature, the CO_2 is not condensate in the high pressure-side of the system and the system operates in transcritical mode. Therefore, when system operates in transcritical cycle the cooling capacity and the system efficiency is lower comparing with other systems. The available techniques back to 1920s could not solve the problem and the new synthetic refrigerants replace the CO_2.

The consequences to the global environment of the release of massive amounts of the synthetic refrigerants were the main reason to start explore about the natural refrigerants again. From the "natural refrigerant" point of view, CO_2 is ideal solution to replace the existing HFCs system. With respect of safety, CO_2 is naturally existing substance and is non-flammable and non-toxic.

The use of CO_2 as a refrigerant it was re-established relatively quickly in the last two decades in varies application such as supermarket systems, automotive applications, air conditioning systems and transportation cooling systems. The available technologies and systems, allow controlling the cooling capacity and efficiency of the system even in the higher pressure cycles. The basic characteristics of CO_2 such as non-toxic and non-flammable make it a promising alternative solution for supermarket applications, where the health and safety regulations for customers and staff have a significant contribution.

2.1.CO_2 AS A REFRIGERANT

The choice of a suitable refrigerant in supermarket applications should be taking into consideration a number of factors which are divided into three main groups: practical – environmental – financial. The first group include the performance and energy efficiency of the individual systems based on the thermodynamic and heat transfer properties of the refrigerant used. The second group including the physical, chemical and physiological properties of the refrigerant which is describe the environmental impact of the refrigerant. System design, operation and maintenance cost are describing from the financial point of view. One approaching gaining the last two decades is the use of natural refrigerants such as ammonia, HC and carbon dioxide. The high toxicity of the ammonia and the size restrictions of the HC systems create the carbon dioxide as a strong competitor for the centralized supermarket systems. Key refrigerants properties for different refrigerants are shown in Table 2.1.

Table 2.1 Key refrigerant properties

Refrigerant	R-744	R-717	R-134A	R-404A	R-410A
Boiling point at 1.013 bar (°C)	-78.5	-33.34	26.15	-45.47(dew) -46.46(bub)	-57.27(dew) -52.35(bub)
Triple point (bar)	5.18				
Triple point (°C)	56.6				
Critical pressure (bar)	73.83	113.53	40.67	37.32	51.74
Critical temp. (°C)	31.06	132.25	101.1	72.07	74.67
Molar mass (g)	44	17	102		

The density of CO_2 saturated vapour is 97.466 kg m-^{3} which is 28 times higher than the ammonia and 6.7 times higher than the R-134a for the same temperature. The higher gas density allows the systems to achieve higher cooling capacity for the same volume flow. This allows designing the system by using smaller pipe diameter in the suction side and reducing the size of the compressors.

The pressure drop is affected by the ratio of gas to liquid density which enabling liquid to be carried faster in wet suction lines (Pearson, 2014).

The high working pressure of the system creates higher vapour density which shown in Fig 2.1, resulting a greater volumetric refrigerant effect comparing with refrigerants with similar values of latent heat of vaporisation/condensation.

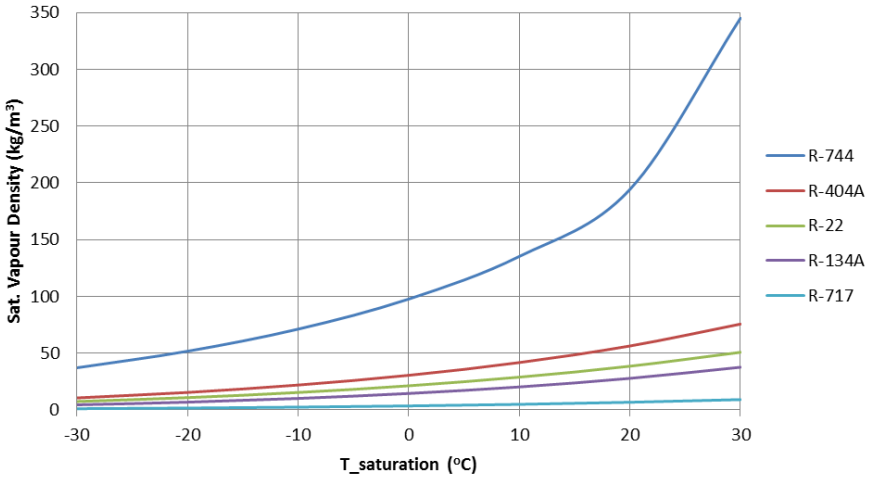

Figure 2.1Saturated vapour density of different refrigerants

The distinguish characteristic of CO_2 is its phase change properties. Table 2.1 shows the triple point of CO_2 is relatively high at -56.6°C temperature and 5.2 atmospheric bar. The critical temperature is lower compering with other refrigerants at 31°C and 73.83 atm. bar. The low critical point of CO_2, results the heat rejection of the system to atmosphere to be at pressures higher than the critical pressure when the ambient temperature is higher than 25 °C (ASHRAE, 2014). The phase change properties for the triple point of CO_2 refrigerant illustrated in Fig 2.2. The phase change properties from solid – liquid – vapour must be taking into account for any potential application of CO_2 in early stages of design.

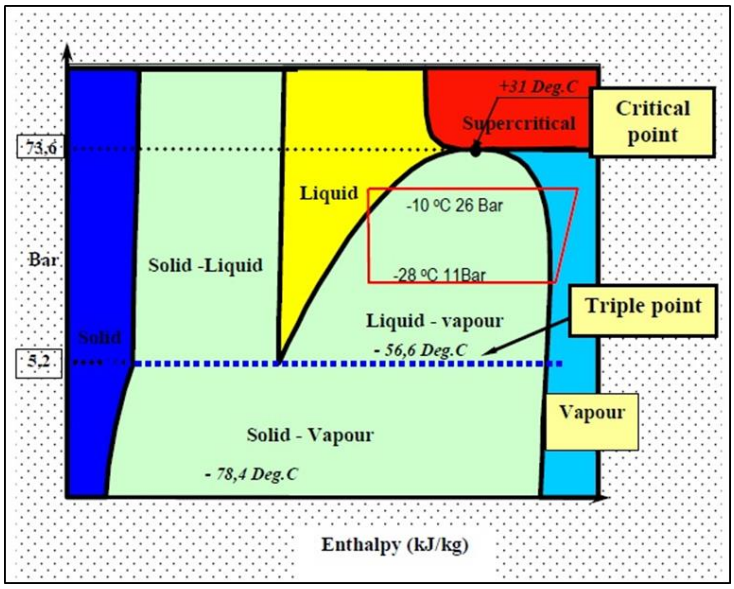

Figure 2.2 - Phase change properties for CO_2 triple point

Adapted from IOR Carbon Dioxide for supermarkets (Campbell, 2007)

The operating pressure characteristics of the CO_2 are significantly different comparing to other refrigerants as shown in Fig. 2.3. The higher operating pressure of CO_2 required more detailed design of the system in order to stand with higher operating pressures.

On the other hand the higher operating pressure causes a much smaller changes in saturation temperature which means that the evaporators and pipework must be designed to operate with higher pressure drop comparing with other refrigerants without severe operating penalties (Pearson, 2014).

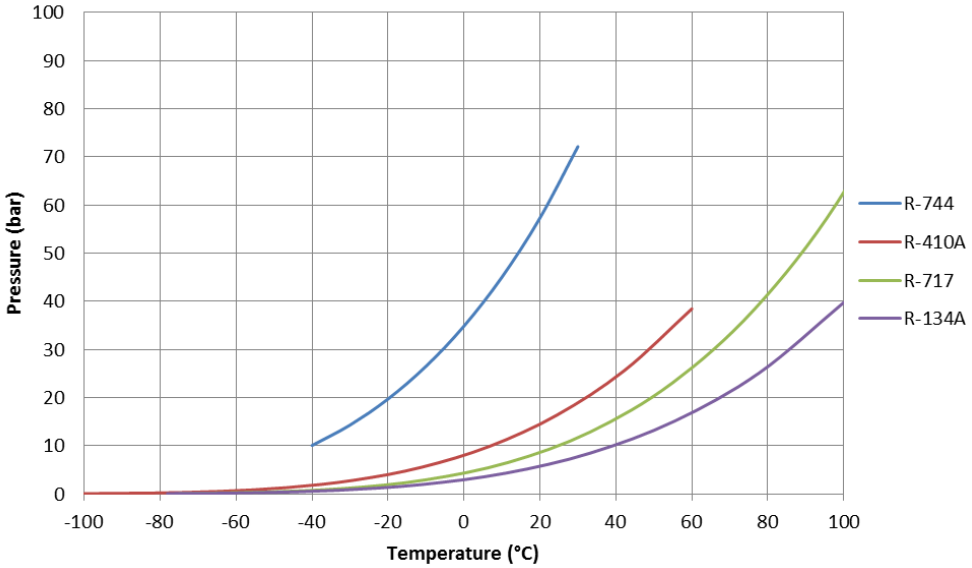

Figure 2.3 Operating pressure for different refrigerants

The high pressure operation results another thermos-physical advantage based on the latent heat of vaporization. Fig. 2.4 illustrates the comparison between common refrigerants used, where the CO_2 is in the same range except the R-717 which has exceptionally high values.

As the proportional of the high vapour density (Fig. 2.1) of CO_2 the volumetric refrigerant effect is higher comparing with the refrigerants with similar values of latent heat of vaporization.

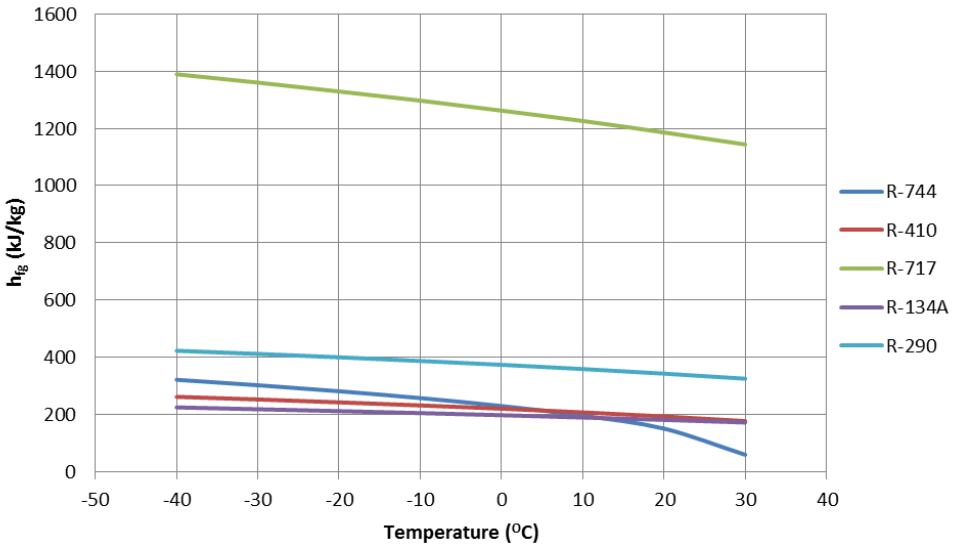

Figure 2.4 Latent heat of vaporization

Figure 2.5 shows the comparison of volumetric refrigeration effect on the selected refrigerants. The CO_2 values are relatively much higher comparing with the other refrigerants which means that the system need smaller refrigerant vapour volume flow rate for the same cooling capacities.

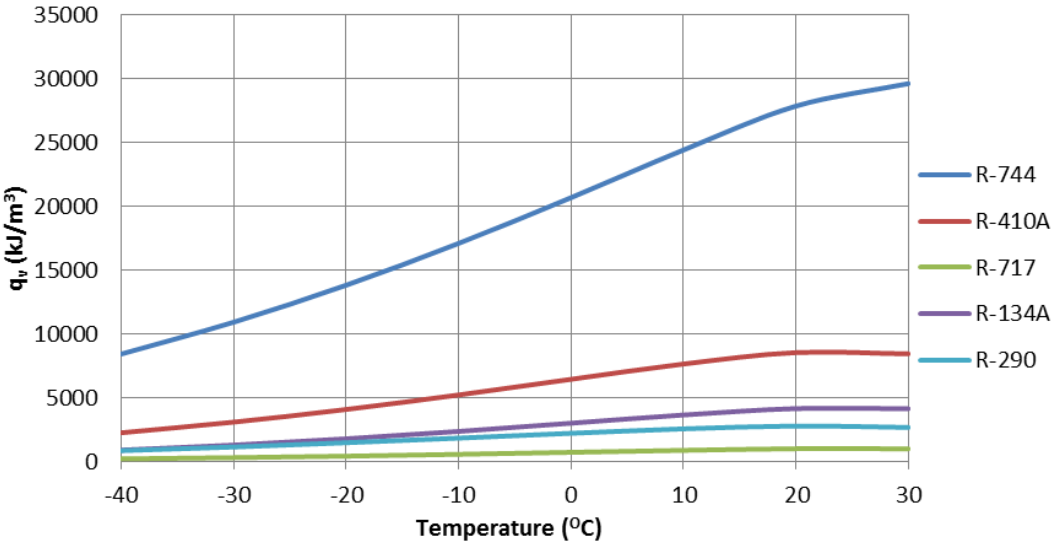

Figure 2.5 Volumetric refrigeration effect on the selected refrigerants

Enthalpy of vaporization (kJ/kg)*Density (kg/m^3) – Complete evaporation
Derived using EES

The unique thermos-physical properties of CO_2 lead to deliver higher rates of evaporative heat transfer as a proportional of the gas/liquid density ratio as discussed in this section. Furthermore, the boiling heat transfer coefficient of the CO_2 is twice higher comparing with other fluorocarbons fluids but lower than the ammonia. The very low viscosity increases the heat transfer without effect on the pressure losses. In the early stage of the CO_2 condenser-evaporator design, the refrigerant flow path can be extensive than other refrigerants. By using the advantage of favourable pressure-temperature relationship allows designing the system with higher mass flux values and increases the internal coefficient. Along the excellent heat transfer rates of the CO_2 as a refrigerant, should be noted that for the design on air-to-refrigerant heat exchangers the air side coefficient will effect to the overall performance of the system. Therefore, the overall structural dimensions of the heat exchanger are really important to achieve the higher heat capacity (Pearson, 2014; Kim, 2004). The surface tension of the fluid is another parameter which effect on the heat transfer. The lower surface tension decrease the superheated required for nucleation and growth of vapour bubbles which in some case can effect to the heat transfer positively. Therefore, the evaporative heat transfer is a proportional of the wetting characteristics of the liquid refrigerant thus affected from the surface tension of each fluid (Pettersen, 2004).

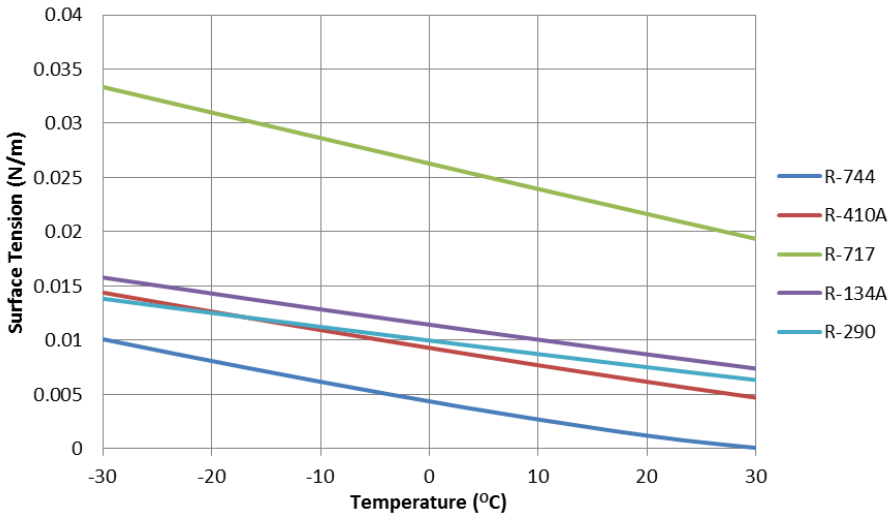

Figure 2.6 Surface tension for given refrigerants

Figure 2.6 presents the surface tension for specific refrigerants at different temperatures. The surface tension of the CO_2 is lower than those refrigerants.

Other important characteristic of supercritical fluids such as CO_2 is the rapidly change of the properties with respect in temperature in an isobaric process, especially near to pseudocritical point. The pseudocritical point (Tps) is defined as temperature where the specific heat reaches the highest value at specific pressure (Liao and Zhao, 2002).

As discussed, when the ambient temperature is higher than the CO_2 critical temperature the saturated gas is not condensate at the high pressure side of the system. Subsequently, the heat exchanger is act as a gas cooler in nearly isobaric operation with high temperature drop across the coil.

Figure 2.7 illustrates the specific heat and density of CO_2 at supercritical pressures. The pseudocritical temperature of CO_2 is calculated by Lorentzen (1993):

$$T_{pseud} = -122.6 + 6.12P - 0.1657P^2 + 0.01773P^{2.5} - 0.0005608P^3 \qquad 2.1$$

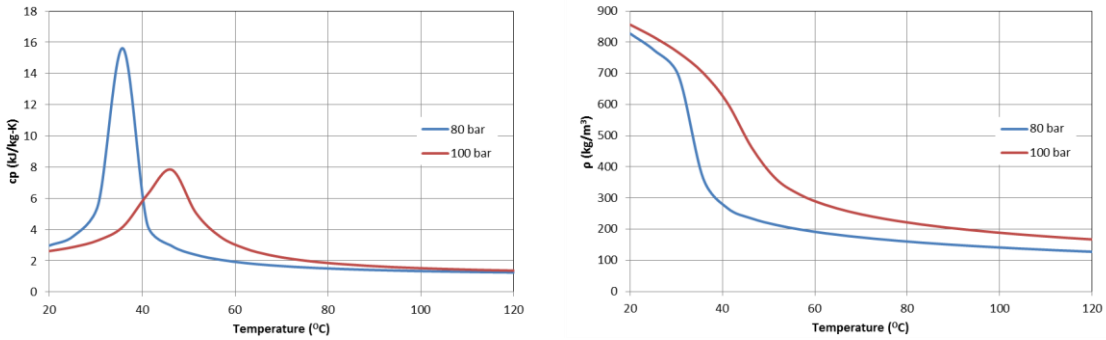

Figure 2.7 specific heat and density of CO_2 at supercritical pressures

The pseudocritical temperature for varies pressure is shown in Fig. 2.8. It follows that the Tps is 34.63°C at 80 bar and 45°C at 100 bar.

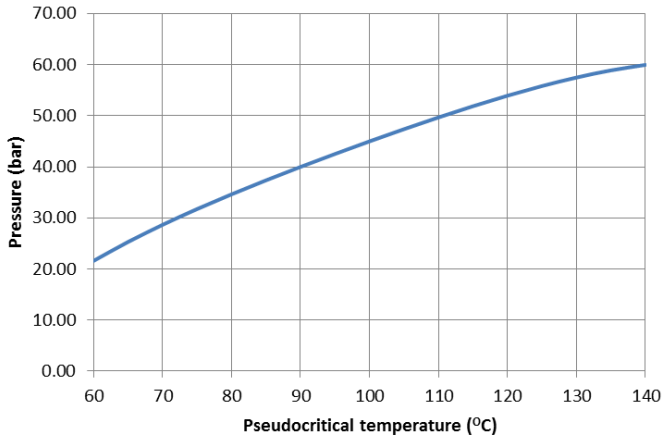

Figure 2.8 Pseudocritical temperature for varies pressure

The heat transfer coefficient is a proportional of the refrigerants transport properties such as thermal conductivity and viscosity. The higher thermal conductivity of the fluid can increase the heat transfer coefficients both in single phase or two phase flow. Viscosity is important parameter for the fluid flow behaviours, convection characteristics and pressure drop (Pettersen, 2002). Fig. 2.9 shows the transport properties of CO_2 refrigerant under different pressure operations.

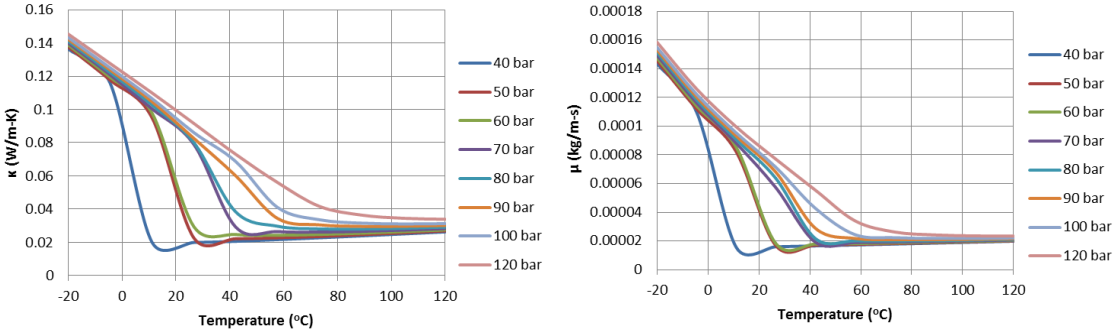

Figure 2.9 Transport properties of CO_2 refrigerant

Comparing with other refrigerants, the thermal conductivity of saturated CO_2 liquid and vapour at 0 °C are 20% and 60% higher comparing with R-134A liquid and vapour respectively (Kim, 2004).

Another important parameter for the local heat transfer coefficient is the Prandtl number. It is a proportional of temperature and pressure and associated with the specific heat. Fig. 2.10 depicts the Prandtl number of CO_2 at different temperatures.

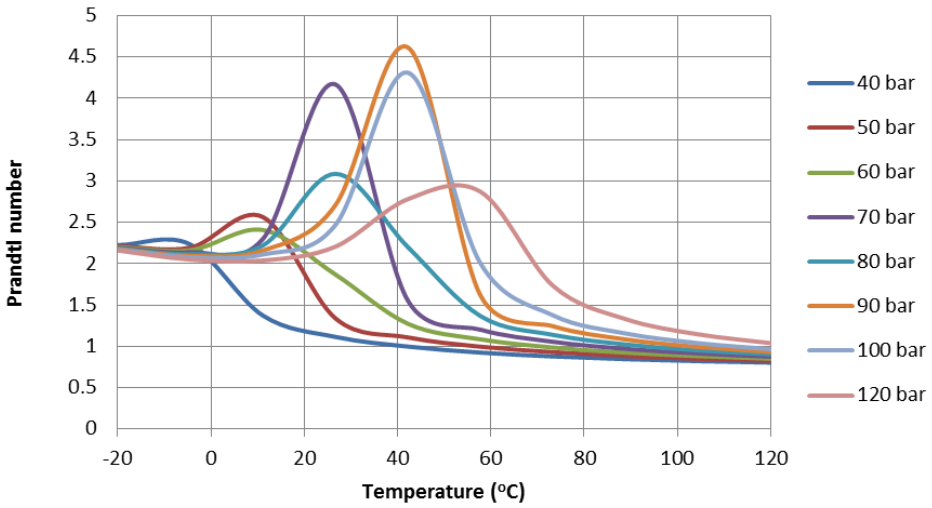

Figure 2.10 CO_2 Prandtl number under different temperatures

2.2.REFRIGERATION CYSLES BEHAVIOUR

The comparison between CO_2 and other commons refrigerants can be misleading because the unique properties of the CO_2 such as low critical temperature. The CO_2 can be compare reasonably with R-404A only when the condensing temperature is below 20°C and the pressure of 56.3 bar (Pearson, 2014). However, is really difficult to achieve these conditions all the time.

The low critical temperature usually leads to design the CO_2 systems in different way comparing the other refrigerants. Therefore, like-for-like comparisons between CO_2 and other common refrigerants are not easy to predict.

Table 2.3 represents the performance comparison between CO_2 and selected refrigerants under the same operating conditions for medium (MT) and low temperature (LT) refrigeration applications. The comparison operating conditions are shown in Table 2.2.

The refrigerants which are selected for comparisons are: CO_2, R-134A, R404A, R-290, R-1270 and R-717. The refrigeration capacity for the comparison is lower in order to be served from HC refrigerants as well.

Table 2.2 Operating conditions

	MT	LT
Refrigeration capacity (kW)	5	5
Degree of superheat (K)	5	5
Sub-cooling (K)	0	0
Evaporating Temperature (°C)	-8	-32
Condensing Temperature (°C)	28	28

The refrigeration effect of CO_2 is higher comparing with R-404A but lower than the other natural refrigerants. The mass flow rate required to be circulated in the refrigeration system is a proportional of the refrigeration effect. CO_2 required 30% lower refrigerant charge comparing with R-404A and 6% than the R-134A for the LT applications under the same conditions. On the other hand, CO_2 refrigeration systems required more refrigerant charge compare with the other natural refrigerants.

Table 2.3 shows that CO_2 has really low pressure ratio than the selected refrigerants. The lower pressure ratio leads to the higher isentropic and volumetric efficiencies of the system. As shown in table, the pressure ratio of CO_2 is 20 to 64% for LT applications and 8 to 33% lower for MT refrigeration system.

Table 2.3 Performance comparison between CO_2 and selected refrigerants

Refrigerant	Refrigeration effect	Refrigerant mass flowrate	Evaporator Pressure	Condenser Pressure	Pressure Ratio
	kJ/kg	**kg/s**	**bar**	**bar**	
LT application					
R134a	144	0.035	0.8	7.3	9.5
R404A	112	0.045	1.9	13.6	7.1
R290	272	0.018	1.5	10.3	6.6
PROPYLENE	281	0.018	2.0	12.5	6.3
R717	1100	0.005	1.1	11.0	10.2
R744	153	0.033	13.3	68.9	5.2
MT application					
R134a	159	0.031	2.2	7.3	3.4
R404A	126	0.040	4.7	13.6	2.9
R290	301	0.017	3.7	10.3	2.8
PROPYLENE	306	0.016	4.6	12.5	2.7
R717	1134	0.004	3.2	11.0	3.5
R744	152	0.033	28.0	68.9	2.5

Continue from the Table 2.3 the suction gas specific volume and latent heat of evaporation for the given refrigerants are shown in the Table 2.4.

Table 2.4 Suction gas specific volume and Latent hat of evaporation

Refrigerant	Suction gas specific volume	Latent heat of evaporation
LT application		
	m^3/kg	**kJ/kg**
R134a	0.253	221
R404A	0.102	191
R290	0.285	415
PROPYLENE	0.234	421
R717	1.082	1366
R744	0.030	307
MT application		
R134a	0.095	205
R404A	0.043	173
R290	0.126	386
PROPYLENE	0.105	390
R717	0.397	1290
R744	0.014	253

Another important advantage of the CO_2 operation in both LT and MT applications is the very small suction gas specific volume comparing with HFCs and other natural refrigerants. The suction gas specific volume for CO_2 is 0.030 m^3/kg for LT applications when the values for R-717 and R-404A are 1.082 and 0.102 m^3/kg respectively. It is mean by reducing the suction gas specific volume we can reduce the diameter of the pipework in the system and the compressor size. For the same operating condition the ammonia compressor is much bigger comparing with the CO_2. This directly influence on the capital cost of the system, maintenance cost, safety and direct and indirect emissions from the system to environment. The table also shows CO_2 has higher latent of evaporation values comparing with HFCs refrigerants but lower comparing with other natural refrigerants.

The main advantage associated with the high working pressure of the CO_2 is the low vapour pressure. This allows us again to design the system by using smaller compressor size and distribution pipework.

The comparison between CO_2 and selected refrigerants can be related by applying the same operating conditions, geometry and load with Table 2.3 to the following pressure drop equations (Moreno and Thome, 2007a; Moreno and Thome, 2007b).

$$\Delta P = 4\, f\, \frac{L}{D}\, \frac{G^2}{2\rho} \qquad 2.2$$

The friction factor is calculated by Blasius equation for laminar flow conditions (Cheng et al, 2008):

$$f = \frac{0.079}{Re^{0.25}} \qquad 2.3$$

Assuming the refrigerant enters the evaporator as saturated liquid and evaporates completely. For the same capacity, pipe length and diameter the above equations used to compare selected refrigerants under different saturations temperatures. The data were derived by using EES.

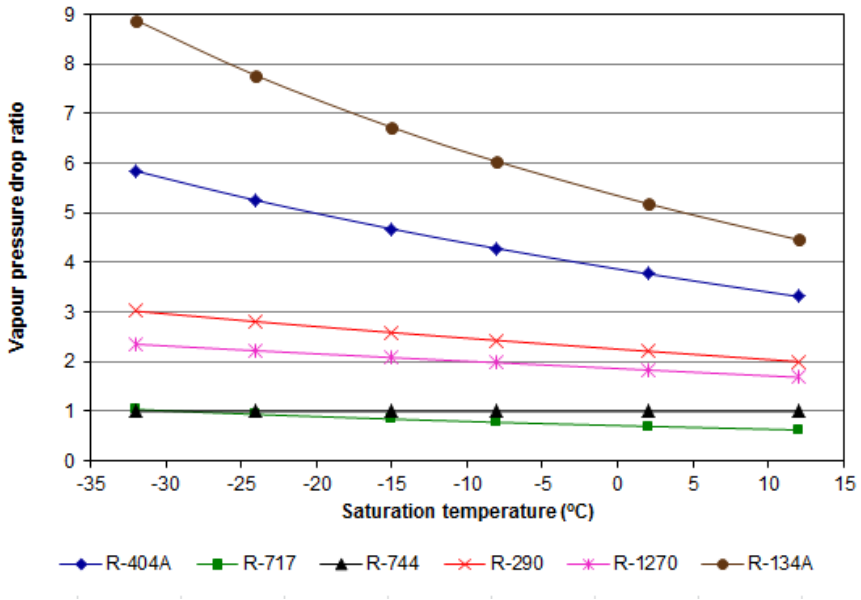

Figure 2.11 Saturated vapour pressure drop ratio

Figure 2.11 illustrates the saturated vapour pressure ratios for selected refrigerants. The values for CO_2 vapour pressure drop is much lower comparing with other refrigerants

apart from ammonia. For the saturation temperature below 0 °C the gap between CO_2 and other selected refrigerant is getting bigger. The saturated vapour pressure ratios for CO_2 and ammonia is nearly the same for different for saturated temperatures between -10 and -32 °C.

In Fig. 2.12 the comparison between CO_2 and selected refrigerants based on the saturated liquid pressure drop are presented. Eq. 2.2 and 2.3 used to define the liquid pressure drop under different saturation temperatures and assuming that the quality entering is 100% liquid.

It can been seen from the graph, that the liquid pressure drop of CO_2 is lower comparing with R-404A for saturation temperatures below 5 °C. The pressure drop values for CO_2 and R-134A related with the saturation temperature. As is can been seen for saturation temperature below -24°C, CO_2 shows higher pressure drop. Pressure drop ratios of R-290 and R-1270 shows much lower pressure drop ratios comparing with CO_2. Ammonia gives a pretty constant liquid pressure drop characteristics for varying evaporating temperature.

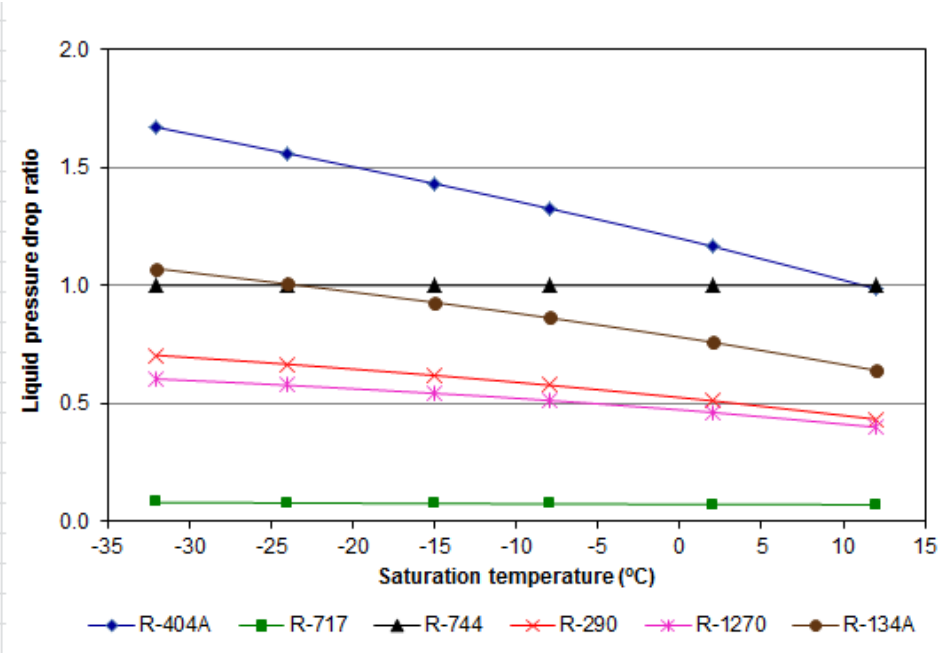

Figure 2.12 Saturated liquid pressure drop ratio

The acceptable liquid pressure drop of the applications where the CO_2 used is higher comparing with other refrigerants as a proportional of the unique thermos-physical properties. Based on that, CO_2 and R-717 can performed better compared with the other

selected refrigerants. Due to the low saturated pressure drop CO_2 is suitable to use as a secondary fluid in centralized refrigeration systems.

2.3.SAFETY GROUP & PRECAUTIONS

Safety classification of the refrigerants describes the toxicity level in case released to environment and flammability standards in case of fire for each refrigerant fluid.

BS EN 378 (2012) standards have the intension to minimize possible hazards to persons, property and the environment causes from refrigerating systems and refrigerants fluids. These hazards are associated essentially with the physical and chemical characteristics of refrigerants as well as the pressures and temperatures occurring in refrigeration cycles. Table 2.5 represent the safety classification for natural refrigerants.

Table 2.5 Natural refrigerants safety group

Natural Refrigerants				
Type	Ref. Code	Safety Class	ODP	GWP
Butane	600	A3	0	3
Ammonia	717	B2	0	0
CO_2	744	A1	0	1

Source: BS EN 378 (2012)

CO_2 is non-toxic and non-flammable. Ammonia carries a B2 safety classification which indicates that it is a high toxic refrigerant and also carrier a medium flammability risk. Butane is non-toxic but carrier a high risk of flammability. Also butane has a higher GWP number instead of CO_2 and ammonia (ASHRAE Standard 34, 2007; BS EN 378-2012). Comparing with other two natural refrigerants, the CO_2 may offer the same environmental and personal safety.

Although CO_2 is present in the atmosphere, safety precautions are necessary in order to prevent accidents, casualties and fatalities. The effects of carbon dioxide exposure for a typical person under normal situations are given in Appendix B. Along the attractive thermos-physical characteristics which discussed in this chapter; the high operating pressure of the systems presents an additional hazard. System must be designed to stand with high operating pressures avoiding any damage which will release huge amount of the CO_2 in the environment. Typical values for standstill and operating

pressures which the CO_2 system must be design are illustrated in Table 2.6. The standstill pressure referred on the pressure existing in the liquid receiver where the CO_2 fluid storage when the system is off. Subsequently, operating pressure is the pressure on the particular equipment such as gas cooler/condenser and evaporator, when the system is running.

Table 2.6 Standstill and operating pressures for R-744 systems

Operation	Pressure Limitation (bar-gauge)
Standstill Pressure at 10 °C	44
Standstill Pressure at 30 °C	71.1
LT Evaporator	10-17
MT Evaporator	25-30
Cascade Condenser	30-35
Cascade HP cut-out	36
Cascade PRV in HP side	40
Transcritical in HP side	90-100
Transcritical HP cut-out	108-126
Transcritical PRV in HP side	120-140

In order to ensure that pressure inside the liquid receiver does not rise above the relief pressure levels in the event of system fault or high ambient temperature, a small condensing unit proposed to install to cool down the system. The condensing unit must be supplied by an uninterruptable power supply and switch on when the pressure rises above the set point. The auxiliary condensing unit must be designed to remove sufficient heat from the receiver in sort time and keep the pressure in safe levels.

2.3.1. SAFETY RECCOMENDATIONS

In case CO_2 liquid try to escape from vent valve which is opened then the liquid will transfer to solid peace of ice and block the valve. By adding heat to the valve in order to melt the ice could cause an extreme rise in pressure which might damage the valve or system equipment which located near to the blocked area. When the pressure rise above the designing levels the relief valves will open and a part of CO_2 release to the atmosphere. For that reason, the relief valves should be placed in good ventilated place

and avoid exceeding the prescribed limit for the space. This limit is described by BS EN 378 (2012), ASHRAE 15 (2013) and ISO5149 (2013). CO_2 applications where the charge is much higher than the limit the safety relief valve must be installed outside in a safe place away from costumers and stuffs.

The safety relief valves for CO_2 systems are operated in a different way comparing with the ammonia and HFC systems. For CO_2 the relief valve will open in case of the pressure is higher than the setting point of the body valve. On the other hand, the valves for ammonia and HFC systems will operate in case of hydraulic lock or fire. A huge amount of refrigerant can escape under abnormal circumstances from the system. In order to prevent a huge loss of refrigerant it is recommend to install a pressure regulating valve in parallel before the relief to allow controlled the venting of vapour at set pressure slightly lower than the relief valve setting (ASHRAE, 2014). The system relief valve sizing should be made by using the following formula.

$$C = f_{,constant}\, D_{,vessel}\, L_{,vessel} \qquad 2.4$$

Where: C is the capacity required (kg/s of air), f is the refrigerant specific constant (1 for CO_2), D is the diameter of the vessel (m.) and L is the length of the vessel (m.). Another important issue for the safe operation is the water in the system. CO_2, like all the refrigerant fluids is very sensitive to any moisture within in the pipework. System must be evacuated every time before charging the refrigerant fluid in order to remove the atmospheric moisture. The acceptable water level in the system for CO_2 applications is much lower comparing with other refrigerants. In case the water concentration exceeds the saturation limit it creates carbon acid which can cause possibly corrosion on the internal pipe work or even equipment failure (ASHRAE, 2014). Then, it is recommended to install filters-driers before all main liquid feel equipment.

Additional considerations based on the high operation pressure and high liquid density of the CO_2 must be taken to prevent the risk of liquid hammer in the control valves operation. The hammering effect creates change in the operation pressure of the system, which can be calculated as below.

$$\Delta P = c_{,sound\ speed}\, v_{,liquid\ velocity}\, \rho \qquad 2.5$$

Common design strategies to prevent the risk of hydraulic shocks are the use of slow acting valves and installation of flexible hose as a part of the pipework. In the high

pressure side of the system the installation of ball valves instead of solenoid valve is recommend.

Liquid CO_2 is dispensed and stored in the pressurized vessel. The vessel must be cooled down with independent condensing unit as described in above paragraphs. It is recommend it to install number of valves at every inlet and outlet of the vessel to isolate it in case of failure and maintenance. A single pipe line which has to be connected with pressure relief valve must be installed at the top part of the vessel to prevent the unsafely pressure levels inside the vessel.

In general the system must charge and test with higher pressure than the system designed. Before the first charge the system must be cleaned and evacuated for acceptable period of time to ensure that no moisture exist in the system. It is recommend it to vacuum the system for one hour for each 30 m^3 of the system. After finish vacuum the system should be kept in vacuum conditions for at least one day. If the system keeps the vacuum condition over the day then dry nitrogen should be added to the system slightly above the design operating conditions for another day. A special leak detector spray must use to check every single join in the system. When the authorised stuff are confident with the system integrity, the dry nitrogen must be realized to the air and the system pull back into vacuum conditions. Break the vacuum by insert CO_2 to the system. Open the valves slow and allow the CO_2 flows on the system. Maintenance stuff must use protective clothing, industrial gloves and safety glasses to entry the plant room. In additional, a number of detectors must install in the plant area. Number of acoustic and flashing alarm devices must be in a visible place from both inside and outside area of the plant room.

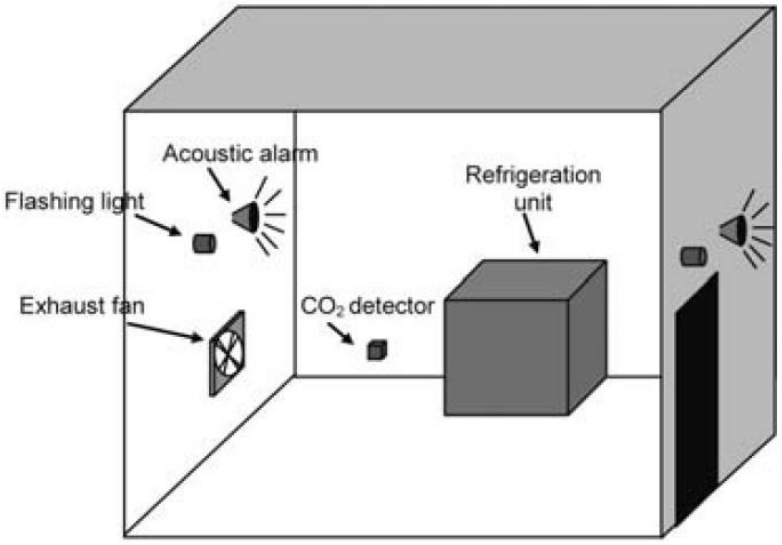

Figure 2.13 CO_2 machine room construction recommendations

Adapted: GTZ Proklima, 2008

2.4.REFRIGERANT PRICE

Due to high heat transfer ratio the use of CO_2 refrigerant allowing selection of smaller equipment compared with HFCs systems. Therefore the smaller equipment and component selection reduce the size of pipe diameter of the CO_2 systems as discussed in previous paragraphs. The refrigerant charge for CO_2 centralised supermarket systems is 50% lower than HFC refrigerants. The specific refrigerant charge of a CO_2 for centralized supermarket applications is between 1.0 to 2.5 kg/kW as shown in Table A-1 (Appendix A). CO_2 gains market acceptance due to its low refrigerant charge comparing with HFCs and on the other hand the low price of the carbon dioxide as a refrigerant. Table 2.7 shows the price for selected refrigerants

Table 2.7 Price for given refrigerants

Refrigerants	Price (£/kg)	Ratio
R-134A	14.58	6.2
R-404A	10.42	4.6
R-290	17.30	7.4
R-1270	19.00	8.1
R-717	6.20	2.6
R-744	2.34	1

2.5.REFRIGERANT CO_2 APPLICATIONS

Increasing the environmental concerns about the potentials direct emissions from HFCs refrigeration system into the atmosphere have led the used of CO_2 refrigeration around the world. CO_2 is already used in a massive range of applications including supermarkets, food processing, vending machines, cold storage, heat pumps and transportation refrigeration units.

Over the last 30 years the choice of refrigerants in food industry application systems has been undergoing a rapid change. Supermarket application has been increasing alongside the growth of the world population and the human needs. The solution of natural refrigerant has emerged as one of the most promising environmental friendly refrigerants. As an alternative of the HCFCs and HFCs systems, CO_2 gains the market acceptance in the supermarket applications. Cascade and transcritical systems are recognized as good opportunity in countries with moderate temperature. A number of investigators and companies are now focusing on the performance increasing for hot climates countries (Rolfsmann, 1999; Tassou et al, 2010).

More than 200 supermarkets have been used CO_2 as a working fluid in Europe the last decade, with cooling capacity varies of 50 to 1200 kW. The use of carbon dioxide led to reduce the direct emission in zero level. The energy consumption has been reported to be in the same range such as R-404A systems (Tassou et al., 2010). The initial capital investment for CO_2 systems is 10 to 20% higher comparing with R-404A. A comparison based on the energy consumption between CO_2 and R-404A system with heat recovery showed that the CO_2 system have lower power consumptions. Therefore, the life-time assessment is lower for the CO_2 systems (Neksa et al., 2010). In the high temperature countries, the efficiency of the system is more challenging. When the temperature is higher than 30 °C the overall performance of the CO_2 system is 10% lower comparing with R-404A (Girotto, 2007). A number of existing options can be taken under consideration to improve the system performance. Finckh et al (2011) have been reported a number of comparisons between CO_2 and R-404A supermarket refrigeration systems. For the ambient temperature below 24°C the performance of the CO_2 systems are higher. Both systems shows the comparable efficiency when the ambient temperature is above 30°C.

CO_2 has been widely used in stand-alone applications the last five years. It is a self-contained refrigeration system such as ice-cream freezers, ice-cream machines, beverage vending machines and display cases. Stand-alone equipment are used in medium size supermarket because of ease of installation and maintenance. Europe, Asia and lately in other countries, CO_2 used as the heat transfer fluid for stand-alone equipment (UNEP, 2014).

The use of all-CO_2 transcritical cycle in heat pump applications is very common for the last decade. The heat pumps used to heat the water in the range of 10°C to 65°C (Neksa et al., 1998). About 1.7 million units were installed between 2001 and 2008 in Japan. The aim to achieve by 2010 was the installation of 5.2 million units and reduces the CO_2 emissions about 2.9 MT-CO_2/year.

Another important application of CO_2 is the Rankine Cycle (ORC). It is similar to the process used for power generation in steam turbines but is operates in lower temperatures which depending on the working fluid used. The ORC systems use heat to evaporate the CO_2 fluid at high pressures, and then the gas passed through the expansion engine. The useful work done by the engine used to drive the alternator and the produce electrical power. The low pressure gas at the expander outlet is condensed by rejecting the heat to the atmosphere and change to the liquid form. The liquid is pumped up to evaporating pressure by using a liquid pump. The typically conversion rate from thermal to electrical power is in the range of 10 to 15% (Leslie et al., 2009). The power generations systems were used CO_2 operate with the heat input from the transcritical operation or with both heat input and heat output above the supercritical point (UNEP, 2014).

The environmental and thermos-physical opportunities of the use of CO_2 as a working fluid and the widely range of applications encourage researchers and companies to investigate new directions of CO_2 applications. The development of new more strong components and more efficient equipment gains the confidence in dealing with its systems and provide an excellent background for new implementations. Supermarkets, food processing, vending machines, cold storage, heat pumps and transportation refrigeration units are some of the application areas for which the CO_2 fluid is an excellent refrigerant to replace the HFCs and minimize the direct emissions.

2.6.LUBRICATANTS

The main function of the lubricant is to reduce the friction and minimize wear in the compressor. There are several compatible oils for use with CO_2. The most commonly oils used for CO_2 systems are the polyol ester (POE), alkyl benzene (AB), alkyl naphthalene (AN), polyalfaolefin (PAO) and polyalkyl glycol (PAG). For the cascade applications the use of more common oil such as POE is suitable for the compressors. On the other hand, for the transcritical operations where the pressure and temperature is much higher, the systems required more special lubricants to stand with these conditions. The performance of the compressor and the compressor longevity is a common area for researches over the last years. Different oils based on viscosity and thermodynamic behaviour have been tested and reported (Bobbo et al., 2006; Rohatgi, 2010). The most common oils for CO_2 supermarket applications are the POE and PAG for subcritical and transcritical applications respectively.

2.7.OTHER ASPECTS

Along the above advantages, CO_2 also has some disadvantages. The main drawback of CO_2 as a refrigerant is its inherent high standstill and operating pressures, which are more hazardous and increase the leak potential. The systems required specially designed components to stand with this extremely conditions. Compressors body, motor and displacement combination must be design to operate in high refrigeration capacity. The special systems and components design leads to higher capital cost for installation and maintenance. The operating conditions on the high pressure side of the transcritical CO_2 systems required the pipework to include steel or stainless steel and proper joints techniques. Specially licenced welders need to be carried out this job. Time, materials and licenced welders is another reason to increase the capital cost of a CO_2 plant (Emerson, 2015). Additionally, the fact that CO_2 has no smell and it can displace the oxygen in the space may cause a serious health problem for the people expose on it. The special detectors and its positions have been explained above.

2.8. SUMMARY

This chapter outlines advantages and disadvantages of the CO_2 natural refrigerant as a fluid into a refrigeration system. Furthermore, some of the key applications have been discussed. Due to less environmental impact and the attractive thermo-physical properties, CO_2 refrigeration system has been widely applied over the last decades. The attractive thermos-physical properties of the CO_2 leads to its good heat transfer

properties which allows to design the system by using smaller equipment comparing with HFCs systems. Moreover, CO_2 gains the market acceptance due to its good safety characteristics and very low price than other refrigerants. High toxicity risk of ammonia and risk of flammability of the HC make the CO_2 more advantageous than other natural refrigerants. Table 2.8 summarize the properties of various refrigerants which have been discussed earlier.

Table 2.8 Various properties for investigated refrigerants

	GWP	Flammability	Toxicity	Cost of fluid	System cost
HFCs	High	No	No	Moderate	Low
Ammonia	Low	Ignited	Yes	Low	High
HCs	Low	Yes	No	Low	Medium
CO_2	Low	No	In very high concentration	Low	Medium

The following chapter will describe the different CO_2 refrigeration system arrangements for supermarket applications. The recent developments of the CO_2 refrigeration systems will discuss as well.

3. SUPERMARKET APPLICATIONS – NOVELTIES – CASE STUDIES

3.1.INTRODUCTION

In supermarket application three types of refrigeration systems are employed which include the remote systems (plug-in/stand-alone equipment), condensing units and finally the centralised systems (UNEP, 2014). The stand-alone equipment consists of individual refrigeration systems where the whole circuit is brazed. The remote systems are applied for freezer, beverage coolers and vending machines applications. For refrigerating capacities ranging from 1 kW to 20 kW the condensing unit solution are applicable. Condensing unit is typical solution for butcher shops and convenience stores. For supermarket applications the centralised systems are one of the best choices. The centralised applications are divided in two sub-categories, the direct and indirect systems. For the direct systems the fluid flows from the machine room to the sales area where it evaporates in the refrigerated display cabinets. The vapour phase from the evaporator outlet is flows back to compressor suction to start the process again. For the indirect systems the use of secondary refrigerant is necessary. Both refrigerants and secondary fluid are exchange the temperature at the heat exchanger. The secondary fluid exchange the temperature at the heat exchanger with the primary fluid and it's pumped to the display cabinets. The use of the indirect systems are becoming more popular in recent years because the design is allows to us a flammable or toxic fluid for the high temperature circuit side (UNEP, 2014).

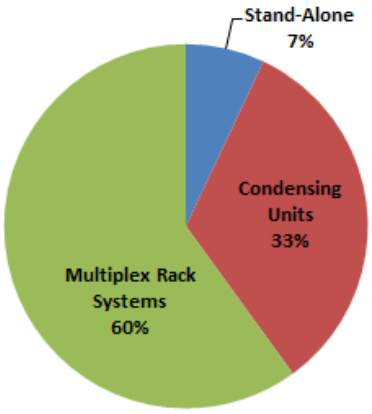

Figure 3.1 Global Commercial Refrigerant Stock by System

(EPA, 2010)

One approaching gaining the last two decades is the use of natural refrigerants such as ammonia, HC and carbon dioxide. The high toxicity of the ammonia and the size restrictions of the HC systems create the carbon dioxide as a strong competitor for the centralized supermarket systems. As discussed earlier, the unique thermo-physical properties of CO_2 lead to deliver higher rates of evaporative heat transfer as a proportional of the gas/liquid density ratio as discussed in this chapter. Furthermore, the boiling heat transfer coefficient of the CO_2 is twice higher comparing with other fluorocarbons fluids. The very low viscosity increases the heat transfer without effect on the pressure losses. In the early stage of the CO_2 condenser-evaporator design, the refrigerant flow path can be extensive than other refrigerants. By using the advantage of favourable pressure-temperature relationship allows designing the system with higher mass flux values and increases the internal coefficient. The unique thermo-physical properties of the refrigerant CO_2 has been discussed extensively in Chapter 2.

3.2.CO_2 CENTRALISED SYSTEMS

For the centralised refrigeration systems the application of CO_2 for the food retail refrigeration system can be adopted that fall into three major categories: indirect/secondary, subcritical cascade systems and all-CO_2 system. For an indirect system, the CO_2 is commonly used as a two-phase secondary coolant while a HFC refrigerant such as R404A is conventionally charged in the primary side. In a cascade layout, the system constitutes of two single stage sub-systems, integrated by a cascade heat exchanger. The CO_2 is applied in the low cascade side while a working fluid such as R404A, NH_3 or hydrocarbon is operated in the high cascade side. In all-CO_2 system, the CO_2 refrigerant is the only working fluid employed without need of a second refrigerant on the high pressure side. The main advantages of the CO_2 booster system over other ones include the simpler design requirements, less installation cost and less environmental impacts from the refrigerant leakage comparing with cascade systems use a HFC's as a secondary fluid. However, the CO_2 as a working fluid has a quite low critical temperature of 31.1°C and very high critical pressure of 73.8 bar. Consequently, the CO_2 operates in relatively high pressure comparing with other refrigerants. In case the ambient temperature is higher than the critical temperature, the CO_2 is not condensate in the high pressure-side of the system. The high pressure-side in the system can thus act as either a condenser or gas cooler depending on the ambient conditions. This necessitates high pressures which can lead to high power consumption. Therefore,

the pressure of the gas cooler becomes very important operating parameters which need to be controlled in order to obtain best performance of the system.

3.2.1. ADVANTAGES AND DISADVANTAGES OF CO_2 SYSTEMS

Before discuss the different CO_2 system arrangements for supermarket applications, it is important to describe the advantages and disadvantages of those as reported from the number of companies and researchers. Table 3.1 shows the advantages and disadvantages for secondary/indirect, cascade and transcritical systems.

Table 3.1 Advantages and disadvantages for secondary/indirect, cascade and transcritical systems

	Secondary/Indirect	Cascade	Transcritical
Advantages	• Very low pump power required due to the latent heat of CO_2 • Constant pressure at the system • Combine LT and MT	• Higher efficiency in warm climates • Standard HFC components well known in the market	• One refrigerant • Lower capital cost • Higher efficiency in cold climates
Disadvantages	• Additional equipment (heat exchanger) • Leaks and losses on the CO_2 pump	• Two different refriger. systems • System faults in coupled systems affect both MT and LT	• LT requires additional compressor • High operating pressures • Low efficiency in warm days

(Emerson, 2015)

3.3.INDIRECT/SECONDARY

The basic schematic design diagrams of the two possible arrangements for CO_2 indirect/secondary systems are illustrate in Figure 3.2. The main components for those two typical retail secondary systems are shown in Table 3.2. The CO_2 works as a secondary fluid for this arrangement. Both systems are connected in the cascade heat exchanger where the high stage system cools the liquid CO_2 in the secondary circuit. The evaporating temperature of the primary stage refrigeration system must be lower than the saturation temperature of the corresponding CO_2 secondary loop circuit. This arrangement can be applied for both chilled and frozen food display cabinet applications which can be arranged as parallel units. For that reason, the saturation temperature of the secondary circuit must be low enough to keep the product temperature at the ISO standards (ISO, 2012), where for chilled food the temperature is between -1°C to +7°C and for frozen food the product temperature must be keep from -15°C to -18°C. For the

supermarkets applications the saturation temperature is usually in the range of -6.5°C to -10°C for chilled food and -28°C to -35°C for frozen food. The typical pressure are 26 bar and 13 bar respectively. Based on the corresponding pressures the use of the available refrigeration pipes and components on the market is it possible to handle the CO_2 with further actions.

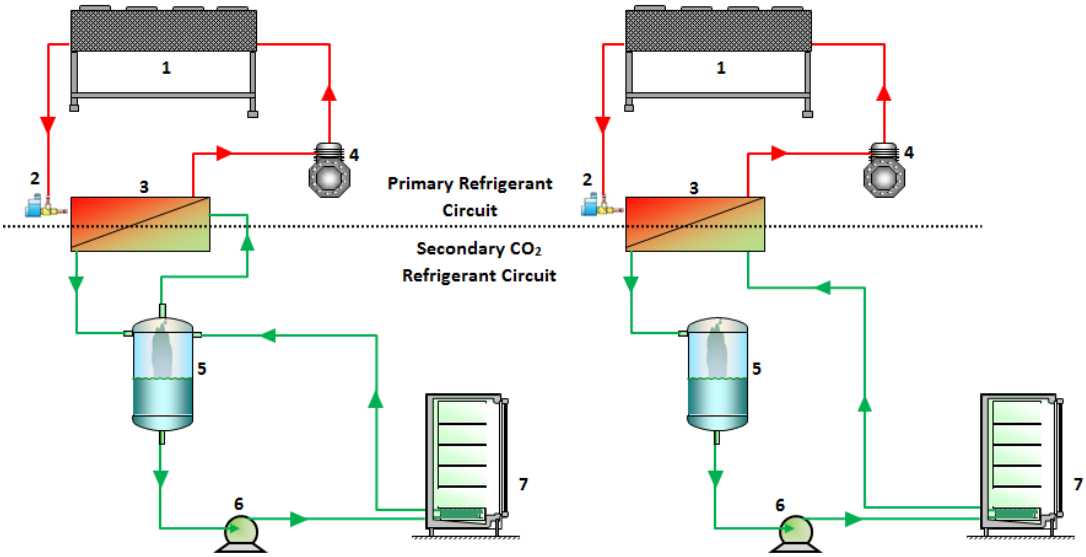

Figure 3.2 CO_2 indirect/secondary system arrangements

For the secondary circuit, the CO_2 is pumped around the load. The great advantage against other secondary fluids such as glycol it is volatile. Therefore, does not remain as liquid all the time, instead it partially evaporates. Because it partially evaporates the cooling capacity of the CO_2 is greater comparing with other secondary fluids. Moreover, it required lower pump power and temperature difference across the evaporator is lower comparing with other fluids.

Table 3.2 CO_2 indirect/secondary system components

Ref.	Component	Description
1	Condenser	Typically air-cooled/multi-fan type or convectional chiller
2	Expansion	Electronic expansion valve
3	Heat exchanger	Typically plate heat exchanger
4	High stage compressor	HFC or HC typical compressor
5	Receiver	Standard receiver (not for high pressure)
6	Liquid pump	Centrifugal pump are usually used
7	Evaporator	Standard evaporator is used (not for high pressure)

Figure 3.3 illustrate the relationship of the circulation ratio with the refrigerant quality exist from the flooded evaporator. The relation of the circulation ratio with the evaporator exit vapour fraction of the CO_2 can be ensured a higher heat transfer in the evaporator comparing with other fluids.

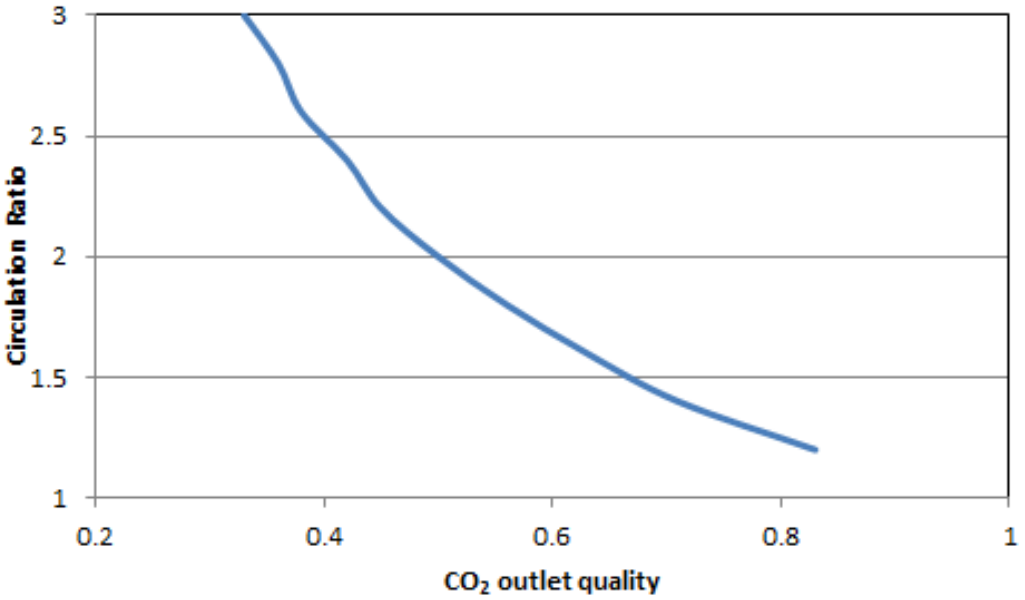

Figure 3.3 CO_2 Circulation ration in different outlet quality

As it mention before, the CO_2 system contains the liquid receiver where the liquid CO_2 is returning from the cascade condenser. The liquid receive act as a reservoir for the pump. The control strategies of the pump must be link with the level of the liquid in the

receiver to ensure the pump works at the acceptable net positive suction head avoiding any damage of the pump. Therefore the size of the receiver is essential for those systems and should be carefully designed to be able to accommodate the fluctuation of the liquid CO_2 caused by the variation of the cooling load for the normal or defrost operation.

Cavitation is the major problem with the liquid CO_2 pumps. The flow conditions must be then proper designed in order to avoid the cavitation problems. For example the feed velocity must be < 0.3 m/s, the sufficient head higher than 0.5 meters and a vortex breaker should be used in liquid receiver. The typical industrial refrigeration pumps can be applied to circulate the CO_2 in the secondary loop. The typical pressure across the pump is between 1 to 3 bar. The pump circulates the liquid CO_2 and keeps the evaporator wet for all the conditions. The liquid CO_2 absorbs the heat from the hot air at the evaporator and some of it evaporates. The liquid/gas mixture flows to the liquid receiver for the case A or directly to cascade condenser for case B. For case A the heat is rejected at the low temperature CO_2 liquid inside the receiver and for case B the heat is rejects to the high stage system. For both cases the saturated mixture becomes liquid again.

Another arrangement for the indirect/secondary CO_2 system is illustrate in Fig. 3.4. The system design is very similar to the previous one but the pressure control (by-pass) valve has been added on the system.

The pressure regulator valve prevent overfeed of the evaporator and also is act as a pressure controller in order the evaporator supply pressure to be constant all the time. In general words, the pressure controller regulator is another safety issue that must be take into account when design an indirect/secondary refrigeration system.

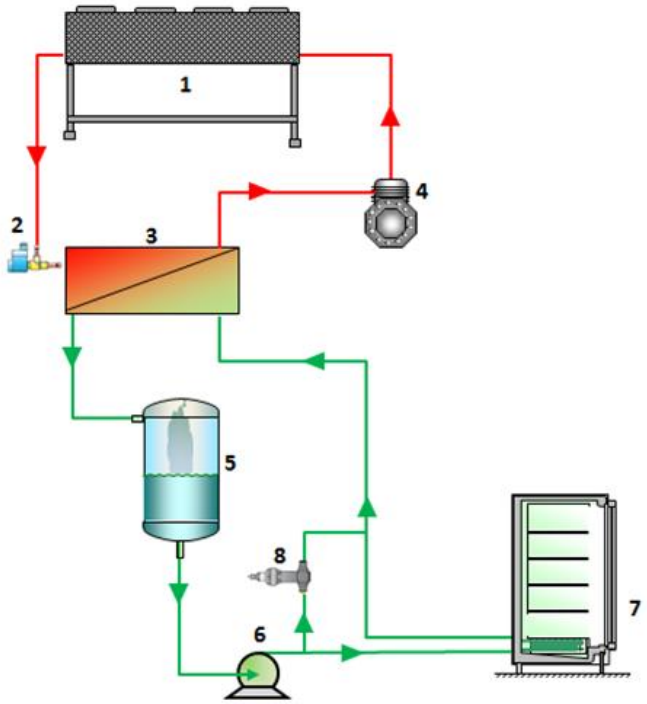

Figure 3.4 Indirect system arrangement

The simple indirect/secondary CO_2 arrangement systems use two parallel systems in order to supply the chilled and frozen food cases. This has a disadvantage the refrigerant charge and safety risk for the high stage system. In case of ammonia or hydrocarbon used for the high system side the risk of fire and toxicity is really high.

In Figure 3.5 the indirect/secondary CO_2 arrangement supply both MT and LT cases with only one high stage circuit. The system employs an MT flooded evaporator and LT DX cascade low system. Therefore, for this arrangement a pumped secondary system coupled with cascade system.

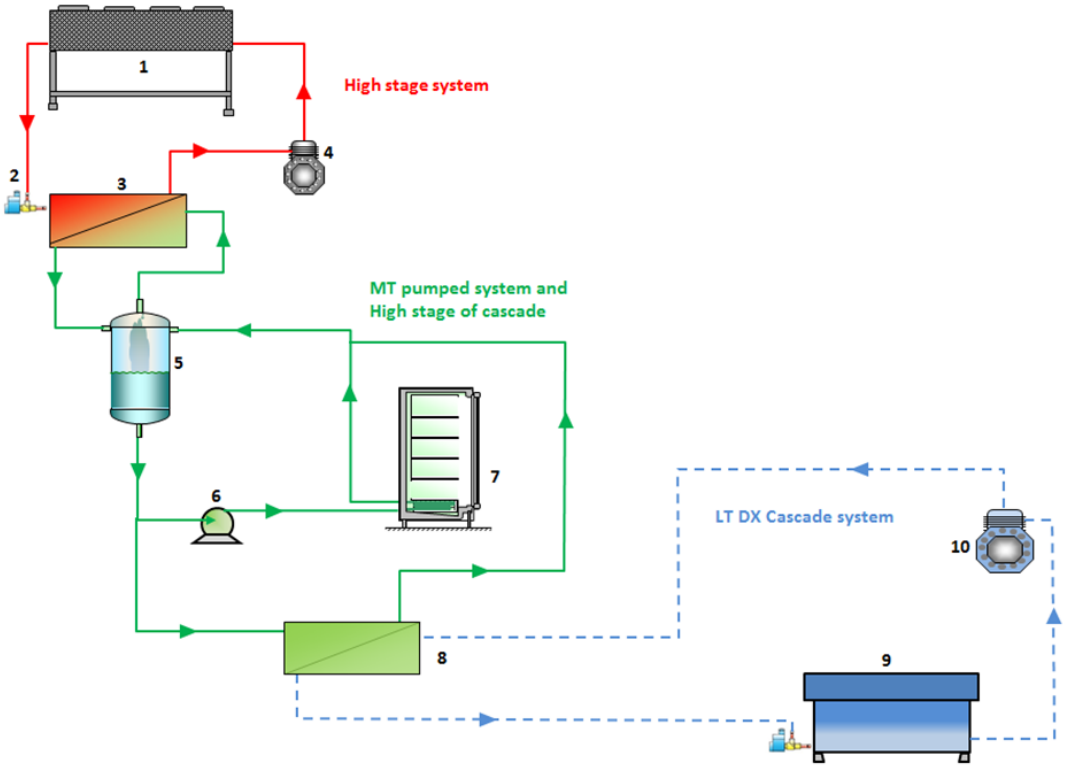

Figure 3.5 MT / LT indirect system

The high stage system cools and condenses the evaporated pumped CO_2 on the high stage heat exchanger. The primary system for application like this uses either and HFC or HC refrigerant.

The pumped CO_2 flows and cools the MT load. For this arrangement it is also cooling the medium in the cascade condenser. The LT DX load is cooled by the low stage of the cascade system. Both pumped and LT DX cascade system uses CO_2 as a refrigerant.

The CO_2 gas from the outlet of the evaporator is return to the cascade heat exchanger to close the circle. The disadvantage of this system is the complex design and the number of the different components in order to couple both systems. The main components for those two typical retail secondary systems are shown in Table 3.3.

Table 3.3 MT / LT indirect system components

Ref.	Component	Description
1	Condenser	Typically air-cooled/multi-fan type or convectional chiller
2	Expansion	Electronic expansion valve
3	Heat exchanger	Typically plate heat exchanger
4	High stage compressor	HFC or HC typical compressor
5	Receiver	Standard receiver (not for high pressure)
6	Liquid pump	Centrifugal pump are usually used
7	Evaporator	Standard evaporator is used (not for high pressure)
8	Cascade heat exchanger	Typically plate heat exchanger cab be used
9	LT Evaporator	DX standard evaporator is used (low pressure)
10	Compressor	Suitable for low temperature CO_2 applications

3.3.1. INDIRECT/SECONDARY SYSTEMS DISCUSSION

The indirect/secondary arrangements are relatively simple systems to implement and can be applied in number of different arrangements depending on the application. The great reduced pumping and pipework cost against the glycol systems are made the CO_2 indirect systems as the most cost effective solution (Pearson, 2014).

The Table 3.4 illustrates the estimation of the power consumption made by pumps for 500 kW load for different secondary fluids.

Table 3.4 Estimation of power consumption by pumps with different working fluids

Secondary Fluid	**Power (kW)**	
	-10°C	**-20°C**
CO_2	0.97	0.85
Ethylene Glycol	15.87	18.8
Propylene Glycol	14.03	16.63

In additional, the comparison of pipe diameters based on CO_2 and glycol application is illustrate in Figure 3.6 (Mikhailov, 2011).

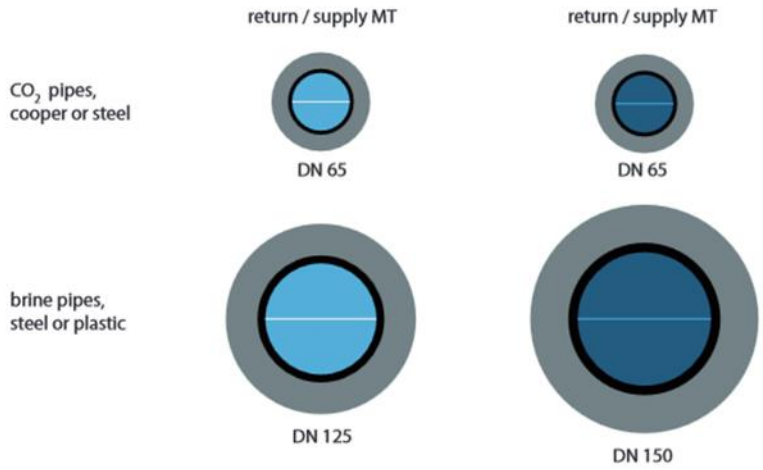

Figure 3.6 Pipe diameters for CO_2 and glycol applications

(Adapted: Shecco, 2013)

Further, Rogstam et al. (2010) reported that by using CO_2 as a secondary refrigerant is possible to achieve 90% energy reduction compared with the fixed speed brine pumps and 50% redaction compared to brine pump with integrated variable speed controller. The lifetime cost comparison between glycol and CO_2 systems are shown in Fig. 3.7.

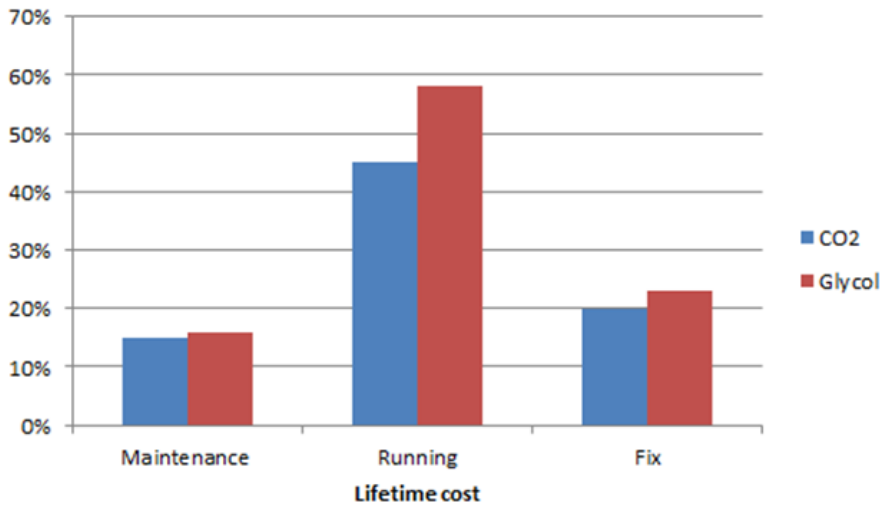

Figure 3.7 Lifetime cost comparison between glycol and CO_2 systems

(Source: Mikhailov, 2011)

3.4.SUBCRITICAL CASCADE DESIGNS

The CO_2 cascade arrangement has been applied in supermarket applications over the last two decades and is becoming a really promising alternative especially for warm climates. The great advantage of the cascade configuration is that the CO_2 system running in a subcritical mode in the whole year around without affecting from the ambient conditions. This system are divided in two sections the high stage and low temperature stage. The high stage is usually an HFC refrigerant such as R404A or R134A, or NH_3, or an HC such as R1270 (propene, propylene) or R290 (propane). The operation of the high stage of the system is controlled by the pressure in the CO_2 receiver. Both systems are exchange heat on the cascade condenser which acts as an evaporator for the high stage and as a condenser for the low CO_2 stage. This arrangement can feed both MT and LT cabinets. Based on that, the refrigerant charge on the high stage circuit can be significantly reduced as a proportional to minimize the impact to the environment when HFC is used. In case the high stage of the system uses HC or NH_3, the circuit can be located in the secured distance machine room away from the sales area. A typical subcritical cascade system applied in supermarket is shown in Fig. 3.8.

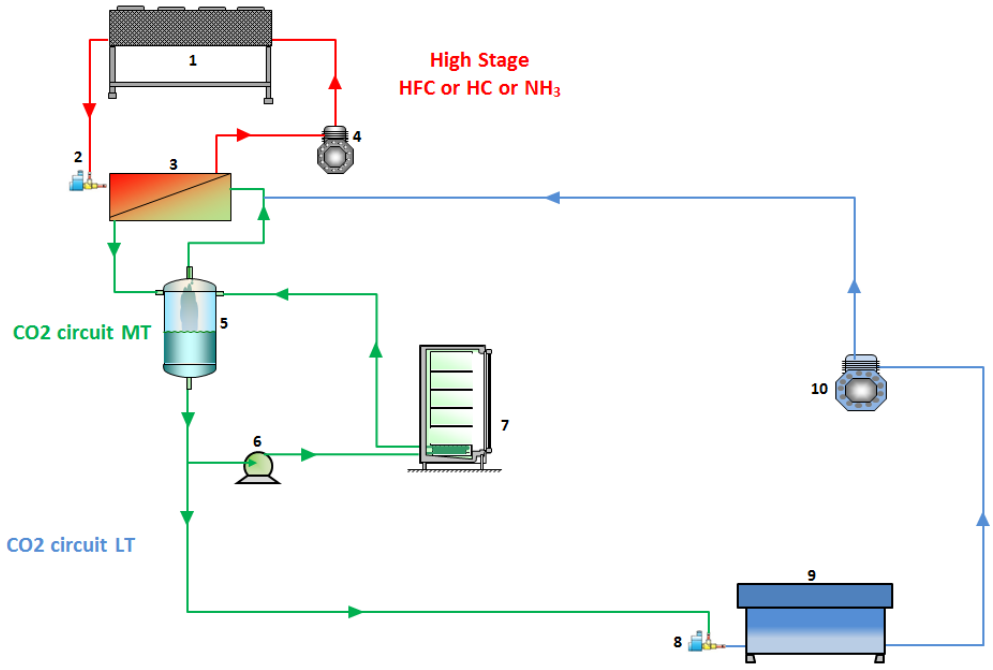

Figure 3.8 Typical subcritical cascade system arrangment

As mentioned before, within the cascade systems, the evaporating high-stage refrigerant absorbs the heat rejected by the condensing CO_2. The condensing temperature of the CO_2 must be maintained to be lower than the critical point. The main components for the cascade system in Figure are described in Table 3.5 below.

Table 3.5 Cascade system components

Ref.	Component	Description
1	Condenser	Convectional chiller can be used
2	Expansion	Electronic expansion valve
3	Heat exchanger	Cascade heat exchanger
4	High stage compressor	HFC or HC typical compressor
5	Receiver	CO_2 receiver – Design only for subcritical operation
6	Liquid pump	Centrifugal pump are usually used
7	Evaporator	MT Standard evaporator is used (not for high pressure)
8	AKV	Electronic expansion device for CO_2 applications
9	Evaporator	Low temperature evaporator
10	Compressor	Low temperature compressor suitable for CO_2

In this arrangement the CO_2 receiver collect the liquid after the condensation on the cascade heat exchanger. The CO_2 flows through the pump to the MT flooded evaporator and the expansion device at the DX LT evaporator. At the outlet of the DX LT evaporator the CO_2 gas entry to the suction line of the LT compressor. The discharge gas from the low-stage compressor is mixing with the saturated vapour from the receiver before entry to the cascade heat exchanger. At the mixing point, the CO_2 will become de-superheated before entry to the cascade condenser where further de-superheating will happened before the condensation process. This cascade arrangement is well known as hot gas de-superheating arrangement (Sawalha, 2008).

Another possible solution for CO_2 cascade systems is shown in Figure 3.9. For this arrangement the high stage of the cascade system provides the cooling for the MT load. Except the cooling load for the chill food, the high stage refrigerant flows through the cascade condenser where removes the heat from the condensing CO_2 at the low stage of

the system. The low-stage CO_2 then delivers the LT DX cabinets. This CO_2 cascade arrangement is well known as hybrid system (Emerson, 2015).

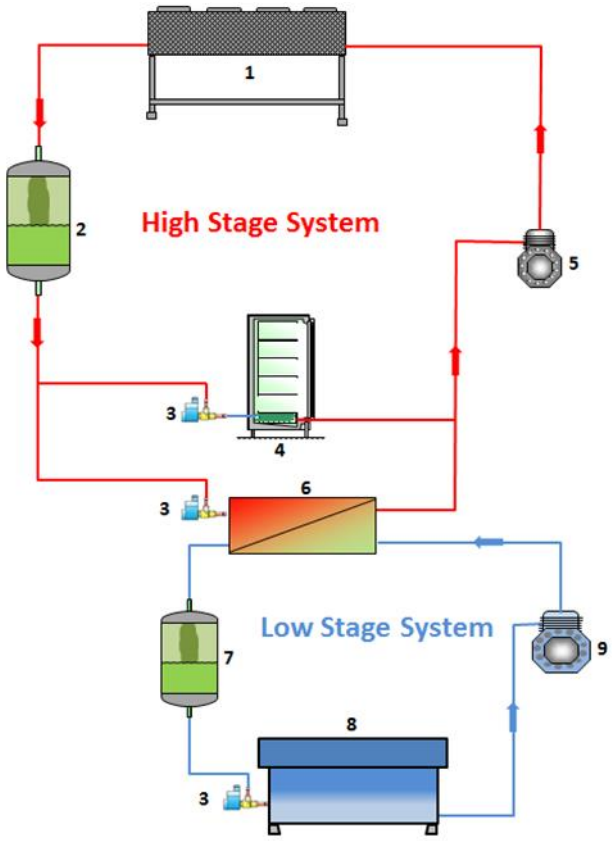

Figure 3.9 LT/MT cascade system arrangement

The main components of the cascade system are listed in Table 1.6. In the simplified diagram in Fig. 3.9, smaller components such as oil separator, filter driers, pressure regulators are not represented.

Table 3.6 LT / MT cascade system components

Ref.	Component	Description
1	Condenser	Air-cooled / multi-fan
2	Receiver	High stage refrigerant receiver
3	Expansion devices	Electronic expansion valve
4	Evaporator	Typical HFC or HC evaporator
5	Compressor	HFC or HC standard compressor
6	Cascade heat exchanger	Plate heat exchanger
7	Receiver	CO_2 receiver – Design for sub. operation
8	Evaporator	Low temperature evaporator
9	Compressor	Low temperature compressor suitable for CO_2

The diagram in Fig. 3.10 is a simplified cascade system similar with Figure 3.9. The difference with this system is that the saturated vapour from the receiver is mixing with discharge gas from the low-stage compressor and enters to the cascade heat exchanger with passing from the receiver. This is more simplified circuit compared with the initial system, based on the pipework arrangement and control strategy. However, the main components of the system are the same and illustrated in Table 3.6.

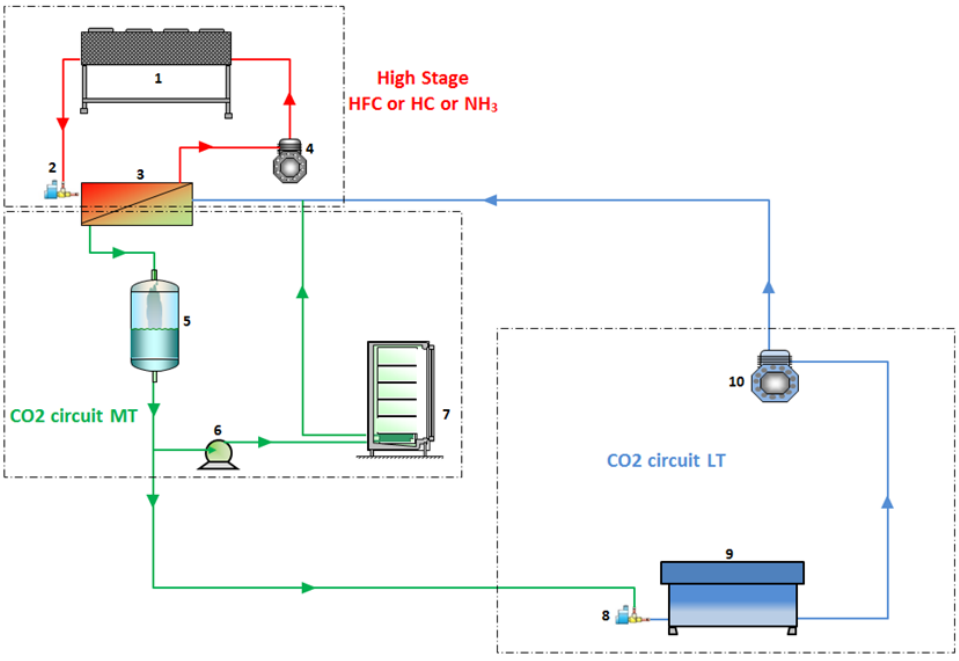

Figure 3.10 Cascade with saturated vapour mixture

3.4.1. CASCADE SYSTEMS DISCUSSION

The use of CO_2 as secondary refrigerant in a cascade supermarket solution allows the reduction of primary HFC refrigerant by 75%. In additional, the use of cascade system in industrial applications allows the reduction of ammonia charge by 90% compared to system which uses ammonia as an only refrigerant fluid and minimizes the safety risk in such a systems (ASHRAE, 2010).

In more technical aspects for the typical retail subcritical systems, the operation temperature in the most of the pipe line for the CO_2 circuit is below -5°C; therefore the pipework must be insulated to avoid the heat gain into refrigerant. In the most of the cases, only the pipe line after the LT compressor discharge is not insulated where the temperature is much higher. The liquid line temperature is much higher than the ambient condition for moderate climates, so there is no subcooling at the CO_2 flows along the liquid line. The cooling capacity of the LT DX evaporator is reduced due to the saturated liquid at the inlet of expansion device. Based on that approach, the AKV valve is sized to be 30% greater than the standard due to lack of subcooling (Emerson, 2015).

In the retail applications, the heat exchanger is located above the CO_2 liquid receiver to ensure there is no back flow. For the cascade applications, is more common the used of plate or shell-and-tube heat exchanger which operates as condenser for low stage CO_2 and as evaporator for the high stage of the system. The temperature difference across the heat exchanger depends on the effectiveness of the cascade condenser. As this temperature difference increases the overall system efficiency decreases caused the cooling capacity of the system and affecting on the product temperatures. Based on that, the cascade heat exchanger must be insulated to prevent the losses to the warmer ambient. For the cascade systems with high degree of superheat, a de-superheater need to installed in order to reduce the load on the high temperature side of the circuit (Danfoss, 2010). Therefore, the de-superheater must be placed between the discharge line of the LT compressor and suction line of the low cascade stage. In general, the control strategies for the cascade systems are divided into five main levels: the compressor capacity control, condenser capacity and cascade injection control for the high stage of the system and the MT evaporator mass flow control strategy and LT evaporator expansion regulator for the low CO_2 circuit.

The number of cascade installation using CO_2 as a MT and LT refrigerant has been increased since 2001. The first installations of cascade systems from 2001 to 2005 were used an HFC or hydrocarbon on the high stage (Funder-Kristensen et al., 2012). The phase-out of some of the HFC fluids used force the researchers and companies to explore new substances for the high stage side of the system. However, there as yet not been consensus on which refrigerant to use on the high side of the system in order to condensate the CO_2 on the low side. Ming et al., (2014) presented the use of falling film evaporator-condenser as the cascade heat exchanger for a NH_3/CO_2 refrigeration system. The results shows lower temperature difference across the proposed cascade heat exchanger which drives the system to higher COP values compared with the system where the plate, shell-and-plate or shell-and-tube heat exchangers are used. Rezayan and Behbahaninia (2011) investigated the thermoeconomic optimization for CO_2/NH_3 cascade refrigeration cycle. The authors proposed method included the thermal and economical aspects of the system design and operation. Based on the proposed design and operation of the system and for constant cooling capacity of 40 kW the annual cost reduction of the system is equal to 9.34% compared with the base case design. Messineo (2012) compered the R744-R717 cascade system with a R404A two-stage system based on the similar operating conditions. The author reported the effect of the overall COP for different condensing temperatures, degrees of subcooling and evaporating temperatures. Sanz-Kock et al., (2014) evaluated experimentally a $R134A/CO_2$ cascade refrigeration system. It is reported that the cooling capacity of the system is negatively linear dependent with the condensing temperature of the low stage cycle of the cascade system. Also, the use of the gas cooler on the low cycle in order to reject an amount of the heat before the refrigerant flows to cascade heat exchanger increased the overall COP of the system.

The experimental analysis of a CO_2/Ammonia cascade system for supermarket refrigeration applications has been presented from Sawalha, (2008). The CO_2 refrigerant used to cool-down the LT and MT where a DX and flooded coil used respectively. Sawalha concluded that the COPs for the CO_2/Ammonia cascade solution were 50 to 60% higher than that of a direct R404A system installed in the same laboratory environment.

The energy efficiency comparison for a convectional R404A system, R22 system and a subcritical CO_2 cascaded has been reported (Silva et al., 2010).The comparison based

on the given cooling capacities of the system were 20 kW of MT and 10 kW for LT used. The initial cost of the CO_2 cascade system was 18.5% higher comparing with the other two solutions. The high side of the cascade system were charged with 15 kg of R404A. On the other hand, the conventional R404A system had a charge of 125 kg of refrigerant. The author reported that the CO_2/R404A cascade refrigeration system can provide great performance and be a more environmental friendly solution comparing with the other two systems. The size of the three compared system are shown in Fig. 3.11.

Figure 3.11 R22, R404A and CO_2/R404A refrigeration systems trailed by BITZER for supermarket application

(Silva et al, 2010)

3.5.ALL CO_2/TRANSCRITICAL DESIGNS

After the first installations of cascade systems were the CO_2 operates as a low stage refrigerant, the real breakthroughs for the new all-CO_2 systems began around 2005. The use of CO_2 as the only refrigerant for small, medium and large supermarket applications has been introduced in transcritical booster systems. By using CO_2 as the only refrigerant minimises the environmental impact from the refrigerant leakage when HFC

is used and the system is safer comparing with the cascade systems where NH_3 and HC used for the high stage of the system.

Another important advantage of the all-CO_2 systems comparing with the cascade installations is the absence of the cascade heat exchanger and the temperature different issues between the two refrigerants. However, when the ambient is above 27 °C, then the system will operate over the critical point and transcritical mode is enforced. For the transcritical operation the heat exchanger will act as a gas cooler where the operating pressure becomes independent of the gas cooler outlet temperature. The high operating pressure in the gas cooler can lead to high power consumption of the system and loss on the overall COP. Therefore, the control strategies for the individual pressure stages for the transcritical operation need to be regulated in order to achieve best performance of the system. The important consequence of controlling the high pressure side of the system has to do with the pressure inlet at the throttling valve and the specific refrigeration capacity provided for each given pressure exit (Kim, 2004). Therefore, the optimum value for each ambient temperature need to be obtain in order to keep the COP in the higher levels.

All-CO_2 systems are more suitable for cold climates conditions. Comparing the all-CO_2 systems with the HFCs installations, it found to be more energy efficient when the ambient temperature is lower than 22 °C, about equal when the temperature is between 22 to 26 °C and lower when the ambient temperature is higher than 26 °C and the system operate in transcritical mode (Finckh et el., 2011). For new installations or replaced systems from HFCs to CO_2 can reduce the carbon footprint of supermarkets by 25% (EPA, 2010).

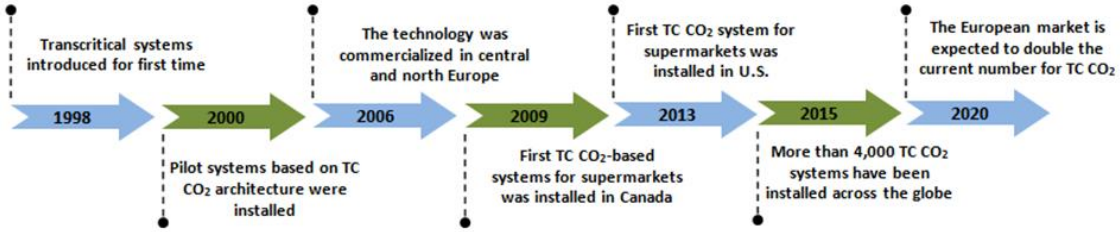

Figure 3.12 Transcritical systems market trend

(Adapted: MarketsandMarkets, 2015)

For moderate and warm climates the recovered heat from the refrigeration plant it is a really promising option. This recovered heat could be used for hot water heating or sanitary. An additional heat exchanger between the discharge compressor line and gas cooler inlet must be installed in order to recover the waste heat from the transcritical operation. The refrigerant enters to the heat exchanger at a very high temperature and exchange heat with the cold water entering from the other side. The refrigerant is de-superheated before flows to the gas coolers and potentially increased the overall system COP.

The recovered heat for supermarket applications can lead to 30% energy savings annually (Hafner and Neska, 2014).

3.5.1. ALL-CO_2 CYCLE

The diagram in Fig. 3.13 is a single stage transcritical supermarket system. The layout of the system is very similar with the common HFC arrangements. The CO_2 system consists by the gas cooler/condenser, the expansion valve, the evaporator and the compressor.

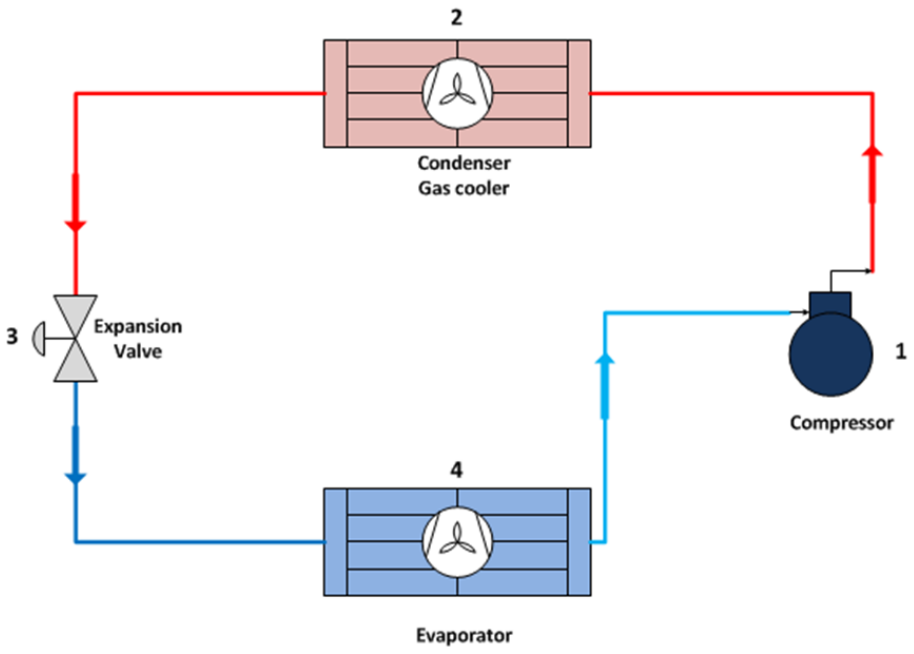

Figure 3.13 Single stage transcritical system

After the CO_2 refrigerant discharge from the compressor enters to condenser/gas cooler where the heat is removed from the colder air passing throw the heat exchanger. At temperatures above the critical point the refrigerant does not condensate and it's called

transcritical operation. In this operation the refrigerant pressure at the outlet of the gas cooler becomes independent of the refrigerant temperature and the temperature outlet depends on the approach temperature. On the other hand, the pressure associate with the control valve degree opening.

The refrigerant then flows through the expansion valve where the refrigerant change phase. When the pressure drop at this point the refrigerant condensate before enters to evaporator. The saturated refrigerant is superheated at the evaporator before enters to compressor and complete the cycle. The Pressure-Enthalpy (P-h) diagram for the transcritical and subcritical operation for varies conditions is illustrated in Fig 3.14.

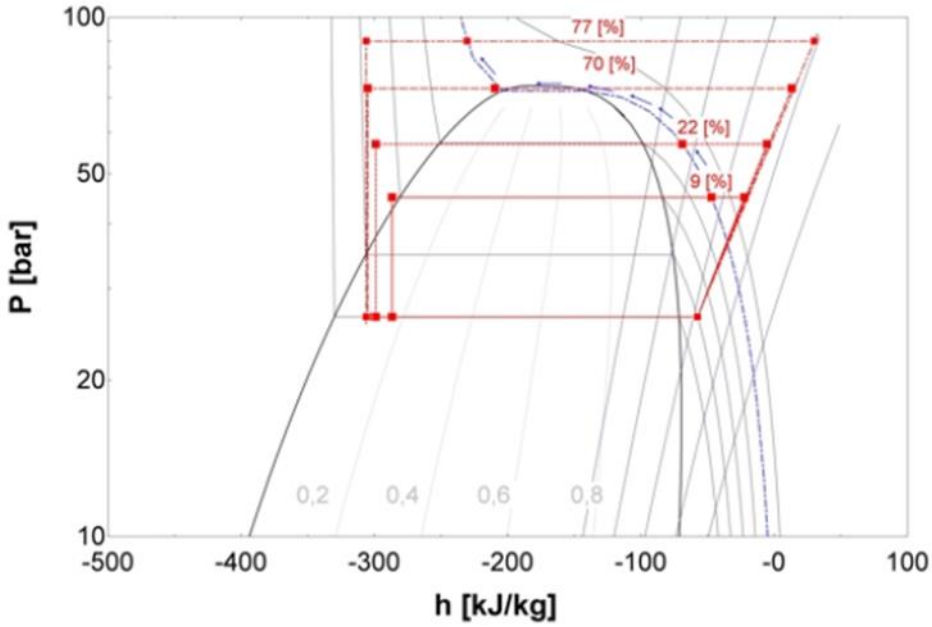

Figure 3.14 CO_2 subcritical and transcritical Ph diagram

(Source: Madsen, 2010)

It is very important to mention the temperature and pressure at the outlet of the gas cooler, the ambient temperature and the pressure drop at the expansion device of the system is very important for the overall performance of the system. The control strategies for the above parameters will be discussed in the next sub-chapter.

3.5.2. TRANCRITICAL RETAIL APPLICATION

All-CO_2 systems can operate in both subcritical and transcritical cycles depending on the ambient temperature. Those systems can feed both LT and MT evaporators. The MT cabinet is a flooded or DX evaporator depending on the system arrangement (Bansal, 2012).

The main advantages of this arrangement comparing with the existing HFCs systems are the smaller direct global impacts, the refrigerant price and availability and the safety classification. Comparing with the other natural refrigerants such as HC and ammonia, the CO_2 is non-flammable and non-toxic. Moreover, the CO_2 application can be varied from a small cooling unit such as vending machine to a large supermarket arrangement by suppling both LT and MT. The first all-CO_2 supermarket refrigeration system was installed in Italy in 2005 (Better Buildings, 2015). The lack of the retailers awareness about this new technology has been slows the uptake of this new alternative refrigerant solution.

The high operating pressure, the unavailability for the components such as compressor and valves, the method to maintain the system and the lower performance for the higher ambient temperature applications are some of the barriers.

After the first installation in 2005, nearly 1500 supermarkets in Europe have successfully installed and operate this system architecture. In the next sub-chapter the transcritical installations across the Europe and the rest of the world will be discussed.

Fig 3.15 is represents a simplified typical transcritical system which is really common in retail applications. The system consists from the condenser/gas cooler, the ICMT motorized valve which act as an expansion valve, the liquid receiver the ICM or CCM gas bypass valve and the DX evaporator.

This configuration is very similar with the system has been experimentally investigated which is present in Chapter 5.

The transcritical CO_2 booster in Fig. 3.15 comprised of three pressure sections: high, intermediate and medium. The high pressure section begins at the discharge line of the compressor, follows through the gas cooler/condenser and finally at the inlet of the ICMT valve. At the outlet of the ICMT valve the intermediate pressure section starts, where the CO_2 exits as a two phase and flows into the liquid receiver.

At the outlet of the liquid receiver the intermediate pressure section continues, where the saturated vapour CO_2 flows back through the ICM bypass valve and the liquid phase to the AKV expansion valves and then to MT cabinet.

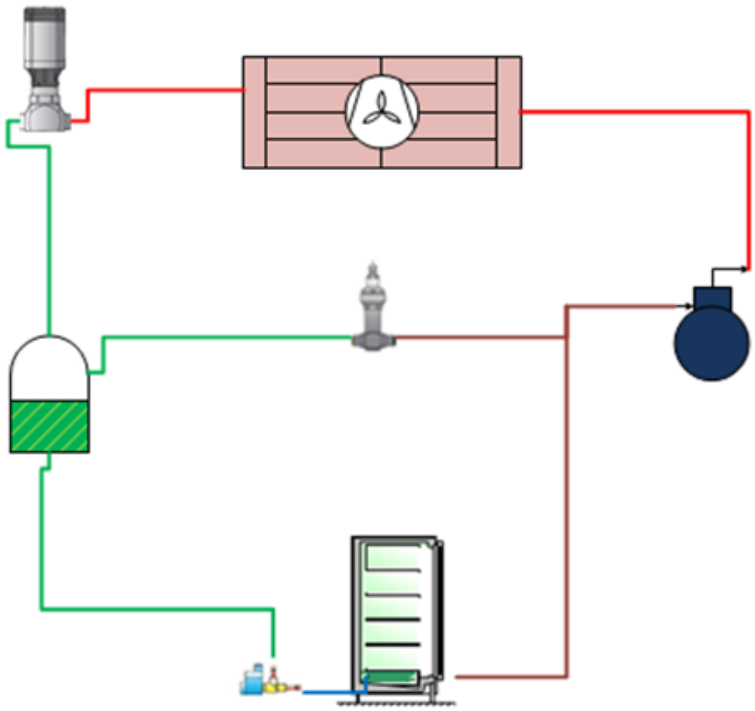

Figure 3.15 MT or LT Transcritical arrangement

After the expansion valve the medium pressure section begins. The refrigerant coming out from the MT cabinet is mixed with the saturated vapour from the CCM bypass valve before entry to accumulator and then to compressor where the cycle is complete.

The thermodynamic analysis of a similar CO_2 system has been done by Ge and Tassou (2009, 2011), where the control optimisation and the optimal high side pressure has been established.

3.5.3. CONTROL STRATEGIES

The control strategies for the transcritical applications can be divided into four groups based on the different side of the system; the evaporator control, gas cooler/condenser control, compressor capacity and the receiver pressure control which involved also the amount of the liquid on the receiver and the bypass gas to the compressor. This system also is known as a booster system.

In general, the control strategy of the CO_2 system involves three main control valves which are integrated with individual electronic controllers. Moreover, the signal from those transferred to the main controller gives us the opportunity to monitor and record

the system under different conditions. The main control valves and each corresponding electronic controller are shown in Table 3.7.

Table 3.7 Control valves for TC system

Position	Valve	(PID) Controller
High pressure side	ICMT	EKC 347
Intermediate side	CCM	EKC 326A
MT cabinet	AKV	AK-CC550A

The high pressure ICMT valve controls the high pressure side of the system in order to achieve an optimum high pressure when the system operates in transcritical mode. It also acts as an expansion valve/device to reduce the high pressure to an intermediate pressure stage before reaching the liquid receiver.

A pressure transmitter and temperature sensor have been installed at the outlet of the gas cooler/condenser (Danfoss, 2012). When the system operates in transcritical mode at particular ambient conditions, the electronic controller receives the signal from those sensors and sends a signal back to motorize the valve to open or close to achieve the optimal COP.

The size calculation of the ICMT valve is a relatively complex process as the refrigerant mass flow changes when the system moves from subcritical to transcritical conditions. The most appropriate way to accurately size the ICMT valve is to calculate it as an expansion valve and take into account the temperatures at the gas cooler/condenser outlet and inside the intermediate vessel as well as the degree of subcooling for condenser only (Danfoss, 2010b).

For the transcritical operation the pressure outlet from the gas cooler becomes independent of the temperature outlet. The next chapters will described the difference of the temperature drop across the coil and the nearly isobaric process on the high side of the system. The different operating pressures with respect of gas cooler exit temperatures are showing in Fig. 3.16. The graph also represents the optimum operating pressures regarding to the gas cooler exit temperature.

The ICM or CCM motorized valve is also referred to as a gas bypass valve with a PID controller, which keeps the pressure in the liquid receiver down to a level determined by the system user. After the ICMT valve, the flow enters into the receiver and is divided into gas and liquid flow.

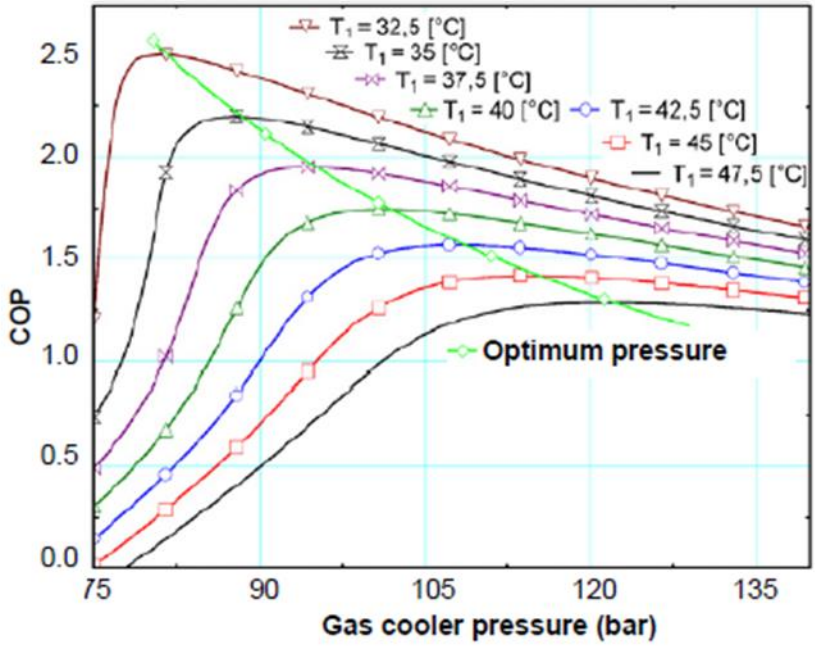

Figure 3.16 Optimum operating pressures

(Source: Sawalha, 2008)

The CCM valve has been installed on top of the liquid receiver, thereby bypassing the gas phase and mixing with the refrigerant outlet from the evaporator before flowing to the accumulator and then the compressor suction line. Moreover, the bypass valve ensures that the evaporator is feeding only the liquid phase, which gives us the opportunity to use a higher-grade copper pipe instead of the steel used in the rest of the system.

The electrically operated expansion valve, AKV, is usually installed before the DX MT evaporator. The AKV is integrated with the AK-CC 550A case controller supplied by Danfoss. The superheat degree control of CO_2 evaporators is more complex procedure comparing with the HFC evaporators.

3.5.4. TRANSCRITICAL INSTALLATION IN RETAIL STORES

The simplified drawing in Fig. 3.17 shows a transcritical CO_2 system serve both LT and MT evaporators. The main components of a transcritical booster system are listed in the Table 3.8. Both MT and LT evaporators are using a direct expansion solution. The oil management is not showing in this drawing and will be discussed in Chapter 5.

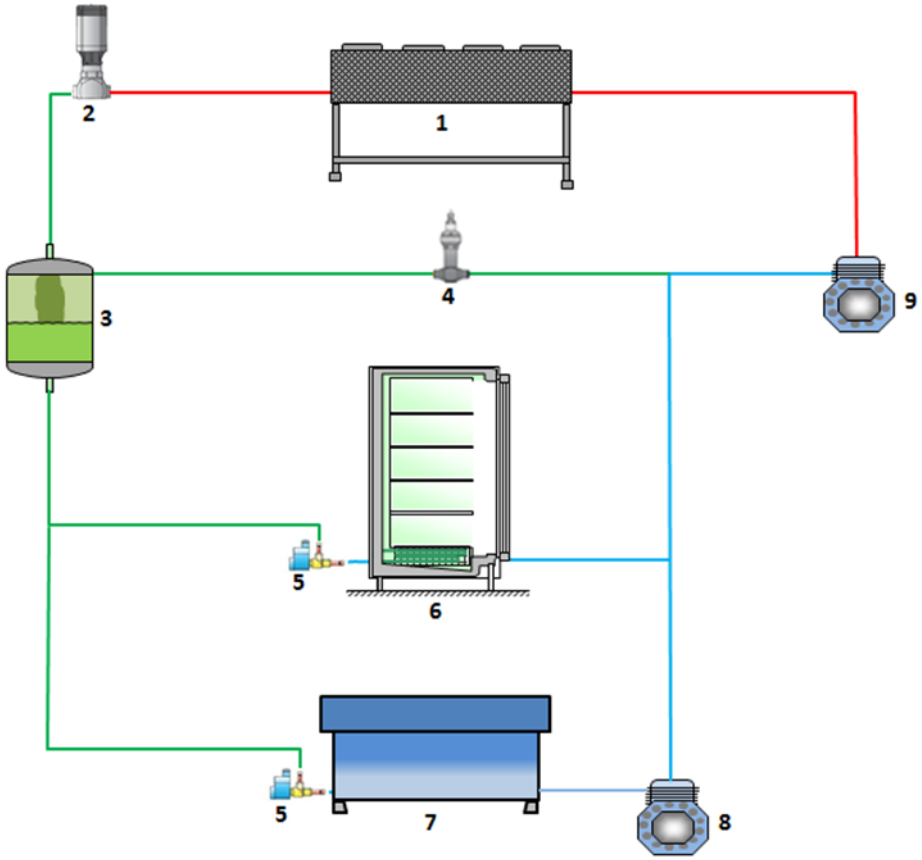

Figure 3.17 Both MT and LT transcritical booster system

The MT/LT transcritical system is divided into four pressure levels; high, intermediate, medium and low. The high pressure level it incorporates the discharge line of the HT compressor, the gas cooler/condenser and the inlet line of the ICMT valve. Normally this section is operating between 60 to 90 bar depending on the ambient conditions.

The intermediate pressure is between 30 to 60 bar depending on the application and the MT evaporator control. In case of a flooded evaporator is used for the MT application, a high pressure can be used on the intermediate side.

Table 3.8 Booster system components

Ref.	Component	Description
1	Condenser/Gas cooler	Air-cooled / multi-fan to stand with high pressures
2	ICMT	Control the high side of the system
3	Receiver	Liquid Tank/Separator
4	CCM or ICM	Control the intermediate pressure
5	AKV	Electronic expansion valve
6	MT cabinet	Standard medium temperature evaporator
7	LT cabinet	Standard low temperature evaporator
8	LT compressor	Low temperature compressor
9	HT compressor	High temperature compressor

At the outlet of the motorized ICMT valve the intermediate pressure section begins and includes the liquid receiver, the CCM bypass valve, and the suction of the HT compressor and the inlet line of both AKV expansion valves. The medium pressure level incorporates the MT evaporator and the normal operation pressure range is between 25 to 30 bar. The corresponding temperatures for the saturated CO_2 enter to evaporator for the given pressure varies from -10 to -5 °C.

The low pressure section is on the pressure range from 11 to 14 bar with corresponding temperatures of -35 to -29° C. The low pressure side includes the LT evaporator and the suction line of the LT compressor. The refrigerant outlet from the LT evaporator mixed with the outlet from the MT evaporator and the gas bypass from the liquid receiver before enters to the suction line and start the cycle again.

The liquid receiver has been designed for two main reasons. For the first one, the receiver is operate as a storage capacity when the components of the system must be serviced or the system must be shut down due to the tests having complete or maintenance purposes. For maintenance purposes, in each inlet and outlet pipe of the

receiver a high standard ball valve has been installed to separate the receiver from the main system. An addition standalone system connected with a separated condensing unit need to be install in order to keep the pressure at the lower levels in case of power failure or standstill operation. The standalone condensing unit must be connected with a coil which has been placed at the bottom of the liquid receiver. The second purpose for the liquid receiver is to act as a separator, where the liquid CO_2 flowing to evaporator and the gas return to compressor suction line through the CCM by-pass valve.

The intermediate pressure must be designed based on the requirement pressure on the shop floor of the supermarket and the requirement maximum allowable pressure of the pipe joints and pipe work which must be above the pressure equivalent to the higher ambient if the CO_2 system is at standstill operation. Moreover, the intermediate pressure is affect to the overall system COP. When the transcritical system use a DX solution for both MT and LT evaporators, the intermediate pressure does not influence on the medium and low pressure side of the system. Based on that fact, the power consumption of the LT and MT compressor are not changing for different intermediate pressures. On the other hand, the refrigeration effect of the LT and MT evaporators will increased for lower intermediate pressures. With lower intermediate pressure the refrigerant quality will diminish at the inlet of the receiver and the enthalpy values will be lower at the inlet of MT and AL evaporators. In such circumstances, the COP of the system will be increased. The effect of the intermediate pressure on the system COP will discussed in the next Chapters.

The control strategies for such as systems have been discussed in Chapter 3.5.3. The system in Fig. 3.17 is very similar with the system has been used for the experimental investigation and model validation in Chapter 5.

3.5.5. NOVELTIES – CASE STUDIES

The main advantages of the CO_2 transcritical system over the other available arrangements include the simpler design requirements, less installation cost and less environmental impacts from the refrigerant leakage comparing with cascade systems use a HFC's as a secondary fluid. The use of CO_2 as an only refrigerant on the system create a great opportunities to eliminate entirely the direct GHG emissions to the atmosphere and diminish potentially the indirect effects by optimising the system

designs and operations. Therefore, to increase the performance of the CO_2 transcritical systems is a challenge for the researchers. The use of the internal heat exchanger (IHX) has drawn lots of concern over the last decade (Ma et al., 2013). The IHX usually is placed after the gas cooler condenser. The system in Fig. 3.18 illustrates a parallel CO_2 arrangement with two separates DX circuits for both LT and MT display cabinets. Both systems using a multi-compressor pack and the number of the compressors based on the total capacity of the application. For the LT system two-stage compression is used. An intercooler is used between the two compressors in order to de-superheat the refrigerant before entering to the second compressor. The MT system uses single stage compression without an intercooler. When the additional IHX placed in this stage we ensure that the suction line of the compressor feted with superheated CO_2 vapour. A very similar parallel arrangement has been investigated by Girotto et al. (2003).

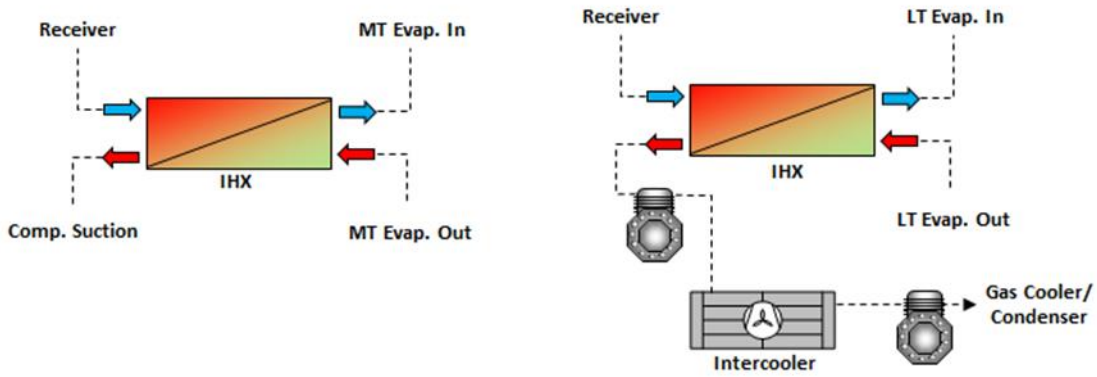

Figure 3.18 Booster system with IHX and intercooler

For the case of the LT system the use of two-stage compression with intercooling process in between can reduce the pressure ratio (Rp). By reducing the Rp the discharge temperature is becomes lower and results a better efficiency of the compressor. As it mention before, the intercooler de-superheats the vapour CO_2 before entering to second stage and keep the discharge temperature on the acceptable levels for these kind of compressors.

Another great potential of the transcritical CO_2 systems comparing with other refrigerants is the heat reclaim because of the higher discharge temperatures. Heat reclaim has been applied with other HFCs refrigerants such as R134A. Comparing these two refrigerants, the R134A will deliver 35 °C and on the other hand the CO_2 can supply a hot water of 55 °C (Sawalha, 2012).

The heat recovery process is usually taking a place after the HT compressor and before the gas cooler/condenser of the system where the vapour CO_2 temperature is extremely high. The Figure 3.19 illustrates the heat reclaim installation position for a typical CO_2 transcritical system. A plate heat exchanger is usually used in order to exchange the heat from the hot CO_2 vapour inlet to the cold water enters to the heat exchanger. This process is also act as a de-superheating for the gas cooler/condenser.

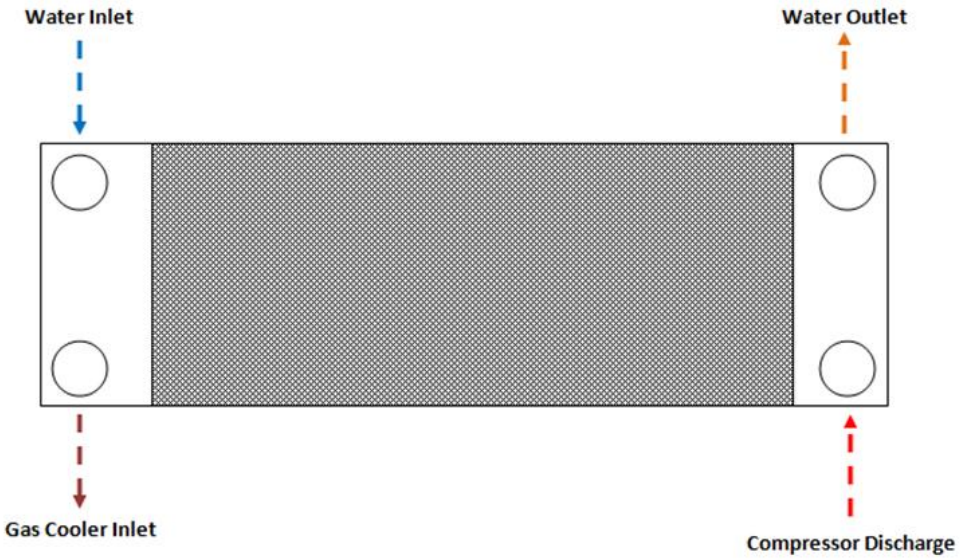

Figure 3.19 IHX for water heat reclaim

The heat reclaim is relatively new topic for the transcritical CO_2 installation. The great opportunity to save energy is evolving rapidly this heat reclaim technology for the new installations. This type of heat reclaim is commonly known as a series heat reclaim.

The hot water produced from this process can be used for heating during the winter months and reheat during active dehumidification in the summer months. Also, in some cases the hot water produced from the heat reclaim can be used for utilities inside the supermarket area.

- **The Danfoss solution**

Solution 1: Warm climate – Parallel Compression

One of the first solutions proposed by Danfoss is called a parallel compression. This solution is also known as an economizer or equal compression solution. The

arrangement of this transcritical system is very similar with the traditional CO_2 system which served both MT and LT load by using DX evaporators. It is more suitable for medium and large applications where the parallel compression technology is need it.

The difference with the traditional CO_2 transcritical systems is the use of an additional compressor on the intermediate pressure side of the system. Figure 3.20 illustrates the proposed system by Danfoss.

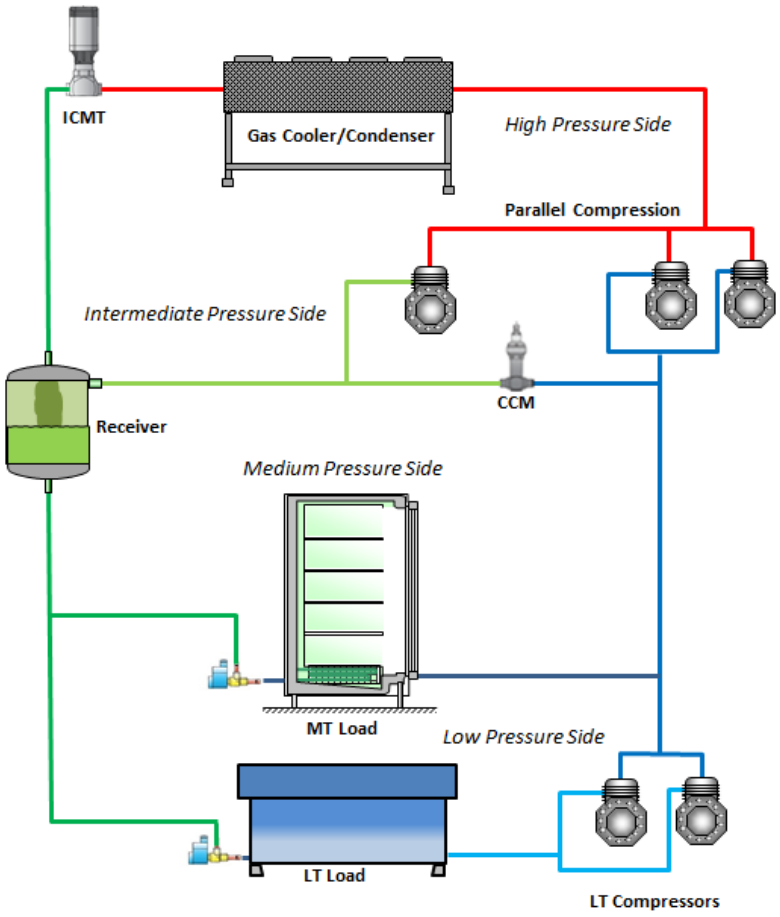

Figure 3.20 Booster system with bypass compressor

As Danfoss proposed, this is a very good solution for warm climates applications. An additional compressor is installed at the intermediate pressure section of the system and especially in the gas bypass side. With this technology will keep the receiver pressure on the designed levels for the warm days. For the cold months the system will switch automatically to use the CCM gas bypass valve. The energy improvement by using the

parallel compression technology found to be 5 to 10% based on the annual power consumption.

The intermediate pressure in such as systems is around 30 to 40 bar depending on the application. On the convectional transcritical systems the gas exit from the receiver is mixed with the lower pressure saturated gas from the LT and MT and then compressed to the gas cooler/condenser. Based on that, the power consumption of the compressor must be much higher in order to compress the low pressure level gas to higher pressure. By using the additional compressor in the intermediate pressure level, the gas pressure enters to this compressor is much higher comparing with the mixed of LT/MT. Therefore, the power consumption can be minimised. In this point we have to mention that for warm climates applications and especially during the warm months the gas bypass volume may be higher than 50% of the total CO_2 mixed enters to receiver. Also, the parallel compression solution will save an amount of the compressor install capacity because the density of the high pressure CO_2 gas is much greater. The function of the parallel compressor will be discussed and analysed in Chapter 8.

Solution 2: Warm climate – Sub-cooling

Another possible solution for the warm climates applications is to integrate the system by using a sub-cooler. The sub-cooler is installed at the outlet of the gas cooler/condenser and before the ICMTS or ICMT motorized valve. Figure 3.21 illustrates the implementation of sub-cooler on the transcritical CO_2 system.

As it mention before, for the warm days the gas bypass volume is higher than 50% of the total CO_2 volume circulate at the system. Therefore, a large amount of the CO_2 is return to the compressor through the CCM valve. By using the sub-cooler we can reduce a lot the refrigerant temperature entering to the ICMT and then change the percentage of the bypass gas to the compressor. With this solution we can save 5 to 10% of the compressor power consumption as reported from Danfoss.

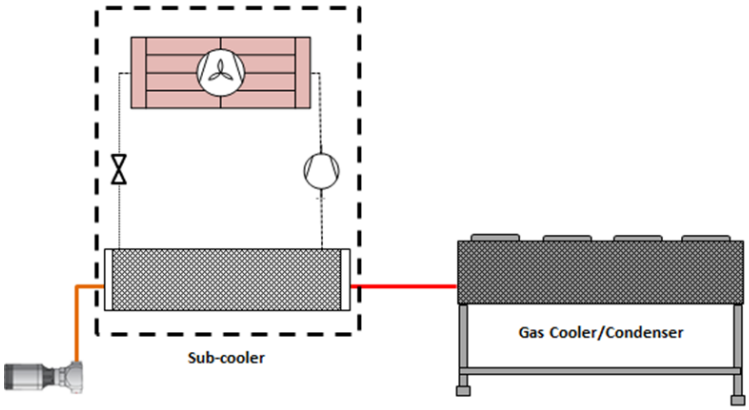

Figure 3.21 Sub-cooler solution in booster system

The sub-cooling process it can be combined with the AC system of the building for use of de-humidification during the summer months or heating during the colder periods.

This solution is applicable for small, medium and large applications. The disadvantage of this solution is the difficulty to implement with other features.

3.6.INSTALLATIONS REVIEW

The total equivalent warming impact (TEWI) for various aspects such as building, transportation/distribution and refrigeration are required to publish by the supermarkets every year. For the refrigeration plants the TEWI report includes both direct and indirect emissions as discussed before.

In the UK, food retail is responsible for approximately 40% of the indirect GHG emissions. Refrigeration technology, which is important in the processing, transportation and preservation of the food, is potentially responsible for the significant GHG emissions. Total GHG emissions from food chain refrigeration in UK are 13,720 kT CO_2, where the 35% are created from the direct emissions and 65% from indirect emissions. The split between direct and indirect emission in food retail sector shows that the direct emission are responsible for 3,000 kT CO_2 from the total of 6,530 kT CO_2. Moreover, the direct emissions from the food retail sector are responsible for the 63% of the total direct emission (SKM Enviros, 2011).

From the first CO_2 supermarket refrigeration installation there has been a rapid growth across the world. The previous sections described the different CO_2 arrangements and

novelties through the years for the supermarket applications. A number of documents published in details the number of systems installed across the world.

Recently MarketandMarket (2015) published a report on the transcritical CO_2 market for the time being and the global forecast until 2020. The report includes all the range of the applications for the CO_2 transcritical systems. Shecco (2014) reported the natural refrigerant market growth by type and application for the European market.

Figure 3.22 illustrates the number of the transcritical installations in Europe as reported. The geographical illustration shows the market growth from 2011 to 2013.The total number of installation back to 2011 was 1330 across the Europe. As it shown in the geographical representation the total installation of transcritical systems is 2885 for 2013. The enormous growth of the transcritical systems is due to the phasing down of the common refrigerants used for supermarket applications such as HFCs

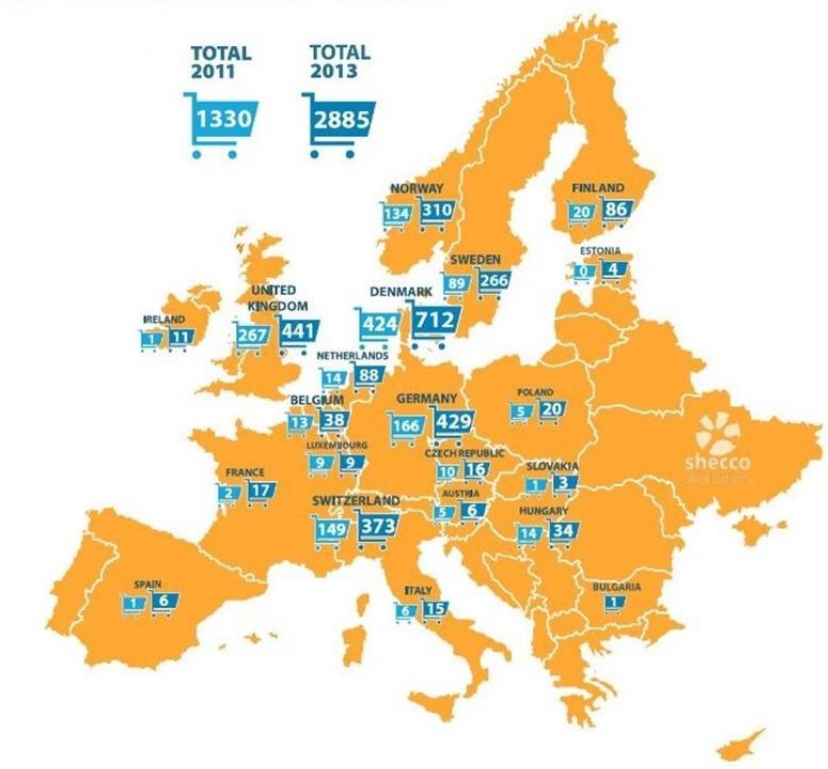

Figure 3.22 Transcritical installations in Europe

(Source: Shecco, 2014)

Another barrier was the low performance of the CO_2 transcritical systems and the safety issues of the high pressure side. The new installations of the CO_2 systems are considering the performance of the systems and implement different solutions in order

to increase the efficiency even for warmer climates. The new control equipment and components ensure the safe operation of the CO_2 in stores even for extremely high pressures. In additional, thanks to those new technologies the transcritical systems are being used in the smaller convenience stores. Another important parameter when we compare the geographical representation of 2013 with the one of 2011 is that the market expands to southern regions where the ambient temperature is much higher.

Denmark is the leader of the installations of CO_2 transcritical systems and this is expected to continue in the future. The low ambient temperatures is made the CO_2 solution a really promising alternative to switch from the old type HFCs. Moreover Denmark has introduced a new tax policy on the imports of bulk HFCs.

The number of the transcritical stores in the UK has been increased from 267 on 2011 to 441 in 2013 and bring UK second on this list. The first UK transcritical system was installed in 2006 in Swansea for Tesco. Since that time the transcritical system is gaining momentum even without the UK government force the retail companies with additional taxes in case the use high GWP refrigerants. On the other hand, the UK climate change legislation, which includes the 2001 Climate Change Levy (CCL) and the 2008 Climate Change Act (CCA) are strongly encourage the retail companies for new investments for more friendly systems and energy saving based on the refrigeration technology. The target of the CCA is to reduce the carbon emissions by 80% of the total emissions based on 1990 levels by 2050 (NAO, 2007 – CCA, 2008).

The retail companies including Tesco, Sainsbury's, Marks and Spencer and Waitrose have a target to phase down the old HFCs systems and switch to CO_2 transcritical installations.

At the beginning of 2013, Tesco have 65 stores running with transcritical CO_2 technology and planning to at least double this number by the end of this year (Shecco, 2014). Sainsbury's was operating 166 big stores and 1 convenient store as reported on April of 2013. Based on the published data by Sainsbury's, by using CO_2 transcritical systems the carbon footprint reduced by 33%.

The published report by Shecco (2014) shows the number of CO_2 cascade stores in Europe. The geographical illustration shown the cascade installations divided by type,

including CO_2/HFC, CO_2/NH_3 and CO_2/HC. Figure 3.23 shows the number of the cascade systems use a CO_2 as a low side refrigerant across the Europe.

As the Figure shows, 1638 stores using CO_2/HFC in Europe. Germany is leading on the cascade installations with 314 stores. In additional, 5 German stores use an HC for the high stage side of the system.

The cascade installations are more popular comparing with the transcritical systems at the southern part of Europe where the ambient temperature is relatively higher. In Italy 199 stores operates with cascade systems and only 15 use transcritical system. Also, countries such a Greece and Croatia are started to implement cascade systems for the supermarket application. For both countries the ambient temperature is higher comparing with the countries in north and the transcritical system is not a good option for the time being.

In UK, Marks & Spencer (M&S) use the cascade solution in 82 food halls. Morrison and Iceland run 5 stores with CO_2 in the low stage and HFC for the higher operation stage.

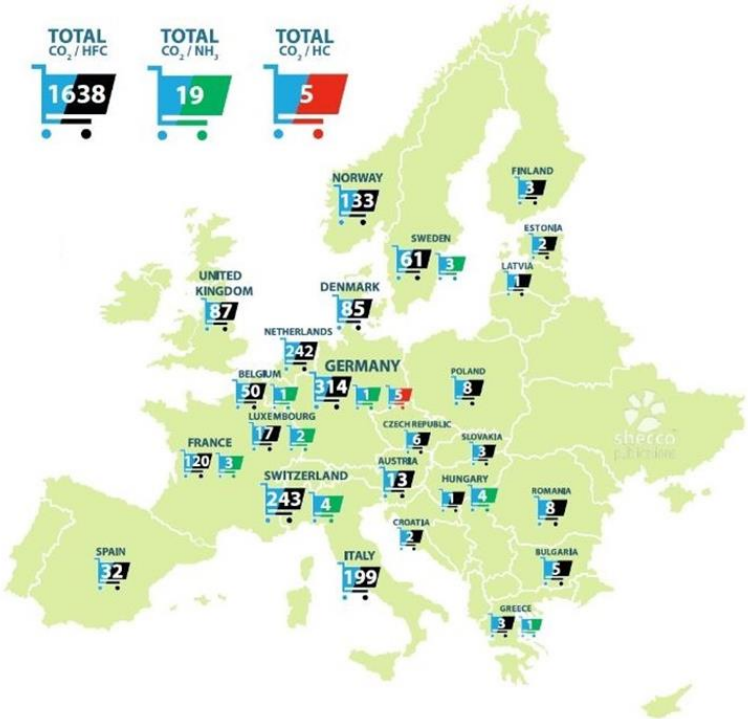

Figure 3.23 Number of the cascade systems use a CO_2 as a low side refrigerant across the Europe

(Source: Shecco, 2014)

As the Fig. 3.24 shows at the beginning of the CO_2 installations the cascade systems was more popular in supermarket market. The HFC phase down policy and the great potential of using CO_2 as the only refrigerant bring the transcritical systems in higher position after 2008.

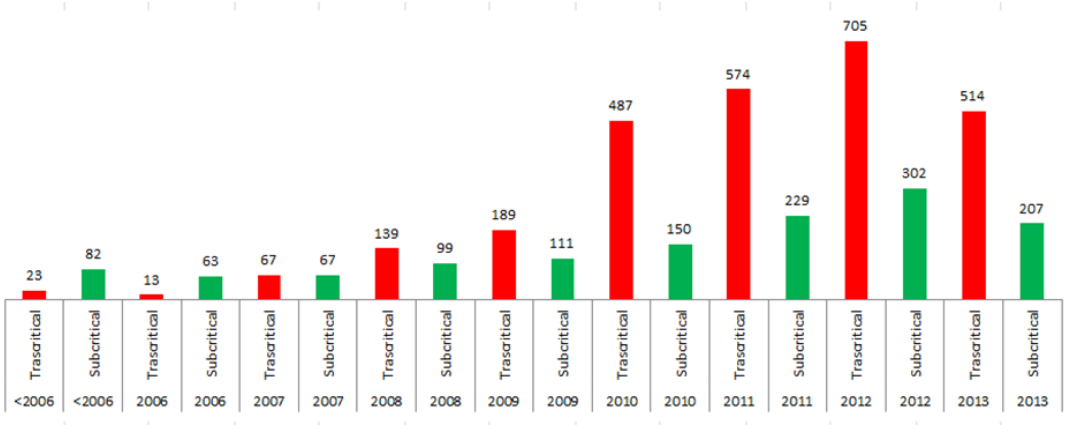

Figure 3.24 System installation over the last decade

(Data from: Shecco, 2014)

The Figure 3.24 illustrates the number of the installations per year for both transcritical and subcritical systems in Europe. The data for the 2013 includes the findings for the half year.

The Environmental Investigation Agency published reports based on the number of surveys sent to the retail companies in UK. The reports focused on the intentions of the main supermarket operators to move from the old style HFCs systems to natural and more environmental friendly refrigerants (EIA, 2014). As reported, Waitrose and M&S are using cascade systems where the CO_2 is operates in low stage side and for the high side both HC or HFC used (Arthur, 2011).

For the UK retail sector Tesco was leading at the CO_2 installation until 2010 (Walravens and Hailes, 2010). Two accidents inside stores have been discourage the Tesco engineers and placed them to a position to re-evaluate the system and components where used. Both explosions were due to pipe rupture on the CO_2 side (Milnes, 2011). Apart those two accidents in Tesco stores there is no any other accident has been reported.

The EFCTC (2013) published the accidents database happened from the refrigeration systems across the world from 2006 to 2013. As it shown in the report the largest

number of accidents happened for the systems used ammonia and hydrocarbon as refrigerants. For the CO_2 systems only the two blasts are reported and a number of small leaks without any crucial damage.

The CO_2 installations around the world are shown in Fig. 3.25. The total number of CO_2 installation is reported to be 5100 and the 3080 of these are transcritical for the 2013.

Figure 3.25 CO_2 systems installation over the world

(Source: Shecco, 2014)

3.7. SUMMARY

In the application of CO_2 as a refrigerant to food retail refrigeration systems, a number of different design approaches can be adopted that fall into three major categories: indirect/secondary, subcritical cascade systems and all-CO_2 system. The indirect/secondary was first applied due to the attractive thermos-physical properties of the CO_2 as a secondary refrigerant comparing with the propylene glycol which commonly used. On the existing systems the CO_2 replaced the fluid only in the shop area while the existing system can still operate.

In a cascade layout, the system constitutes of two single stage sub-systems, integrated by a cascade heat exchanger. The CO_2 is applied in the low cascade side while a working fluid such as HFC, NH_3 or HC is operated in the high cascade side. With this arrangement the CO_2 will be subcritical all the year around even if the ambient temperatures are high. As it mention in the previous sub-chapters the cascade solution is really promising for applications where the ambient temperatures are warm enough.

In an all CO_2 or transcritical system, a booster configuration is commonly employed where CO_2 is the only refrigerant charged. The main advantages of the CO_2 booster system over other ones include the simpler design requirements and less installation cost. However, the CO_2 working fluid has a quite low critical temperature of 31.1°C and very high critical pressure of 73.8 bar. Consequently, the CO_2 operates in relatively high pressure comparing with other refrigerants. In case the ambient temperature is higher than the critical temperature, the CO_2 is not condensate in the high pressure-side of the system. The high pressure-side CO_2 heat exchanger in the system can thus act as either a condenser or gas cooler depending on the ambient conditions. In such a circumstance, the CO_2 gas cooler/condenser must be well designed and controlled to match the cooling capacity requirement of the system at the least cost and in the meantime improve the system performance.

The three main solutions of the CO_2 as a refrigerant in supermarkets have been clearly discussed on the previous sub-chapters. Moreover, the novelties and case studies proposed for the existing and new installations have been described.

The geographical representations for the cascade and transcritical system and the growth over the last years are clearly illustrated before. The literature review revealed a lack of research in the CO_2 applications for warm climates. As it mention before, the all-CO_2 systems it found to be more energy efficient when the ambient temperature is lower than 22 °C, about equal when the temperature is between 22 to 26 °C and lower when the ambient temperature is higher than 26 °C and the system operate in transcritical mode.

New system arrangements applicable in warm climates have been proposed from a number of companies and researchers. The biggest problems for the transcritical systems operate in higher ambient temperatures are the power consumptions by the compressors and the low cooling performance of the system.

It is hard to recommend one of these proposed systems and draw conclusion based on the companies' measurements since the operating conditions and application requirements are not usually the same. Therefore, a computer simulation model supported by experimental results seems to be the best way to evaluate the different and alternatives solutions. In the next chapter the computer simulation model used is described in details.

4. COMPUTER SIMULATION DESCRIPTIONS

4.1.INTRODUCTION

Refrigeration systems are crucial parts in retailed superstores to ensure proper merchandise and safety of the food products. Two temperature ranges are designed in a supermarket to store frozen and chilled food products at -18°C to -35°C and -1°C to 7°C respectively. It is noted that the supermarket refrigeration systems contribute greatly to both direct greenhouse gas emissions due to refrigerant leakage and indirect greenhouse gas emissions by energy consumption. From the environmental and safety point of view, CO_2 is a very attractive refrigerant with negligible GWP, non-toxic and non-flammable. It also offers a number of advantages over other refrigerants such as superb thermo-physical properties and excellent heat transfer behaviours. Subsequently, the utilisation of CO_2 as a refrigerant can not only eliminate the direct emissions to the environment but also possible energy savings.

In order to evaluate and enhance the performance of CO_2 refrigeration systems in a supermarket, a small-size CO_2 refrigeration system was built to investigate experimentally the system performance under different operating conditions and control strategies. The test rig was comprehensively instrumented to enable a detailed performance evaluation of the system and individual components. A medium temperature open vertical multi-deck refrigerated display cabinet was used for the investigation at controlled conditions in an environmental chamber. The chilled cabinet was loaded with M-type test packages which were used as food simulators in the unit.

This chapter describes the development of numerical simulation model used to simulate the performance of the CO_2 refrigeration system for a supermarket application. Models are written using Engineering Equation Solver (EES, 2014) software. The numerical models enable the detailed thermodynamic analysis of refrigeration cycles and individual components under different model boundaries. A detailed model also used to investigate the medium temperature (MT) evaporator under different evaporating temperatures and air flow conditions.

In additional, mathematical models were established for the modification of the existing system which including the installation of the additional evaporator, pipe sizing for new evaporator, brine side model to calculate the thermodynamic properties of the brine

side, model to calculate the effectiveness of the plate heat exchanger used for the additional load and system integration.

A very detailed model based on the performance of the gas cooler will be presented separately in Chapter 7.

4.2.CO_2 REFRIGERATION SYSTEM MATHEMATICAL MODEL

The CO_2 refrigeration systems have been verified against the existing technologies based on the advantage, disadvantages and ambient condition limitations. The CO_2 refrigeration systems are usually compared with the existing R404A systems for supermarket applications.

Although the performances of the CO_2 refrigeration systems have been extensively compared with the existing systems using both experimental and theoretical methods, the detailed investigation and comparison between the existing and new proposed CO_2 refrigeration arrangements is still limited. During the last decade the convectional CO_2 booster systems have been undergoing a rapid change. The new technologies are trying to reach equal or higher COPs comparing with the existing HFCs systems especially in warm climate applications. The theoretical analysis of those systems is therefore essential. In order to analysis the existing systems a validated model is then required.

The mathematical model enables thermodynamic analysis of the existing CO_2 refrigeration cycle and individual components. The numerical models used to select the components for the experimental system have been integrated to complete the whole refrigeration cycle.

4.2.1. MATHEMATICAL EQUATION-SOLVING SOFTWARE

The mathematical models based on the experimental system have been developed using Engineering Equation Solver - EES (EES, 2014). This program can be solving up to 12,000 of non-linear algebraic and differential equations. The equation must be inputted on the program and the key parameters to solve must be define by the user. EES is extremely fast computational software including the thermodynamic and transportation functions of a number of fluids. In additional, EES can be used for single or multi-variable optimization process, check the unit consistency and provide uncertainty analysis for the calculated results.

4.2.2. TRANSCRITICAL BOOSTER SYSTEM

The system consists of two parallel semi-hermetic compressors, an oil separator, an oil receiver, a gas cooler/condenser, an ICMT motorized valve, a liquid receiver, an ICM by-pass valve, a direct expansion (DX) medium temperature (MT) refrigeration cabinet, a CO_2/Brine evaporator to get additional load, two electrically operated expansion valves (AKV) and a CO_2 accumulator (HT Acc.). The booster system includes three pressure levels: high, intermedium and medium in which the CO_2 gas cooler, liquid receiver and two evaporators are installed respectively. Figure 4.1 shows the P-h diagram of the cycle. A schematic diagram of the refrigeration cycle is shown in Fig. 4.2. The design of the system is similar to that presented in chapter 3.5.4. Instead of the LT load an additional medium temperature brine load has been added to the system.

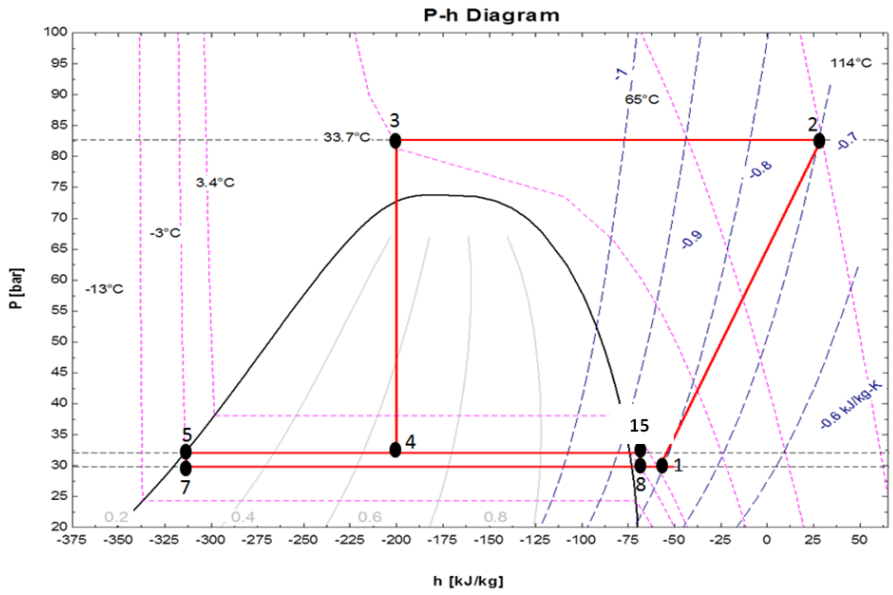

Figure 4.1 System P-h diagram

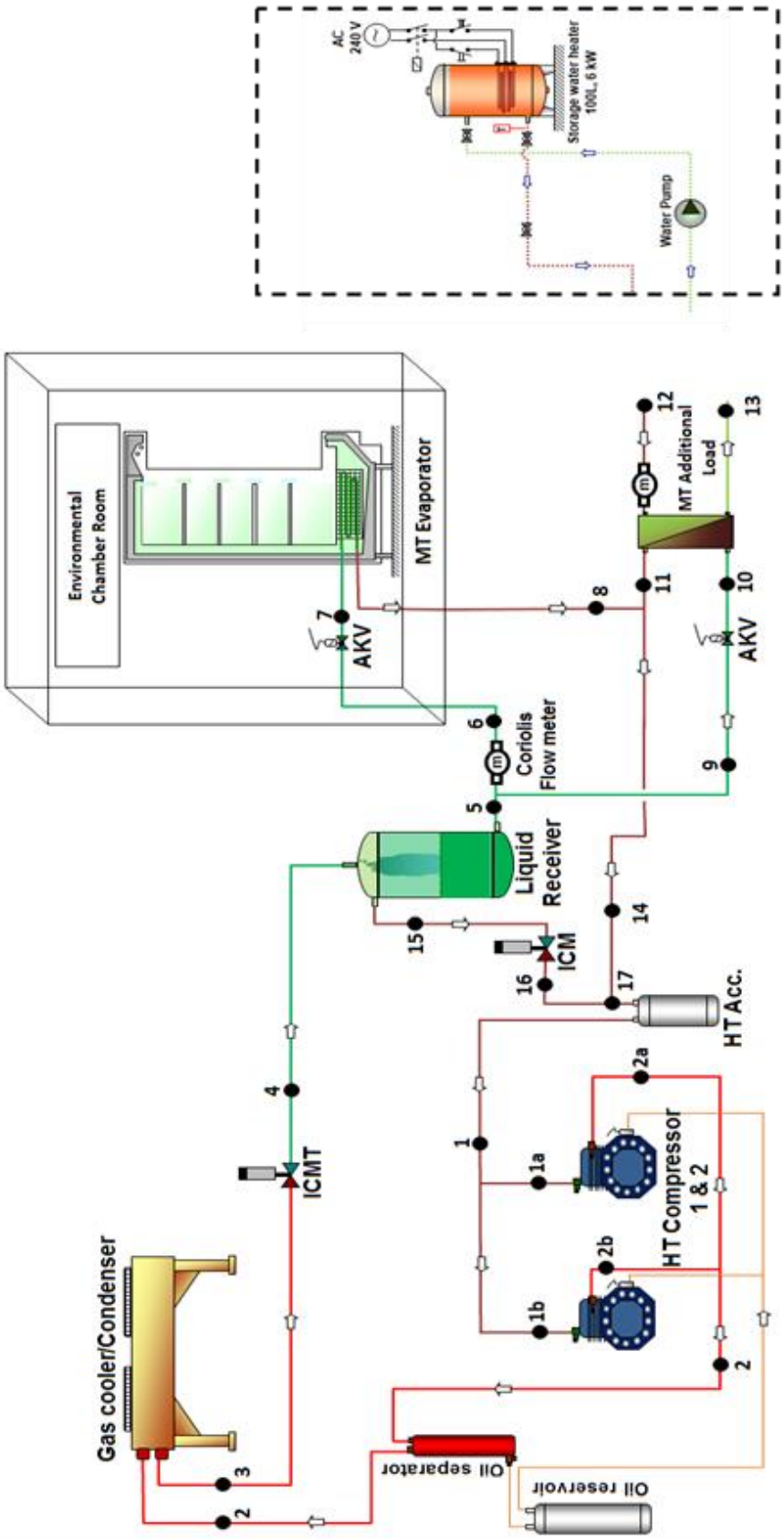

Figure 4.2 Simplified schematic diagram of the refrigeration system

4.2.3. TRANSCRITICAL BOOSTER INTEGRATION MODEL

The transcritical booster model uses the ambient conditions as boundary conditions for the high pressure side of the system such as the condenser/gas cooler and the suction line of the ICMT valve. The ambient temperature is also used to calculate the bypassed gas escaped from the CO_2 liquid receiver. For the intermediate pressure level of the system the normal set points used during the experiments and the most common values in real supermarket application are used to analyse the system performance. For the low pressure side of the system the evaporating temperature was assumed to be -8 °C. Later the evaporating temperature has been updated based on the experimental results. For the first stage the temperature of the products was assumed to be in M1 "M" packages temperature class (ISO, 2012) -1 °C to 5 °C. Later the "M" packages products were measured and the model values have been updated.

In order to simulate the transcritical booster refrigeration system, some assumptions were made as shown below.

- Steady state flow conditions
- Negligible thermal losses to the environment
- Pressure drop across the pipe line is negligible due to the short distance
- Refrigerant leaving the condenser is saturated liquid (Subcritical operation)
- Degree of superheat of the MT evaporator 5 K – updated afterwards from experimental results
- Degree of superheat of the AL HX/evaporator 7 K – updated afterwards from experimental results

The transcritical model involved all the components which influenced the performance of the CO_2 system. The individual components were treated as a single control volume. The mass and energy balance principles were applied for each individual component.

$$\sum_{inlet} m = \sum_{outlet} m \tag{4.1}$$

$$Q - W + \sum_{inlet} m\, h_{inlet} - \sum_{outlet} m\, h_{outlet} = 0 \tag{4.2}$$

4.2.4. CO_2 COMPRESSORS SYSTEM

The system is equipped with two HT parallel connected compressors and one LT compressor. As explained before the LT side of the system was not operated for this series of experiments. In order to validate the model including the LT side later, additional tests have been done in order to analyse and validate the LT compressor model.

In this case the HT compressor is used to compresses the superheated refrigerant from the outlet of MT evaporator, discharge line of AL and bypassed gas from the ICM valve to the condensing/gas cooling pressure depending on the ambient conditions. It is assumed that there any change as the mixed CO_2 refrigerant passes from accumulator before enter on the compressor suction line. The work of the compressor is calculated by the following equation.

$$W_{HT} = m_{total}(h_2 - h_1) \quad 4.3$$

or

$$W_{HT} = m_{total}\left(\frac{h_{2s} - h_1}{\eta_s}\right) \quad 4.4$$

$$m_{total} = m_{MT} + m_{AL} + m_{ICM} \quad 4.5$$

The actual isentropic efficiency of the HT compressor was calculated from the test results from the experimental system at CSEF in Brunel University. For the simulation purposes the isentropic efficiency of the compressor can be expressed as a function of the pressure ratio (R_p) across the compressors. Lee et al., (2006) equation are used to calculate the above.

$$\eta_s = 0.00476\, R_p^2 - 0.09238\, R_p + 0.89810 \quad 4.6$$

P_2 = discharge P_1 = suction 4.7

$$R_p = P_2/P_1 \quad 4.8$$

The enthalpy before and after the HT compressor were calculated by the model and is a function of the temperature and pressure. Both, temperature and pressure were calculated by the model iterative solution technique.

$$h_1 = f(P_1, T_1) \text{ – Suction enthalpy} \quad 4.9$$

$$h_2 = f(P_2, T_2) \text{ – Discharge enthalpy} \quad 4.10$$

The correlations for isentropic efficiency values were adapted as a good approximation for the real performance of semi-hermetic CO_2 compressors.

4.2.5. CONDENSER – GAS COOLER

In cases where the ambient temperature is higher than the critical temperature, the refrigerant cannot be condensed as the heat rejection temperature is above the critical point of CO_2, therefore a gas cooling process occurs. At this supercritical operation the pressure is independent of the temperature. When the system operates at supercritical region, the ICMT valve trying to maintain the optimum gas cooler pressure where the system reaches the higher COP. The optimum gas cooler pressure is a function of the refrigerant outlet temperature. The function of the optimum gas cooling pressure has been studied by many researchers in the past were they have proposed a different formulas to calculate this.

The effect of the compressor efficiency in the optimum pressure at the gas cooler exit pressure has been discussed by Sawalha (2008) and Srinivasan (2010). According to Kauf (1998) and Chen and Gu (2005) the evaporating temperature has significant influence on the optimum discharge pressure. However, Liao et al. (2000) included the evaporating temperature in the optimum discharge pressure correlation.

Ge and Tassou (2011b) investigated the optimum discharge pressure for a CO_2 booster system very similar to the experimental test rig which has been used for this work. The authors have been developed a correlation for the optimum discharge pressure when the ambient conditions are above 27 °C.

Table 4.1 HP side correlations

$P_{opt}=2.3426\ T_{amb}+11.541\ [R^2=0.9991]$	Ge and Tassou (2011b)
$P_{opt}=2.7(T_{amb}+T_1)-6.1$	Sawalha (2008)
$P_{opt}=2.68\ T_{amb}+0975=2.68\ T_3-6.797$	Chen and Gu (2005)
$P_{opt}=(2.778-0.0157\ T_{eva})Tc+(0.381T_{eva}-9.34)$	Liao et al (2000)
$P_{t,H}=2.6\ T_{amb}+7.54$	Kauf (1998)

More extensive analysis for the optimum pressure at the condenser/gas cooler will be described in Chapter 6 and 7.

The approach temperature for the cross-counterflow heat exchanger is defined as the temperature difference between the refrigerant outlet and the air entry to the heat exchanger.

$$Approach\ temperature\ (AT) = T_{ref,out} - T_{air,on} \quad 4.11$$

The approach temperatures at the gas cooler outlet are influenced by the air-on temperature, gas cooler fan speed, compressor controller and ICMT motorized valve opening.

For the first series of modelling analysis the approach temperature difference in the condenser/gas cooler was assumed to be constant 5K for both subcritical and transcritical operations. Then the values have been updated using the experimental results as approach settings. Finally the approach temperature values have been compared with the values for the detailed gas cooler model and the modelling settings for the transcritical solutions have been also updated.

The total refrigerant mass flow rate passing through the heat exchanger is calculated by the energy balance of air and refrigerant sides based on the experimental values. Then the experimental values were compared with the modelling values for similar conditions.

$$\dot{m}_{ref} = \dot{m}_{CO2,TOTAL} \quad 4.12$$

$$\dot{m}_{ref}\ (\Delta h)_{ref} = \dot{m}_{air}\ c_{p,air}\ (\Delta T)_{air} \quad 4.13$$

A more detailed model will present in Chapter 7 of this thesis. The discrete heat transfer model will use to analyse the effects of different design heat exchangers on the overall system COP. The model will be validated against the experimental results.

4.2.6. ICMT VALVE

This valve regulates the pressure inside the gas cooler to maintain an optimum COP during transcritical operation and degree of sub-cooling during the subcritical operation. The ICMT valve is the point where the high pressure side of the system separated with the intermediate side. In simple words, the valve expands the refrigerant from the gas cooler pressure level to the lower level of the receiver pressure for the transcritical operation. For the subcritical operation the saturated liquid pressure is used.

For the mathematical model purposes the following equations are used. Equations 4.14 and 4.15 referred to Fig. 4.2.

If transcritical:

$$\left.\begin{aligned} P_{GC,opt} &= P_{ICMT,in} \\ P_{GC,out} &= P_{ICMT,in} \\ P_{ICMT,out} &= P_{Rec} \\ h_{ICMT,in} &= f(P_{GC,out}, T_{GC}) \\ h_{ICMT,in} &= h_{ICMT,out} \rightarrow Isenthalpic \end{aligned}\right\} \quad 4.14$$

If subcritical then:

$$\left.\begin{aligned} P_{Cond} &= P_{ICMT,in} \\ P_{Cond,out} &= P_{ICMT,in} \\ P_{ICMT,out} &= P_{Rec} \\ h_{ICMT,in} &= f(P_{Cond,out}, T_{Cond,out}) \\ h_{ICMT,in} &= h_{ICMT,out} \rightarrow Isenthalpic \end{aligned}\right\} \quad 4.15$$

4.2.7. LIQUID RECEIVER

The liquid receiver has been designed for two main purposes. Firstly, the receiver operates as storage to maintain fluid when the system components require servicing or when the system shuts down after an operation or due to scheduled maintenance requirements. The second purpose is to act as a separator, where the liquid CO_2 flows to the evaporators and gas phase returns to the compressor suction line through an ICM by-pass valve.

Thermodynamic analysis of the preliminary experimental results shows that the separation ratio of gas by-pass to liquid flowing to the evaporators ranges from 36.5% to 63.5% respectively for the 3–row heat exchanger system and 38.29% and 61.71% each for the 2-row gas cooler/condenser system. Those are based on the average values

for ambient conditions between 19 °C to 36 °C. The variation of the separation ratio is determined by the CO_2 vapour mass fraction at the receiver inlet which is mainly a function of the gas cooler/condenser outlet parameters (temperature and pressure) and intermediate pressure. Considering of large variation of ambient temperature, these outlet parameters can be greatly altered and therefore the separation ratio. The liquid receiver is simulated by assumed the quality at the outlet of the liquid side and gas bypass side. Figure 4.3 illustrates the gas and liquid mass flow rate separation.

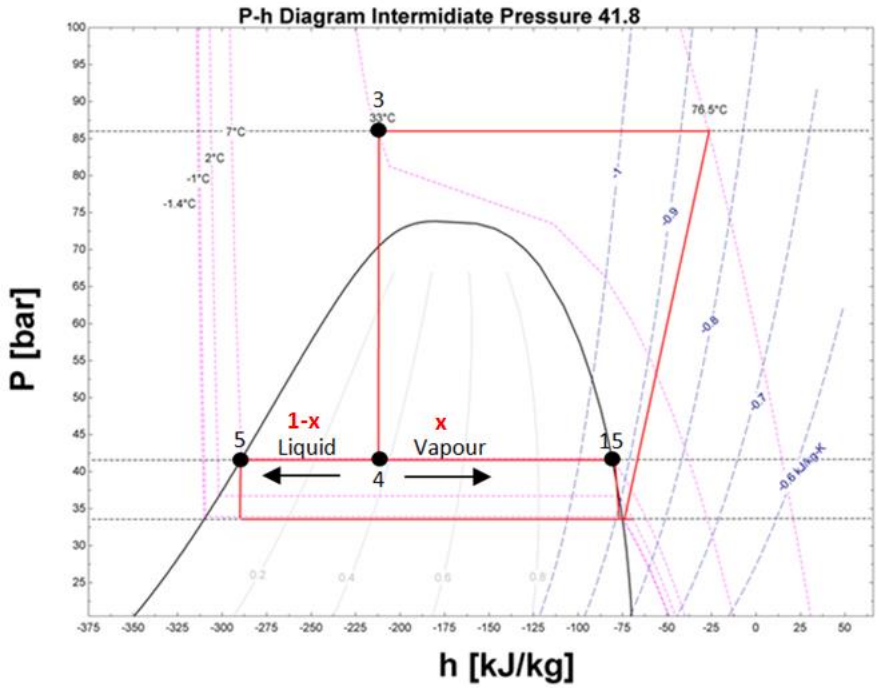

Figure 4.3 P-h Diagram use for mass flow rate calculations

The mass balance across the CO_2 liquid receiver is analysed as shown the following equations. The numbers refer to Fig. 4.3.

$$\left.\begin{aligned} \dot{m}_{CO2,TOTAL} &= \dot{m}_3 \\ \dot{m}_3 &= \dot{m}_4 \\ \dot{m}_4 &= \dot{m}_5 + \dot{m}_{15} \\ \dot{m}_5 &= \dot{m}_4 - \dot{m}_{15} \\ \dot{m}_5 h_5 &= \dot{m}_4 h_4 - \dot{m}_{15} h_{15} \end{aligned}\right\} \quad 4.16$$

The mass flow rates flow a liquid and gas side were calculated as shown in Fig. 4.3.

$$x = \frac{h_4 - h_5}{h_{15} - h_5} \qquad 4.17$$

Liquid mass flow rate: $\dot{m}_5 = (1 - x)\dot{m}_4$

Bypassed mass flow rate: $\dot{m}_{15} = x\,\dot{m}_4$

4.2.8. BY-PASS ICM VALVE

The ICM valve has been install at the top side of the liquid receiver where the gas phase is bypassed and mix with the refrigerant outlet form the evaporator before flow to accumulator and then to compressor suction line. Therefore, the bypass valve ensured that the evaporator is feeding with only liquid phase.

The valve has negligible effect on the system efficiency but ensures an operating pressure below the maximum operating pressure of the receiver and liquid pipe line.

The valve expands the vapour refrigerant from the intermediate pressure to the medium pressure of the MT before enters to the compressor suction. For simulation purposes the ICM valve is model using an isenthalpic expansion process. From Fig. 4.2 and 4.3 the isenthalpic expansion is described by the Equation 4.18.

$$h_{15} = h_{16} \qquad 4.18$$

4.2.9. AKV ELECTRONIC EXPANSION VALVES

There are two AKV valves before both MT and AL evaporators. For simulation purposes it is assumed in both expansion valves is isenthalpic. The enthalpy at the inlet and outlet of the evaporators are calculated by the pressure at the intermediate level of the system. At the initial stage the evaporating temperature assumed to be -8 °C for both MT and AL evaporators. Then the values were updated with the experimental results. The effect of the evaporating temperature on the system COP has been investigated and will present in the next chapter. The energy and balance equations for both MT and AL are illustrated below, the numbers of the parameters refer to Fig. 4.2.

$$h_{6,9} = f(P_{intermidate}, T_{evaporator}) \qquad 4.19$$

$$\left.\begin{aligned} h_6 &= h_7 \\ h_9 &= h_{10} \\ \dot{m}_6 &= \dot{m}_7 \\ \dot{m}_9 &= \dot{m}_{10} \\ \dot{m}_5 &= \dot{m}_6 + \dot{m}_9 \end{aligned}\right\} \quad 4.20$$

4.2.10. MT REFFIGERATED CABINET

The MT display refrigerated cabinet which is located inside the environmental chamber room generate a part of the CO_2 system load. The evaporation process takes place between points 7 and 8 and the cooling capacity is calculated as follows:

$$Q_{MT} = \dot{m}_7(h_8 - h_7) \quad 4.21$$

For the first running of the simulation models the cooling capacity of the MT refrigerated cabinet is used as an input based on the design consideration in order to calculate the mass flow rate of the refrigerant passing through the coil. The results have been compared with the experimental values.

The same procedure is used to calculate and compare the mass flow rate passing through the AL evaporator and by using the equations in Chapter 4.2.7 the total mass flow rate is calculated. Finally, the total mass flow rate calculated from the model was used to compare with the calculated values from the experimental results.

During the experimental tests the refrigeration capacity of the system varies as the MT cabinet was ON/OFF based on the set point or the defrost period. For the purposes of the simulation investigation a constant evaporator load is assumed. Therefore, the comparison between experimental and simulation results were made based on steady state conditions for both. For this comparison, defrost and off-cycle data were neglected.

4.2.11. MT REFRIGERATED CABINET DETAILED SIMULATION

For the initial simulation model run the energy and balance equations are used to calculate the mass flow rate based on the design capacity of MT refrigerated cabinet. The mass and energy equations are shown below.

$$\dot{m}_7 = \dot{m}_8 \quad 4.22$$

$$\dot{m}_7 h_7 + Q_{MT} = \dot{m}_8 h_8 \quad 4.23$$

For the supermarket applications the most common type of the evaporator used is the finned-type heat exchangers. The performance of evaporators coils directly effect on the medium and low temperature levels and finally at the overall supermarket system performance.

When the CO_2 refrigeration system operates in subcritical cycle do not direr so much from the common HFCs systems usually operate in supermarket applications. In case of the transcritical operation the unusually operating pressure at the high pressure side of the system effect on the whole system as well in medium and low pressure side.

The evaporators as an individual component has been investigated by many researchers and the influence of different design and operation parameters were analysed. To date, there has not been much research into the evaporator effects on the whole CO_2 refrigeration system. In the most of the research work for the CO_2 refrigeration systems the evaporator is taken into account my assuming the isenthalpic work at the expansion valve, the evaporating temperature and the superheat value.

In this subchapter, the numerical model for the MT evaporator is presented. Key parameters such as air and refrigerant conditions varied in order to investigate firstly the evaporator as an individual component of the system. Secondly, the results of the individual evaporator unit will integrate with the whole system model and the influence of the evaporator side and the system COP will discuss.

To integrate both models, the evaporator model was written in EES software. One main model was established and can be applied for both MT and LT refrigerated cabinets. The assumptions made for the model as described below:

- The heat exchanger operates under steady state conditions – independent of time

- Intermediate pressure is used as a pressure in the suction of the AKV
- Heat losses to or from the surroundings are negligible
- There are no thermal energy sources in the heat exchanger walls such as electric heater
- Uniform air temperature across the coil
- Refrigerant flows inside the tubes in one dimensional flow

For the simulation purposes the tube are arranged in coordinates along width, depth and height axes and denoted with i, j and k respectively. The coil is divided into two regions: single phase region at the outlet of the evaporator and two phase region at the inlet. For the mathematical model the regions are called control volumes. The mass and energy balance must be satisfied for each of these control volumes in order to precede the model for further calculations.

Refrigerant side:

$$\left.\begin{aligned} \dot{m}_{ref,in} &= \dot{m}_{ref,out} \\ Q_{ref} &= \dot{m}_{ref}(h_{ref,out} - h_{ref,in}) \\ \dot{m}_{ref}\left(h_{ref,out,sp} - h_{ref,in,sp}\right) + \dot{m}_{ref}\left(h_{ref,out,tp} - h_{ref,in,tp}\right) &= Q_{ref} \end{aligned}\right\} \quad 4.24$$

Air side:

$$\left.\begin{aligned} \dot{m}_{air,in} &= \dot{m}_{air,out} \\ h_{air} &= f(T_{air}, P_{air}, RH_{air}) \\ Q_{air} &= \dot{m}_{air}(h_{air,in} - h_{air,out}) \end{aligned}\right\} \quad 4.25$$

Energy balance:

$$Q_{MT} = Q_{ref} = Q_{air}$$
$$Q_{MT} = UA_o\Delta T_{lm} \quad 4.26$$

The logarithmic mean temperature difference is defined as (Shah R., Sekulic D., 2003):

$$LMTD = \Delta T_{lm} = \frac{\Delta T_I - \Delta T_{II}}{\ln(\Delta T_I/\Delta T_{II})} \quad 4.27$$

$$\Delta T_{lm} = \frac{(T_{h,in} - T_{c,out}) - (T_{h,out} - T_{c,in})}{\ln\left((T_{h,in} - T_{c,out})/(T_{h,out} - T_{c,in})\right)} \quad 4.28$$

Extended surface efficiency:

$$\eta_o = 1 - \frac{A_f}{A_a}(1 - \eta_f)$$
$$\eta_f = \frac{\tanh(mr_o\varphi)}{mr_o\varphi}$$
$$m = \sqrt{\frac{2a_o}{k_f\delta_f}}$$
$$\varphi = \left(\frac{R_{eq}}{r} - 1\right)[1 + 0.35\ln(\frac{R_{eq}}{r})$$
$$\frac{R_{eq}}{r} = 1.27\frac{X_M}{r}\left(\frac{X_L}{X_M} - 0.3\right)^{1/2} \quad 4.29$$

The same procedure is used to calculate the DX LT evaporator by only changed the temperature profiles for air and refrigerant sides. The model results are used to integrate with whole CO_2 model. In the next chapter the results from the model and the effect on the system COP are illustrated.

4.2.12. BRINE PUMP

The power consumption of the brine pump is calculated based on the brine mass flow rate, pressure head and the efficiency of the pump. The equation below illustrates the equation inserted to the mathematical modelling.

$$W_{brine,pump} = \frac{\dot{m}_{brine} v_{brine} (\Delta P_{brine})}{\eta_{brine,pump}} \quad 4.30$$

The mass flow rate was calculated based on the refrigeration load, v_{brine} is calculated by M. Conde (2011), ΔP_{brine} and $\eta_{brine,pump}$ and were assumed to be 250kPa and 0.5 respectively based on the manufacturer data.

4.2.13. ADDITIONAL LOAD EVAPORATOR

The additional load refrigeration capacity was calculated from the energy balance between brine (water/glycol mixture) and refrigerant side, assuming an adiabatic heat transfer. The refrigeration capacity was determined by calculating the heat absorbed by the refrigerant from the brine. The properties of the refrigerant were calculated from the EES software, while the properties of brine side were calculated by using the equations from M. Conde (2011).

$$Q_{AL,CO2} = \dot{m}_{10}(h_{11} - h_{10})$$

$$Q_{AL,brine} = \dot{m}_{12} cp_{brine}(T_{12} - T_{13})$$

$$\dot{m}_{10}(h_{11} - h_{10}) = \dot{m}_{12} c_{p_{brine}}(T_{12} - T_{13})$$

$$c_{p_{brine}} = 4.476 + 0.6086\,\xi + 0.715\left[\frac{273.15}{T_{brine}}\right] - 1939\,\xi\left[\frac{273.15}{T_{brine}}\right] + 0.4787\left[\frac{273.15}{T_{brine}}\right]^2 \quad 4.31$$

The effectiveness of the HX is calculated by the model.

$$C_h = \dot{m}_{brine} c_{p_{brine}}$$

$$C_c = \dot{m}_{ref} c_{p_{ref}}$$

$$C_{min} = \min(C_h, C_c)$$

$$q_{max} = C_{min} * (T_{h,i} - T_{c,i})$$

$$q_1 = C_h * (T_{h,i} - T_{h,o})$$

$$q_2 = C_c * (T_{c,o} - T_{c,i})$$

$$q_1 = q_2$$

$$\varepsilon = {q_1}/{q_{max}} \quad 4.32$$

As the MT evaporator load, the cooling capacity of the AL additional load is used as an input based on the design consideration in order to calculate the mass flow rate of the refrigerant passing through the coil. Then the mathematical model has been updated by using variables from experimental results.

4.2.14. MIXING POINTS

After the liquid receiver the system is divided in three flow lines including the MT, AL evaporators and the bypassed vapour refrigerant. Before the CO_2 refrigerant enters to the HT compressor to close the cycle, there are two mixing points where the refrigerants with different properties values are mixed. For the simulation purposes the mixing points were inserted to the mathematical model as follows. The numbers refer to Figure.

Mixing Point 1: MT & AL evaporators

$$\dot{m}_{14}h_{14} = \dot{m}_{8}h_{8} + \dot{m}_{11}h_{11} \quad 4.33$$

Mixing Point 2: Mixing Point 1 & bypassed vapour

$$\dot{m}_{17}h_{17} = \dot{m}_{14}h_{14} + \dot{m}_{16}h_{16} \quad 4.34$$

The mass flow rates for points 14 and 17 are calculated as explained in Chapters 4.2.7, 4.2.10 and 4.10.12. Therefore the refrigerant enthalpy for both coils is calculated by the model. The enthalpy of mixing point 2 value is used as a suction line for the HT compressors.

$$\left.\begin{aligned} T_{17} &= f(P_{17}, h_{17}) \text{ – HT suction temperature} \\ h_{17} &= h_1 \\ T_{17} &= T_1 \end{aligned}\right\} \quad 4.35$$

4.2.15. PERFOMANCE OF CO_2 REFRIGERATION SYSTEM

The performance of the refrigeration system was determined based on the requirements for each test and variables which are under investigation. The performance of the CO_2 refrigeration system can be determined by the following equation:

$$COP_{CO2} = \frac{Q_{MT} + Q_{AL}}{W_{TOTAL}} \quad 4.36$$

$$W_{TOTAL} = W_{HT,com} + W_{brine,pump} \quad 4.37$$

In order to take under consideration the effect of the different air volume flow rates passing through the condenser/gas cooler, the power consumption of the fan has been taken into account on the overall system COP. Therefore the system COP is calculated by the following equation.

$$COP_{CO2} = \frac{Q_{MT}+Q_{AL}}{W_{TOTAL}+W_{fan}} \quad 4.38$$

The power consumption of the fan was measured by power quality analyser and then the values inserted at the simulation model. Those results will present in Chapter 7 with the detailed gas cooler model.

4.2.16. ADDITIONAL AIR COOLER (AAC)

One of the modifications was required for the system during the experimental tests was the installation of an additional evaporator coil. The air cooler was connected in parallel with the MT refrigerated display cabinet and was feed with the same liquid line. Therefore, the consideration for the liquid line has been done from the early stage of the MT evaporator design. The pressure drop of the liquid line was designed to be below 78 kPa. For the outlet of the AAC the refrigerant is in single phase. The pressure drop of the single phase AAC outlet was calculated from the equation below:

$$\Delta P = 4f\frac{L}{d_i}\frac{G^2}{2\rho} \quad 4.39$$

- f = friction factor
- L = is the required length to connect with the mix point before compressor
- d_i = internal diameter of the pipe
- G = mass velocity
- ρ = refrigerant density

The friction factor is calculated from Blasius equation (Incropera F.P., DeWitt D.P., 1996):

$$f = \frac{0.079}{Re^{0.25}} \quad 4.40$$

$$Re = \frac{G\ d_i}{\mu} \quad 4.41$$

Different lengths and pipe diameters were used for simulation purposes. The pressure drop at the single phase designed to be lower than 55 kPa with equivalent saturation temperature drop 1 K as recommended by ASHARE (2010).

For the simulation model the energy and balance equations are used to calculate the mass flow rate based on the design capacity of AAC. The mass and energy equations are shown below.

$$\dot{m}_{19} = \dot{m}_{20} \quad 4.42$$

$$\dot{m}_{19} h_{19} + Q_{AAC} = \dot{m}_{20} h_{20} \quad 4.43$$

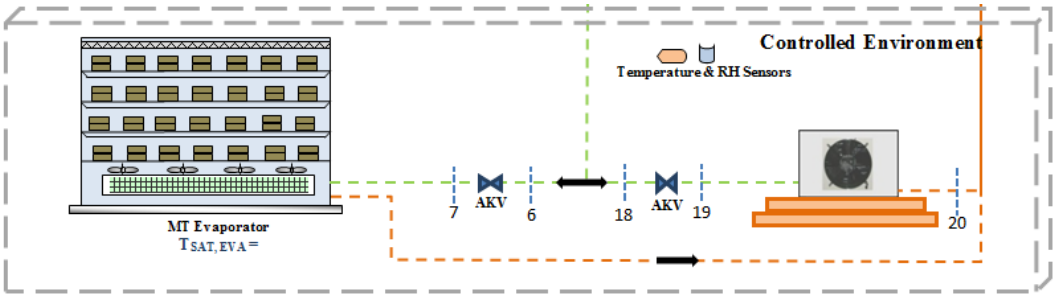

Figure 4.4 AAC installation point

Additional experimental tests have been done in order to investigate the mass flow rate fluctuation in the AAC with respect to ambient conditions and ICM by pass rate. Based on those results, the simulation model was updated. The results are illustrated in Chapter 6.

4.3.SUMMARY

The descriptions of the computer simulation for the existing CO_2 system arrangement are described in details in this chapter. Energy and mass balance equations were applied for each system component individually. The condenser/gas cooler model is based on the thermodynamic equations related to air and refrigerant side. In Chapter 7, a very detailed model based on gas cooler design and operation will be present. This model will integrated with the rest of the CO_2 system from this chapter and the final COP results will validated.

In the next chapter the design-construction-modification procedure for the experimental test facilities will be present in details.

5. DESIGN – CONSTRUCTION – MODIFICATION FOR THE EXPERIMENTAL TEST FACILITIES

5.1.INTRODUCTION

In order to evaluate and enhance the performance of CO_2 refrigeration systems in a supermarket, a small-size CO_2 refrigeration system was built in the refrigeration laboratory of the Research Council United Kingdom (RCUK) Centre for Sustainable Energy use in Food chains (CSEF), Brunel University.

The CO_2 transcritical system consists of the gas cooler/condenser, an ICMT motorized valve which act as an expansion valve of the system, ICM gas bypass valve, liquid receiver, a CO_2 accumulator and two semi-hermetic compressors. A medium temperature (MT) direct expansion (DX) open vertical multi-deck refrigerated display was used for the investigations and the tests were carried out at controlled conditions in an environmental chamber. An additional CO_2/Brine load has been installed on the system in order to balance the capacity of the compressor.

A simplified drawing illustrates the relative installation positions of the main components in the system are shown in Fig. 5.1.

Some modifications have been made to the refrigeration system during the experimental investigation in order to explore different parameters and how these effect on the overall performance of the system.

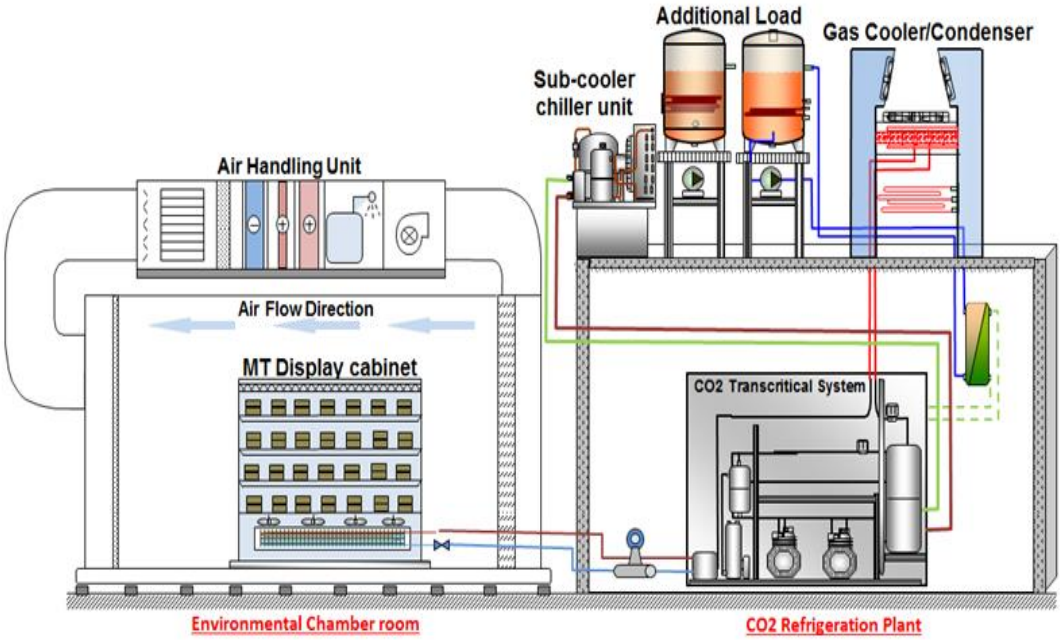

Figure 5.1 Simplified drawing of the relative component installation positions

The system is divided into three pressure sections, high, intermedium and medium; where the high pressure section begins at the outlet of the compressor and continues through the gas cooler/condenser and inlet line of ICMT motorized valve. Intermediate pressure section exists at the outlet of the ICMT valve and through the receiver where the flow is divided into gas and liquid. The gas phase returns back to the compressor suction line through the by-pass ICM valve. The liquid flows to the expansion valve where the medium pressure level begins. The liquid is expanded prior to MT display cabinet and additional load (AL). The gas outlet from the MT and AL flows back and mixing with the gas by-pass from the receiver before enter to compressor suction line and complete the circuit.

For a real supermarket application the transcritical booster system can supply both MT and LT loads or the system can supply only MT or LT for the parallel applications. For this particular work which the main object is investigate the effect of condenser/gas cooler design on the system COP is decided only the MT circuit operate during the experimental tests.

Figure 5.1 and 5.2 shows the installed relatively position of the CO_2 booster system in the initial and final stage. The components of the system are illustrated in Table 5.1. The selection process for each of these components is detailed in the next sections.

Figure 5.2 CO_2 booster experimental test rig

When the system was being designed and installed the availability of the CO_2 components was very limited. During the last years the CO_2 components market has been extended and many companies involve with innovation and installations of CO_2 refrigeration systems.

To avoid any component failure during the tests, the system has been designed with by-pass pipes for all the main components. The components which have been designed to by-passed in case of failure are included in Table 5.1.

Table 5.1 Main system components

Component	Notes	By-pass design
Compressor HT	Operated	Yes - Connect parallel
Compressor LT	Not in operation	Yes
Gas cooler compressor	Operated	No
ICMT valve	Operated	No
Receiver	Operated	Yes - Part
ICM	Operated	No
Refrigerant Flow meter	Operated	Yes
MT cabinet	Operated	Yes
Additional Load	Dep. Test requirements	Yes
Other Components		
Relief valves	-	-
Accumulator	-	-
Oil separator	-	-
Oil receiver	-	-
Expansion valves	-	-
Brine side pump	-	-
Brine tank	-	-

5.2.SYSTEM LAYOUT

The CO_2 test rig is consisted by CO_2 main plant room, the roof platform and the environmental chamber room. Those three main parts of the system has been on designed based the space availability and system needs.

Inside the CO_2 main plant room the CO_2 rack system has been installed including the liquid receiver, compressors, oil system, control panels and auxiliary components. Figure 5.3 shows the CO_2 rack design.

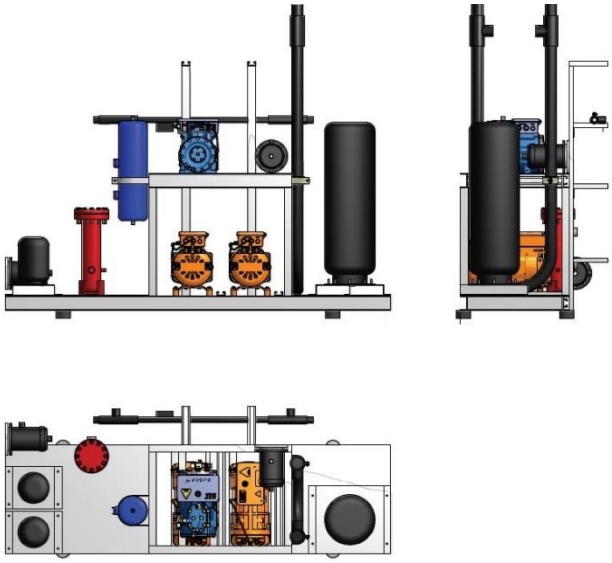

Figure 5.3 CO_2 system rack

The C/GC test unit, the standstill condensing unit and the AL heat exchanger have been placed at the roof above the CO_2 main plant room. Figure 5.4 shows a picture of the roof.

Figure 5.4 Condenser/Gas cooler relative position

The MT display cabinet of the refrigeration load system was placed in an environmental test chamber. In order to maintain constant temperature, relative humidity and air velocity the environmental room incorporates and air handling unit (AHU) which was installed above the roof next to CO_2 main plant room roof. Figure 5.5 shows a picture of the environmental chamber room.

Figure 5.5 Environmental chamber room

The useful test area of the chamber room is 6.14 m long, 3.1 wide and 3.05 m high. The supply and return duct of the AHU are terminating at the technical walls of the sides of the chamber room. The technical walls of the supply and return air plenums were constructed from perforated metallic plates supported by a wooden frame. The MT cabinet has been positioned 1.9 m. from the supply wall and 0.8 m. from the back wall.

5.2.1. HT CO_2 COMPRESSOR

As it mentioned before, when the system designed and installed the CO_2 technology was in very early stage and the available components were very limited. To find and select a small capacity compressor was a challenging process. In order to select the appropriate compressor for a CO_2 system a number of parameters must be taken into

account. The total refrigerant mass flow rate is related with the swept volume of the compressor.

In order to calculate the refrigerant mass flow rate the MT total load need to be considered. At the early stage the system designed to supply an additional LT load were taken into consideration to the mass flow rate calculations.

For this case the refrigerant outlet from the LT load is mixed with the outlet from the MT evaporator, additional load and by-passed vapour from the receiver before enters to the HT compressor. There is a number of ways to calculate the total refrigerant passing through the HT compressor. The first option is to calculate the refrigerant mass flow rate based on the designed cooling loads for MT and LT. For this option an assumption must be made in order to calculate the refrigerant by passed from the receiver.

$$\dot{m_{MT}} = {}^{Q_{MT}}/_{\Delta H} \quad 5.1$$

$$\dot{m_{LT}} = {}^{Q_{LT}}/_{\Delta H} \quad 5.2$$

The calculated refrigerant mass flow rate based on the given loads is used to calculate the swept volume of the compressor required to generate the cooling. The swept volume of the LT compressor is a proportional of the mass flow rate of the low pressure side of the system. The HT compressor swept volume is calculated by using the total mass flow rate of the system.

Total mass flow rate: $\dot{m}_{total} = \dot{m}_{MT} + \dot{m}_{LT} + \dot{m}_{bypass}$ 5.3

The equations used to calculate the swept volume of LT and HT compressors shown in Fig. 5.6.

$$\dot{V}_{swept,LT} = \dot{m}_{LT}/(\rho_{suc,LT} \cdot \eta_{vol,LT}) \quad 5.4$$

$$\dot{V}_{swept,HT} = \dot{m}_{total}/(\rho_{suc,MT} \cdot \eta_{vol,HT}) \quad 5.5$$

The volumetric efficiency of the compressor, density in the suction line of the LT compressor and the mixed point of the suction line of the HT compressor has been calculated by the simulation model. The mass flow rate by-passed from the ICM valve assumed as a linear relationship with the ambient temperature.

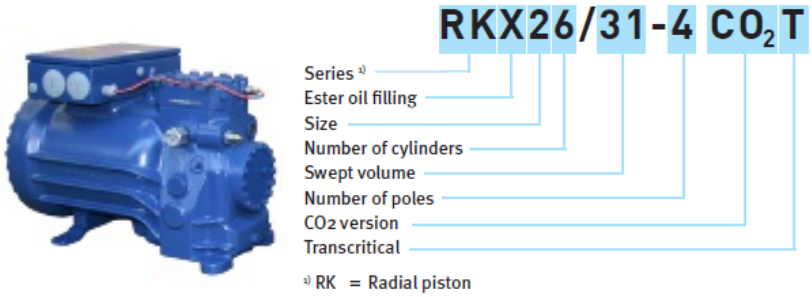

Figure 5.6 Bock HT compressor

The two compressors were selected for the high pressure side are a semi-hermetic radial 2-piston manufactured by BOCK. The two compressors are connected in parallel with the advantage to run in the same time or separately depending on the test conditions.

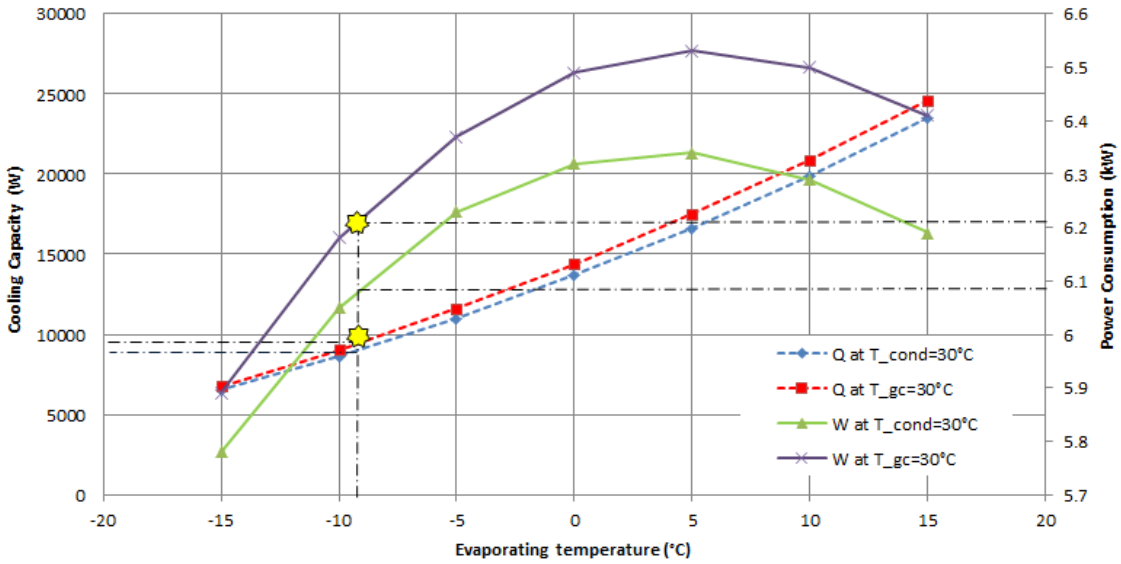

Figure 5.7 Compressor cooling capacity for different evaporating temperatures

(Data source: Bock, 2009)

The designing conditions for the HT compressor was at T_{evap} = -8 °C and T_{gc} = 30 °C and the system designed to operate in transcritical cycle. It can be seen from the graph in Fig. 5.7 that the cooling capacity is around 10 kW for the given values. For both subcritical and transcritical cycles a 10 K suction gas superheat is assumed. The pressure at the outlet of the compressor for transcritical operation assumed to be 75 bar.

For the case of the LT load is not operated the cooling capacity of the compressor is double than the designed load of the MT compressor. Consequently, an additional MT load was added on the medium pressure side of the system in order to balance the load.

In additional, the compressor was equipped with variable speed controller. The variable speed controller is manufactured and provided by Danfoss in order to enable the variation of the capacity.

The compressor equipped with centrifugal lubrication system with oil separation to protect the compressor from running without sufficient lubrication and protect the compressor against the wear. The synthetic ester oil can be used both in subcritical and transcritical systems with the same results.

To ensure the safety operation of the compressors, low and high pressure switches are used to control and protect the compressor from any potential damage. The low and high pressure switches control the suction and discharge pressure levels respectively. The ON/OFF compressor operation is controlled by PID controller which set a time delay of 3 minutes.

Both MT compressors are equipped with service valves mounted on the suction, discharge oil regulator to allow the isolation from the refrigerant circuit.

The compressor suction and discharge lines are connected with flexible heavy duty pipe to prevent from the vibrations. The compressors are bolted to the frame on shock and oil resistance machine feet made of polymer to avoid any damage from the vibrations during start or stop operation. Appendix C illustrates more information regarding the HT compressor.

5.2.2. VARIABLE SPEED CONTROLLERS

Both compressors connected with separate variable speed controllers provided by Danfoss. The variable speed mechanism controls the capacity of the compressor depending on the evaporating load of the system. For this case the variable speed settings was from 0 to 50 Hz.

By changing the frequency the swept volume of the compressor is changing all the time in order to meet the requirement settings. Figure 5.8 shows the VLT 2800 Danfoss variable speed pack which has been used.

Figure 5.8 Compressor variable speed controllers

5.2.3. OIL MANAGEMENT

Figure 5.9 illustrates the simplified drawing of the oil system pipe connections and oil management which integrated with the compressors of the CO_2 system.

When the refrigerant enters to HT compressor is mixed with some oil loosed from the oil sump and circulates with the refrigerant through the system. To make sure that the majority of the oil returns to the compressor the CO_2 refrigeration system equipped with an oil management system. This system ensures the constant lubricated of the system avoiding high temperature tensions and damage of the compressor. In case the oil trapped from the oil management system and the compressor is over heated a high temperature control switch is used to stop the compressor operation and protect the compressor form any potential damage.

The CO_2 compressor oil system consists from the oil separator, oil receiver, oil strainer, oil level regulator and a pressure relief valve. The system controlled by an oil/refrigeration PID controller.

The two HT compressors on the system are connected in parallel. This means only one pipe coming to the compressors and split into the two suction lines. The two discharge lines become one after the HT compressors. The refrigerant from the discharge line passes first through the oil separator. The oil separator designed based on the compressor oil requirements.

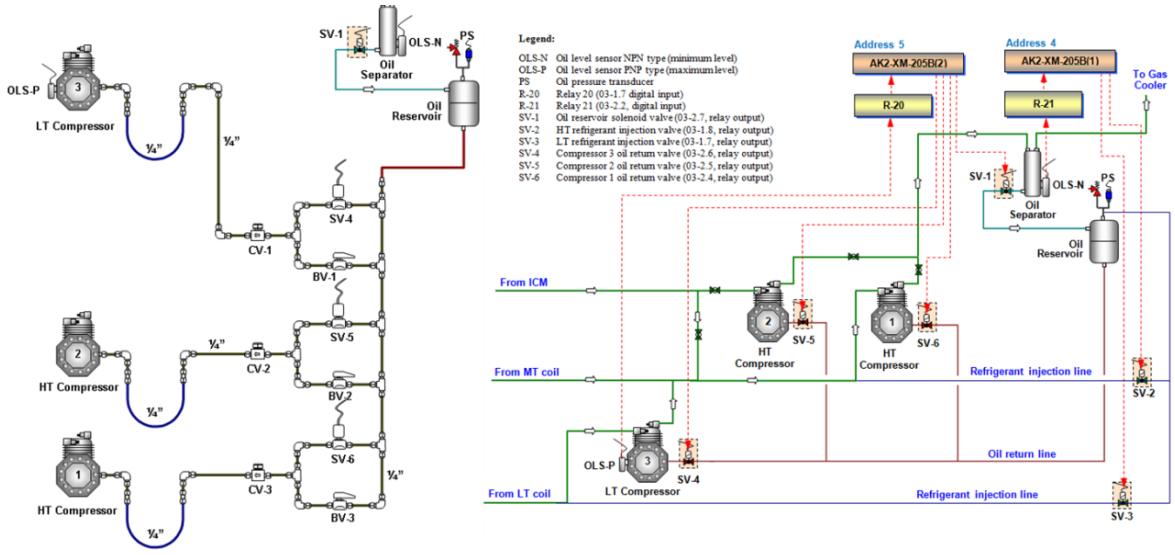

Figure 5.9 Oil system for HT compressors

The oil separator manufactured by Temprite is suitable for CO_2 transcritical configurations. Temprite oil separators used a dual function filters to separate the oil from the refrigerant. The maximum operating pressure is 130 bar and the nominal separation efficiency is found to be 98.5%. The maximum operating temperature is 130 °C and minimum is 0 °C. The maximum oil capacity is 2.5 L with minimum filling volume of 0.6 L. The system equipped with a built-in float valve which opens when the oil level rises above the minimum charge level and the excess oil is returned back to the compressor trough the oil reservoir.

As it mentioned before the oil from the separator returns to oil reservoir, which acts as an oil storage and oil supply of the compressor. The oil reservoir designed with volume of 8.2 L and maximum working pressure of 42 bar. The normal operating temperature of the oil reservoir is between -10 to 110 °C and is manufactured by Henry Technologies LTD. The oil level inside the reservoir is checked by the two sight glasses. The two sight glasses placed in the same line to be the one above the each other. The first one denote the minimum oil level and the second one the maximum oil level on the reservoir.

An oil regulating system consists by the oil level sensor and a solenoid valve is used to regulate the oil to the compressor. When the oil inside the compressor reach the low

level indicator the solenoid valve opens and allows the lubricant oil to flow to the compressor. Oil regulator and compressor power supplied from the same PID controller. When the compressor is out of operation, the solenoid valve is shut and stops feeding the compressor with oil. In case of any potential fail on the solenoid operation, the compressor is stop running when the oil level is lower than the minimum level.

Additional information for the oil system, charging procedure, maintenance and problems during the operation described in Appendix D.

5.2.4. CONDENSER/GAS COOLER TEST RIG & UNITS

To further examine the performance of CO_2 system with different gas coolers/ condensers sizes and operating conditions, a test unit has been built as shown in Fig. 5.10. The CO_2 heat exchanger is suspended tightly between two upright metal frames. A propeller air fan with variable speed control is installed above the heat exchanger to maintain a passage of fixed air flow. Above this are a number of smaller air fans installed oppositely along the direction of pipe length, which will be switched on if the air on temperature is controlled to be higher than ambient. As such, part of the hot exhaust air will flow back through the return air tunnels, the return air grills and finally mix with the lower temperature ambient air flow. If the mixed air flow temperature is still lower than the designed air on temperature, an electric air heater installed just below the heat exchanger is controlled to turn on in order to maintain the air on temperature.

Consequently, the gas cooler air on parameters, temperature and flow rate, can be well controlled to specified values.

The test rig has been comprehensively instrumented to detailed measurement data and overall performance description of the heat exchanger itself and its integrated CO_2 refrigeration system. These include two thermocouple meshes with 24 points each to measure air-on and air-off temperatures; pressure difference of air flow through the heat exchanger to get the air side pressure drop, air flow velocity to obtain the air flow rate. For the refrigerant side, 2 to 6 (depends on the test) pressure transducers are installed inside the inlet and outlet headers and one circuit of the heat exchanger to measure overall and heat exchanger refrigerant side pressure drops.

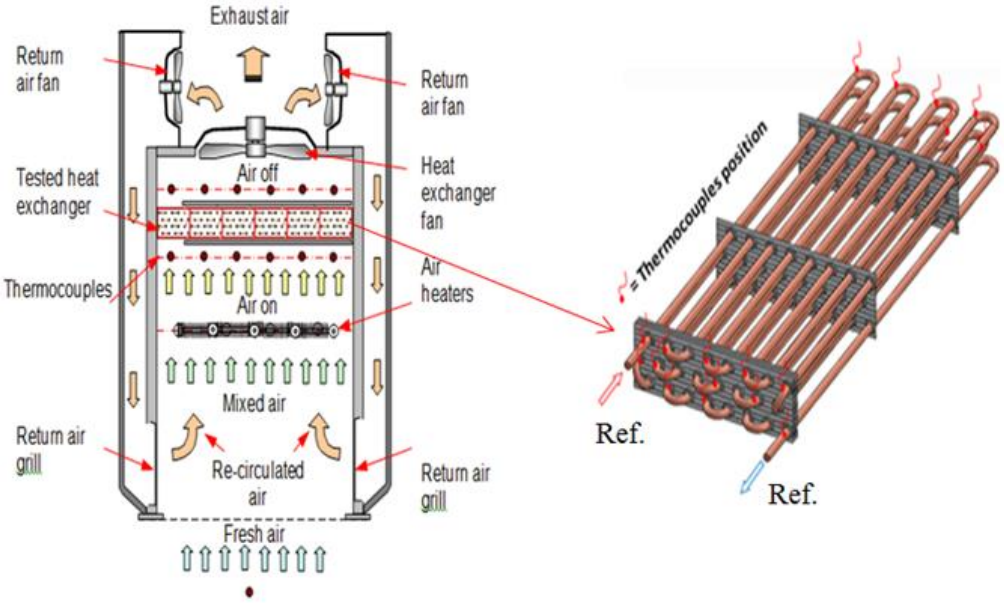

Figure 5.10 C/GC test unit

In addition, as shown in Fig. 5.10, a large number of thermocouples are attached on all the pipe bends along the pipes of one circuit to measure the refrigerant temperature variation or profile from inlet to outlet. Instead of directly measuring the refrigerant mass flow rate, it is calculated from the heat exchanger heat balance between the air and refrigerant sides.

In order to experimentally examine the effect of different size of CO_2 gas coolers/condensers on the system performance, three gas coolers/condensers have been purposely designed and manufactured with different pipe arrangements and circuit numbers which are denoted as coil A – B – C.

As shown in Fig. 5.11, coil A has three rows and four pipe circuits with total pipe number of 96 and overall dimension of 1.6m×0.066m×0.82m (L×D×H). Correspondingly, coil B has two rows and two circuits with total pipe number of 64 and overall dimension of 1.6m×0.044m×0.82m (L×D×H). Coil C has the same pipe arrangement with the coil A with the only difference that has the half-length with 0.8m×0.066m×0.82m.

The remaining structural parameters are the same for both coils including: copper pipe inner diameter, aluminium fin thickness, fin density which are 6.72mm, 0.16mm and 453fins/m respectively.

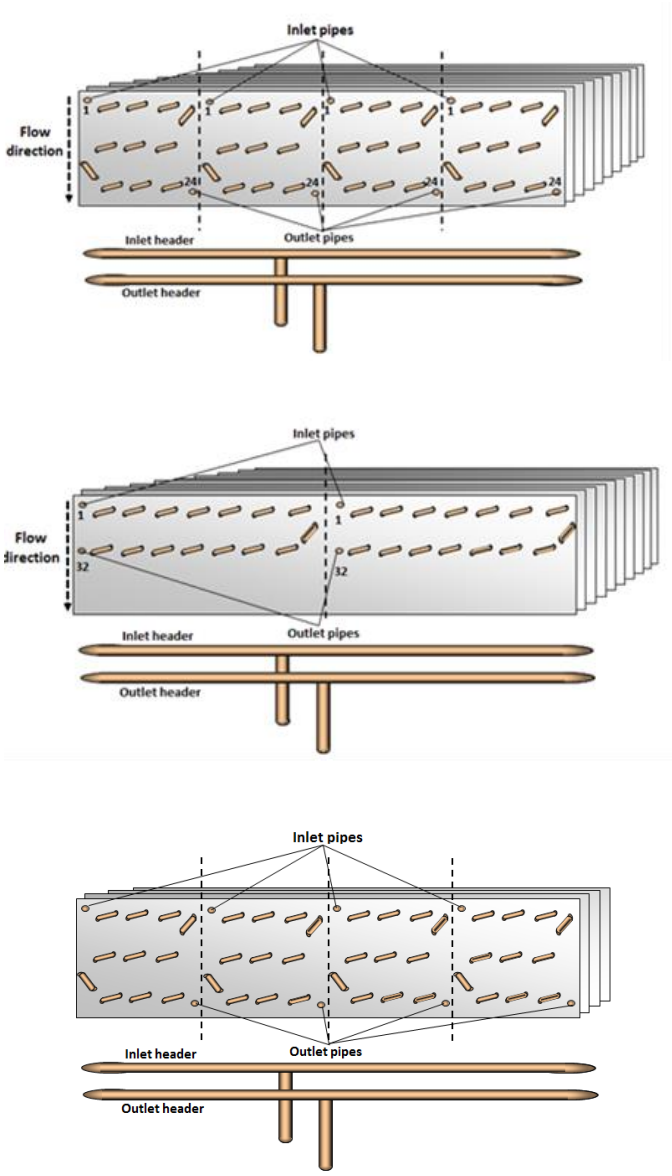

Figure 5.11 Air cooled heat exchangers under investigation

These three heat exchangers were installed in the CO_2 system separately and tested at the same operating stages of intermedium and medium temperatures and pressures and air flow parameters. The air-on flow temperatures varied between 19°C to 36°C and flow rates were modulated from 2000l/s to 2800 l/s through fan speed controls. Consequently, both heat exchangers operated at condenser and gas cooler modes.

All the pipes, bends and couplings used to connect the gas cooler/condenser with the rest of CO_2 circuit complied with EN 10216 (2014) and EN 10305 (2010) standards.

The condenser/gas cooler pipes joints made by a specialist who certified as the EN 287-1 (2011) specified.

The gas cooler employs two main fans located above the heat exchanger coil and support it by the metallic enclosure frame of the gas cooler. Those fans are manufactured by EBM-PAPST Mulfingen GmbH & Co. KG and the type of fans is S3G500-AE33-11. The blades are made by PA plastic and the rotor by cast-in with PA plastic. The nominal speed is 1250rpm and the maximum power input is 0.69 kW. The maximum operative range is 110 Pa. The fan speed controlled from 0% to 100% by using a power inverter. The power consumption of the fan for different power inputs is described in Appendix E.

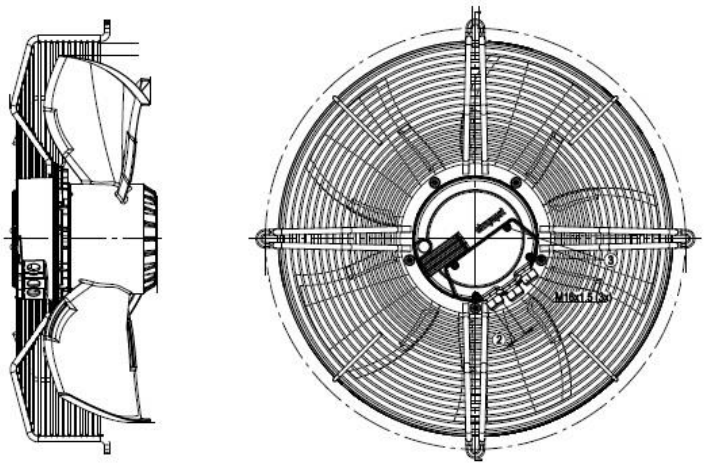

Figure 5.12 C/GC propeller fans

As it mention before, above the two main fans there is four smaller air fans installed oppositely along the direction of pipe length, which will be switched on if the air on temperature is controlled to be higher than ambient. The recirculation fans have been integrated with PID temperature controller which take a feedback from the air outlet temperature and depending on the set point, operate the fans with the required speed.

If the mixed air flow temperature from the ambient and by-passed air temperature is still lower than the designed air on temperature, an electric air heater installed just below the heat exchanger is controlled to turn on in order to maintain the air on temperature.

The air heaters have been installed exactly below the coil to minimize the temperature losses to the ambient. Figure shows the air heaters installed positions.

Figure 5.13 Air heaters

The air heaters capacity is 3 kW each with total capacity of 12 kW. The heaters are divided into group of 6 kW each and controlled separately. The heaters control is integrated with the by-pass air inlet temperature to maintain the requirement temperature. The CO_2 gas cooler/condenser test rig is illustrated in Fig. 5.14.

Figure 5.14 C/GC test apparatus

The side of the gas cooler has been isolated by using thin metallic sheet in order to avoid the air coming from the side to mix with the air from by-pass tunnels and air heaters. For that reason the floor constructed with metal open type material.

5.2.5. HIGH PRESSURE VALVE - ICMT

The high pressure valve is made up of two Danfoss components, the ICMT valve and the ICAD 600TS actuator. The actuator can be dismantled by three small sockets without breaking into the refrigerant circuit and the valve can be controlled by manual valve.

This valve regulates the pressure inside the gas cooler to maintain an optimum COP during transcritical operation and degree of sub-cooling during the subcritical operation. The valve is designed for high pressure CO_2 systems where the pressure is equal or below 140 bar.

Figure 5.15 ICMT motorized valve

The ICMT valve can be used in systems with flash gas bypass, parallel compression as well as for stand-alone applications. The most typical application where the ICMT applied is the flash gas bypass.

The degree of opening for the ICAD 600TS is controlled via a modulating analogue signal 4 – 20 mA for normal running operation or a digital ON/OFF signal. At the top of the actuator there is an advanced Man Machine Interface (MMI) including a small display where the opening degree is displayed.

The ICMT valve is controlled by the Danfoss EKC 326A controller. The controller received a feedback from a S2 Gas temperature probe and a high pressure transducer. Both are located at the outlet of the gas cooler/condenser.

The design parameters of the ICMT valve and the integrated EKC controller are also involving the intermediate receiver pressure independently. The temperature difference at the receiver is not significantly affects the sizing the valve. The valve is act as a pressure control device for the gas cooler/condenser and expansion valve of the refrigeration circle.

In order to find and use the correct ICMT valve for this system calculations have been made at the early stage of the designing process. At the beginning the valve has to be calculated as a simple expansion valve in the liquid line of the refrigeration system. As recommended by the manufacturer the expansion valve has to be calculated with the following conditions of 30 °C condenser outlet temperature, assume that the evaporating temperature is equal with the refrigerant temperature at the receiver and there is 0 K of subcooling. For a winter conditions the valve has to be calculated for condenser temperature equal to 15 °C and 5 K subcooling.

The temperature range for the valve is -60 to 120 °C and the maximum operating pressure is 140 bar-atm. The minimum opening degree which has been tested is 12% of the total opening. Below this value the pressure at the gas cooler/condenser was extremely high and the system COP was reduced dramatically.

5.2.6. BY-PASS ICM VALVE

For new CO_2 systems a CCM valve is introduced to operate as a by-pass valve at the gas side of the receiver. When the CO_2 system at Brunel University designed the CCM was not available at the market. For this reason an alternative ICM valve was designed and installed in the system.

The ICM motorized valve employs a PID controller, which keeps the pressure in the liquid receiver down to a level the user of the system decides. The valve consists of three main components: the valve body, the combined top cover / operating module, and the actuator.

After the ICMT valve the flow is divided in into a gas and liquid and entry to the receiver. The ICM valve has been install at the top side of the liquid receiver where the gas phase is bypassed and mix with the refrigerant outlet form the evaporator before flow to accumulator and then to compressor suction line.

Moreover, the bypass valve ensured that the evaporator is feeding with only liquid phase, which gives us the opportunity to use higher-grade of copper pipe rather steel that we use in the rest of the system. The maximum opening pressure differential is 52 bar and the temperature range is -60 to 120 °C. In order to ensure that the operating pressure is kept below the maximum allowance of the valve; a pressure relief valve

(PRV) has been installed between the receiver and ICM. The design consideration for the PRV valves is illustrated in the next sub-chapters.

The motorized ICM valve integrated with a PID controller supplied by Danfoss. The EKC 347 controller is regulates the liquid level controller. A feedback signal transmitter constantly measures the refrigerant liquid level in the receiver.

The liquid level and the pressure inside the receiver are two different parameters. The pressure inside the receiver is not a proportional of the level of the refrigerant. The refrigerant level is calculated by the cooling load and the number of the evaporator which the system must be supply. As it mention before, the pressure is controlled by the ICMT valve and the integrated EKC 326A controller. This controller has a Failsafe feature in the event the receiver pressure drops below the set point of the system. In case of the pressure of the receiver reach the lower pressure level then the controller send a signal to the ICMT valve to open fully and increase the pressure at the receiver.

5.2.7. LIQUID RECEIVER

The liquid receiver has been designed for two main purposes. Firstly, the receiver operates as a storage to maintain fluid when the system components require servicing or when the system shuts down after an operation or due to scheduled maintenance requirements. At each inlet and outlet pipe of the receiver, for maintenance purposes, a high standard ball valve has been installed to separate the receiver from the main system. The second purpose is to act as a separator, where the liquid CO_2 flows to the evaporators and gas returns to the compressor suction line through an ICM by-pass valve.

After the ICMT valve, the gas and liquid enters to the receiver where the ICM valve used to reduce the pressure in distribution systems. By suppling only liquid to the evaporators we ensure the possible use of standard pressure components in the liquid side and greater cooling performance in the system.

The design criteria were used to determine the size of the receiver described in the following bullet points.

- Vessel size should be sized to enable full pump-down of the system. The total volume of the vessel should be equal with the full refrigerant charge of the system.

- The gas by-pass pipe outlet connection should be at the top of the receiver to avoid trap of liquid refrigerant.
- The orientation and outer diameter of the vessel must be calculated based on the available space inside the compressor rack.

By considering the volume of all the components of the CO_2 transcritical booster system including the pipework between each component, the dimension of the liquid receiver and the fluctuation of the liquid level during standstill or normal operating condition were investigated. In additional, considering the available space for the liquid receiver, only the vertical solution has been investigated. The refrigerant charge for each component and the state and volume for each component has been calculated.

Some assumptions have been made such as the standstill pressure in the receiver equal to 26 bar and running pressure of 32 bar. The fluctuation in the liquid level is investigated under different ambient conditions and running pressures.

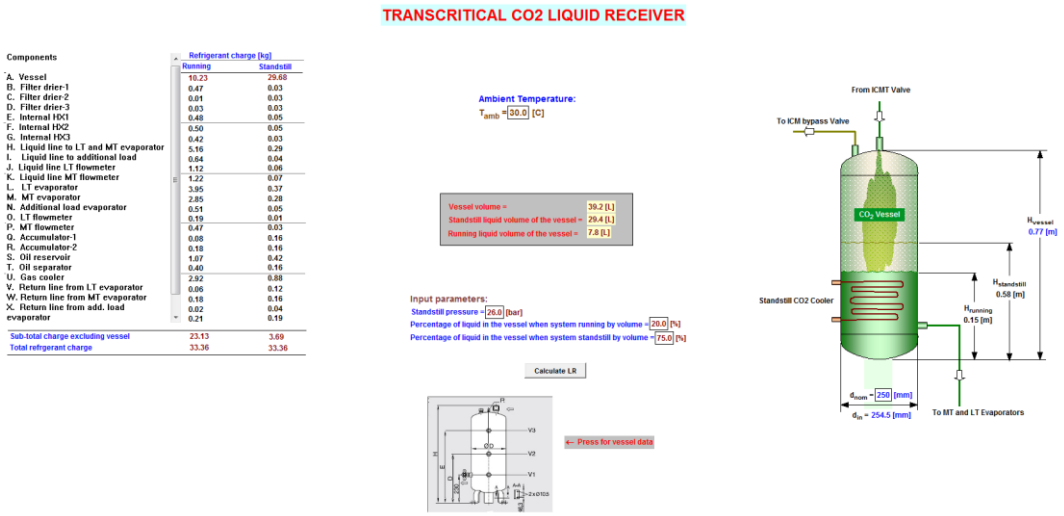

Figure 5.16 Liquid receiver design model

The CO_2 liquid receiver is a vertical custom build receiver manufactured by Klimal Italia Srl with total volume of 40 litres with external surface area of 0.8 m^2 and 33.6 kg of total mass charge. The liquid vessel was tested at 71.5 bar with specified maximum allowable pressure of 55 bar. Three sight glasses have been fitted at the bottom, middle and top of the vessel in order to detect the CO_2 liquid level during the charging, normal operation and shut-down operation.

Figure 5.17 Liquid receiver installed in CO_2 system

In case of a power failure during the running operation of the system, an additional standstill condensing unit has been installed inside the receiver. This unit is connected to an additional safety cooling circuit and preventing the CO_2 inside the receiver dangerously high pressures above the design pressure of the receiver. The condensing unit and communications and controller layout are described in 5.3.8.

5.2.8. STANDSTILL CONDENSING UNIT

The standstill condensing unit is a safety unit feature of the system. It consists of hermetic scroll compressor with capacity of 1.5 HP, accumulator, condenser, a single one speed fan, oil filter and dryer, thermostatic expansion valve and a pressure switch to avoid damage the hermetic compressor for any extremely high pressure. The condensing unit based on the plate and deigned to allow easy installation. It is located at the roof next to the condenser/gas cooler test unit as it shows in Fig. 5.18 and referred as a sub-cooler chiller unit. The condensing unit at the top of the roof integrated with the coil which is located at the bottom part inside the liquid receiver. The thermostatic expansion valve has been installed exactly before the receiver at the liquid side of the system. The unit uses R-404A as a refrigerant with maximum refrigerant charge of 8.4kg.

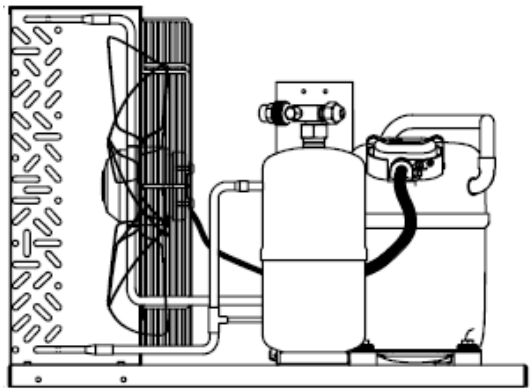

Figure 5.18 Liquid receiver condensing unit

In additional the condensing unit keep a constant pressure of 32 bar when the system running under really high ambient temperature conditions. A set pressure of 26 bar used when the system is out of operation but filled with CO_2 gas to avoid any extremely high pressure and damage of the components.

5.2.9. FLOW DIAGRAM OF RECEIVER CONTROL

The integrated flow diagram of the receiver pressure control layout and control communication is illustrated in Fig. 5.19

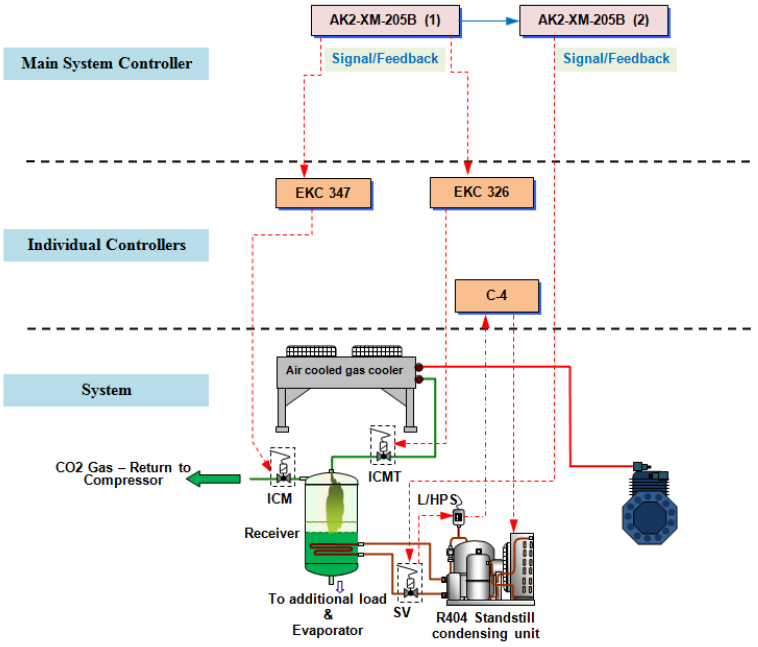

Figure 5.19 Receiver control and feedback

The control layout consists of the ICM and ICMT valves, the condensing unit expansion valve, the integrated individual controllers for each valve and the main CO_2 control system.

5.2.10. COMPONENTS BEFORE THE MT EVAPORATOR

In this section the components which have been installed before the MT evaporator are described. These include the coriolis refrigerant flow meter, pressure transducer and the AKV valve.

5.2.10.1. REFRIGERANT FLOW METER

The refrigeration capacity of the MT display cabinet is determined by calculating the amount of heat absorbed by the evaporator coil. The calculations procedure involves the enthalpy difference across the coil and the mass flowrate of the refrigerant circulating through the evaporator coil.

Figure 5.20 KHRONE mass flow meter

In order to ensure that the mass flow rates are reasonably measured a KROHNE – Optimass 3000-S03 is used. The measurement uncertainty for this type of flow meter is ± 0.035%. However, the level of the accuracy effected from the gas bubbles arising in the liquid line. The risk of inaccuracies is higher when the ambient temperature is above the critical point of CO_2 refrigerant. For that reason, the liquid line from the outlet of the receiver until the inlet at the evaporator coil was insulated with Armaflex 25 mm–class 0 insulation.

The maximum flow rate capacity for this type is 0.036 kg/s and ambient operating conditions between -40 °C to +55°C.

5.2.10.2. PRESSURE TRANSDUSER

The inlet pressure before the evaporator coil was measures by using a Danfoss pressure transmitter with ratiometric output signal. The measurement accuracy for this type of transmitter is equal to ± 0.3% with response time of < 4 ms. The operating temperature range is between -40 °C to +85°C.

Figure 5.21 Pressure transducer used on the system

(Source: Danfoss 2008)

5.2.10.3. EXPANSION – AKV VALVE

The electrically operated AKV expansion valve has been chosen for the DX evaporator. The electronic expansion valves are installed exactly before the evaporator inlet (liquid line). The main advantage of this type of valves is the possibility to integrate with the cabinet controller and change easier the operating conditions for the cabinet even if the system is running.

Figure 5.22 AKV expansion device

(Source: Danfoss 2008)

The superheat control of the CO_2 evaporators is difficult to controlled comparing with the traditional HFC refrigerants.

The AKV valve is a pulse-width-modulating valve supplied by Danfoss and it is especially designed for supermarket application. The valve maintains the superheat value at the evaporator based on the operator settings by closing and opening 0 to 100%. The maximum operating pressure difference across the valve specified to be equal to 18 bar with maximum operating pressure of 52 bar.

Based on the available AKV types on the market the following Fig. 5.23 illustrates the performance characteristics of the AKV type.

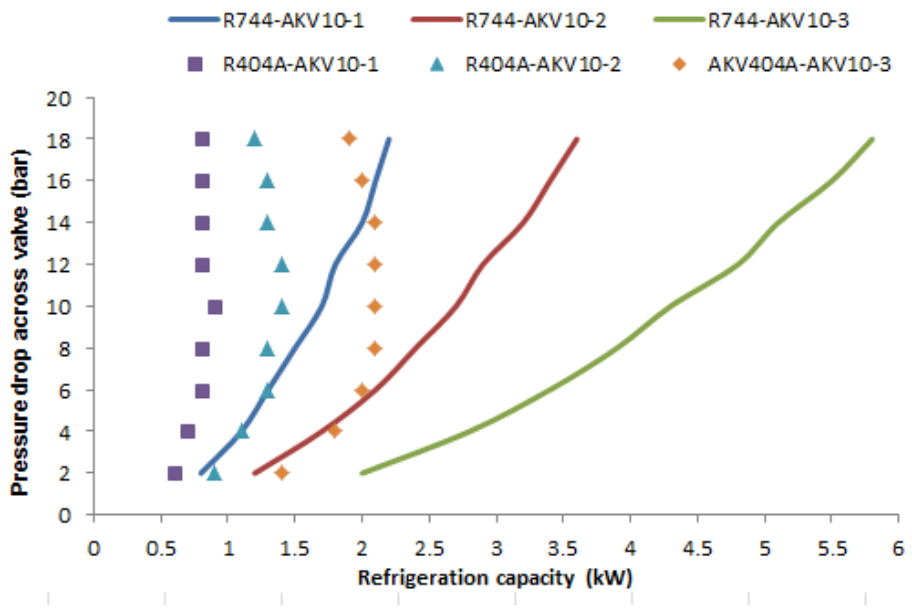

Figure 5.23 Performance characteristics of the AKV valves

5.2.11. COMPONENTS BEFORE THE ADDITIONAL LOAD

The liquid line feed the additional load divided with the one which supplies the MT evaporator after the receiver and before the coriolis flowmeter. A pressure transmitter and AKV valve are fitted on the pipe line before the entering to additional load coil. The type of the pressure transmitter and AKV valve are the same with the evaporator pipe line and described in 5.3.10.2 and 5.3.10.3.

The mass flow rate is calculated by the energy balance between refrigerant and brine side. Moreover, the refrigerant passes through the additional load is double checked by the total amount refrigerant passes through the condenser/gas cooler by subtract the bypassed refrigerant in ICM valve and the refrigerant travels to MT evaporator coil. This will be explained in details in the next chapters.

5.2.12. REFRIGERATION LOAD SYSTEM

The initial design of the system involved two refrigerated display cabinets with full load refrigeration capacity of 9 kW which provided by 6 kW medium temperature (MT) cabinet and a 3 kW low temperature refrigerated display cabinet. Because the lowest LT compressor was not stable due to the higher capacity of the LT compressor which was commercially available at the time; the LT cabinet was removed from the chamber room and the valves supplied this side of the system was shut. However the capacity of the system by using those three condensers/gas coolers was much higher than the cooling capacity of the MT by its self, the system was unstable. Even the application of a variable speed controller could not reduce the compressor capacity as low as the designed MT load; a medium temperature additional load (AL) was added to the loading system to balance the capacity of the system when one or two compressors worked in parallel.

How the additional load effect to the piping pressure drop has been also been investigated using an EES model. The pressure drop in the short pipe from after the liquid receiver and where the MT and AL pipes are split; and at the mix point where the MT and AL outlet are connected before the compressor were still in acceptable range.

5.2.12.1. REFRIGERATED DISPLAY CABINET

For the medium temperature refrigerated display cabinet a chilled open vertical multi-deck cabinet was used. The cabinet was initially designed for R-404A refrigerant. However, this cold was removed and a new direct expansion (DX) coil was fitted in the cabinet.

The MT cabinet manufactured by Carter ELFM with open length 2.47 m. and 4.2 m^2 display area. The depth is 1.13 m. and the length equal to 2.05 m. The circulation fans are located below the base self of the cabinet.

Figure 5.24 shows the schematic diagram of the MT cabinet and the installation point at the test chamber.

The cabinet were loaded with products to simulate the real supermarket situation which consists of “M”- packages and plastic containers which have been filled with water – glycol (60/40%).

Figure 5.24 MT display cabinet

The location of the cabinet inside the room, the loaded configuration and the test chamber room conditions are specified by ISO (International Organisation for Standardisation) standards, BS EN ISO 23953-2:2005 Refrigerated display cabinets – Classification, requirements and test conditions, (BSI, 2005).

For monitoring and recording purposes a number of thermocouples were installed at the specified from the ISO standards positions and where a calibrated T-type thermocouple inserted into the geometric centre of the package.

The MT refrigerated cabinet is controlled by Danfoss AK-CC-550A controller. The controller takes the feedback from the air temperature inside the cabinet and controls the flow of the refrigerant enters to evaporator coil by opening/closing (100%/0%) the AKV valve and maintain the superheat at the set point from the user. The feedback from refrigerant temperature at the inlet and outlet of the coil and a pressure transmitter are send to controller which calculates the superheat degree and regulates the cooling capacity of the evaporator. The controller also maintain a constant interval defrost period based on the time settings of the user. Once the cabinet reach the set point

temperature or operates in defrost period the controller shut AKV valve and stops the flow to the evaporator. During this period the fan are operates as normal.

5.2.12.2. ADDITIONAL LOAD

The additional load has been installed to the CO_2 test rig in order to balance the capacity of the HT compressors and also provide better results for the condenser/gas cooler. The system has been tested without this additional load; the compressors were worked for a few minutes and then stop. Once the MT cabinet temperature was higher than the set point a feedback signal send back to compressors in order to run again. If this happened really fast a safety feature of the compressor kept those OFF-running for 3 minutes after the last run. This issue caused a really high temperature inside the MT cabinet, the system was unbalanced and the power consumption was higher than the compressor run in variable speed control mode.

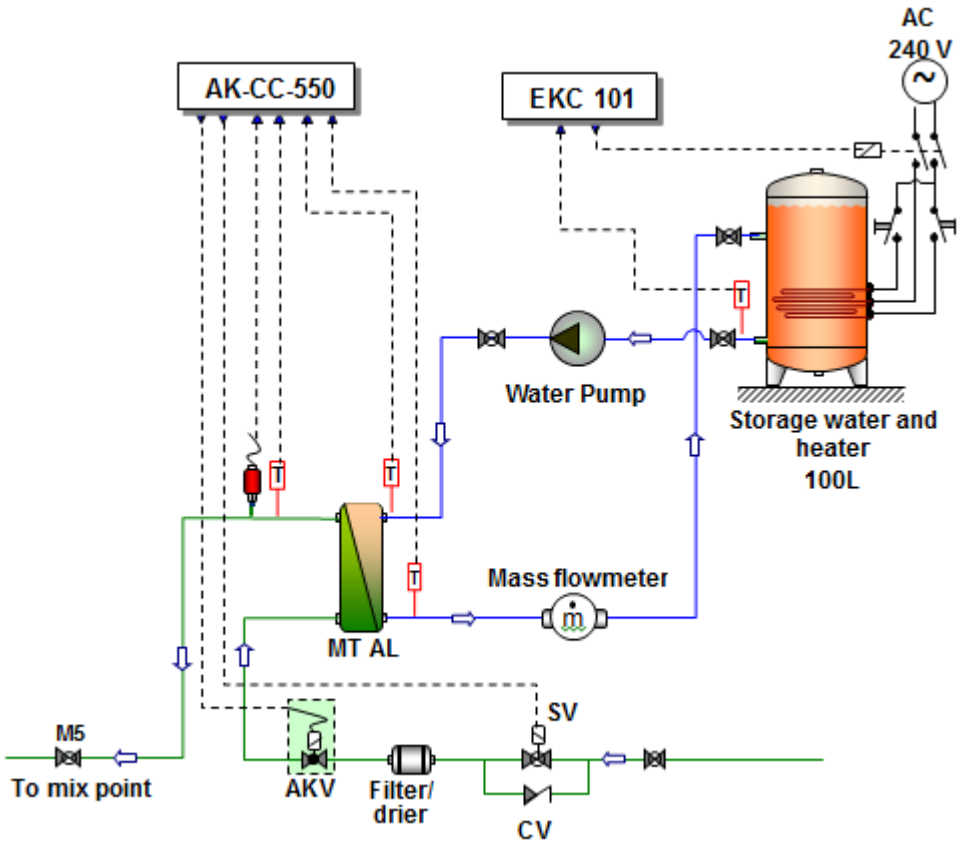

Figure 5.25 Additional load configuration

The additional load consists from a storage water tank where a heater has been installed inside and heat-up the brine (water/glycol) side. In additional on the brine side of the system a water pump, a water mass flow meter and manual flow control valves have been installed. For the refrigerant system an AKV expansion valve has been installed at the liquid side.

The evaporator HX of the additional medium temperature load system is a plate type heat exchanger (PHX) HX: B15Hx30/1P-SC-M from SWEP Inter. with capacity 6-8 kW at evaporating temperature –6°C to - 8°C respectively, and 10K superheat. The cold-stream (refrigerant CO_2 side) of the heat exchanger absorbs heat from the hot-stream (brine side) of the heat exchanger. In this case the system acts as a MT DX evaporator.

The function of the AKV is controlled by a Danfoss AK-CC-550A which is the same like the MT display cabinet controller. The controller maintains the degree of superheat based on the operator settings.

The solenoid valve (SV) is used to regulate the refrigerant flow at the liquid line as it illustrated in Fig. 5.25. Once the system reaches the set point temperature the SV valve is shut. The refrigerant which flows to this side escapes from the non-return valve (CV). This safety feature protects the pipe line and HX from damage that may be caused by backflow or liquid trapped in the pipe.

For the brine side of the additional load, the circuit was filled with propylene glycol of 40% mass fraction in water solution. The solution has a freezing temperature of -15 °C and used in order to protect the pipe line and HX from ice blockage. The circulation brine pump is a manufactured by Grundfos type CH-2-30 with flow capacity of 1.5 m^3/h, minimum operating temperature of -20 °C and maximum head 30 m. The water circulated around the system is storage in 100 litres water tank which has been insulated with 50mm polyurethane foam to avoid the heat losses to the environment. At the bottom part inside the water tank two immersion heaters of heating capacity 4 kW each has been installed. Both regulated by Danfoss EKC 101 temperature controller. Depends on the temperature settings on both immersion heaters the capacity can vary between 1 to 8 kW. For those series of tests the capacity which used varied between 6 to 8 kW. The flow meter is used to measure and record the brine mass flow rate. In additional this flowrate was used to determine the duty of the additional load and

calculates the mass flow rate for the refrigerant side by using the energy balance equation.

5.2.13. AUXILIARY-CONTROL-ISOLATION-OVER PRESSURE PROTECTION

The auxiliary components which have been installed on the system include a refrigerant accumulator, sight glass, filter drier and pressure gauges. The control and isolation valves should be located so they cannot trap liquid refrigerant during the normal period. Another important parameter for the CO_2 refrigeration systems is the safety actions that the designer has to consider. The system is protected from the abnormal pressure levels with a number of pressure relief valves (PRV).

5.2.13.1. AUXILIARY COMPONENTS

The accumulator is installed at the suction line of the HT compressors. For the parallel arrangements compressors only one accumulator is required. Therefore, the accumulator has been design to facilitate when both compressors working in full load. The suction line accumulator manufactured by ESK Schultze and is a type FA-12-CD with 0.8 litres volume. The main function of the accumulator is to protect the compressors from damage by preventing liquid droplets (after mixing point of bypass/MT/AL) from entering from the compressor suction line to main body.

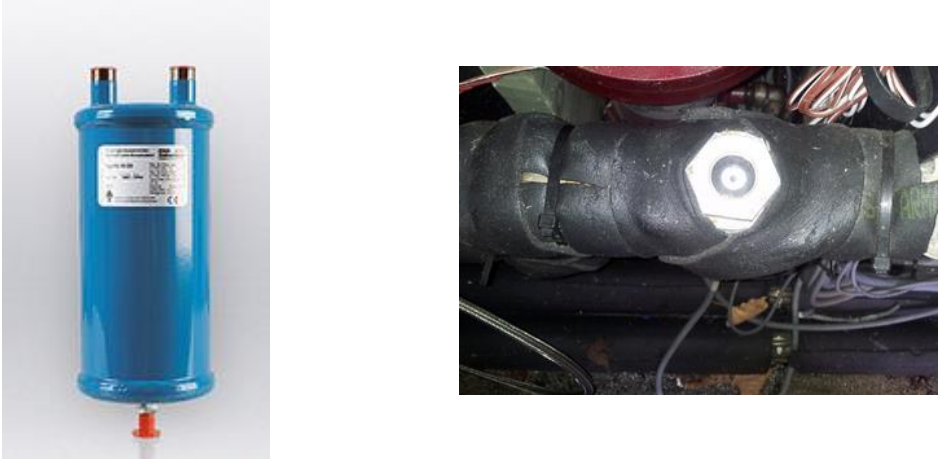

Figure 5.26 Auxiliary components

The sight glass has been fitted at the liquid line of the MT refrigerated display cabinet before the coriolis mass flow meter. This is manufactured by Danfoss and is a type SGN. The sight glass is used to monitoring the refrigerant flow downstream to evaporator coil.

A number of gauges have been fitted on the side of the CO_2 rack to monitoring the pressure during the normal operation, charge or maintenance procedure.

A total number of five pressure gauges have been installed on the system including HT and LT suction pressure, liquid pressure inside the receiver, gas cooler outlet pressure and HT discharge pressure (bottom to top in Fig 5.27).

Figure 5.27 Pressure gauge used on the CO_2 system

The gauges pressure range varies from 0 to 160 bar and are suitable to use for high pressure applications such as a CO_2 refrigeration systems. The gauges are OMEGA ENGINNERING type PG63-70S. The gauges were an additional safety feature when the system was charging.

On the liquid lines upstream of the expansion valves of both MT display cabinet and AL, two filter drier are installed to prevent any debris to enter and damage the valves.

5.2.13.2. CONTROL & ISOLATION VALVES

Sufficient valves have been fitted to minimize danger and loss of refrigerant during the service and maintenance of the system. The seals have been replaced a frequently opened/closed process.

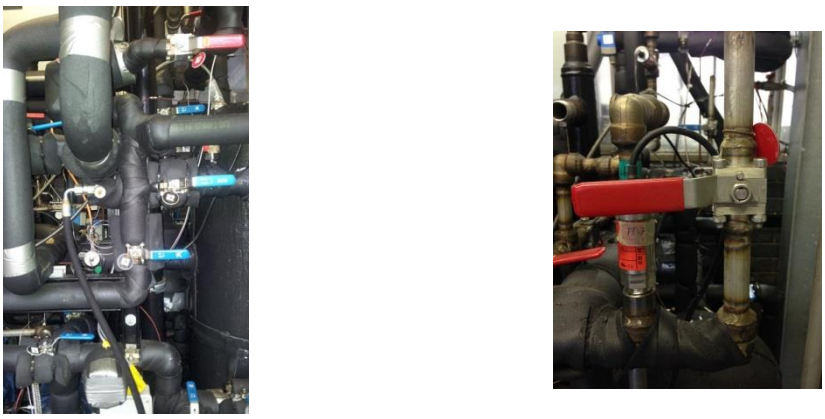

Figure 5.28 Control ball valves

A three piece stainless steel ball valve with reinforced PTFE sat and ISO mounting top have been used. The two pieces are welded to the stainless still pipe and four bolts are used to touch and seal the three pieces including the main body. This make easier to replace the PTFE sealing in case of damage.

During the normal operation of the system a problems with ice formation were faced, especially on the liquid lines downstream to MT and LT and the receiver liquid side. To protect the valve body thick pipe insulation is used to cover the body of the valve and main pipe line. In case of emergency one of the valve had to shut and ice formation was covered this, the sealing was broker and a tinny leak was appear. This part of the system was isolated and the refrigerant was disposal. Then the PTFE sealing was replaced with a new one.

5.2.13.3. OVER PRESSURE PROTETCION

The CO_2 refrigeration system is protected from abnormal pressures by using pressure relief valves (PRV). Main considerations and design criteria for the over pressure protection are described below.

- The PRV must be design and operates at the maximum allowable pressure (PS) as defined in EN378 or for individual items.
- PRV is fully open at 1.1 x PS for pipework or individual components
- The PRV must be vent to a safe place
- The high pressure switch on the control system should be set at 0.9 x PS

Figure 5.29 PRV valves

The relief valves have been fitted in MT, LT, AL liquid lines to protect the system for high pressure and cause any damage to pipe itself of the evaporator coils and plate heat exchanger respectively. Another PRV has been fitted in high pressure side of the system and especially at the condenser/gas cooler. During the charging process or power failure the pressure inside the receiver is become uncontrolled even if the safety feature of condensing unit is used. Therefore, a PRV valve has been installed at the liquid receiver. The minimum required capacity of the PRV for the liquid receiver is a proportional of the external area of the receiver, the density of the heat flow rate and the heat of vaporization at the set pressure which is based on the bullet points above. The Equation 5.6 illustrates the minimum discharge pressure which is required for the PRV.

$$Q_{PRV} = \frac{3600\ \varphi\ A_{rec,out}}{H_{vapor}} \qquad 5.6$$

Where Q_{PRV} = minimum required discharge capacity of the pressure relief valve (kg/h); φ = density of heat flow rate (kW/m^2); for the standard vessel used this is 10 kW/m^2; $A_{rec,\ out}$ = external surface area of the liquid receiver (m^2) and H_{vapor} = heat of vaporization (kJ/kg) at the set pressure. On the end of PRV there is no pipe work installed in order to avoid a potential dry ice form which can cause a blockage on the PRV. All the PRVs were vented to a safe area without cause a potential problem to operators or other equipment next to it. The PRVs supplied by Seetru Limited. The main body is made by bonze brass seat and use a viton a seal material. In case of the receiver the set pressure for the PRV to open is 46 bar. The total flow area is 70.8mm^2 with maximum flow area of 0.77 kg/s.

5.2.14. PIPING DESIGN

The higher operation pressure of the CO_2, especially in high temperature side of the system means further consideration must be given on the distribution pipe work materials and supports used. Therefore, all pipe work must design to withstand the pressure associated with the operation of CO_2 system. The outside diameter (OD) is usually smaller than the system of same capacity working with HFC refrigerants because the CO_2 has greater capacity as has been explained in Chapter 2.

Table 5.2 below illustrates the reference suction and liquid lines pipe diameters (OD) for CO_2, R717 and R404A.

Table 5.2 Suction and liquid lines diameters

	CO_2	R717	R404A
	mm	mm	mm
Suction	12	28	22
Liquid	6	8	5

The internal dimensions (ID) of the pipes are selected to be large enough to keep the pressure drop higher between the individual components. Also, with bigger internal diameter the refrigerant circulates with higher velocity which means that the oil carried by the refrigerant is distributes around the system more efficiently. Base on the above considerations the recommended pipe dimensions, lengths and materials are shown in Table 5.3.

Table 5.3 Pipeline circuit design materials

Pipe line	Max allowance	ID	Length	Vel.	Material
Suction HP	52	13.9	5	16.4	5/8 Copper
Discharge HP	130	12.5	10	7.5	3/8 Stainless
C/GC out	130	12.5	10	-	3/8 Stainless
Liq. After rec.	52	13.7	10	0.6	5/8 Copper
MT liquid	52	10.7	25	0.55	½ Copper
MT suction	52	10.7	25	7.5	½ Copper
AL liquid	52	10.7	20	0.55	½ Copper
AL suction	52	10.7	20	7.5	½ Copper
LT liquid	52	7.52	10	0.7	3/8

					copper
LT suc.	52	10.7	10	12.3	½ Copper

During the construction of the CO_2 test rig a few changes have been made based on the pipe material between the individual components.

5.2.15. SYSTEM MODIFICATIONS

Additional modifications have been made on the system arrangement in order to investigate the effect of the higher cooling capacity on the C/GC operation. Higher cooling capacity means more mass flow rate of refrigerant circulate on the system. One of these modifications was the installation of an additional evaporator coil. The air cooler was connected in parallel with the MT refrigerated display cabinet. This is manufactured by GEA-Searle and is a type KEC 30-6L.

The coil used aluminium "D" fins with fin spacing 6mm and tube pitch along the air flow of 37.24 mm.

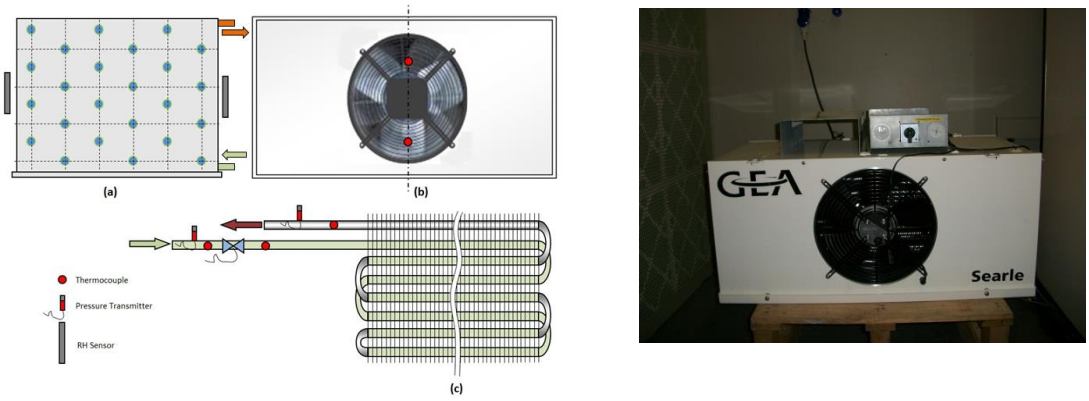

Figure 5.30 AAC unit

The additional evaporator coil is used to balance the system when both of compressors are running and push the condenser/gas cooler to reach the higher heat capacity. The air cooler is controlled by using AK-CC-550A Danfoss controller same as the MT and AL. The controller is associated with a pressure transmitter and AKV same as the MT and AL as described in 5.3.10.3 and 5.3.10.2 respectively. The pipe line specifications for additional air cooler are illustrated below in Table 5.4.

Table 5.4 AAC pipeline design

Pipe line	Max allowance	ID	Length	Vel.	Material
MT liquid	52	10.7	25	0.55	½ Copper
MT suction	52	10.7	25	7.5	½ Copper

Additional tests were done in order to investigate the fluctuation of the air cooler capacities under different tests conditions. The results represented in Chapter 6. The final arrangement illustrated in Figure 5.31.

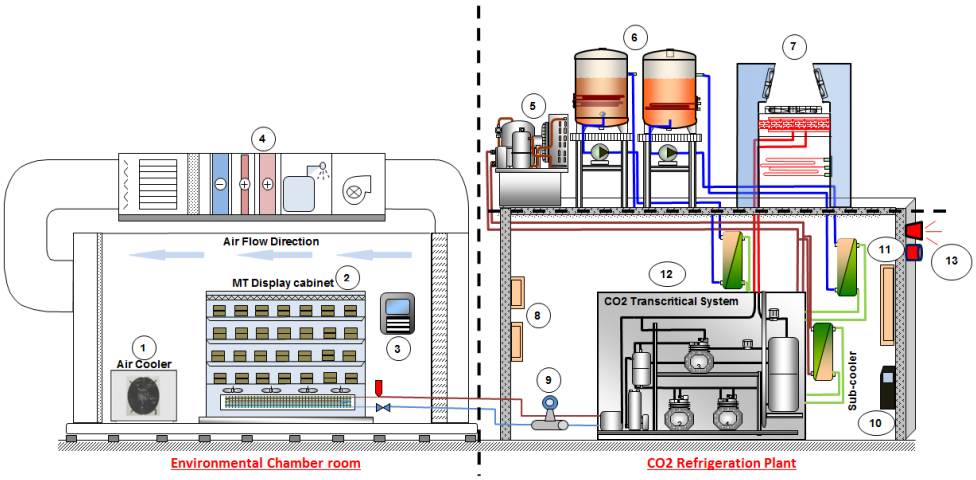

Figure 5.31 CO_2 booster system experimental apparatus

1) Air Cooler (Additional Evaporator) – GEA KEC35-6
2) Medium Temperature Display Cabinet
3) CO_2 System Main Controller – Control CO_2 system equipment (compressor, etc) - Danfoss AK-SC255
4) Air Handling Unit - using for maintain temperature and RH in chamber room
5) Standstill condensing unit – maintain pressure inside the CO_2 receiver (26bar when the is OFF/31bar when its ON)
6) Water/Glycol additional load
7) Condenser/Gas cooler
8) Electrical boxes – Controllers (Fans – Heaters – Additional Load)
9) Coriolis flow meter
10) Compressor Inverter – linked with main controller (3)
11) Electrical/Electronic/Controller main box
12) Main Transcritical CO_2 System
13) CO_2 Sensors/Alarms

5.3.SYSTEM CONTROL COMMUNICATIONS AND CONTROLLER LAYOUT

The control strategy of the CO_2 booster system involves three main control valves, ICMT, ICM and AKV that integrate respectively with three different electronic controllers: EKC 347, EKC 326A and AK-CC550A. Moreover, the signals transferred to a main controller from the above controllers give us the opportunity to investigate and record system performance under different conditions. The high pressure ICMT valve is installed at the high pressure side of the system just after the gas cooler/condenser in order to control and achieve an optimum discharge pressure (corresponding to the maximum system COP) when the system operates in transcritical mode. It also acts as an expansion valve/device to reduce the high pressure to an intermediate pressure stage before reaching the liquid receiver. A pressure transmitter and temperature sensor have been installed at the gas cooler/condenser outlet. These two measured parameters, temperature and pressure, will be used as inputs to the ICMT controller. When the system operates in a transcritical mode at higher ambient temperature conditions, the controller will calculate the optimal discharge pressure based on the gas cooler outlet temperature and use it as a setting point for the pressure control by modulating the ICMT valve position. When the system performs in subcritical mode at lower ambient temperature conditions, the controller calculates the actual subcooling at the condenser outlet based on its measurements and controls and obtains a specified subcooling by modulating the ICMT valve position.

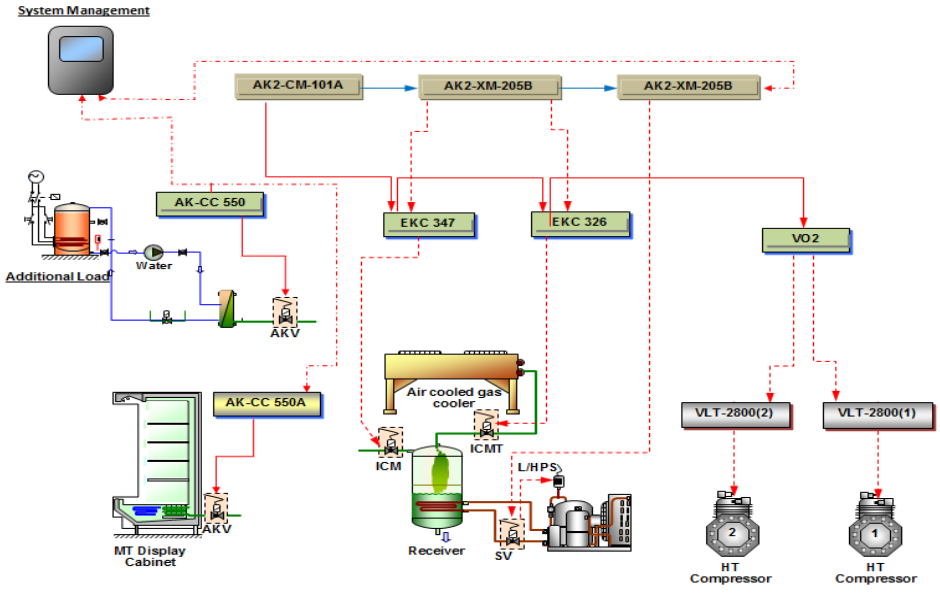

Figure 5.32 System control communications and controller layout

The size selection and calculation of the ICMT valve is a relatively complex process as the refrigerant mass flow changes when the system moves from subcritical to transcritical conditions. The most appropriate way to accurately size the ICMT valve is to calculate it as an expansion valve and take into account the designed pressures and temperatures at the gas cooler/condenser outlet and inside the intermediate vessel as well as the designed refrigerant mass flow rate. After the ICMT valve, the CO_2 flow enters into the receiver and is divided into gas and liquid flows. The ICM motorized valve is also known as a gas bypass valve with a PID controller. The valve is installed on top of the liquid receiver to control a specified liquid level in the receiver which will ensure the evaporator is feeding only during the liquid phase. It can also allow the saturated CO_2 gas to pass and mix with the refrigerant flow from the evaporator outlet before flowing to the accumulator and then the compressor suction line. Two electrically operated expansion valves, AKVs, have been chosen for the DX MT evaporator and additional load. The AKV valve of either the cabinet or additional load also offers the possibility of integrating with the unit controller to simplify operational settings for further investigation of the system. The same capacity control procedure is used for the additional air cooler which has been added to the system later. In general, the overall control communications and controller layout of the CO_2 booster system are shown in Fig. 5.36.

In additional, for the condenser/gas cooler test apparatus an integrated PID control is used to control the air heaters operation based on the air temperature set point from the user. A PT1000 temperature sensor is located at the air inlet; very close to coil which detects the air temperature enters to coil. A feedback signal sends back to a Millennium 3 – SP24 controller where the user used to set the requirement air temperature. If the air temperature is lower than the set point, a signal is transmitted to the air re-circulation fans. As such, part of the hot exhaust air will flow back through the return air tunnels, the return air grills and finally mix with the lower temperature ambient air flow. If the mixed air flow temperature is still lower than the designed air on temperature, the controller is send the signal to the electric air heater installed just below the heat exchanger is controlled to turn on in order to maintain the air on temperature. The Millennium controller is also used to set the main air fan speed according to the test conditions and procedures.

Figure 5.33 Control module

A Danfoss full-store AK-SC 255 controller is used to monitoring all the above individual controllers for each component including alarm functions. This is connected with the communication module with the Universal Analog Input Module (AK2-CM-101A) and Digital Output and Combination Digital Output Universal Analog Input Module (AK2-XM-205B) solutions. Except the main controller which has been located at the environmental test chamber room, all the other electrical and electronic control systems have been installed at the CO_2 machine room. The design has been made based on the "easy to reach" criteria and manual monitoring during the normal operation or service of the system.

Inside the CO_2 test rig, 3 control panels have been installed and operated including the main control panel, additional load (HX evaporator) panel and the condenser/gas cooler air side control panel.

Figure 5.34 CO_2 booster control panel

Figure 5.35 AAC and C/GC control panels

The control strategies for the liquid CO_2 receiver and additional load have been described in 4.3.9 and 4.3.12.2 respectively. The MT compressor is controlled by the main controller AK2-XM-205 which is modulated based on the suction pressure and temperature. The upper and lower limits of the compressor used as the set point for the on/off switch to avoid any damage on the system. The VLT-2800 controllers are used to

operate the compressor with variable speed between 65 to 100% or for fixed speeds of 80% and 100% depending on the test procedure.

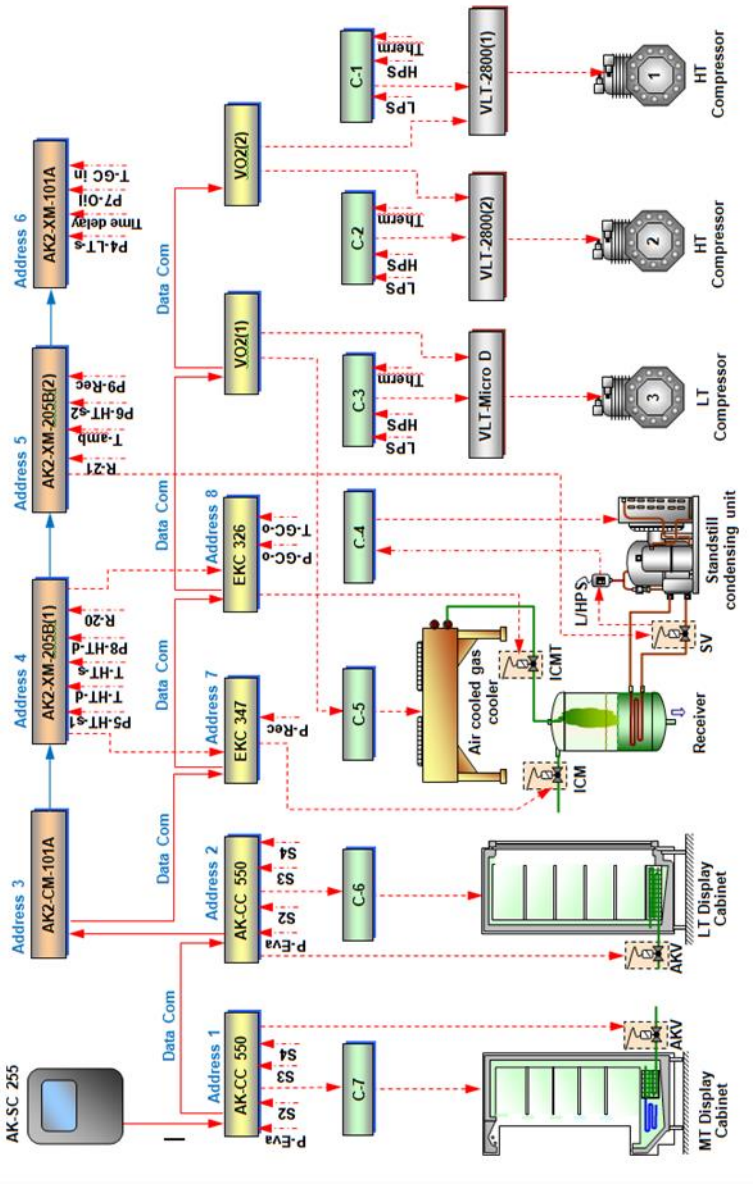

Figure 5.36 Control strategy applied to the CO_2 refrigeration test rig

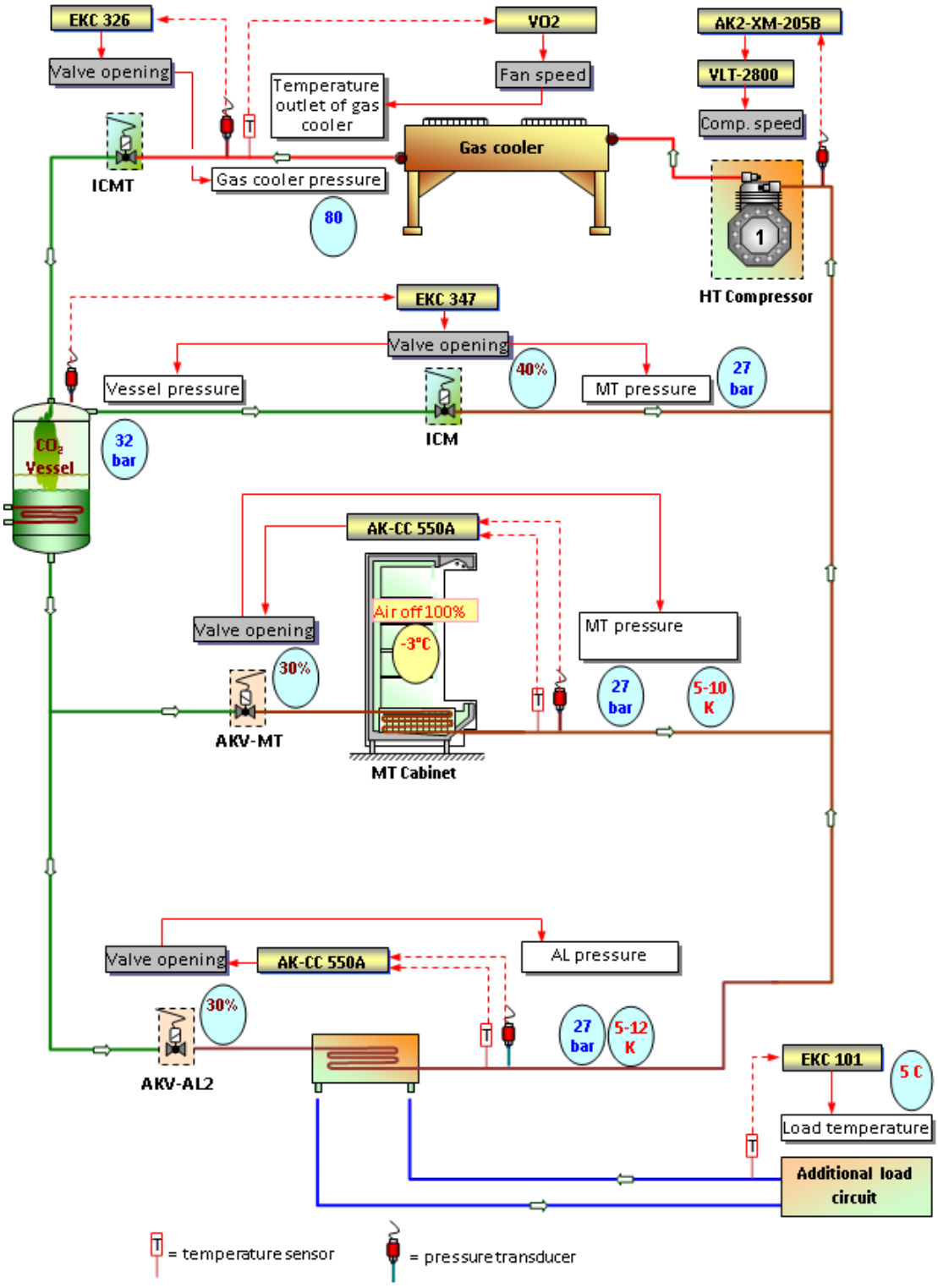

Figure 5.37 System communication and feedbacks

The values shows in Figure 5.37 are the set values on the controllers which have been described in this chapter for the individual components.

5.4.EXPERIMENTAL TEST MONITORING

The test facility is comprehensively instrumented with pressure transducers, thermocouples and coriolis refrigerant flow meter to enable a detailed experimental investigation of the system and individual components under different operating conditions. In addition, the relative installation positions of the main components in the system are shown in previous sub-chapters. A number of hand held equipment have been used for data monitoring and record such as thermometer, relative humidity, air velocity, infrared camera.

5.4.1. TEMPERATURE & PRESSURE SENSORS

For the temperature measurements a T-type and K-type thermocouples were used. The K-type thermocouples have been used for the condenser/gas cooler test rig and the T-type for monitoring and recording the rest of the CO_2 booster system. 1Both thermocouple types have a temperature measurement range -250 °C to 300 °C with a specific error of ± 0.5 °C. All the thermocouples have been calibrated before installed in the system. For the calibration purposes, a calibration bath with a precision hand held thermometer (ASL type F250 MK II, probe J 100-250-10-NA) is used. The reference probe has an uncertainty equal to ± 0.04 °C and the temperature range of the calibration was -12 °C to 120 °C depends on which side of the system are connected.

For the PIDs controller the thermistors type PTC-1000 were used which, is recommended from the controller manufacturer.

A number of pressure transducers were installed along the pipe line of the test rig. Those are connected on the inlet and outlet of the main components of the system. All the pressure transmitters are supplied by Danfoss. The pressure range was varied based on the pressure side of the system. The type AKS 32 with output voltage of 0-10V d.c. is used to integrated with the individual controllers. The higher pressure measuring range transducers are used for discharge line of the compressor and inlet and outlet of the condenser/gas cooler.

Based on the input voltage and output current of each transducer have to be circuited with a resistor in order to change the output current to become an output voltage and allow the data logger to record the real values. The coefficient of correlations of the pressure transducers were above 99.9% with manufacturer uncertainty of ± 0.3%.

The refrigerant flowmeter which has been installed and record the CO_2 liquid which the system feed the MT display cabinet are shown in 5.3.10.1.

5.4.2. CONDENSER/GAS COOLER MONITORING

The condenser/gas cooler test rig has been comprehensively instrumented to detailed measurement data and overall performance description of the heat exchanger itself and its integrated CO_2 refrigeration system. These include two thermocouple meshes with 24 points each to measure air-on and air-off temperatures; pressure difference of air flow through the heat exchanger to get the air side pressure drop, air flow velocity to obtain the air flow rate. For the refrigerant side, 2 to 6 pressure transducers are installed inside the inlet and outlet headers and one circuit of the heat exchanger to measure overall and heat exchanger refrigerant side pressure drops. In addition, a large number of thermocouples are attached on all the pipe bends along the pipes of one circuit to measure the refrigerant temperature variation or profile from inlet to outlet. Instead of directly measuring the refrigerant mass flow rate, it is calculated from the heat exchanger heat balance between the air and refrigerant sides.

A number of equipment were used to monitoring and record the transition and steady state condition in condenser/gas cooler (C/GC) test apparatus including the air pressure difference transmitter, air velocity meter, infrared thermography (IR) camera and power meter.

In additional, the number of the sensors which have been used to record the C/GC data required to build an individual data monitoring station separate from the rest of the CO_2 system.

A KIMO CP 200 pressure transmitter is used to measure the air pressure difference. Two pitot-tubes have been fitted at the inlet and the outlet of the coil is used to calculate the pressure difference.

To measure the air face velocity a Velocicalc Plus 8386A-M-GB, a TSI product, with measurement range 0m/s to 50m/s and uncertainty ± 3% is used. The air velocity is measured for main fan speed range from 10 % to 100 %. Based on the air velocity, the air mass flow rate was calculated. The measured air mass flow rate is used to calculate the refrigerant mass flow from the energy balance of the system.

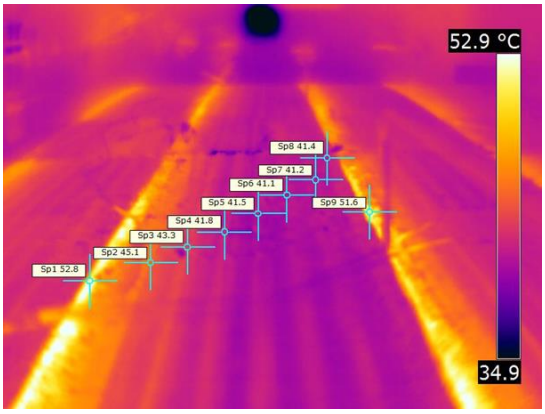

Figure 5.38 IR image from C/GC

An IR camera is used to record the temperature profile colour pattern of the C/GC. A small access-hole has been done on the metallic cover of the C/GC coil which allows capturing the temperature variation along each circuit. Figure 5.38 shows the temperature distribution across the C/GC as recorded by using the IR camera.

A portable FLUKE 435 power quality analyser was used to record the main fan power consumption for different air volume flow rates. The fan power was modulated by the inverter. Therefore, the fan power consumption was recorded from 10% to 100% of the total power. The recorded values were used for the COP calculations.

5.4.2.1. C/GC MONITOR STATION

The large numbers of the sensors were installed in the C/GC test rig requires an individual data logging and monitoring system separate with the rest of the CO_2 system.

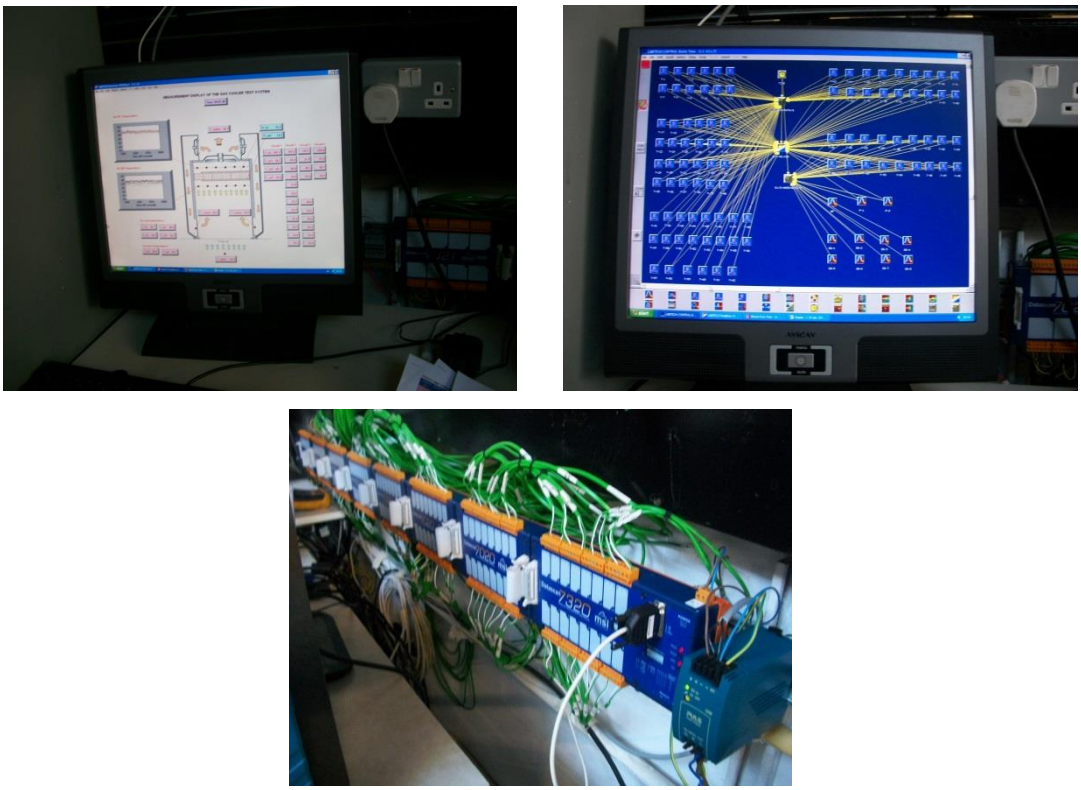

Figure 5.39 System monitoring modules

The output signals from the instrumentation sensors are logged by a data logging system which comprises data acquisition modules and a recording and display system. For the data acquisition modules where all the sensors are connected a DATASCAN 7000 series modules are used. Those are communicating with RS232 cable with the computers where the appropriate software has been installed. The LABTECH software allows recording the data based on the user requirements. In additional, the software has a build-up function to use a display figure of the system and make the monitoring from the user to be easier and act faster in case of emergency.

5.4.3. CO_2 REFRIGERATION SYSTEM MONITORING

The same data logging software is used to monitoring and recording the rest of the CO_2 refrigeration system. For this case the data logging station is installed inside the environmental test room.

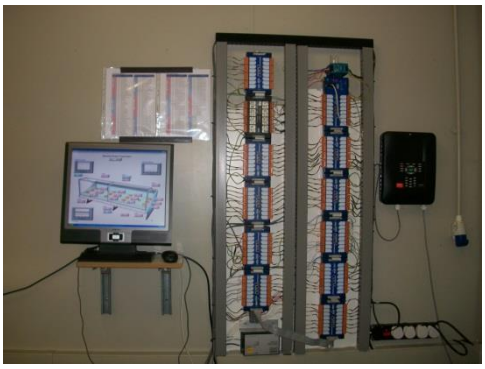

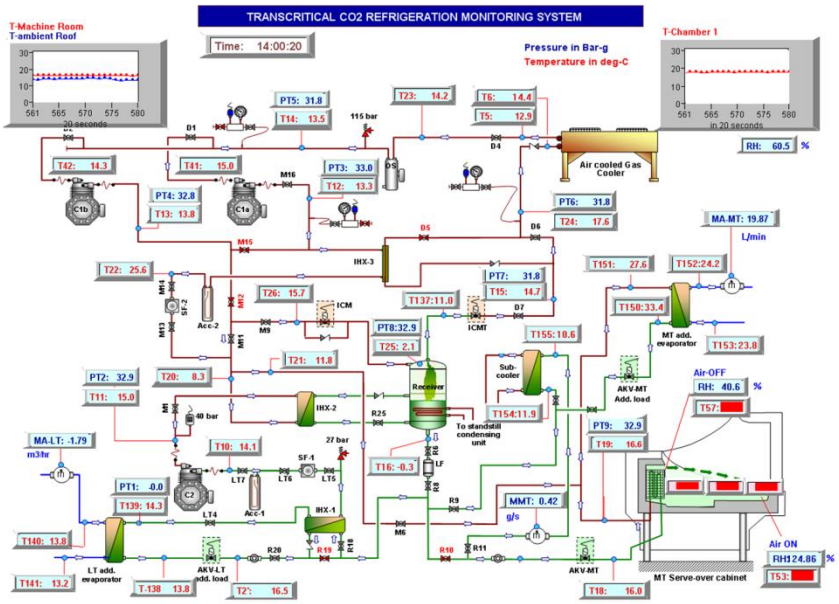

Figure 5.40 Monitoring of CO_2 test rig – Graphical illustration of the test rig

One screen is installed inside the chamber room and another one has been installed inside the lab area.

5.5.REFRIGERANT CHARGE & SYSTEM PREPARATION

The CO_2 cylinders are heavier than the standard HFC cylinders and contain refrigerant at a higher pressure level (57.3 bar at 20 °C). The charging process was carried out by using equipment suitable for the CO_2 refrigerant and pressure concerned. The test rig is equipped with a fixed permanent charging point to reduce cylinder handling.

Before charging, the system was pressure tested by using nitrogen at the certain amount and kept it for 24 hrs to ensure there is no leak on the system. Then the system evacuated for long time to ensure there is no air. The air/moisture in transcritical system causes major problems because it is non-condensable gas and the system pressure may be increased in abnormal levels.

In order to prevent the dry ice formation and thermal it is important to charge the system with the following procedure:

- Charge gas by using the gas/vapour offtake cylinder until the system pressure is above 6 bar – above triple point (4.2 bar).
- Then replace the cylinder with the liquid offtake cylinder.

It was important to make sure that the standstill condensing unit was normal operate before started charging the system. The set pressure point during the charging process was 26 bar. The R404A standstill condensing unit operates when the pressure in the liquid receiver is higher than the set point. The charge process was a step by step process by opening and closing the valve when the pressure was lower than 26 bar and higher than 31 bar respectively. The receiver filled until the liquid of the refrigerant inside this is slightly above the second sight glass.

Before run the system each time a number of actions were made to ensure the normal run of the system and avoid abnormal situations may damage the system. The first action is to check the general system conditions including compressor, valves, receiver and cooling load equipment. The compressor oil level must be check regularly. In case the system was already charged the level of the refrigerant inside the receiver was pointed. Before run the system the inspection of the instruments and manometers were noted to compare with previous values.

The running process was started by turn ON the MT and AL switches to power-up the AK-CC-550A controllers. Then the settings for both evaporators were checked. Back to CO_2 plant, the receiver feed valve checked to make sure that is open. The main power which supplied the controller of the C/GC was turn it ON. After running both evaporators and C/GC, the compressor was power up. After open the system valves the pressure at the suction line of the compressor was started to increase. Once the system reached the minimum operation pressure level the compressor was operated in full

speed of 100% (50Hz) for certain time. After a while the compressor speed was reduced to the normal operation level in order to supply the system. For the first 15 minutes of the system operation all the pressure gauges were checked to ensure that the system is operated in normal conditions.

The air inlet temperature conditions on the C/GC were programmed to meet the requirement for this specific test conditions. Once the air temperature was stable enough to the set value the recording/monitoring program was checked.

5.6. SUMMARY

This chapter presents in details the procedures which followed to design, select and build the CO_2 refrigeration test facilities. The component selection, piping and safety aspects are clearly identified. In additional, the system monitoring, system charge and preparation are discussed also.

Next chapter will present the experimental results from the experimental test rig which described in this chapter. The model validation from Chapter 4 will be presented also.

6. EXPERIMENTAL RESULTS, SIMULATION CALCULATIONS & MODEL VERIFICATION

6.1. INTRODUCTION

This chapter is divided in four main sections. The first section includes the test conditions, set points of individual components, the test procedure, data collection and finally the results processing including the uncertainty analysis. The second section is described and discussed the results of the tests performed on the transcritical CO_2 refrigeration system in CSEF – Brunel University laboratory environment. The detailed design of the CO_2 refrigeration system was presented in Chapter 5. The third section is included the simulation model validation. This simulation model results are compared with the test results for the same boundary conditions. The detailed mathematical model for each individual component was presented in Chapter 4. In this section, the results of the MT refrigerated display cabinet simulation model are also presented. The last section of this chapter is described the test results for the additional modification which have been done during the experimental procedure. Those modifications have been discussed in Chapter 4.

6.2.EXPERIMENTAL PROCEDURE

A number of tests were carried out to evaluate the cooling performance of a CO_2 booster refrigeration system with hot gas bypass. The system which has been explained in details before comprised by the gas cooler/condenser, ICMT and ICM valves, liquid receiver, MT refrigerated display cabinet, additional load and the two HT parallel connected compressors. In additional, the data monitoring and record system includes a number of pressure and temperature point before and after all the individual components of the test rig. The experimental tests were performed under different ambient conditions which the gas C/GC test rig set-up allows to control. The intermediate pressure was kept constant at 32 bar for all the ambient conditions. The effect of the higher intermediate pressure on the overall system COP has been experimentally investigated. The results of this are used to validate the simulation model. The evaporating temperature is kept constant at -8 °C. This is based on the normal supermarket setting in order to ensure proper merchandise and safety of the food products when displayed on the shelves.

Finally, the system performance parameters were recorded and used to calculate the overall refrigeration capacity of the system and coefficient of performance (COP) of the CO_2 hot gas bypass system.

6.2.1. CONDITION – PARAMETERS - PROCEDURE

The experimental tests were performed in order to examine the effect of different size of CO_2 gas coolers/condensers on the overall CO_2 system performance. The three different heat exchangers are described in Chapter 5. These three heat exchangers were installed in the CO_2 system separately and tested at the same operating stages of intermedium and medium temperatures and pressures and air flow parameters. The air-on flow temperatures varied between 19°C to 36°C and flow rates were modulated from 2000 l/s to 2800 l/s through fan speed controls. Consequently, both heat exchangers operated at condenser and gas cooler modes.

6.2.1.1. COOLING LOAD TEST CONDITIONS

The MT refrigerated display cabinet was placed inside the environmental test room. The conditions inside the room were kept constant at climate ISO 3 at 25 °C and 60 % relative humidity. The cabinet was loaded by using M-packages and water/glycol containers in order to provide the adequate thermal mass. Product temperatures and air side temperatures were measured all the time during the tests. The analysis of the product temperatures was based on the M1 classification which requires the packages to be between -1 °C to +5 °C during the running and defrost period (ISO, 2015). The additional load (AL) consists by a plate heat exchanger where the cold side CO_2 refrigerant is transferring the heat to a brine hot side.

Both MT and AL were controlled by the Danfoss AK-CC-550A controller as explained in Chapter 4. The controller sends a signal to open or close the AKV valve. By controlling the refrigerant mass flow rate passing through the coils; both systems can maintain a nearly constant superheat degree point. The degree of superheat for both is calculated by two temperature sensors located on the inlet and outlet of the evaporator and a pressure transmitter which records the feedback from the outlet of the evaporator.

The AK-CC-550A controller is also monitoring and controls the air temperature and brine temperature for the display cabinet and AL respectively. For the MT cabinet, when the temperature inside the cabinet reach the set point then the controller send a signal to stop the refrigerant flow. The controller must be control the superheat degree

and the air temperature set point inside the cabinet; for that reason a differential set point has been used in order to run the cabinet more stable. For the AL the controller has a reference point the temperature outlet of the brine side. In order to avoid a huge difference between two fluids, a high performance efficiency heat exchanger is recommended to use. The set point which have been used for both cooling capacity loads are illustrated below.

Table 6.1 Experimental control settings

Parameters	MT cabinet	AL (brine/CO_2)
Cut off temperature	- 3 °C	- 7°C
Air differential temperature	2 K	3 K
Air-on / air-off weight	100% air-off	100% *
Evaporating temperature	-6.5 °C to -10 °C **	-6.5 °C to -10 °C **
Degree of superheat	7 – 12 K **	7 – 12 K **
Pressure control	27 to 28 bar	27 to 28 bar
Defrost type	Off-cycle	N/A
Defrost Interval	6	
Defrost maximum time period	30 mins	
Defrost termination temperature	7 °C	

* Brine temperature at the outlet of the heat exchanger
** Depending on the tests series

6.2.1.2. COMPRESSOR TEST CONDITIONS

The parallel connected compressors are controlled by targeting the set point of the suction pressure with a small degree of differential. The Danfoss AKS pressure transmitter is sending the feedback of the suction pressure on the AK2-XM-205B controller. The controller is interconnecting with the VLT power inverter. The power inverter which has been explained in Chapter 5 is regulating the compressor speed to maintain the suction pressure suction point.

The pressure suction target for both compressors were set to be at 26.5 bar and the set point suction temperature of -10 °C. A differential pressure degree of 2 bar was set in order to run the system smoothly. All the parameters and settings were controlled by the AK-SC255 Danfoss main system controller.

Four different test series were performed based on the compressor speed. The compressors speed settings were changed in order to investigate the effect of the mass flow rates passing through the C/GC. The variable speed control set up was found to be the most efficient for the CO_2 system. Table 6.2 illustrates the number of the different tests.

Table 6.2 Test series with different control speeds

Test Series	Compressor number and speed
Test 1	Variable speed 65% to 100%
Test 2	1 compressor x 80% of full speed
Test 3	1 compressor x 100%
Test 4	2 compressors x 65% of full speed

6.2.1.3. ICMT – ICM – RECEIVER

All the three gas cooler/condenser coils have been investigated under similar air-inlet temperatures which varied from 18 °C to 36 °C with 2 °C step. Based on those settings, the system was investigated in subcritical, transcritical and transitions mode operations. The ICMT and ICM valves are controlled both subcritical and transcritical operations.

A Danfoss EKC326A PID controller is used to control the ICMT valve. The controller is receiving a signal from a pressure and temperature sensor allocate at the outlet of the coil.

For the subcritical operation a sub-cooling degree is used as a referee point. For the first series of tests the degree of sub-cooling was set to be 2 K. Then the setting was changed to be 0.3 K. For the transcritical operation the system is used the optimum gas cooling pressure as explained in Chapter 5. For both operations the minimum and maximum opening degree of the valve was set to be 0% to 100% respectively. This allowed to the system to fully control the subcooling degree and optimum pressure outlet for both system modes. When the system is moving from subcritical to transcritical operation or vice versa the controller uses a transition zone control theory. By adjusting the maximum opening degree of the valve to be below 50 % can cause a really high pressure of the HP pressure of the system and cause problems on the system equipment or pipeline.

For the preliminary tests the strength of the system was tested by using low enough values for the maximum opening of the valve. The results from those tests were analysed and the most efficient set values were used.

The *ICM* valve controls the pressure at the liquid receiver and the intermediate pressure of the system as explained in Chapter 5. An EKC 347 Danfoss controller is used to control the flow of vapour refrigerant from the receiver back to HT compressors. This type of the controller is used to maintain the liquid level of CO_2 inside the receiver by using the feedback of pressure transmitter to sense the pressure inside the receiver. The ICM valve was the only available valve on the market in order to maintain the pressure inside the receiver by adjusting the liquid level. By the experimental results found that for 64% of liquid level inside the receiver the intermediate pressure was constant at 32 bar. This constant pressure was used for all the series of experiments for the three different GC/C designs. A higher liquid level and higher intermediate pressure was tested and the results are shown in the next sub-chapters.

The receiver control is a function of the ICMT and ICM controller as explained before. In additional another condensing unit is used to maintain the pressure inside the receiver in normal levels in case of power failure. If the ICMT, ICM and condensing unit were failing to operate the liquid receiver was compromised with a PRV.

6.2.2. EXPERIMENTAL RESULTS DATA COLLECTION

The measured performance parameters including the temperature, pressure, relative humidity, mass flow rate and power were logged by using two different data logging systems. The first system was specially built to accommodate the measurements on the high pressure side of the system including the refrigerant and air temperature profiles in the C/GC. The second data logging system is used to record the data from the rest of the system including intermediate and medium pressure levels. Both logging system were produced a live image from the system and record all the parameters every 20 seconds. Both systems were explained in Chapter 5.

6.2.3. DATA PROCESSING AND THERMOPHYSICAL PROPERTIES

The collected data from both data loggers were stored and processed in an EXCEL spreadsheet. For each measured point a new column was used. The first column of its spreadsheet was denoted the time of the recorded data based on the time interval of 20 seconds which has already set up from the beginning. The time in both computers is

synchronised in order to allow noting manually as well every parameter or setting change. This allows to procced the data easier once each test finished.

As a boundary for the test results analysis the air-inlet temperature at the C/GC were used. For that reason the air-inlet thermocouples are firstly plotted against the time. The transition line between each two air-inlet settings was neglected because the system was not under steady state operation.

The next step after defined the steady-state conditions for the air-inlet parameter is to plot the discharge pressure against the time. As already discussed the air-inlet temperature and the discharge pressure at the C/GC coil is related for the CO_2 refrigeration systems. Both air-inlet/time and discharge-pressure/time graphs are compared and the steady state conditions were founded. Therefore, those conditions were used for the system performance analysis.

The steady state points for each air-inlet and discharge pressure were copied in different spreadsheets for each condition. An EES mathematical model which linked with the spreadsheets was modelled to derive the refrigerant and air properties before and after the CO_2 components. The M. Conde Engineering (2011) equations were written to the model to calculate the brine properties for the additional load. The thermos-physical properties derived from the EES are transferred back to initial excel spreadsheet were the energy performance parameters of the CO_2 refrigeration system were calculated which include the cooling capacity of the MT and AL, the bypassed ratio of the refrigerant at the receiver, the power consumption from the compressors and main fans of the C/GC and finally the coefficient of performance (COP).

6.2.4. COOLING CAPACITY CALCULATIONS

The cooling capacity of the CO_2 refrigeration system includes the MT display cabinet and the AL heat exchanger evaporator. As discussed in Chapter 5 an additional air cooler evaporator has been added on the system. This has been tested by running the MT cabinet as well and the air cooler by itself. The results for the individual tests will present in the next subchapters.

The refrigeration capacity of the MT evaporator was calculated by using the refrigerant mass flow rate and the enthalpy across the coil. The MT load is a DX coil where the expansion of the refrigerant assumed to be isenthalpic for cooling capacity calculation procedure. The enthalpy of the refrigerant liquid entering the coil evaporator and the refrigerant vapour leaving the evaporator were determined from the temperature and

pressure measurements of the refrigerant inlet the AKV expansion valve and the outlet of the evaporator respectively.

$$Q_{MT} = \dot{m}_{ref,MT}(h_{ref,out,MT} - h_{ref,in,MT}) \quad 6.1$$

For the AL, the refrigeration capacity was calculated from the energy balance between the refrigerant and brine side of the heat exchanger by assuming adiabatic heat transfer.

$$\dot{m}_{ref,AL}(h_{ref,out,AL} - h_{ref,in,AL}) = \dot{m}_{brine}c_{p_{brine}}(T_{brine,in} - T_{brine,out}) \quad 6.2$$

The refrigeration capacity of the AAC was calculating by using the refrigerant mass flow rate and the enthalpy across the coil. In additional the refrigeration capacity was calculated by using the air side properties. Calculations of the DX AAC are following the same procedure with the MT display cabinet.

$$\left.\begin{aligned} Q_{AAC,ref} &= \dot{m}_{ref,}(h_{ref,out,AAC} - h_{ref,in,AAC}) \\ Q_{AAC,air} &= \dot{m}_{air}(h_{air,in} - h_{air,out}) \\ Energy\ Balance: Q_{AAC,air} &= Q_{AAC,ref} \end{aligned}\right\} \quad 6.3$$

6.2.5. POWER CONSUMPTION CALCULATIONS

The total power consumption of the CO_2 refrigeration system includes the power of the HT compressors and the brine pump. The power consumptions of both were determined by recording the power of both. Because the complexity of the system and power supply line it was really difficult to measure and calculate the power consumption of the HT compressors, brine pump and main fans from the main power panel. Therefore it was decided to create a mathematical model in order to calculate the power consumption done by the HT compressors.

Based on manufacturer data (GEA BOCK, 2009), similar formulae can be applied to calculate the system compressor power consumption at both subcritical and transcritical modes, as listed in equations 6.4 and 6.5 respectively. However, the former is a function of condensing and evaporating temperatures while the latter is dependent on compressor suction and discharge pressures. The coefficients from these equations are correlated and listed in Table 6.3. The map-based routine was used. This routine use the empirical

performance curves for the compressors obtained from the calorimeter measurements performed by the manufacturer. Coefficients c_1 to c_6 are non-dimensional due to the map based routine.

Subcritical: $$W_{com,sub} = c_1 T_{ev}^2 + c_2 T_{ev} + c_3 T_{cd}^2 + c_4 T_{cd} + c_5 T_{ev} T_{cd} + c_6 \quad (6.4)$$

Transcritical: $$W_{com,trans} = c_1 P_{suc}^2 + c_2 P_{suc} + c_3 P_{dis}^2 + c_4 P_{dis} + c_5 P_{suc} P_{dis} + c_6 \quad (6.5)$$

It should be noted that the manufacturer data of compressor power consumption was measured at constant superheat 10 K at the compressor inlet. If the actual suction superheat differs from 10 K, the following correlation factor C_{suc} is applied.

Correction Factor: $$C_{suc} = \frac{v_{exp}}{v_{10K}} \quad (6.6)$$

The coefficients derived by correlated the manufacturer data are illustrated at the table below.

Table 6.3 Coefficients derived by manufacturer data

	c_1	c_2	c_3	c_4	c_5	c_6
Subcritical	-1.61804	303.794	-0.23315	-299.358	1.955376	-5696.67
Transcritical	-1.79591	40.16467	-0.12544	21.38474	1.473649	2520.822

In additional, a power quality analyser was used to measure the power consumption done by the main fans and the brine pump by attaching the power leads at the components and avoiding interfere with by other equipment.

6.2.6. GAS COOLER/CONDENSER CALCULATIONS

The C/GC heat rejection was calculated from the air side temperature difference across the coil, the air flow mass flow rate and the specific heat capacity of air. The results from the excel file for each control performance parameter was entering to a special programmed EES model where the model was calculated the heat rejection from the air side.

$$Q_{GC/C} = \dot{m}_{air}\, c_{p,air}(T_{air_{out}} - T_{air_{in}}) \quad 6.7$$

The specific heat capacity of air is calculated as the average value of air temperature entering on the coil and the air temperature leaving the coil. The energy balance of air and refrigerant sides were used to calculate the total mass refrigerant flow circulate on the system assuming an adiabatic heat transfer.

$$c_{p,air} = f(T_{ave,air}, P_{air}, RH_{air}) \quad 6.8$$

$$T_{ave,air} = \frac{(T_{air_{out}} + T_{air_{in}})}{2} \quad 6.9$$

$$Q_{GC/C} = \dot{m}_{ref}\,(\Delta h)_{ref} = \dot{m}_{air}\, c_{p,air}\,(\Delta T)_{air} \quad 6.10$$

The refrigerant enthalpy across the coil is derived by using the test recorded data of temperature and pressure. The air mass flow rate passing thru the coil was calculated by using the air velocity for different fan speed values. The velocity of air was measured and recorded on different spots across the coil. Two different graphs for the air velocity with respect of fan speed and air flow rate against fan speed were plotted for three row and two row coils separately. The calculated air flow rate is calculated by those correlations. Then, the air mass flow is calculated as illustrated below.

$$\dot{m}_{air} = \dot{v}_{air}\rho_{air} \quad 6.11$$

$$\rho_{air} = f(T_{ave,air}, P_{air}, RH_{air}) \quad 6.12$$

The approach temperature of the C/GC is also derived by the experimental tests. Ge and Tassou (2009) has been defined the approach temperature of a cross flow heat exchanger as the temperature difference between refrigerant outlet temperature and the air temperature entering to the heat exchanger.

$$Approach\ temperature\ (AT) = T_{ref,out} - T_{air,on} \quad 6.13$$

The approach temperature is used for the analysis of the system when was operating in a transcritical mode. For the subcritical mode the subcooling degree was used for the analysis. The degree of subcooling was calculated as shown below.

$$Degree\ of\ Subcooling = T_{CO_2,sat} - T_{ref,out} \quad 6.14$$

$$T_{CO_2,sat} = f(P_{CO_2,out})$$

The values for $T_{CO_2,sat}$ was derived from EES software.

6.2.7. RECEIVER CALCULATIONS

The variation of the separation ratio is determined by the CO_2 vapour mass fraction at the receiver inlet which is mainly a function of the gas cooler/condenser outlet parameters (temperature and pressure). Considering of large variation of ambient temperature, these outlet parameters can be greatly altered and therefore the separation ratio.

The calculation procedure for the separation ration in the CO_2 liquid receiver has been discussed in Chapter 4.2.7. For both three rows and two rows coils the ratio of the separation was different. This is a function of the higher pressure drop on the two rows coil comparing than the three rows. For the same ambient conditions the liquid ratio of the three row coil is slightly higher. This is the proportional of the ICMT function controller. The lower discharge pressure of the three row coil is resulting higher percentage of liquid ratio flows to the evaporators. The higher refrigerant flow rate passing thru the coils were resulting higher refrigeration capacity.

6.2.8. COEFFICIENT OF PERFOMANCE CALCULATIONS

The COP calculation of the CO_2 booster system was calculated from the equations which have been described in Chapter 4.2.15. The COP calculations included the refrigeration load of the MT and AL evaporators and the power consumption of the HT compressor.

All heat exchangers were being investigated under different main fan speeds and the CO_2 system performance was analysed based on the speed on the air extraction fans. Based on that, the power consumed by the two main fans at the GC/C has been taken into account for the overall system COP calculations.

6.2.9. CALCULATION OF UNCERTAINTY

Considering the uncertainty of the experimental measured variables including the air mass flow rate and air temperature, refrigerant temperatures, refrigerant pressures, refrigerant mass flowrate, and moreover assuming that these measurements are uncorrelated and random, the uncertainties of the COP calculation can be determined using the Engineering Equation Solver (EES) software, which are ± 5.52% and ± 6.1% for the systems with 3-row and 2-row gas cooler/condensers respectively. The display cabinet evaporator cooling capacity uncertainty is calculated as ± 0.77% and the

additional load cooling capacity uncertainty is ± 11.22% which is relatively high due to the calculation involved at the brine side.

6.3.EXPERIMENTAL RESULTS AND DISCUSSION

The following sub-chapter presents and discusses the test results from the booster refrigeration system. The results are following the same structure as the chapter 4.3 "Design – Construction – Modifications for the experimental test facilities". The individual components are initially presented. Then, the performance of the system is discussed under different conditions.

The experimental results are used later to validate the simulation models which has been used to compare the different CO_2 systems. Most of the research investigations carried out in CO_2 a commercial installation which makes the difficult to test the system under different parameters. Therefore, the laboratory CO_2 rig investigation is a real need. In such cases, the boundary parameters can be controlled and recorded.

All the experimental data have been analysed by using the ambient temperature and discharge pressure as a boundary conditions. In additional the analysis based on the different parameters and condenser/gas cooler designs which have been described in Chapter 5.

6.3.1. CO_2 COMPRESSORS

The system was operating by using two parallel connected HT compressors which have been described in section 5.3.2. The system was tested by using the parameters presented in Table 6.2. The results for the different parameters are discussed below.

6.3.2. CONDENSER/GAS COOLER

The performance investigation of the condenser/gas cooler includes both air and refrigerant sides. The performance investigation parameters based on the function of the discharge pressure, C/GC heat rejection, approach temperature, fan power consumption and refrigerant temperature profile across the coil.

The function of discharge pressure of the gas cooler/condenser with the air-on temperature is illustrated in Fig. 6.1. The switching point from a subcritical to transcritical operation is at 26.8 °C and 72.77 Bar. It is clear from Fig. 6.1 that the relationship between the controlled air-on (ambient) temperature and discharge pressure is almost linear for the system with two high-pressure side heat exchangers respectively.

From Chapter 4, it is known that the optimal discharge pressure control is mainly based on the gas cooler/condenser outlet temperature, which is directly related to the heat exchanger air-on temperature. If the relation between these two temperatures can be known, the control strategies from the ICMT controller can be derived.

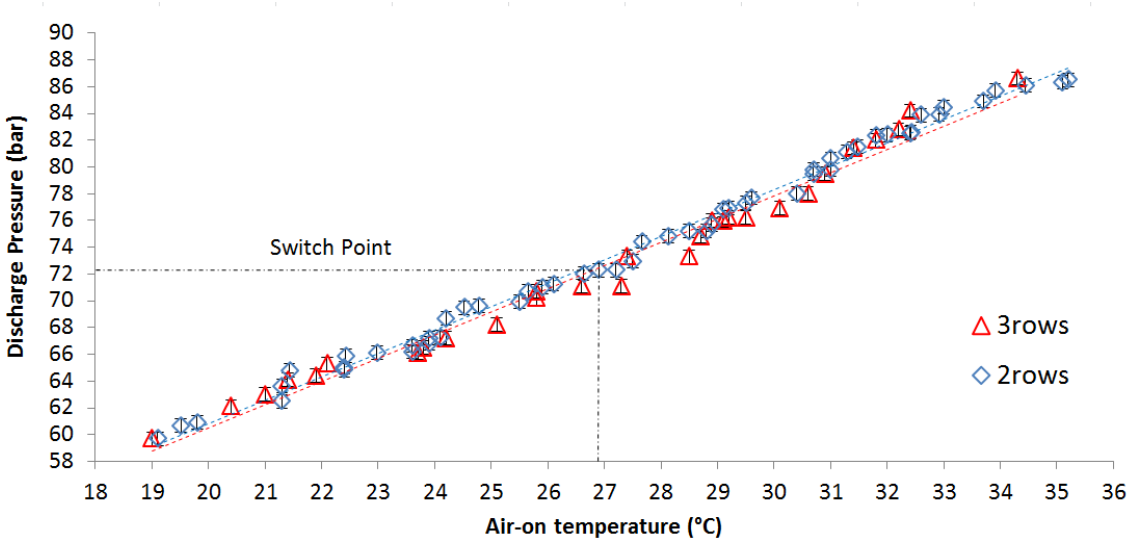

Figure 6.1 Function of discharge pressure of the gas cooler/condenser with the air-on temperature

On the other hand, the air-on temperature can also be used as a one-input parameter to the controller. Furthermore, Fig. 6.1 demonstrates that the optimal discharge pressure for the 3-row heat exchanger system is mostly lower than that of a system with a 2-row heat exchanger. This is because that the larger heat exchanger (3-row) can have a higher heating capacity and thus a lower refrigerant exit temperature or a smaller approach temperature difference at the heat exchanger outlet.

The approach temperatures at the gas cooler outlet are influenced by the air-on temperature, gas cooler fan speed, compressor controller and ICMT motorized valve opening. Figure 6.2 shows that at higher air-on temperatures, the approach temperature drops dramatically.

Moreover, the approach temperature for 70% of the main fan speed (2800l/s) is smaller compared to the 60% fan speed (2400 l/s) due to an enhanced air side heat transfer. Therefore, the heat exchanger outlet temperature or approach temperature can be controlled by modulating the heat exchanger fan speed or air flow rate.

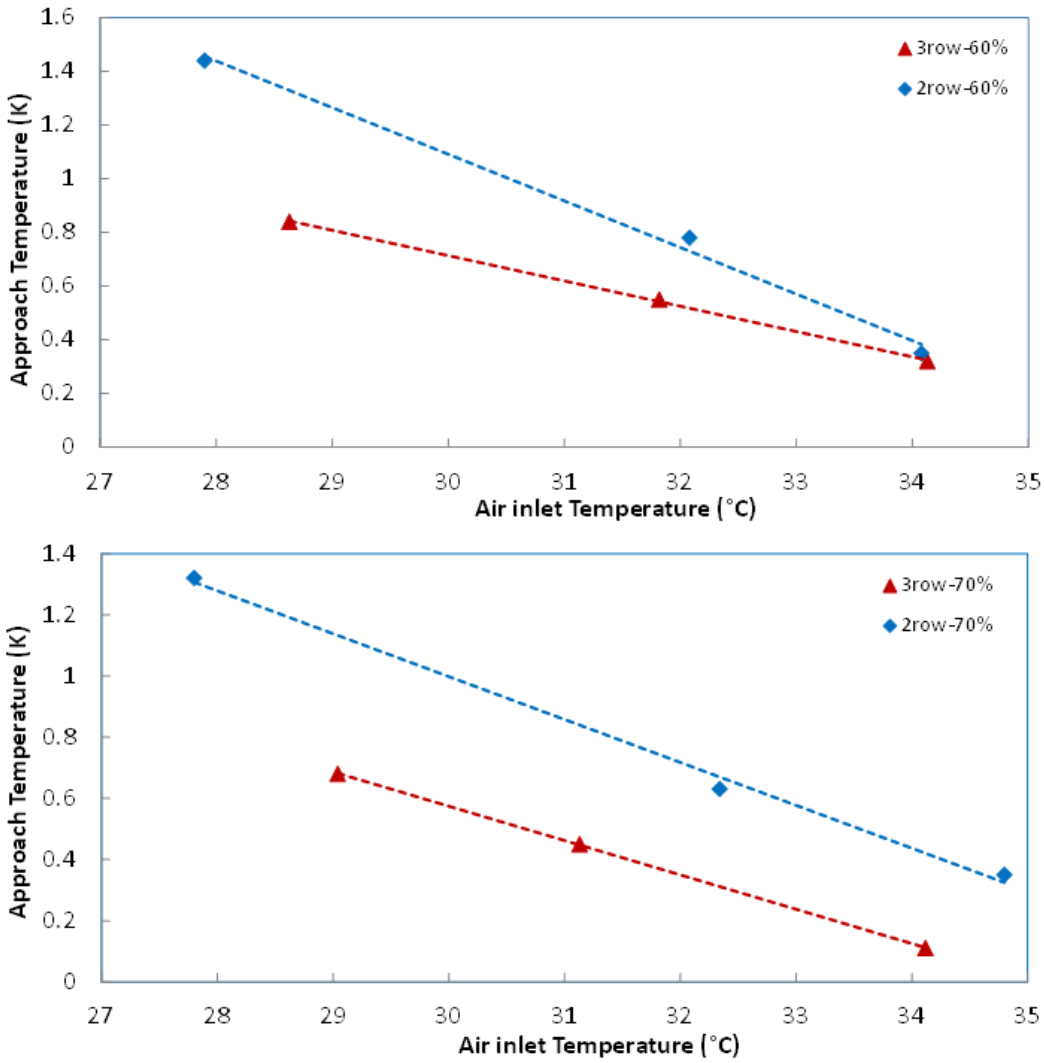

Figure 6.2 Gas cooler approach temperature

However, the higher heat exchanger fan speed significantly affects fan power consumption and the air side pressure drop, as shown in Fig. 6.3 (a) illustrates the power consumption of the fan with respect to different air volumetric flow rates. Apparently, the fan power consumption increases with higher air volumetric flow rates or fan speeds and this increase rate is much higher for higher airflow rates. The more detailed power consumption analysis of the main fans is represented in Appendix E. Figure 6.3 (b) shows the influence of the air volume flow rate on the air side pressure drop for both tested gas coolers/condensers. It can be seen that the air side pressure drop increases with higher air flow rates and greater pressure drops are demonstrated in the 3-row coil due to its greater number of rows.

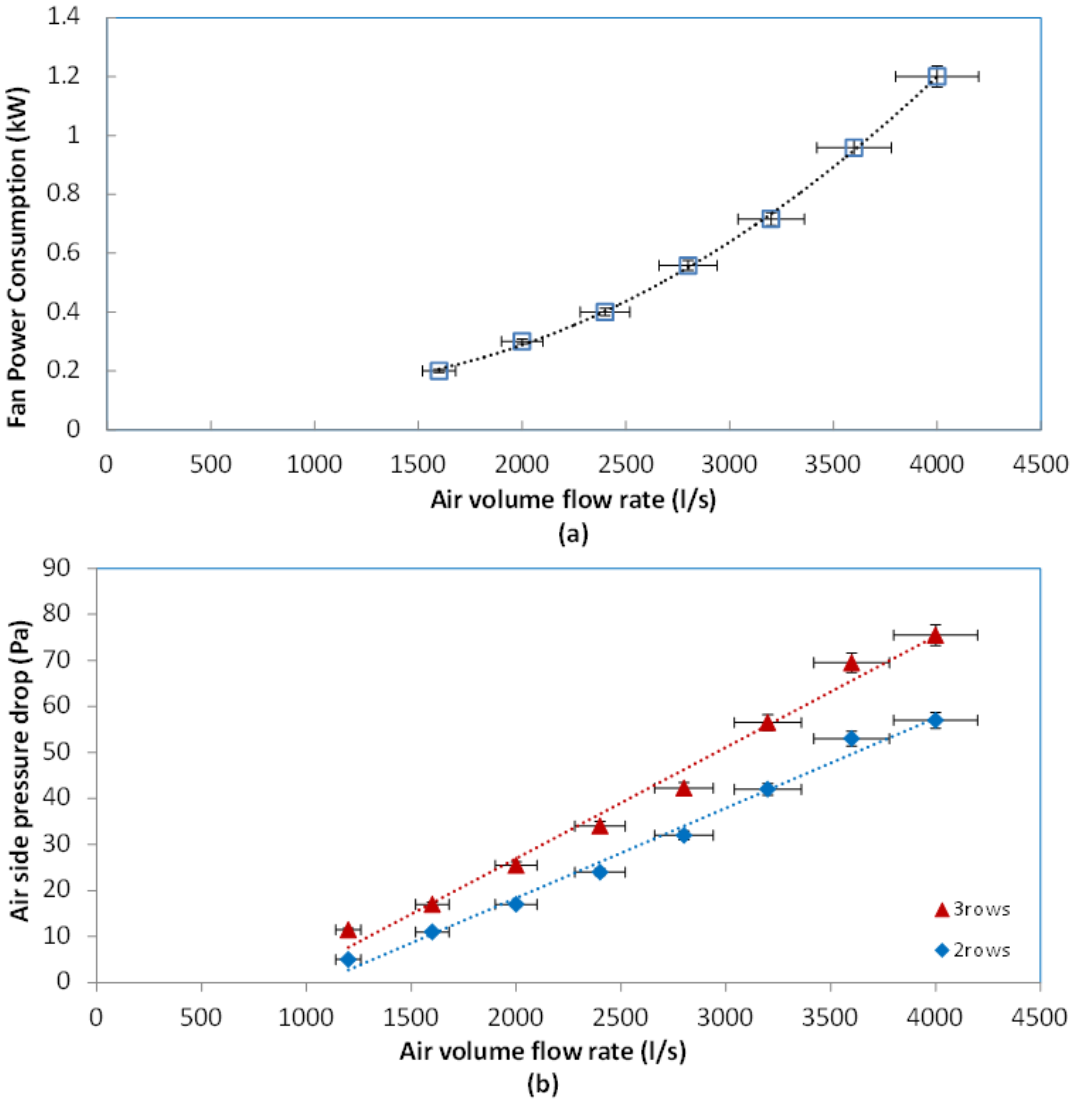

Figure 6.3 Fan power consumption and air pressure drop

The fixed compressor speed of 80%, 100% and 2x 65% were used to investigate the refrigerant side pressure drop of the three different C/GC designs which have been installed separately on the CO_2 system. The pressure at the inlet and the outlet were measured at the header of the coil. The dimension of the three coils were described above including the 3-row, 2-row and 2-row 0.8m with pipe length of 39.20m, 52.50m and 26.25m respectively.

The higher pressure drop found to be in 2-row coil due to the longer distance of the pipe. In additional, the pressure drop affected by the lower number of the circuits as well as the higher refrigerant mass flux.

As can been seen from the Fig. 6.4 the pressure drop reduces as the ambient temperature increases and therefore the discharge pressure is become higher and the system move to transcritical operation. At the transcritical operation, the relation between temperature-pressure is completely changes. The density of the CO_2 refrigerant is related to the pressure which means higher pressure higher CO_2 density. The mass flow rate for 80%, 100% and 2 x 65% were 0.021kg/s, 0.026kg/s and 0.031 kg/s per circuit respectively for the 2-row coil. For the 3-row coil the mass flow rate were 0.011 kg/s, 0.013 kg/s and 0.017 kg/s per circuit respectively.

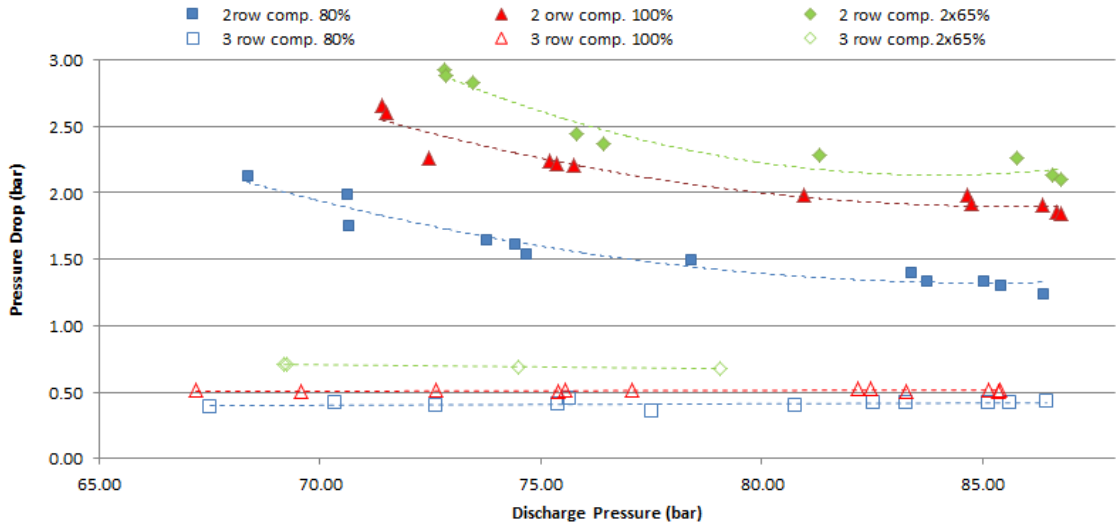

Figure 6.4 Refrigerant pressure drop

From the same graph, it can be seen that the pressure drop across the C/GC increases as the refrigerant mass flow rate increased. The overall pressure drop is much lower comparing with the 2-row coil due to the reasons which explained above.

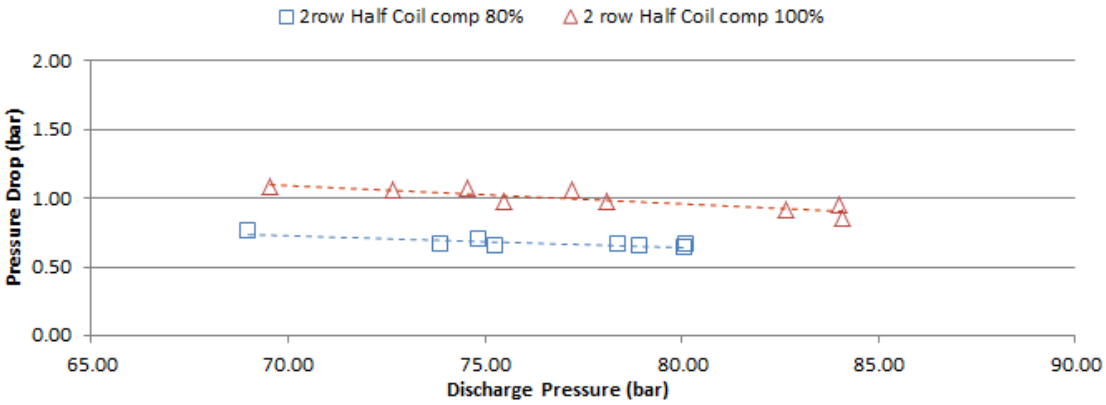

Figure 6.5 Pressure drop across the two different pipe lengths

The mass flow rate for 80%, 100% and 2 x 65% were 0.011kg/s, 0.013kg/s and 0.017 kg/s per circuit respectively.

In Fig. 6.5 the pressure drop across the 2-row coil with length 0.8 m. is illustrated. The pressure drop is much lower comparing with the 2-row 1.6 m coil due to the total distance of the pipe per circuit which is reduced to the half.

The mass flow rate for 80% and 100% were 0.020kg/s and 0.026kg/s respectively.

In Fig. 6.6 illustrated the operating inlet and the outlet conditions of the coil when the system is operated in subcritical and transcritical cycle.

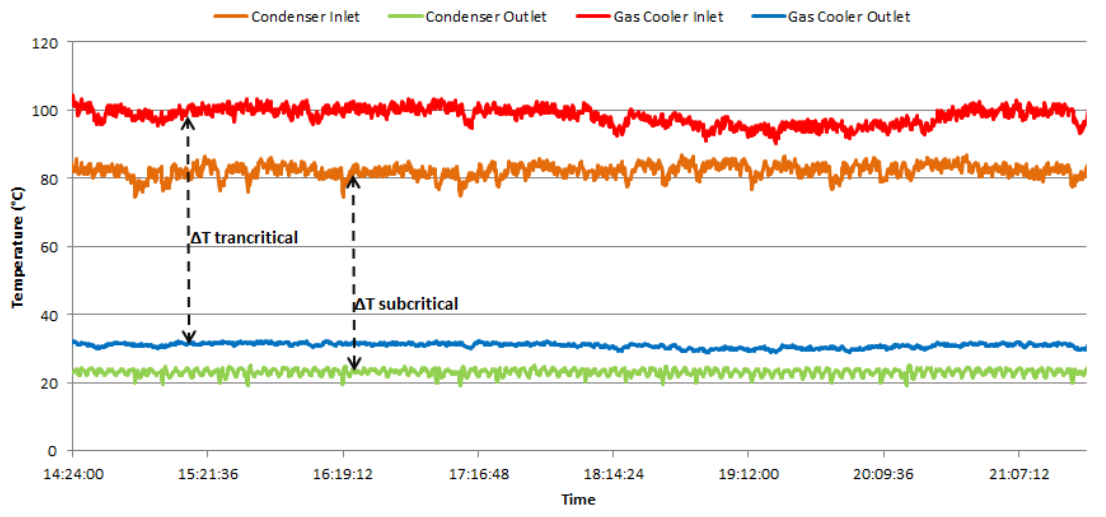

Figure 6.6 C/GC inlet and outlet refrigerant temperatures

In additional the ΔT temperature across the coil is also identified. These results based on the 2 row 1.6m length coil. Very similar line identified for the 3 row coil. On the other hand, the ΔT temperature profile for the 2 row 0.8m. coil is higher due to the

overall pipe length per circuit. The ΔT for the subcritical and transcritical operation is about 55 K and 70 K respectively. This is a very high ΔT compared to that of a R404A condenser, where at the same conditions with the subcritical operation the temperature difference would be 30 K.

The comparison the 3-row and 2-row C/GC based on the heat rejection were performed with varied compressor speed of 65% - 100% and fan speeds from 50% to 70% with step of 10%. The refrigerant mass flow rate was slightly constant for both cases at subcritical and transcritical operation. For subcritical the mass flow rate was 0.37 kg/s and increased when the system moved to transcritical operation to 0.39 kg/s. The refrigerant mass flow rate is a proportional of swept volume, volumetric efficiency, compressor speed and suction line density. It is well known that the refrigeration load is decreased as the system moves to transcritical operation. In order to keep the refrigeration load close to the design values the compressor speed is increased. The higher compressor speed has a proportional to slightly increase the refrigerant mass flow rate. The operating pressure is a function of the air-on temperature which is between 20 to 36 °C for this case. In Fig. 6.7 illustrates the variation of the heat rejection for both C/GC with the discharge pressure.

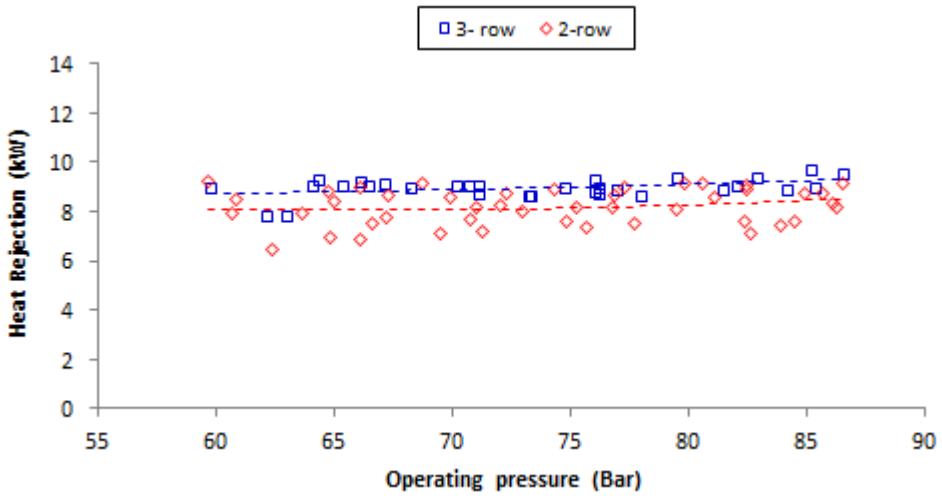

Figure 6.7 Condenser/Gas cooler heat rejection

The heat rejection for the 3-row C/GC was higher comparing the 2-row. This is due to the total heat transfer area where for the 3-row coil was 33% bigger than the smaller 2-row coil.

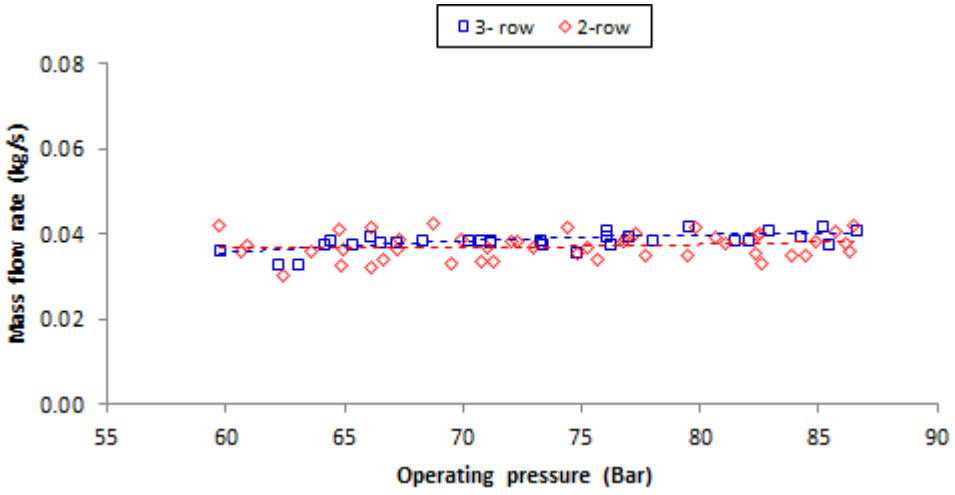

Figure 6.8 Mass flow rate passing through for both investigated coils

The refrigerant mass flow rate of both coils is showing in Fig. 6.8. For the 3-row coil the mass flow was slightly higher due to the total pipe length and nominal capacity of the coil. The operating pressure is related to the air-on temperature at the condenser/gas cooler and the control strategies followed. For Fig. 6.8 the air-on temperature was varied between 20 to 36 °C, the compressor speed controlled by the variable speed controller from 65 to 100% depending on the load. The mass flow rate is fairly constant and slightly increased when the system moves to transcritical condition, which is 73.6 bar-atm.

6.3.3. ICMT –ICM VALVES & LIQUID RECEIVER

The selection of the ICMT valve is described in Chapter 5.2.5. As it described before the ICMT valve maintain the C/GC pressure based on the ambient conditions. In additional, the valve is operating as an expansion valve for the refrigeration system.

The main purpose of the ICM bypass valve is to ensure that the evaporator is feeding with refrigerant liquid only. The valve has negligible effect on the system efficiency but ensures the operating pressure to be below the maximum operating pressure of the receiver and liquid pipe line. More details for the valve and thermodynamic analysis of this can be found in Chapter 4.2.8.

The mathematical model which has been used in order to select the proper CO_2 liquid receiver design was explained in Chapter 5.2.7. In additional, in this chapter presented the relatively installation position of the liquid receiver on the system. The

thermodynamic and mathematical procedure which has been used in order to analyse the operation of the ICMT valve and liquid receiver were explained in Chapters 4.2.6 and 4.2.7. This analysis includes the pressure and temperature status at the outlet of the C/GC, before ICMT valve, suction of liquid receiver and evaporator. Due to the short length of the pipe line between the C/GC outlet and suction of the ICMT valve and the proper insulation method, the pressure and temperature drop was equal to zero.

The temperature profile before and after ICMT is clearly identified from the Fig. 6.9 for subcritical and transcritical operations. This includes the C/GC inlet temperature, the ICMT inlet and outlet temperature profile.

For the subcritical cycle the temperature difference across the ICMT valve was 28.5 K when the ambient temperature was 23.9 °C. For the same ambient temperature the inlet temperature at the condenser was 83.2 °C and the outlet of the ICMT was -3.5 °C which gives a temperature difference of 86.7 K.

For the same test when the system operate in transcritical mode the temperature difference across the ICMT was found to be 34.9 K which is much higher compering with subcritical cycle. For this test the ambient temperature was 32 °C. There is no temperature difference from the outlet of the ICMT to the receiver also. For the ambient temperature of 32°C the inlet temperature at the gas cooler was 100 °C and the outlet of the ICMT was -3.5 °C which gives a temperature difference of 103.5 K.

As it observes from both graphs in Fig. 6.9 the system maintain a constant temperature after the ICMT and inside the receiver without affected from the ambient conditions and the related temperatures and pressure at the high pressure side of the system.

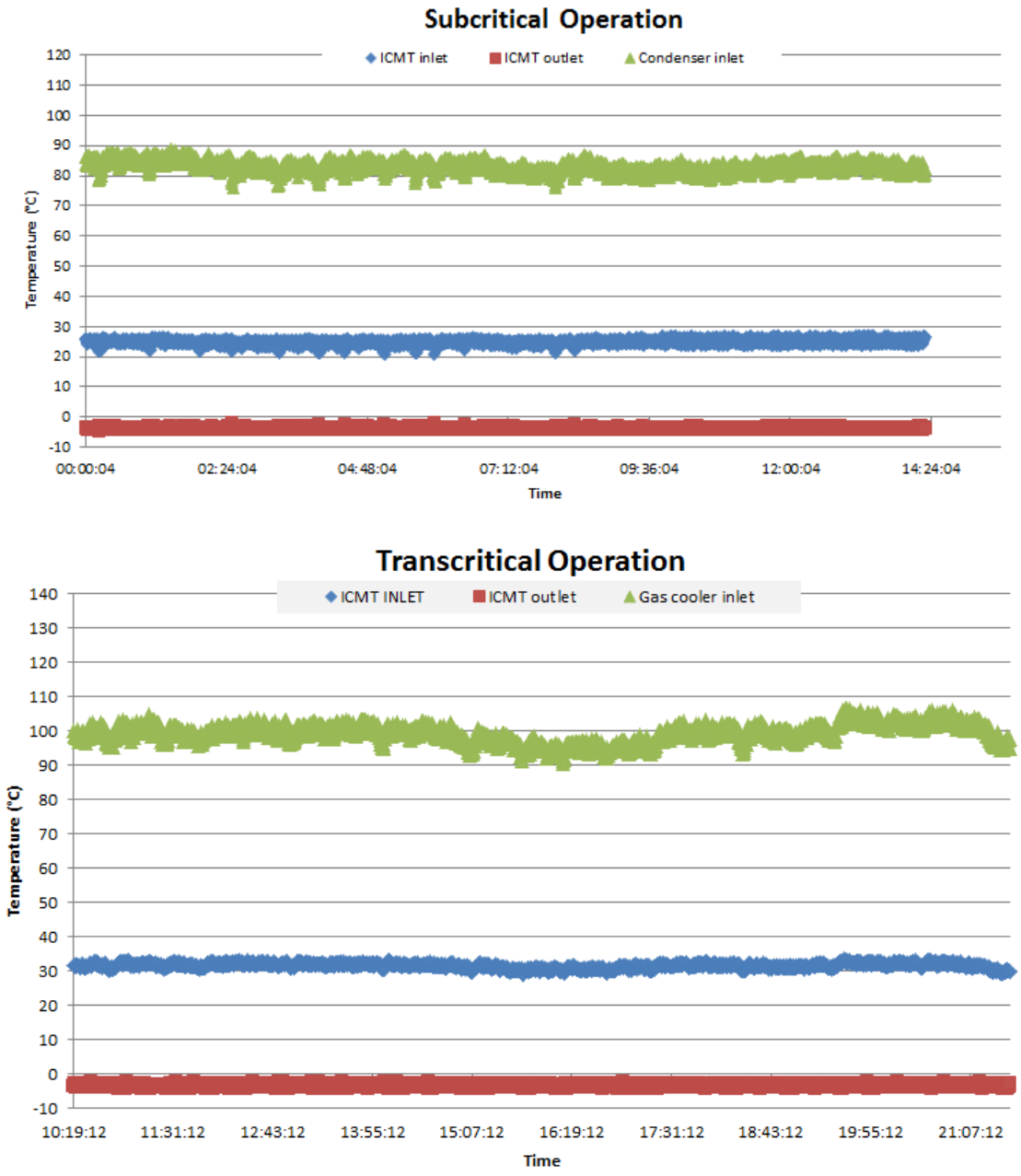

Figure 6.9 Inlet and outlet temperature conditions before and after ICMT valve

Figure 6.10 illustrates the pressure profiles at the inlet and outlet of the condenser/gas cooler and the pressure after the ICMT valve which is the same with the pressure inside the liquid receiver.

The pressure inlet at the inlet of the condenser was found to be 67.3 bar-g when the ambient temperature was 23.9°C. The pressure at the outlet of the ICMT valve found to be 30.8 bar-g which gives 36.5 bar-g pressure drop.

For the transcritical operation and with a ambient temperature equal to 32 °C the inlet pressure at the gas cooler was 81.5 bar-g. The pressure at the outlet of the ICMT valve was found to be constant at 30.8 bar-g. For the transcritical operation the pressure drop between gas cooler inlet and ICMT outlet was 50.7 bar-g, which is much higher comparing with the subcritical operation.

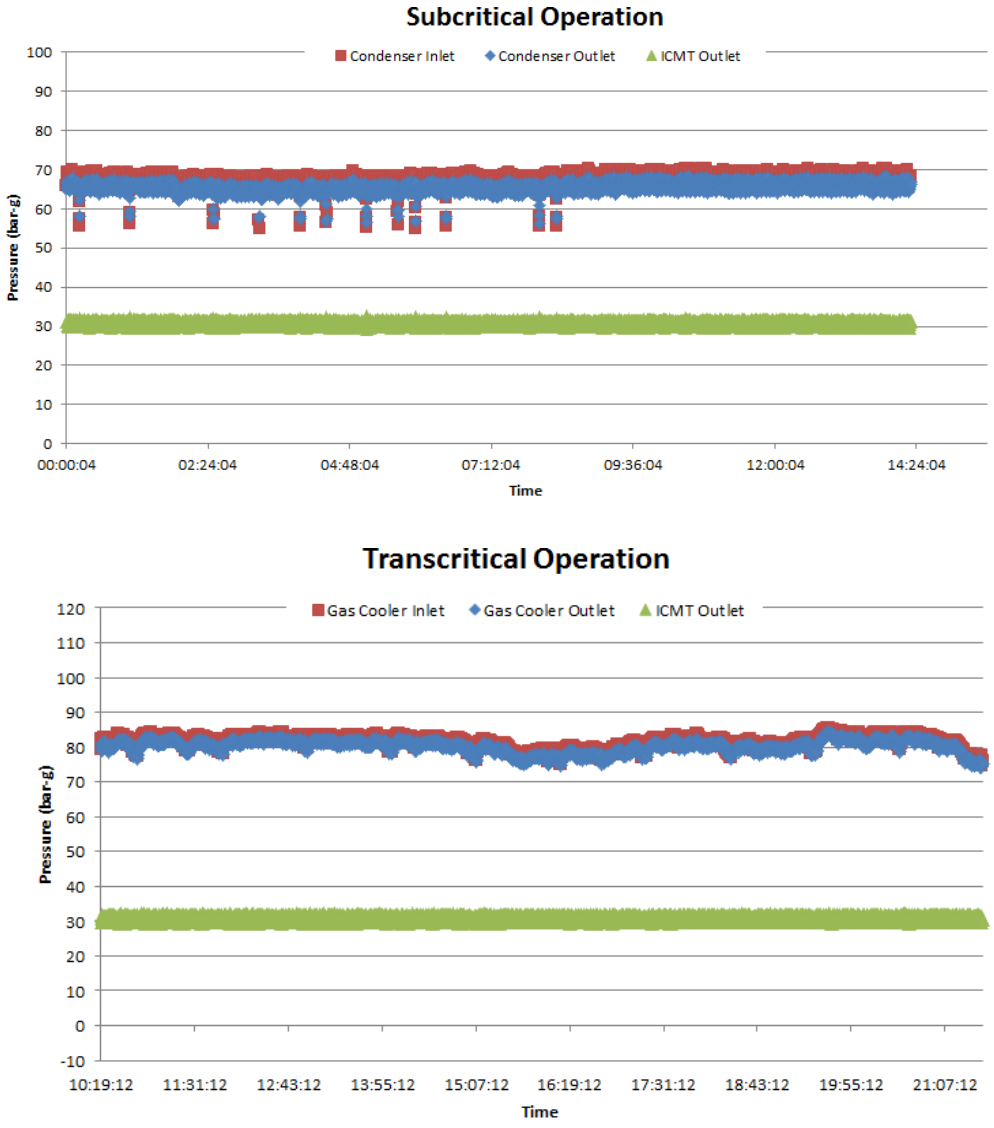

Figure 6.10 Pressure across the ICMT valve

The thermodynamic analysis of the experimental results shows that the separation ratio of gas by-pass to liquid flowing is a proportional of the ambient temperature and intermediate pressure. The C/GC design is slightly effect on the separation ratio due to the outlet values of the heat exchanger.

The variation of the separation ratio is determined by the CO_2 vapour mass fraction at the receiver inlet which is mainly a function of the gas cooler/condenser outlet parameters and as an extension the ambient temperature. More detailed results are presented in Fig. 6.11. The mass flow separation is a function of the enthalpy outlet of the condenser/gas cooler and a constant pressure of 32 bar at the intermediate stage of the system.

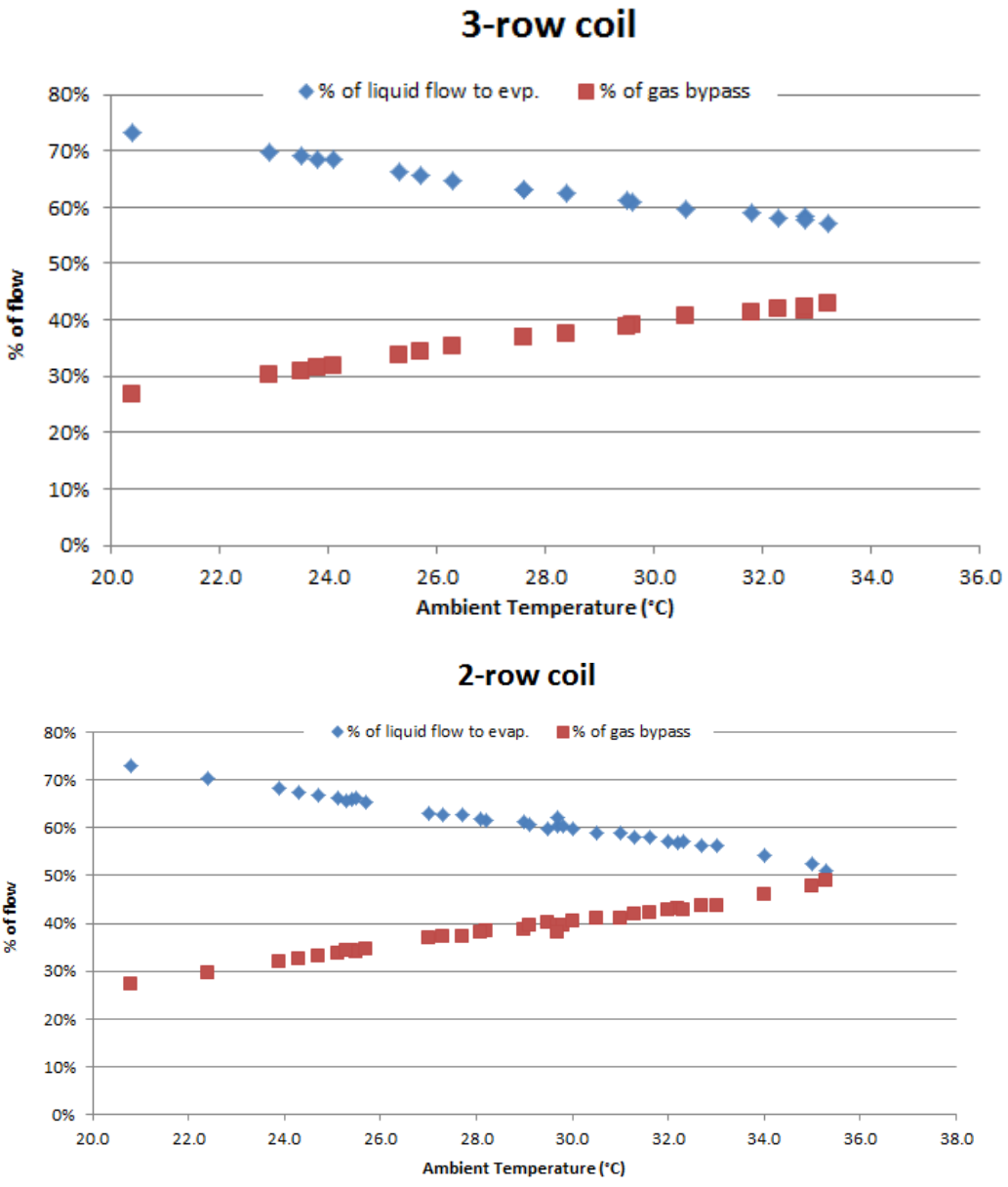

Figure 6.11 Refrigerant mass flow separation ratio

Both graphs in Figure 6.11 have similar trend line. The slightly lower pressure of the 3-row C/GC increased the rate of the liquid to gas by-pass when comparing with the

smaller coil. Both graphs related with the ambient temperature and as a proportional the discharge pressure and temperature. The CO_2 liquid mass flow rate flows to both evaporators and the vapour mass flow rate return from ICM bypass valve to compressor suction are a function of "x" factor as shown in Chapter 4.2.8.

6.3.4. REFRIGERATION LOADS

The refrigeration loads of the system were explained in Chapter 4.3.12. For these experimental tests the refrigeration load is including the MT refrigerated display cabinet and the AL additional water to refrigerant load. The valves to the LT refrigerated display cabinet were shut for those tests. The LT cabinet was operated only to validate the LT side of the model when was needed.

The capacity calculations are compared only between the 3-row and 2-row coils. The 2-row half coil due to the much lower nominal capacity is not included in this comparison.

The relationship between the mass flow rate and the ambient conditions was described in Chapter 6.3.3. The liquid mass flow rate was found to decrease as the ambient temperature increased which effect on the refrigeration load of the system. In Fig. 6.12 shows the relationship of the liquid CO_2 refrigerant flows from the receiver to both MT and AL.

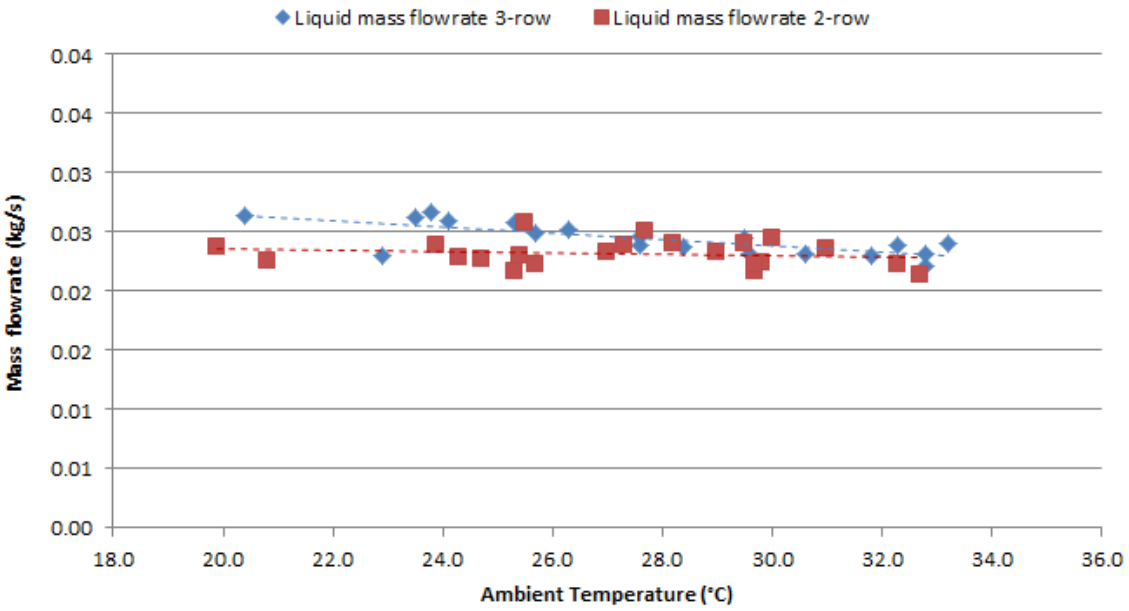

Figure 6.12 Refrigerant liquid flows to both evaporators for different ambient conditions

It can be seen clearly from the graph that the refrigerant mass flowrate of the liquid flows to both MT and AL decreasing as the ambient condition increased. The rate of liquid to gas is changed as the ambient conditions changed.

Figure 6.13 highlights the variation of the refrigeration capacity with respect to ambient conditions for all the fan speeds including the 50%, 60% and 70%. Those results based on the summation of MT and AL loads of the system.

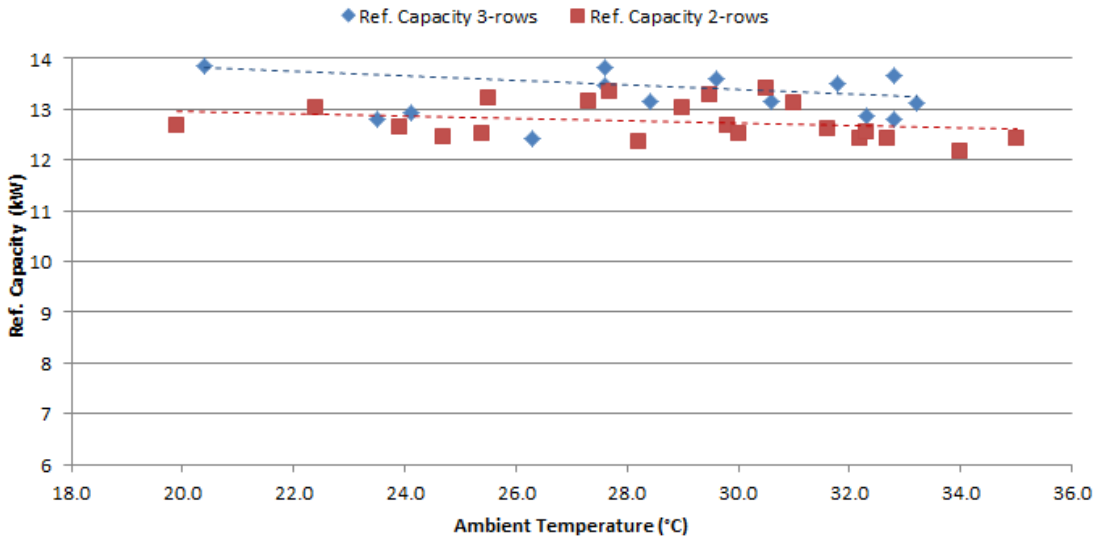

Figure 6.13 Refrigeration capacity with respect to ambient conditions

For both cases as the ambient temperature increased the cooling capacity is decreasing. This is due to the change of the liquid mass flow rate flow to both MT and AL. The refrigeration capacity is higher for the 3-row C/GC due to its lower approach temperature at the coil outlet as explained previously.

The fact that the refrigeration capacity for the 3-rows condenser/gas cooler is higher and the power consumption for both coils were separately installed is very similar leads to the higher cooling performance. When the ambient temperature is around 20 °C the refrigeration capacity of the system when the 3-row coil was installed was around 13.8 kW including MT and AL. On the other hand, for similar ambient temperature the refrigeration capacity of MT and AL together was around 12.9 kW for the 2-rows condenser/gas cooler. When the system operates in transcritical cycles and the ambient temperature was above 29 °C, the gap between 3-row and 2-row was lower.

The relationship between the refrigeration capacities and compressor power consumption with respect to ambient conditions is illustrated in Fig. 6.14 (Tsamos et al.,

2016). The results are represented included the test data for the main fan speed 70% when the two coils were separately installed to the system. Very similar trends may be obtained for the 50% and 60% fan speeds.

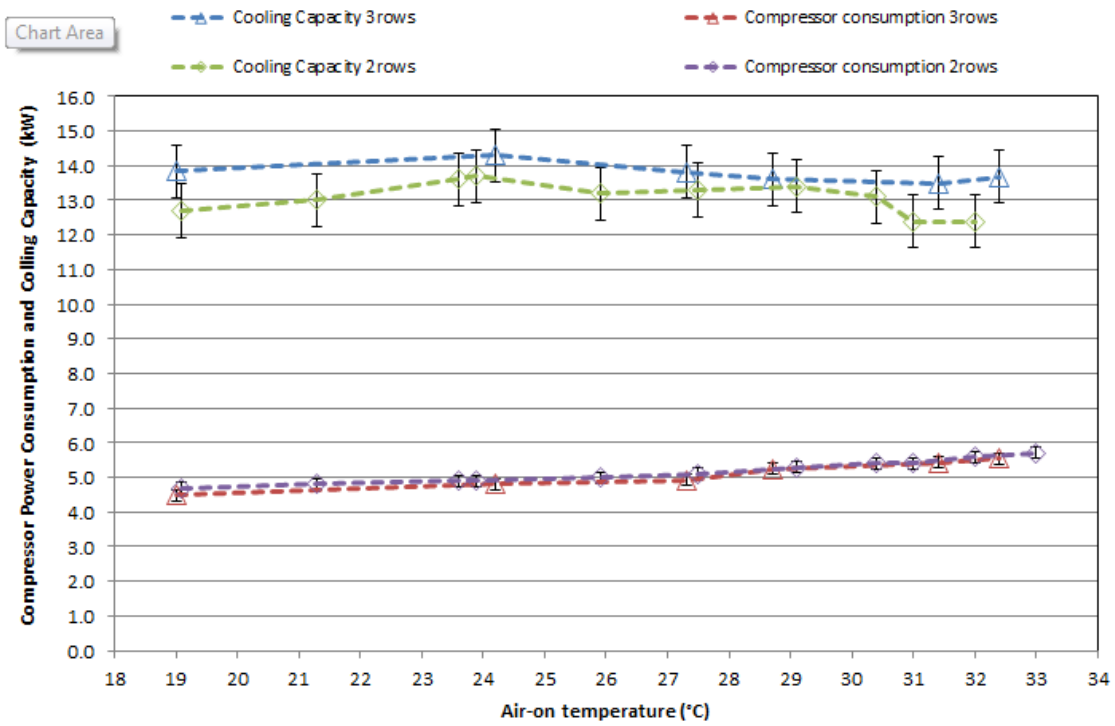

Figure 6.14 Cooling capacity and compressor power consumption for various ambient conditions

In Fig. 6.15 the inlet and outlet pressure at the MT refrigerated display cabinet and the evaporating temperature are illustrated.

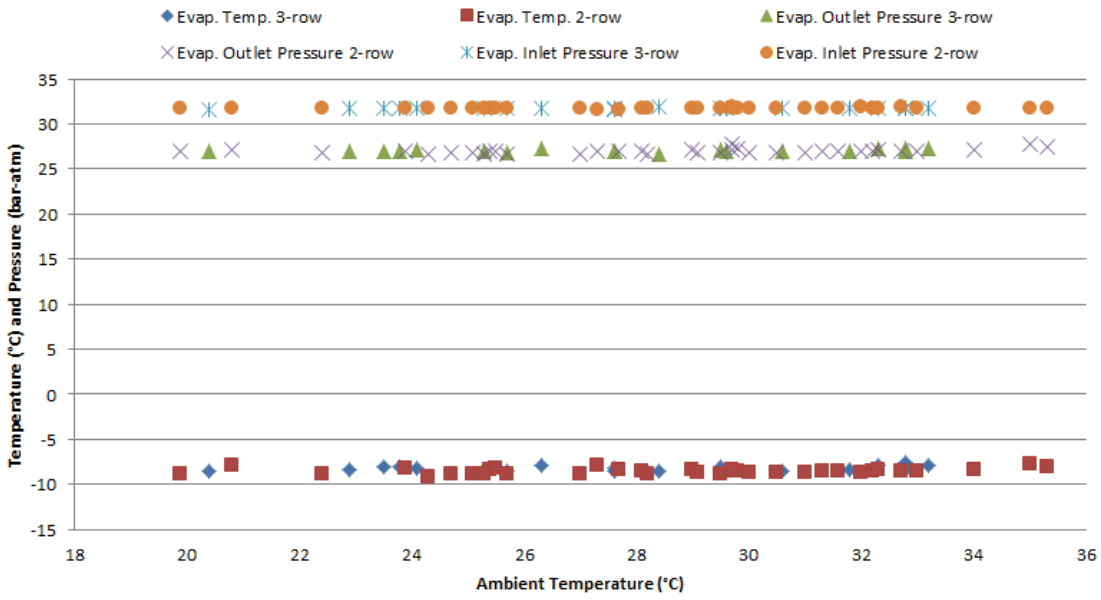

Figure 6.15 Inlet and outlet conditions at the MT evaporator

From the graphs can be obtained that the ambient conditions does not significantly effect on the pressure and temperature at the medium level of the system. The results show a pretty linear line for the ambient temperatures 19 °C to 36 °C.

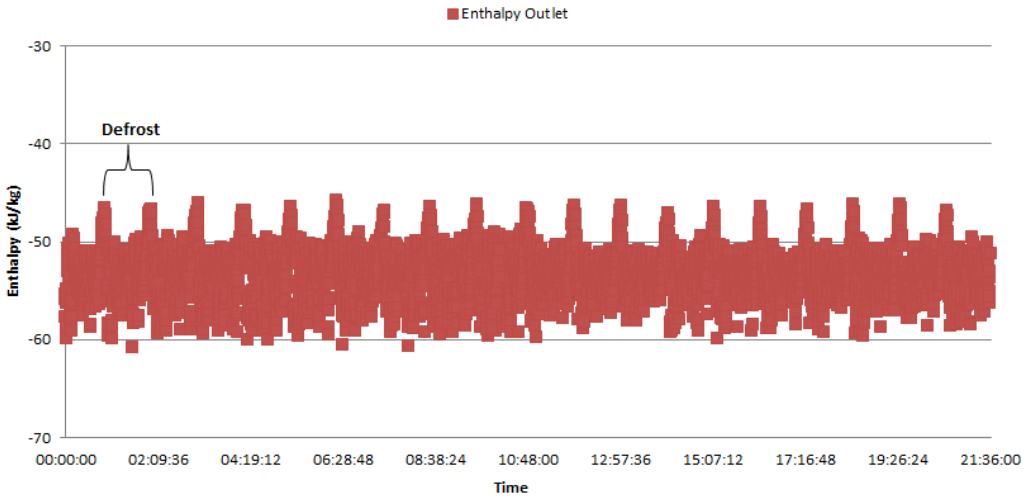

Figure 6.16 Enthalpy variation at the outlet of MT case cabinet

The enthalpy outlet of the evaporator with respect of the time is illustrated in Fig. 6.16. The system tries to maintain the air temperature inside the cabinet by controlling the superheat degree. In additional the defrost periods are clearly identified. The inlet and outlet thermocouples have been installed before the AKV valve and the outlet of the evaporator coil respectively.

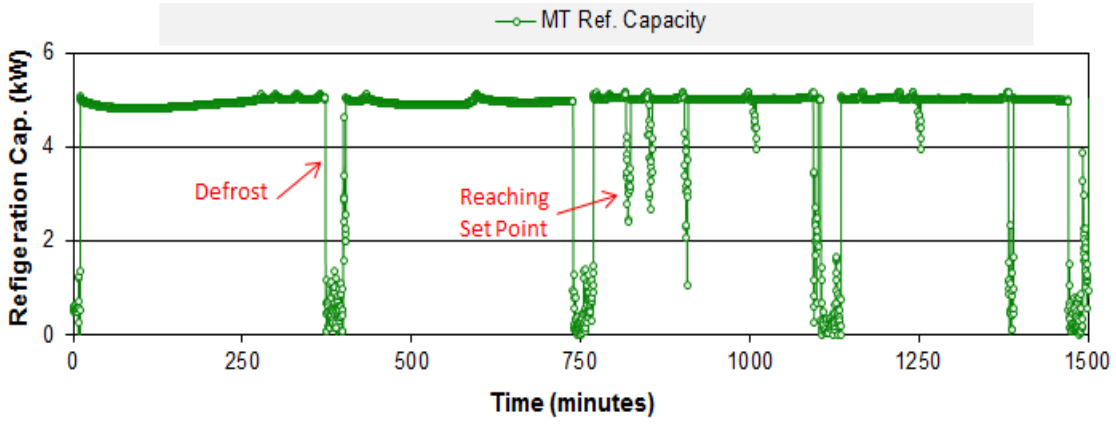

Figure 6.17 Capacity variation over a time period

The capacity variation of the MT refrigerated display cabinet with time at evaporation temperature -8 °C is shown in Fig. 6.17. The capacity was calculated by using the enthalpy difference across the coil and the mass flow rate for the given test. For this test the ambient temperature was 32 °C. The MT display cabinet delivers an average refrigeration capacity of 5.3 kW.

Fig. 6.17 also shows the compressor cycling off or AKV shut period when the air temperature inside the cabinet reaches the set point. It is clearly also defrost cycles, the off-cycle defrost control was set at 4 defrost cycles per 24 hours period. The defrost termination period was controlled on coil air-off temperature (probe) of 7 °C. The maximum defrost period set to be at 30 minutes. These defrost control settings were found to be satisfactory for the conditions tested.

Similar trend lines can be found for all the test results for both 3-row and 2-row heat exchanger when installed and tested separately. The cooling capacity of the 2-row half coil was much lower due to the nominal capacity of the system. In additional, similar graphs can be found for the additional brine load of the system.

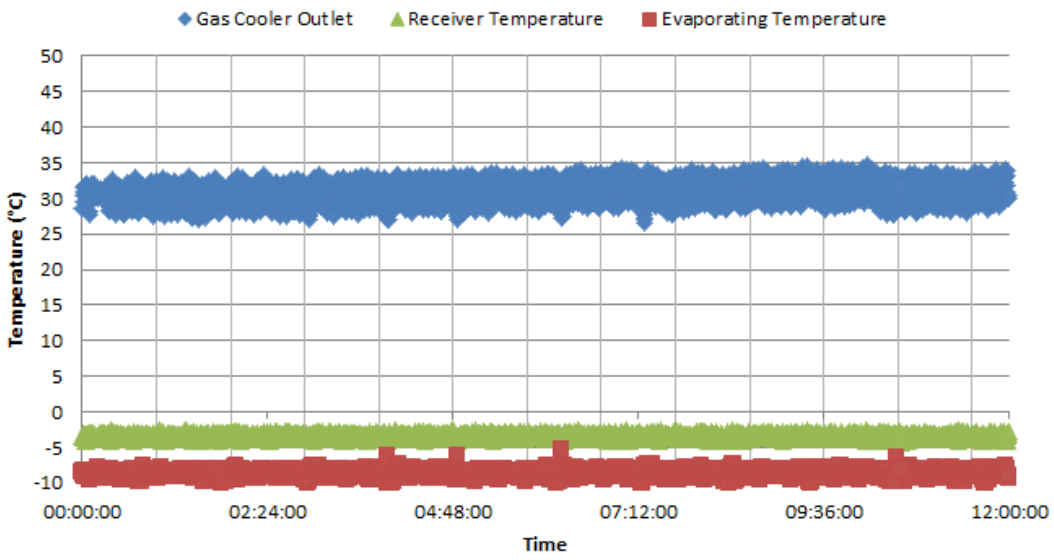

Figure 6.18 Temperature at different levels of the system

The variation of the temperature at the three main stages of the CO_2 system is showing in Fig. 6.18. The gas cooler temperature was measured at the outlet header of the coil, while the receiver temperature was measured at the inlet pipe line of the receiver. The evaporating temperature was measured at the inlet of the MT evaporator just after the AKV expansion valve. The same trend lines can be found for all the tests. The

difference at the C/GC outlet temperature is based on the ambient temperature and coil design 2 or 3 rows. The temperature at the receiver and evaporator were fairly constant due to the control parameters and strategies of the system. The only difference made by the C/GC outlet temperature was intervenes at the rate of the liquid to gas bypassed at the intermediate pressure level of the system, which has been proved above.

6.3.4.1. PRODUCT TEMPERATURE

The product temperature of the MT display cabinet was used to as a measure whether the CO_2 refrigeration system had reached steady state condition. When the temperature of the products located at the MT cabinet was relatively stable in the range of M1 (ISO, 2012) the system was considered to have reached steady state conditions. These conditions were used for the analysis for this chapter.

In additional, the product temperatures have been tested with different evaporating temperatures. The evaporating temperatures between -6.5 °C to -10 °C found to be proper in order to keep the temperature products in M1 classification. When the evaporating temperature was increased above -6.5 °C the air off temperature was high and product temperature rise as well. Below the limit of -10 °C the products with the lower temperatures found to be freeze. This range of the evaporating temperature has been used in order to investigate the effect of the evaporating temperature at the cooling performance of the system by using the mathematical model which created for this system.

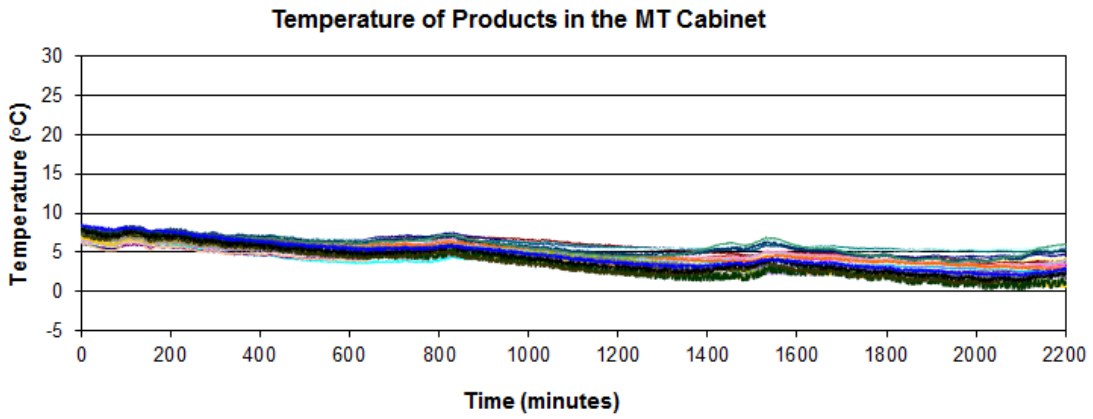

Figure 6.19 Product temperatures

Figure 6.19 shows the product temperature variation of the MT display refrigerated cabinet which has been installed inside the chamber room. The room conditions were kept constant at ISO3 at 25°C and 60% the relative humidity. These results were obtained with evaporating temperature of -8°C. It is also clear that during the defrost cycle the product temperature was slightly increased. More details regarding the MT display cabinet and relatively loaded position can be found in Chapter 5.2.12.1.

6.3.5. COEFFICIENT OF PERFOMANCE CALCULATIONS

The performance of the CO_2 booster refrigeration system which has been installed in CSEF – Brunel University was experimental tested by using three different condenser/ gas cooler which have been separately installed in the system and tested under the same conditions. The ambient condition or air inlet was maintained by using the unique test rig which has been designed and installed for the experimental work.

The analysis of the system used as boundaries the ambient temperatures and as a proportional the condition changing at the high pressure side of the system. Both subcritical and transcritical cycles are clearly identified and analysed. The intermediate and medium pressure levels of the system were kept constant for all the tests. The evaporating temperature for MT and AL was -8 °C and -10 °C respectively and both evaporator coils were used AKV expansion valves. The intermediate pressure was constant at 32 bar and the average temperature after the ICMT valve was equal to -3°C.

Due to the lower nominal capacity of the 2-row half coil the cooling performance of the system was dropped. For that reason, the coefficient performance results of the half coil does not included in this final comparison.

The performance calculations of the CO_2 booster refrigeration system is presented in Chapter 4.2.15. In order to take under consideration the effect of the different air volume flow rates passing through the condenser/gas cooler, the power consumption of the fan has been taken into account on the overall system COP.

The effect of condenser/gas cooler sizes on the discharge pressure and approach temperature can correspondingly affect the compressor power consumption, cooling capacity and cooling COP. The variation of the compressor power consumption and cooling capacity with respect to ambient temperatures were explained in previous chapters.

The cooling capacity is higher for the 3-row condenser/gas cooler due to its lower approach temperature at the gas cooler/condenser outlet while the compressor power consumption is slightly reduced for the system with a larger gas cooler/condenser. This leads to a higher COP for the 3-row CO_2 coil system for all three different fan speeds (Tsamos et al., 2016). Figure 6.20 illustrates the variation of the COP with respect to varies ambient temperatures when main fan speed set to be 50%, 60% and 70% of the total power.

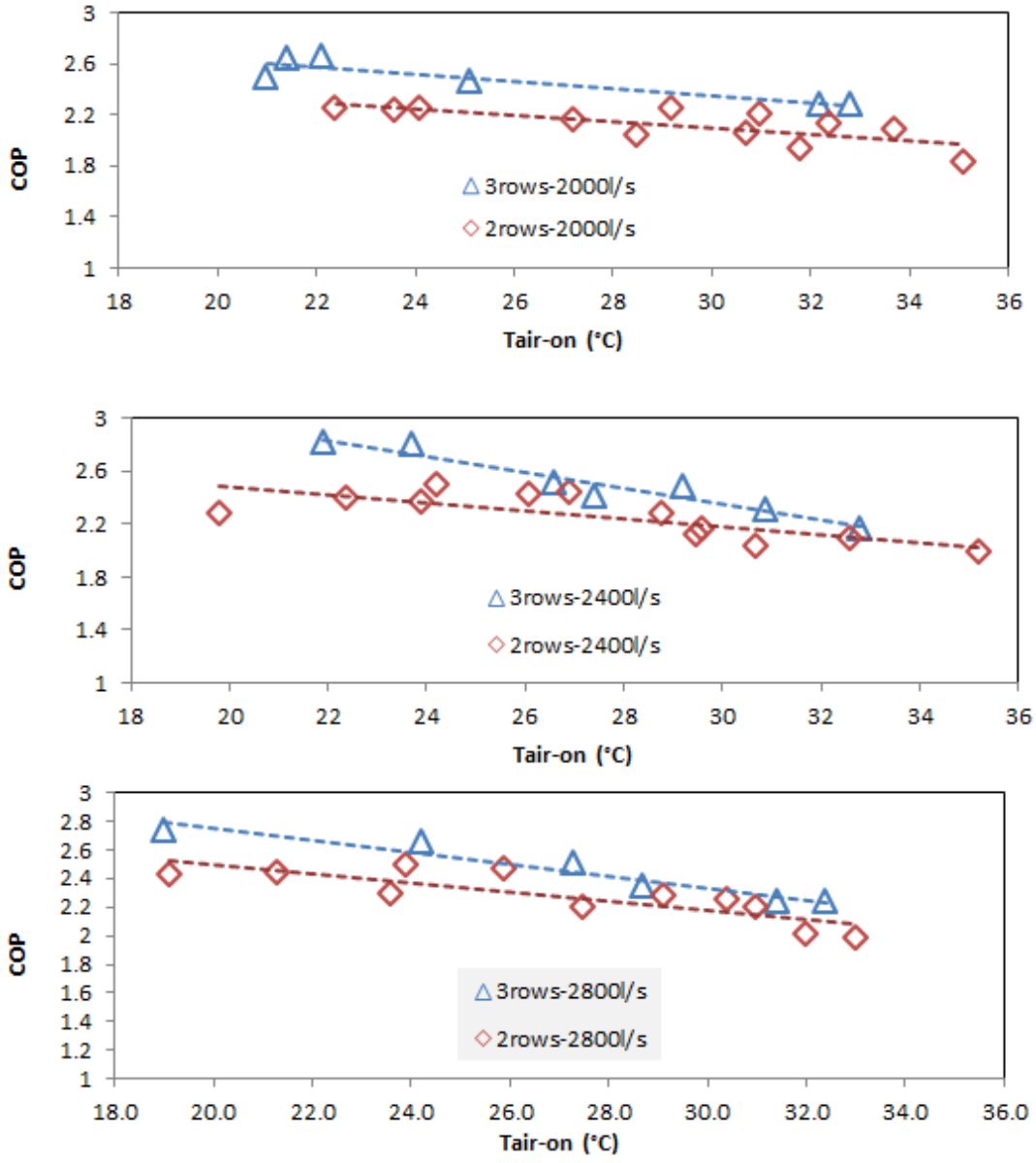

Figure 6.20 Variation of COP for different coil designs and air volume flow rates

It is found that the COP for both circumstances decreases at higher air-on temperatures. A higher COP was found at the 60% main fan speed, corresponding to 2400 l/s of air passing through the coil, and contributes to the lower power consumption of the fan when compared to 70% of fixed fan speed.

It should be noted that these test results are based on varied compressor speeds, a fixed fan speed, constant subcooling at 2K for subcritical cycles and designed discharge optimal pressure control in a transcritical mode.

When the main fans were set to run at 60% of the total fan speed, the COP of the CO_2 refrigeration system when the 3-row C/GC installed found to be 2.82 for the ambient temperature was 21.9 °C. For very similar ambient temperature the COP of the system with 2-row C/GC found to be 2.39. For the transcritical cycle when the ambient temperature was fairly same for both C/GCs at 32.6 °C the COP was found to be 2.16 and 2.09 for 3-row and 2-row respectively. This is due to higher cooling capacity for the 3-row C/GC due to its lower approach temperature.

For similar subcritical ambient temperatures the COP was found to be 2.65 and 2.44 for the 3-row and 2-row respectively. When the system operates at transcritical cycle the COP for the system with the 3-row coil was found to be 2.23 and for the 2-row coil 2.01.

The COP was reduced for both transcritical and subcritical cycles when the system operates with the fan speed to set at 50% of the total fan speed. This is due to the much higher approach temperature at the C/GC side.

Due to the much lower nominal capacity of the 2-row half coil (0.82m) the COP of the system decreased dramatically. For example when the system is operating with fan speed equal to 60% the COP varies from 1.91 to 1.55 for subcritical and transcritical respectively. Due to the much lower values the COP the comparison with the system when the other two coils separately installed is neglected.

6.4.MODEL VALIDATION & FURTHER INVESTIGATION

The third section of this chapter includes the comparison of the experimental results with the simulation model results. The simulation model already discussed in Chapter 4 of this thesis were developed to simulate the performance of the existing CO_2 refrigeration system with the designed capacities of 6 kW of MT and 6-8 kW of AL.

After the experimental tests the model has been updated based on the real delivered capacities of the system and pressure and temperature profiles across the system. The model also predicts the pressure at the high and medium level of the system, the overall refrigerant mass flow rate, the cooling capacity of MT and AL and the power consumption of the system. The capacity at the C/GC is also predicted by the model. The experimental results are inserted to the model to use as references points for the simulation values, for the case that the error is higher than the limits that has been set-up the model is running again. The boundary condition for the simulation model was the ambient temperatures. Figure 6.21 shows the simulation model graphical illustration.

The model is also predicts the additional load plate heat exchanger efficiency. M. Conde (2011) equations to calculate the brine specific heat and density were inserted to the system in order to calculate the capacity of the AL from the brine side. The energy balance equation for the refrigerant and brine side is applied to the model.

The simulation model is also calculates the isentropic and volumetric efficiency of the compressor. The swept volume of the compressor is also calculated and compared with the manufactured data based on the maximum delivered swept volume of this type of compressors.

The mathematical model has been developed using Engineering Equation Solver –EES. Further explanations of equations and procedures used to simulate the CO_2 refrigeration system are detailed in Chapter 4.

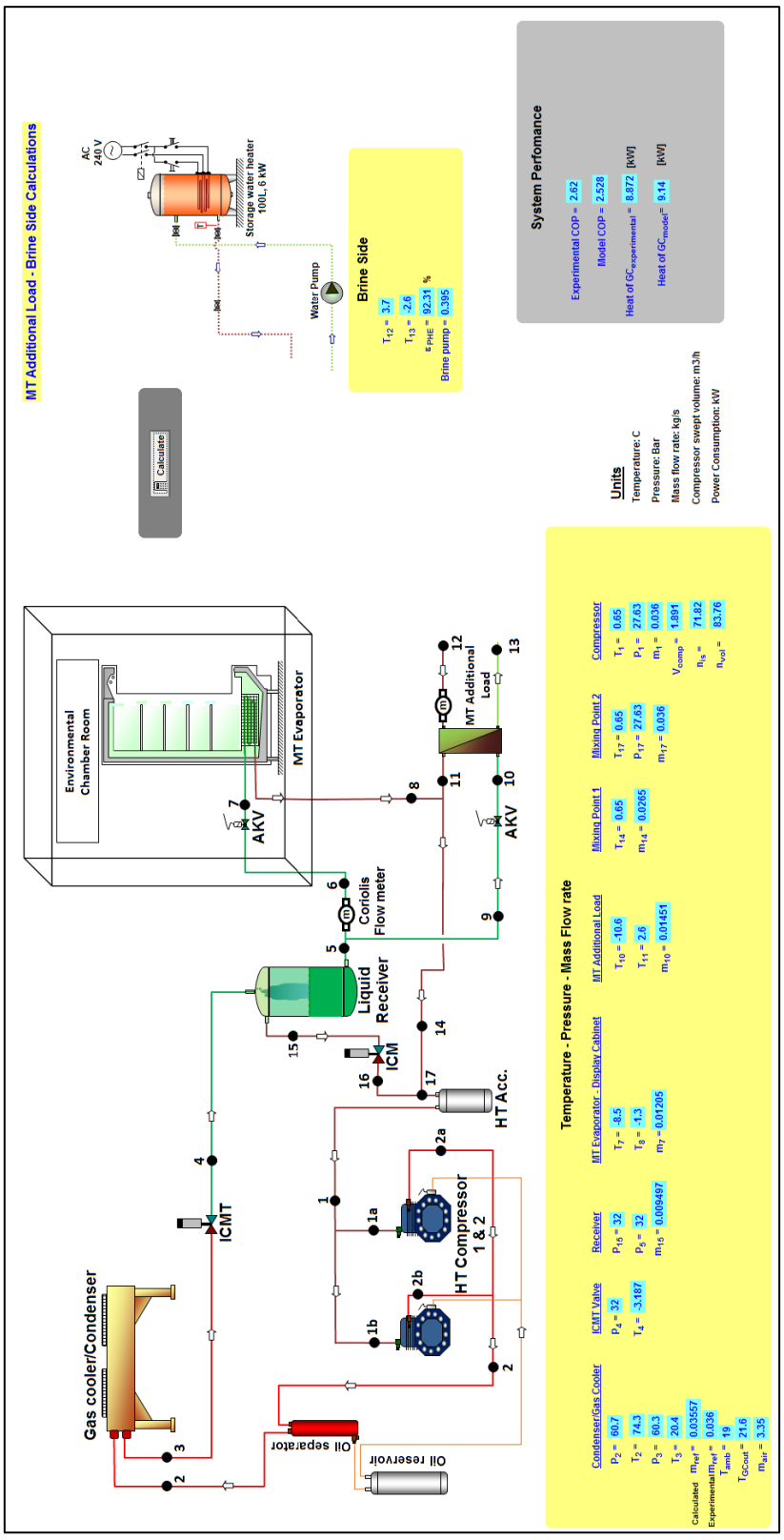

Figure 6.21 Simulation model graphical illustration

6.4.1. MEDIUM TEMPERATURE DISPAY CABINET MODEL

The model has been developed in order to further investigate the evaporator coil of the medium temperature display cabinet. The design parameters entered to the model based on the data provide by the manufacturer. The design parameters of the coil are illustrated below.

Table 6.4 MT cabinet design parameters

Geometry Parameters	Values	Units
Fin Material	Aluminium	
Pipe Material	Copper	
Pipe internal diameter	0.0127	m
Longitudinal tube spacing	0.033	m
Transversal tube spacing	0.038	m
Fin spacing	0.0064	m
Fin thickness	0.00022	m
Number of circuits	4	
Number of rows deep	6	
Number of rows high	4	
Coil height	0.149	m
Coil depth	0.189	m
Coil width	2.085	m
Test Parameters		
Environmental Room Temperature	25	°C
Environmental Room Relative Humidity	60	%
Air mass flow rate	0.30	kg/s

The model validated against the results from the experimental test facility which based on the same coil geometry and test parameters. The comparison between experimental and predicted values from the simulation model was found to be satisfactory based on the refrigeration capacity. Table 6.5 shows the comparison of the results under different conditions.

Table 6.5 MT cabinet model validation

Parameters	Experiment (kW)	Model (kW)	% Difference
Q_{evap} with T_{evap}=-8°C, ΔT_r=5 K, ΔT_a=10 K, ΔRH_a=20 %, Air flow rate=0.26 m^3/s Pinterm=32 bar	5.3	5.8	9%
Q_{evap} with T_{evap}=-8°C, ΔT_r=5 K, ΔT_a=10 K, ΔRH_a=20 %, Air flow rate=0.26 m^3/s Pinterm=35 bar	4.7	4.9	4%
Qevap with Tevap=-8°C, ΔTr=5 K, ΔTa= 8 K, ΔRHa=20 %, Air flow rate=0.26 m3/s Pinterm=32 bar	3.09	3.14	2%
Q_{evap} with T_{evap}=-9°C, ΔT_r=5 K, ΔT_a=10 K, ΔRH_a=20 %, Air flow rate=0.26 m^3/s Pinterm=32 bar	5.07	5.10	1%

The validated model was used for further examination of the MT evaporator coil. The results are inserted to the integrated model later in order to provide more accurate data. The validated model is used for further investigation only for the coil which has been used for the experimental investigation.

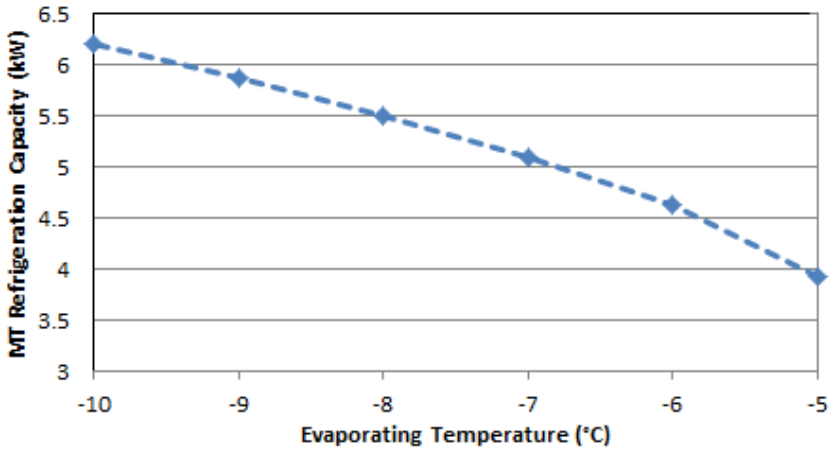

Figure 6.22 Refrigeration capacity for different evaporating temperatures

In Fig. 6.22 the MT refrigeration capacity with different evaporating temperatures is illustrated. It is clear from the graph that as the evaporating temperature decreases the capacity of the coil reduced rapidly. The results presented are based on the constant superheat of 5K. The evaporating temperature is controlled by the pressure drop at the expansion AKV valve. The increased evaporating temperature causes a reduction of temperature difference (ΔT) between the air and refrigerant sides; this has a proportional of the mass flow rate reduction in order to maintain constant superheat of 5K. As the experimental results shows the evaporating temperature is not affected by the intermediate and high pressure side of the system and remains constant.

The experimental results show that the refrigeration capacity of the MT display cabinet is associated with the refrigerant mass flow rate passing through the coil. The refrigerant mass flow rate is a proportional of the refrigerant quality exit the condenser/gas cooler. The quality of the refrigerant exits the C/GC is changing as the ambient temperature is increasing.

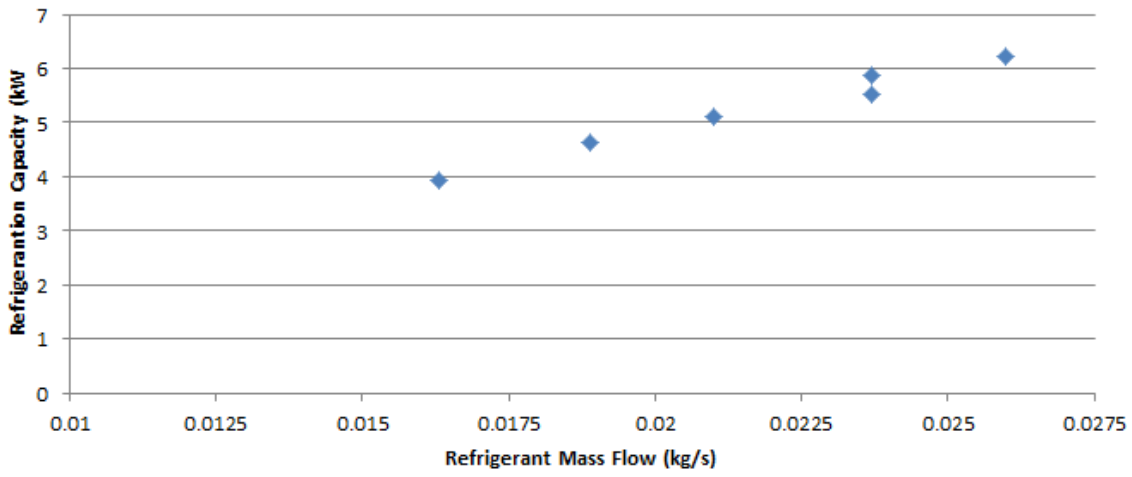

Figure 6.23 Refrigeration capacity with different mass flow rates

In Fig. 6.23 the capacity is plotted against the refrigerant mass flow rate passing through the coil as is calculated by the model. Those based at the same condition with Fig. 6.22. When the ambient condition was lower than 26.8 °C and the system was running in subcritical mode the ratio of the liquid to gas by passed was much higher comparing with the subcritical cycle. Therefore, the refrigeration capacity of the subcritical cycle was higher.

Comparing the 3-row and 2-row coils based on the discharge properties shows that the 3-row coil had lower pressure which means higher liquid to gas ratio. This has been explained analytical in this chapter. The surface efficiency of the evaporator was found to be 0.86 and the average liquid flows to evaporator 4.6 litres.

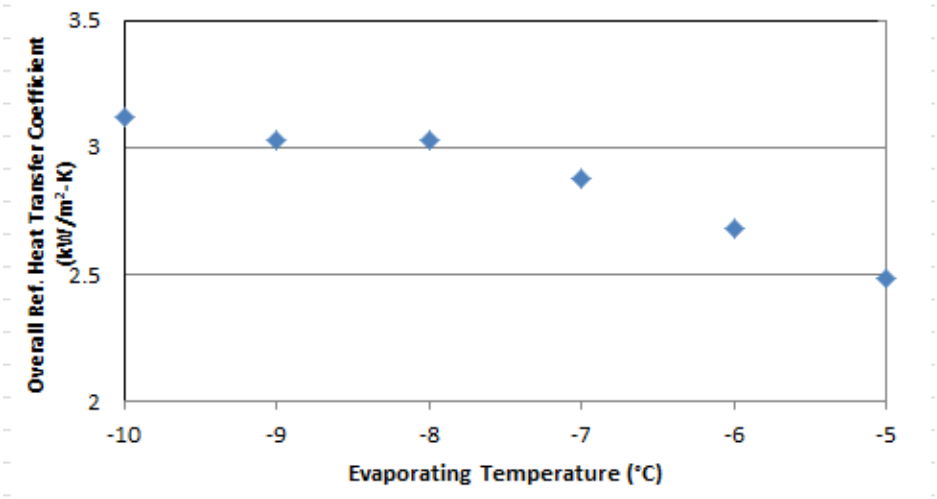

Figure 6.24 Overall refrigerant heat transfer coefficient with different evaporating temperatures

(Overall two-phase heat transfer coefficient for MT-DX evaporator. Calculations are based on the flow regime: Intermittent to Annular and Dryout to Mist regime)

Figure 6.24 shows the variation of the overall refrigerant heat transfer coefficient with different evaporating temperatures. The overall heat transfer coefficient increased as the evaporating temperatures decreased.

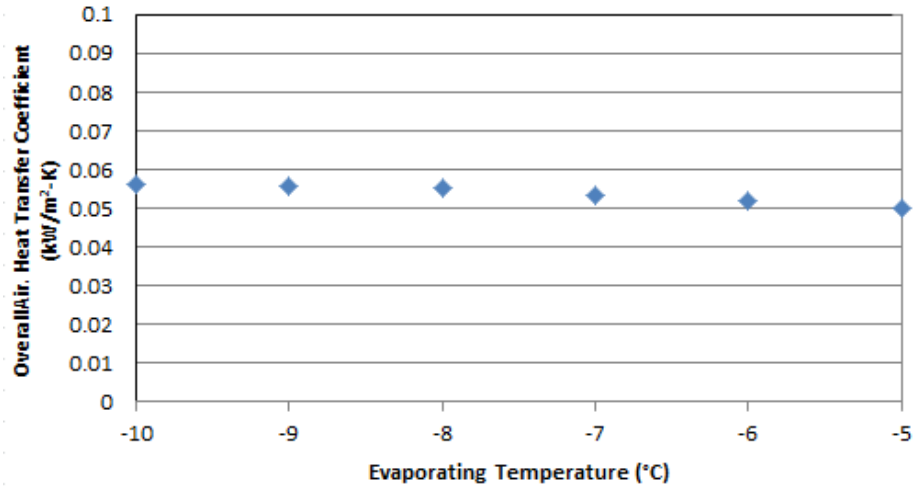

Figure 6.25 Overall air side heat transfer coefficient with respect the evaporator temperature

(The air side heat transfer coefficient consists of convective and latent heat transfer coefficients)

For Fig. 6.24 and 6.25 the investigated conditions were the same and only the evaporating temperature change for this analysis.

Similar trend line can be found for the overall air side heat transfer coefficient with respect the evaporator temperature. In additional the two phase flow coefficient increased as the convective boiling heat transfer coefficient increased which is affect by the mass flux of the refrigerant.

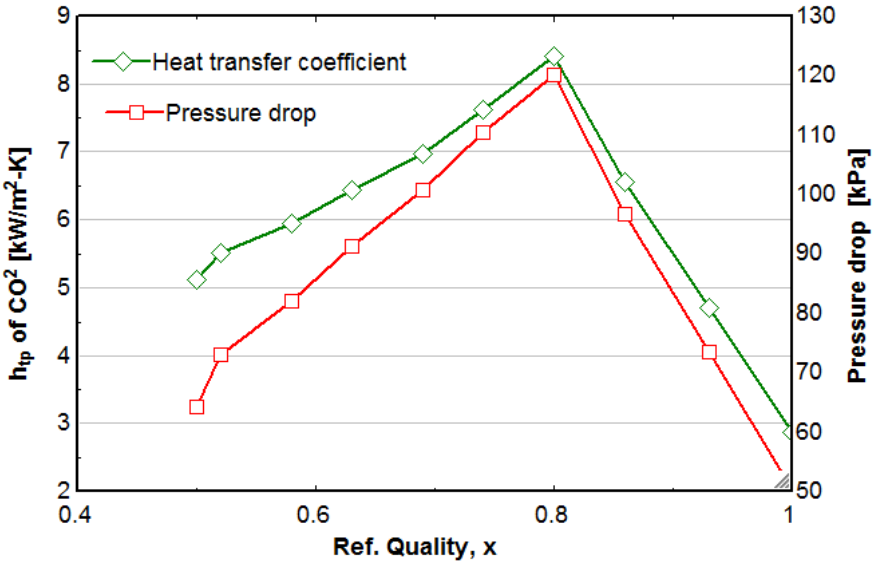

Figure 6.26 Two phase heat transfer coefficient and pressure drop with respect to refrigerant quality along the evaporator coil

(Equations used to calculate both pressure drop and two phase heat transfer coefficient: Cheng, 2008)

Figure 6.26 illustrates the two phase heat transfer coefficient and pressure drop with respect to refrigerant quality along the evaporator coil. Those results were calculated by using the validated model at evaporating temperature of -10 °C, mass velocity 440 kg/s.m^2. The internal diameter of the pipe was 12.7 mm as described before. Very similar trend lines can be found for the rest of the evaporating temperatures which have been investigated above.

It is clear from Fig 6.26 that both two phase heat transfer coefficient and pressure drop increases until the vapour quality reaching their peak values at the vapour quality of 0.8 where the annular flow region ends. When the refrigerant reached the dry out region both heat transfer coefficient and pressure drop are decreased sharply, this is due to the reduction of the thermal conductivity at the dry out region.

The results of the model were used to understand clearly the operation of the MT display cabinet. With respect of the product temperatures the MT display cabinet model has been integrated with the overall CO_2 system model.

6.4.2. VALIDATION OF THE SYSTEM RESULTS

The data obtained from the initial experimental tests with the initial condenser/gas cooler design and pipe arrangement were used to validate the numerical model. Therefore, the predicted parameters are compared with the experimental data results. The model is validated against the overall results of the CO_2 booster system and is does not take into account the different condenser/gas cooler designs and fan speeds. In Chapter 7 a detailed gas cooler model is presented. Then, the detailed model is integrated with the CO_2 system model and the results 6.3.5 for different coil designs and fan speed were validated. The overall COP of the CO_2 refrigeration system without taken into account the fan power consumption is calculated as shown below.

$$COP_{CO2} = \frac{Q_{MT} + Q_{AL}}{W_{comp} + W_{brine,pump}} \qquad 6.15$$

It should be noted that the compared experimental values are based on varied compressor speeds, constant subcooling at 2K for subcritical cycles and designed discharge optimal pressure control in a transcritical mode. The refrigerant mass flow rate remains fairly constant and changes only when the system moves from subcritical operation to transcritical cycle. The evaporating temperature at MT and AL stage was -8°C (±0.5°C). The heat exchanger air-inlet parameters, temperature and flow rate, can be well controlled to specified values without affect from the ambient conditions. The air flow temperatures were varied from 19°C to 36°C for this experimental work. For air inlet temperatures below the 19°C the recirculation fans and air heaters were switched off.

The intermediate and medium pressure levels were fairly constant at 32 bar and 26 bar respectively. The effect of the intermediate pressure level at the final COP of the system is further investigated. The higher pressure level effect at the refrigerated capacity of the system is also experimentally investigated and will present in the next sub-chapter.

The power consumption of the brine pump was measured by using a power quality analyser connected to the pump. This found to be pretty constant at all the ambient conditions and was changed only when the load settings changes. The simulation model

is calculating the power consumption of the pump by using the mass flow rate based on the load and the density of the brine. The pressure drop and the efficiency of the pump are calculated based on the manufacturer datasheet. More details can be found in Chapter 4.2.12.

Figure 6.27 illustrates the experimental and simulation calculations of the COP with respect to ambient temperatures. When the ambient temperature was higher than 20 °C the simulation and experimental results are shown really good agreement. The values presented in the figure when the temperature is below 20 °C shows that the calculated COP is 23% higher than the experimental. One main reason for the deviation is the power consumed by the compressor. The mathematical model used to analyse the experimental results which based on the manufacturer datasheet is predicted lower power consumption made by the compressor when the ambient conditions is between 15 to 20 °C.

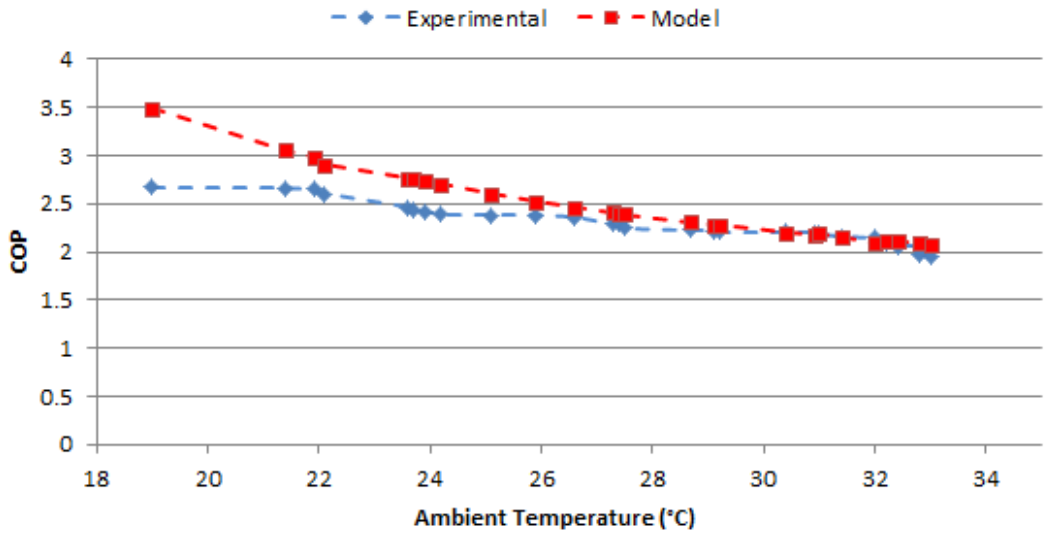

Figure 6.27 Cooling performance model validation

Figure 6.28 presents the power consumption of the system as predicted from the simulation model and calculated from the mathematical model which has been created from the manufacturer datasheet. The difference between experimental and model results is due to the pressure ratio difference between the experimental and calculated power consumption and the enthalpy at the discharge line of the compressor.

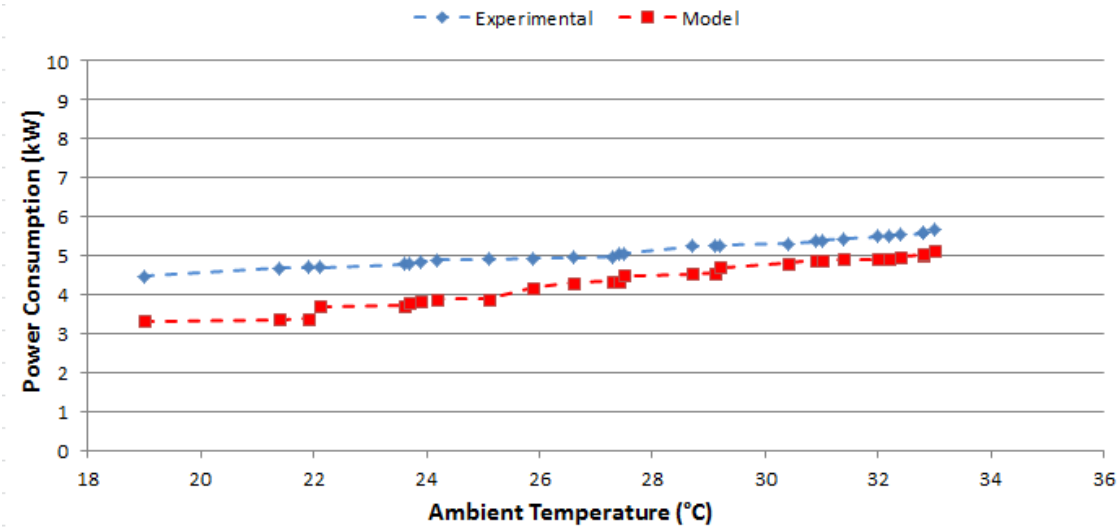

Figure 6.28 Compressor power consumption model validation

Figure 6.29 illustrates the comparison of the experimental and predicted power consumption of the system including the HT compressor and brine pump. It can be seen that the predicted overall power consumption values the absolute average difference is 13%.

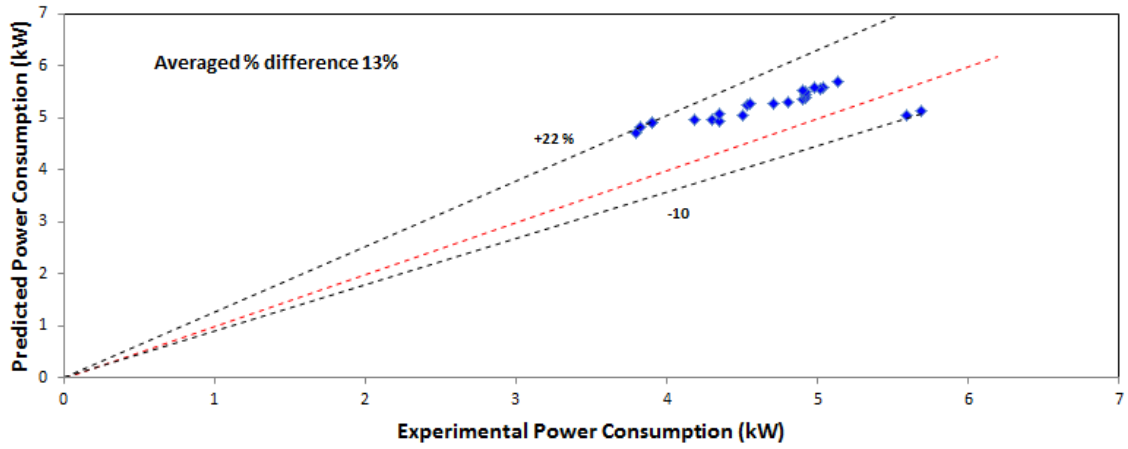

Figure 6.29 Comparison of the experimental and predicted power consumption of the system including the HT compressor and brine pump

Figure 6.30 shows the comparison between the actual and predicted overall COP of the CO_2 booster refrigeration system. It can be seen that 100% of the predicted overall COP data points fall within the average difference of 7%.

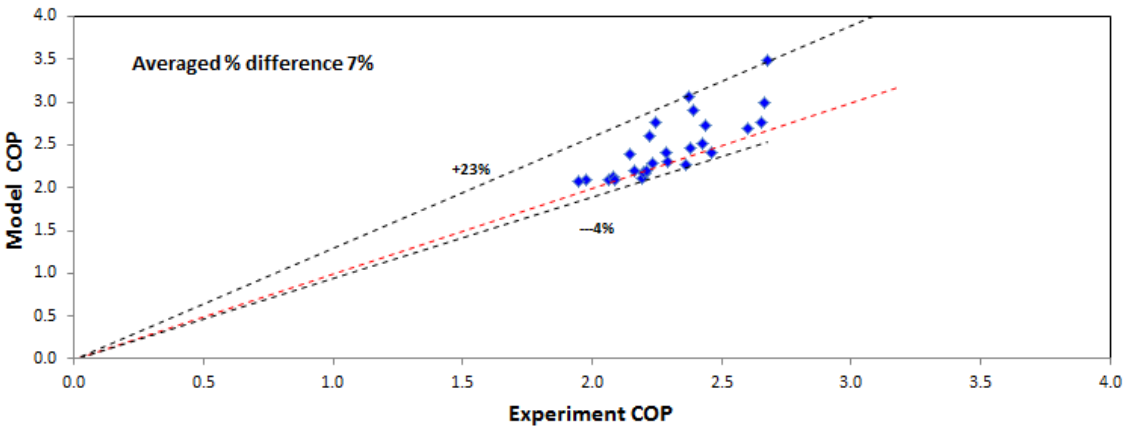

Figure 6.30 Comparison between the actual and predicted overall COP of the CO_2 booster refrigeration system

To determine the validity of the model, the statistical analysis of the COP were performed as shown in Table 6.6. The formula used to calculate the relative difference is given in Equation 6.17.

$$\text{Relative Difference} = \left[\frac{(\text{EES Value} - \text{Experimental Value})}{\text{Experimental Value}}\right] \cdot 100 \qquad 6.16$$

The predicted $COP_{overall}$ have mean difference of 6.6%. This indicates that the numerical model can predict the performance of the CO_2 booster refrigeration system quite accurately.

Table 6.6 Statistical analysis of the model validation

Parameters	Number of data points	Percentage of predicted points within ±14%	Mean difference (%)
$COP_{overall}$	95	92	6.6

The validated model is used for further investigation of the system when the control strategies changes at the intermediate and medium pressure levels of the system. Both are validated in the next subchapter where the results of the additional evaporator installation are explained.

The overall COP of the CO_2 refrigeration system was investigated under different intermediated pressures. For the experimental results the intermediate pressure was set to be above the medium pressure setting of 32 bar where the medium pressure set point was 26 bar. Figure 6.31 shows the variation of the COP under different intermediate

pressures with the ambient temperature. The evaporating temperature input to the model was set to be at -8 °C.

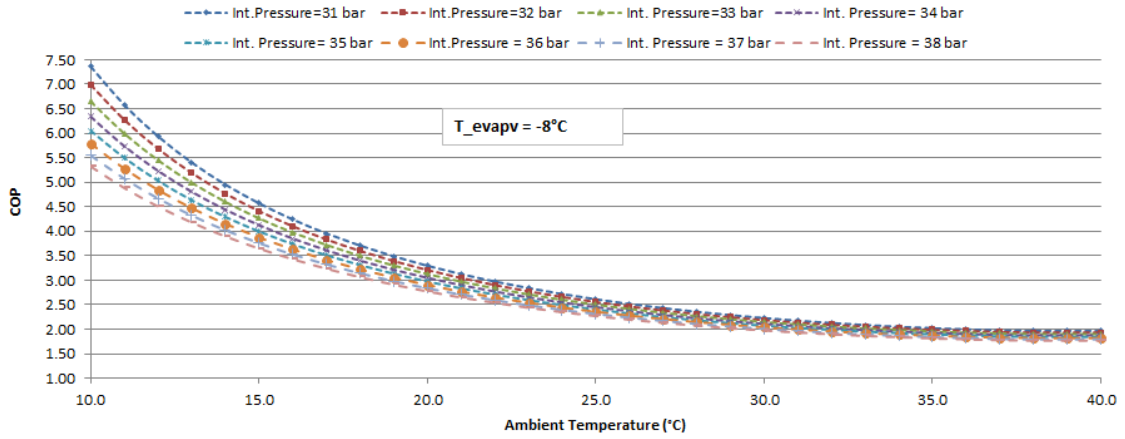

Figure 6.31 COP for different intermediate pressures

It is clear from the graph that as the intermediate pressure of the system increases the overall COP of the system decreases. The enthalpy diminished with the higher intermediate pressure is higher which decrease rapidly the refrigeration capacity of the system. In additional the rate of the liquid to gas by-passed is also decreased and effect on the refrigeration load of the system.

From the experimental results it was found that the evaporating temperature must be varied between -6.5 °C to -10 °C in order to keep the product temperatures at the M1 standard level. Therefore, the effect of the evaporating temperature range as it found from the experimental results is further investigated to identify the effect to overall COP of the system.

Figure 6.32 illustrates the variation of the COP under different evaporating temperatures with respect to ambient temperatures. For this simulation model the intermediated pressure level set to be at 31 bar. The overall mass flow rate of the system found to be fairly constant and changes only when the system moves from subcritical to transcritical cycle. The rest of the settings were kept constant for all the simulation models.

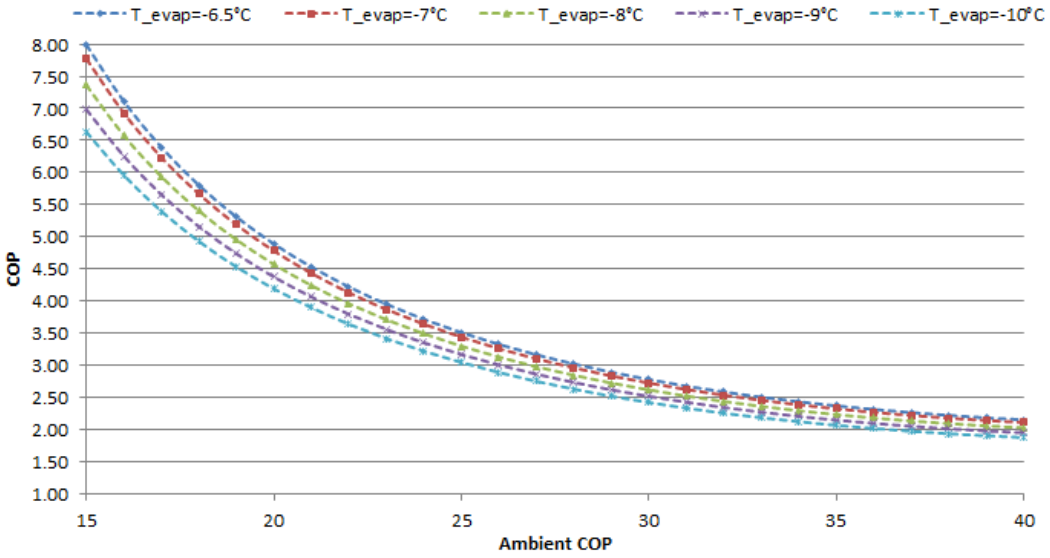

Figure 6.32 COP variation for different evaporating temperatures

6.5.RESULTS FROM TEST RIG MODIFICATIONS

The additional evaporator has been installed at the CO_2 refrigeration system to further investigate the medium pressure level of the system under different conditions. The requirement product temperatures for the MT display cabinet make more difficult the extensive investigation of the system medium level.

In additional the DX air cooler evaporator is used to balance the system when two compressors are running in parallel. More details for this can be found in Chapter 4.3.15.

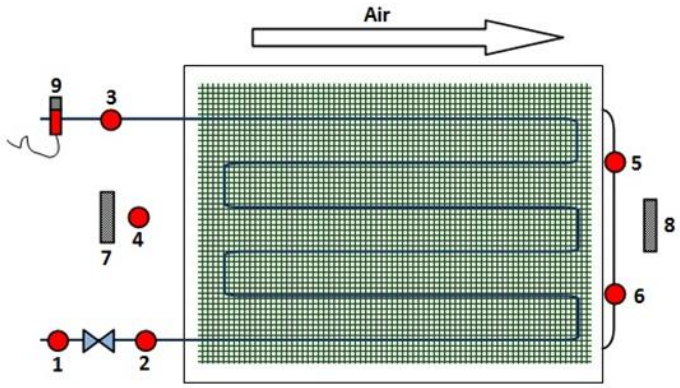

1	Temperature sensor (Inlet - before AKV)	Refrigerant Side
2	Temperature sensor (Inlet - after AKV)	
3	Temperature sensor (Outlet)	
4	Air Inlet	Air Side
5	Air Outlet (Top Fan)	
6	Air Outlet (Bottom Fan)	
7	RH (Inlet)	
8	RH (Outlet)	
9	Pressure Transmitter	Refrigerant Side

Figure 6.33 Relatively installation position of the temperature and humidity sensors

Figure 6.33 illustrates the relatively installation position of the temperature and humidity sensors, which have been used for the data monitoring and recording. To investigate further the effect of the intermediate pressure setting on the refrigerated capacity of the system the MT display cabinet was switched-off. The capacity of the system was included the air cooler evaporator and the AL system.

The chamber room was set at 10 °C with relative humidity of 50% (±4%) to minimize the dew point and avoid the frost at the coil. The same type of controller with the MT display cabinet is used for the air cooler. The settings are showing below in Table 6.7.

Table 6.7 AAC set points

Set Point	-2 °C
Defrost Method	Electric
Defrost Duration	35 mins
Max value of superheat	15 K
Min value of superheat	10 K

The first series of tests included the performance tests of the air cooler based on the cooling capacity under different ambient temperatures at the high pressure side of the system. This is to validate the cooling capacity drop with respect of the ambient conditions and the overall COP reduction of the system.

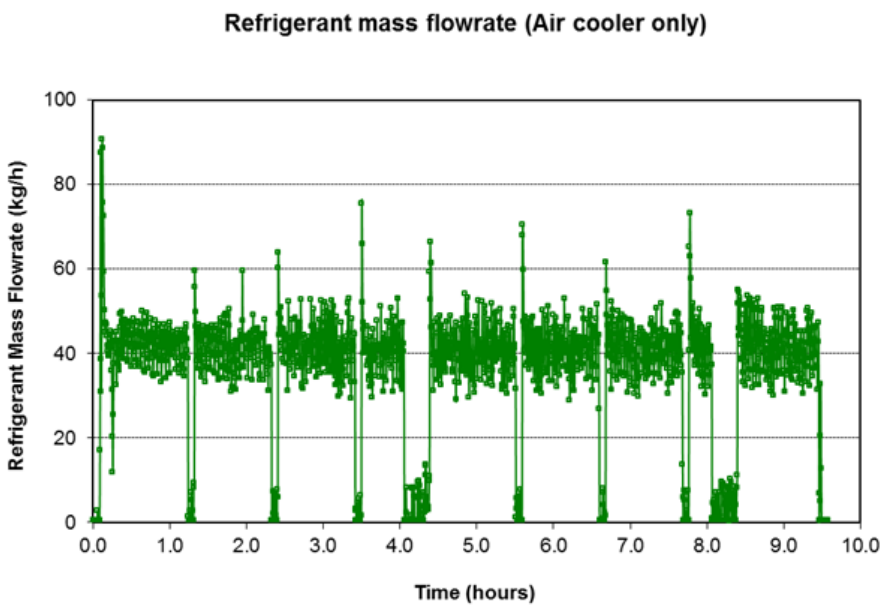

Figure 6.34 Variation of the mass flow rate with the time

Figure 6.34 shows the variation of the mass flow rate with the time when only the air cooler was running and the MT display cabinet was switched-off. It is clear from the graph the defrost periods which set to be every 4 hours. In additional, it is shown when the AKV was closed when the system reached the set point.

The cooling capacities for different conditions were calculated for both air and refrigerant side and the results are compared based on the energy balance of the system. More details can be found in Appendix F.

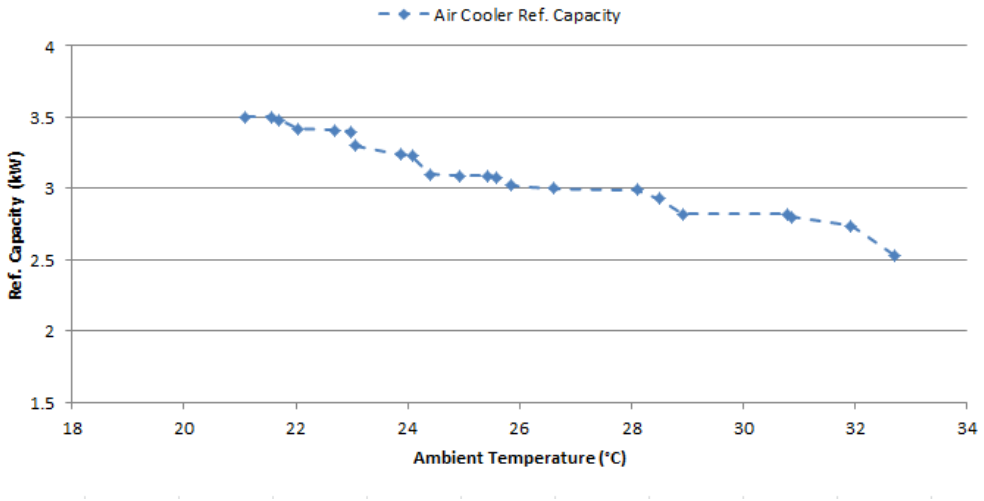

Figure 6.35 Cooling capacity variation with the ambient condition for the AAC

The cooling capacity variation with the ambient condition for the additional air cooler which is connected parallel to the MT display cabinet is shown in Fig. 6.35. As it has been observe it from the MT also the refrigeration capacity is drop as the ambient temperature increased and the system moves from subcritical to transcritical cycle. The rate of the gas bypassed to liquid flows to evaporator increased which reduced the liquid mass flow rate passing through the coil. The trend line is very similar to one found for the MT display cabinet.

In order to validate the model based on the COP reduction when the intermidiate pressure is higher the air cooler capacity was investigated under different intermiates pressures. The available control valves when the system builded makes the change of the intermidate pressure more complicated than the convectional existing system in supermarkets. Appendix G is detailed explained the procedure to increase the intermediate pressure and the associate p-h diagrams are presented.

The air cooler was investigatred under three different intermidiates pressures of 32, 38 and 42 bar. The PRV which has been installed at the liquid receiver is set at 46 bar which limits the range of the higher intermidiated pressure investigation. The evaporating temperature was -8 °C, the control superheat settings were the same for the three pressure levels and the mass flow rate was fairly constant for each experiment.

Table 6.8 illustrate the results for higher pressure at the liquid receiver for very similar test conditions.

Table 6.8 AAC Capacity for different intermediate pressure levels

Receiver Pressure (bar)	Ref. Capacity of the (kW)
32	3.1
38	2.15
42	2.09

As it clear shown from Table 6.8 with higher pressure at the liquid receiver of the system the refrigerated capacity of the air cooler dropped. This is validated the results of the model which has been presented in previous sub-chapter. More details for the higher pressure measurements and data can be found in Appendix H.

6.6.SUMMARY

This chapter was divided in four main sections. In the first section the control parameters and experimental procedure have briefly explained. The analytical results performed on an experimental CO_2 booster refrigeration system were presented in second section of this chapter. The results presented on section two are used to validate and optimise the simulation model developed to simulate the performance of the existing CO_2 system in section three. The four and final section described the results from the modifications have been done in the existing system. In additional, those results are used to validate the model optimisation procedure based on the effect of the intermediate pressure on the overall COP of the system. The validated model will be used later to investigate different CO_2 refrigeration systems solutions.

Chapter 7 will present the detailed simulation for the CO_2 gas cooler. The model will validate against the experimental results and further investigation will be present. As the results from this chapter show the gas cooler design is essential for the system operation and overall COP. The detailed model will be used in order to understand better the operation of the heat exchanger when the system operates in transcritical cycle.

7. MODELLING, VALIDATION AND APPLICATIONS OF CO_2 GAS COOLER SIMULATION MODEL

7.1.INTRODUCTION

In CO_2 refrigeration systems, the system can operate in subcritical or transcritical cycle depending on ambient temperature. When the system is operates in transcritical cycle the heat exchanger at the high pressure side of the system is well known as gas cooler. The gas cooler rejects heat from the superheated refrigerant gas to ambient air without condensation in single phase heat transfer process.

The gas cooler is a major component in CO_2 systems when it operates in transcritical mode. The understanding of its performance parameters under different conditions is essential to adequately design and optimise for specific applications. These important parameters consist of the refrigerant side thermos-physical properties, air inlet effects and local heat transfer coefficients, which after adequate optimisation can lead to higher system Coefficient of Performance.

To date, there has been much research into the optimal control designs and evaluations of their effects on the overall system performance were based on thermodynamic analysis. These theoretical optimal control strategies may or may not match well to actual system performance. When the system is operates in transcritical cycle the gas cooler operation became very sensitive. The changes on the output properties of the gas cooler can lead to lower COP of the system. The experimental verification or analysis presented to Chapter 6 is therefore essential.

In order to investigate further the gas cooler operation, a detailed mathematical model is developed in the EES platform, and validated with data were obtained from experimental test rig at the National Centre for Sustainable Energy use in Food chains (CSEF) and presented in this Chapter. The model was used to calculate the refrigerant temperature profiles across the heat exchanger and the heat rejection rate across the gas cooler, as well as on investigate effect of different gas cooler outlet parameters to the system performance.

7.2.GAS COOLER MODEL DESCRIPTIONS

The dimensional parameters were used for the simulation model are the same with the 2-rows and 3-rows heat exchangers descriptions which have been previously experimentally investigated. The discrete numerical model solution is used in

developing the simulation model of finned-tube air cooled CO_2 heat exchanger. Figure 7.1 illustrates the two coils where used for the simulation models. Table 7.1 also represents the dimensions and constructed materials of both finned-tube air cooled CO_2 gas coolers.

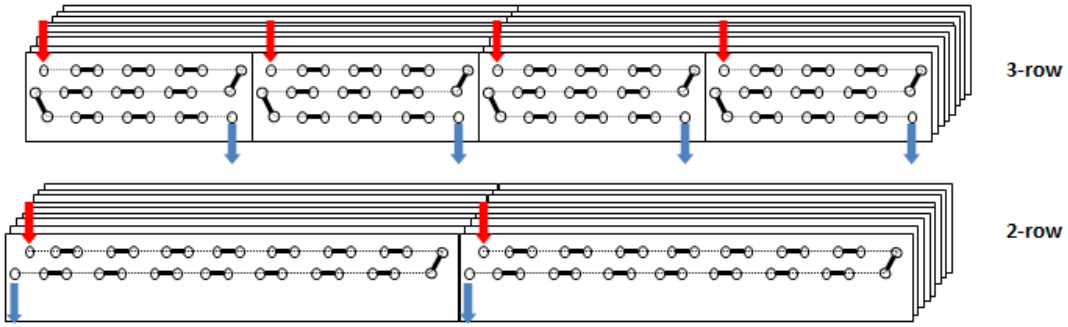

Figure 7.1 Air cooled heat exchangers

Table 7.1 Air cooled heat exchangers design parameters

Specification of tested gas cooler		
	3 rows	**2 rows**
L^xD^xH	$1.6m^x0.066m^x0.82m$	$1.6m^x0.044m^x0.82m$
Front area	1.6m x 0.82m	1.6m x 0.82m
Fin (plate type)		
Material	Aluminium	Aluminium
Pitch	2.11mm	2.11mm
Thickness	0.16mm	0.16mm
Tube (circular and smooth)		
Number of rows	3	2
Number of tube per row	24	32
Outside diameter	8mm	8mm
Inside diameter	6.32mm	6.32mm
Tube shape	smooth	smooth
Material	Copper	Copper
Propeller Fan		
Number of fans	2	2
Fan position (centre of fan/ Front to rear)	1: 400mm 2: 1200mm	1: 400mm 2: 1200mm

The three dimensional diagram of the three row gas cooler is shown in Fig. 7.2. Same procedure has been used for the 2-row coil as well. Copper tubes are arranged parallel to *i* direction, *j* and *k* specified the longitudinal and transverse direction respectively.

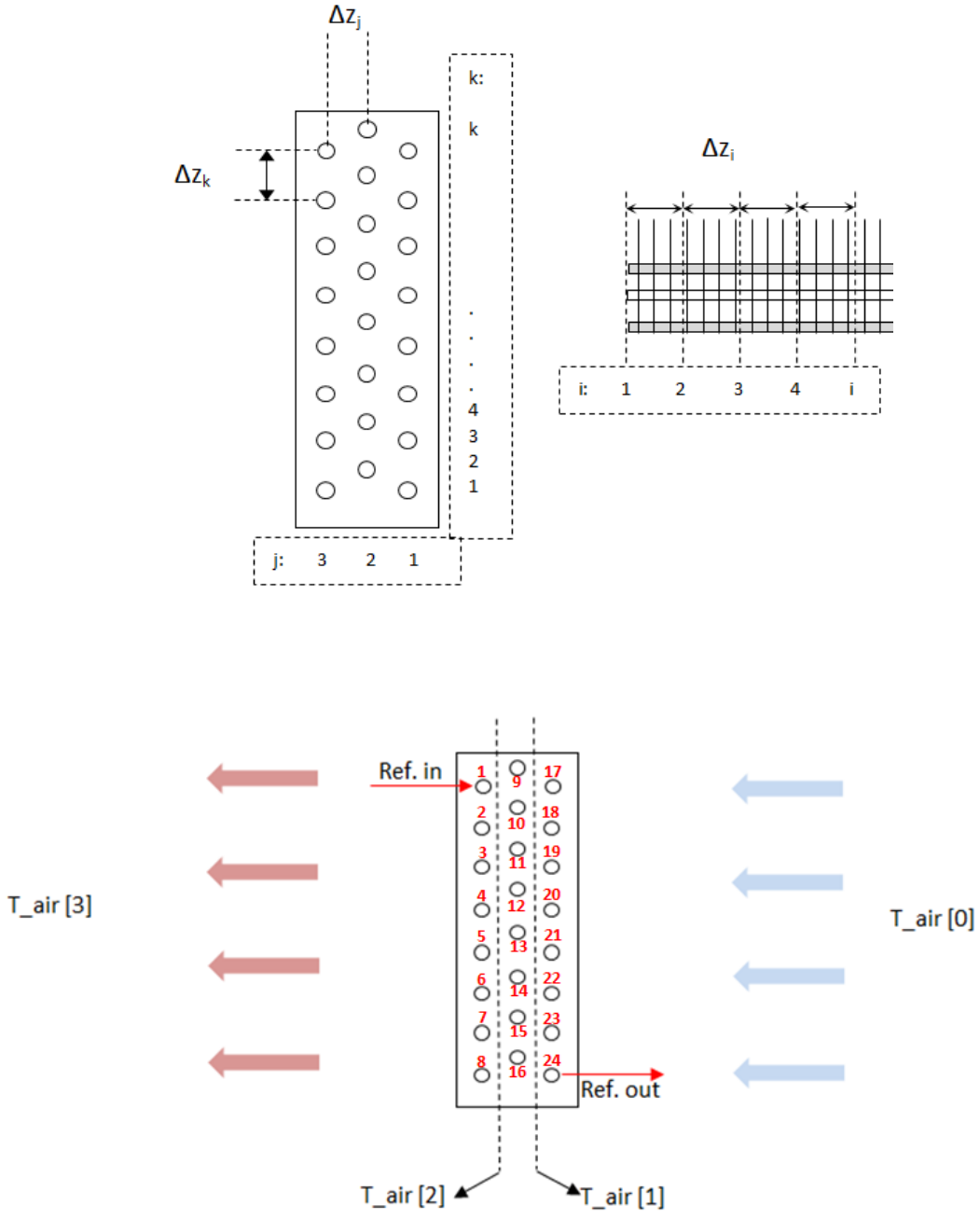

Figure 7.2 Three dimensional diagram of the three row gas cooler

The air is passing through the coil parallel to *j* direction and the refrigerant flows inside the pipe parallel to *i* direction. Each pipe was divided in 16 segments of 0.1 m each for both coils. The larger value of segments is, the more accurate the simulation will be.

The professional version of the EES program can solve 12,000 simultaneous equations. Due to this limitation the number of the segments set to be 16.

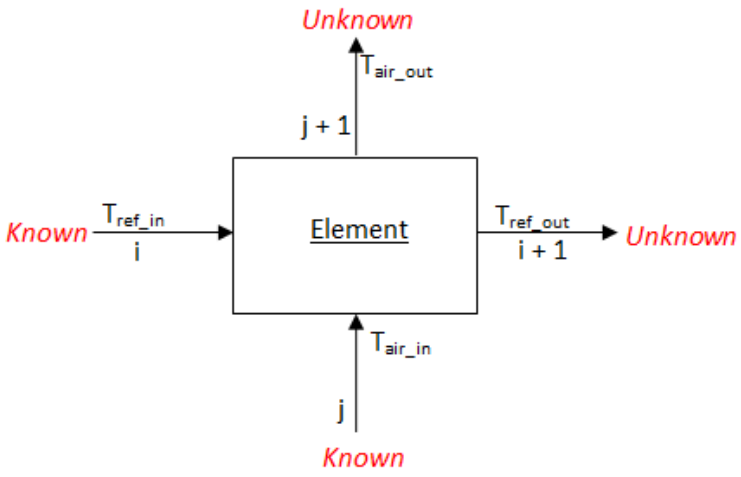

Figure 7.3 Gas cooler element

The equations for refrigerant and air side are solved simultaneously using an iterative method for *i+ 1 and j + 1*. The pipe number starts from the refrigerant inlet to refrigerant outlet to complete each pipe circuit. The gas cooler is a counter cross flow heat exchanger. Due to this, only the refrigerant temperature, pressure and mass flow rate is known as shown in Fig. 7.2 and 7.3 Therefore, the air inlet temperature at each segment must be assumed, which should be higher than the known air inlet temperature. The solution proceeds until the segment No. 1 where the air inlet conditions are known. By updating the guess values of the EES solution the model is looping in order to calculate the real values of T_air [1], T_air [2] and T_air [3] which is the air outlet of the finned-tube air cooled gas cooler.

Starting from the inlet refrigerant conditions the solution of each sub-element is used as the input for the next sub-element until the model completes. Figure 7.4 shows the flowchart of the model for the finned-tube air cooled CO_2 gas cooler.

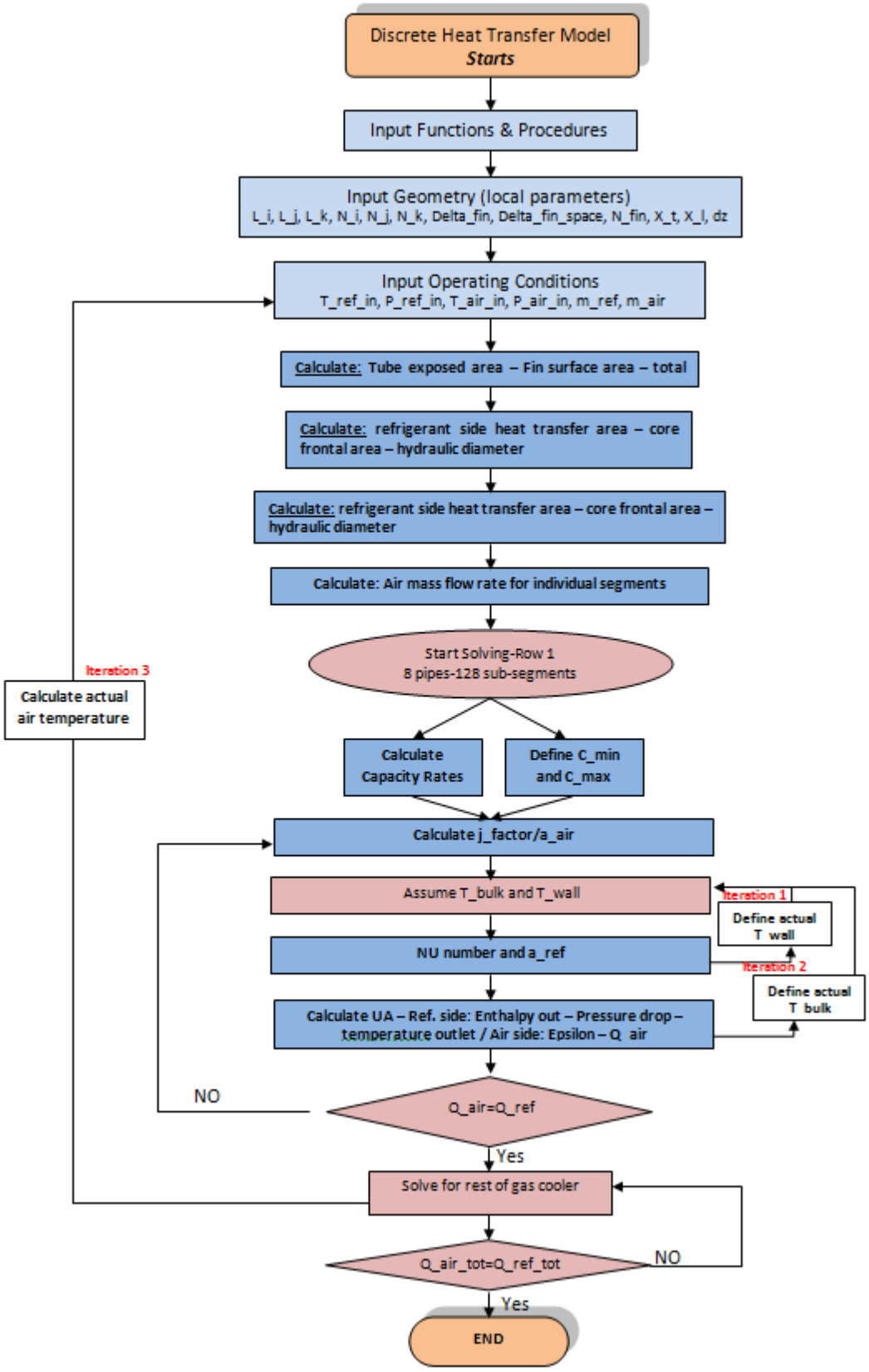

Figure 7.4 Gas cooler solving routing

The model consists of four loops/iterations. The first loop is to define the actual wall temperature of the copper pipe based on the heat transfer coefficients of air and refrigerant side. The detailed calculations will present below. The second loop is used to re-calculate the actual bulk temperature of the refrigerants which is proportional of the inlet and outlet refrigerant temperature for each sub-element. In the most of the theoretical works the bulk temperature assumed to be equal with inlet conditions. To minimise the possible error of the calculations the system is iterate to calculate the actual bulk temperature as will explain in this chapter later. The third loop ensures that the energy balance in the first row can be satisfied. The fourth and last loop ensures that the energy balance between air and refrigerant sides for the whole finned-tube air cooled CO_2 heat exchanger. The key input parameters at the first two boxes of Figure were varied based on the experimental data results in order to investigate the heat transfer performance for the two different coils under different test parameters.

The model also predicted all the refrigerant and air thermos-physical properties for each sub-element, the fin and overall efficiency of the heat exchanger, pressure drop across the coil and temperature profile.

The model makes some assumptions as follows:

- The heat exchanger operates under steady-state conditions. (Constant flow rates and fluid temperatures independent of time)
- Heat losses to or from the surroundings are negligible
- One dimensional flow for refrigerant inside the tubes and air across the coil
- The fluid flow rate is uniformly distributed through the exchanger on each fluid side in each pass
- Heat conduction along the pipe axis and within fins are negligible

7.3.GAS COOLER MATHEMATICAL MODEL APPROACH

The mathematical model uses the discrete solution technique by which the finned-tube air cooled CO_2 heat exchanger is divided into a number of small sub-elements. All the equations which will explain below are applied to individual segments. The tubes are arranged in coordinates *i, j* and *k* as explained before. The number of the rows and pipes per row is specified by the two coils used for the experimental investigation. The 3-row heat exchanger is divided in 384 sub-elements and the 2-row in 320 sub-elements.

The mass, momentum and energy equations are illustrated below. Those equations are discretised for all sub-elements with coordinate (*i*, *j*, *k*) to (*i+1*, *j*, *k*) for the refrigerant side and (*i*, *j*, *k*) to (*i*, *j+1*, *k*) for the air side.

Mass equation:

$$(\dot{m}_r)_{(i+1,j,k)} - (\dot{m}_r)_{(i,j,k)} = 0 \qquad 7.1$$

Momentum equation:

$$\frac{1}{A_{in}}\left[(\dot{m}_r u_r)_{(i+1,j,k)} - (\dot{m}_r u_r)_{(i,j,k)}\right] = -\Delta P - \Delta P_f \qquad 7.2$$

Energy equation:

$$(\dot{m}_r h)_{(i+1,j,k)} - (\dot{m}_r h)_{(i,j,k)} = -(\pi d_o)\dot{q}_{ref,flux}\ \Delta z_i \qquad 7.3$$

7.3.1. AIR MASS FLOW RATE CALCULATIONS

The air mass flow rate is calculated for each sub-element based on the element area. The cross section area of the coil and the mass flow rate is used to calculate the velocity as shown below.

$$\left.\begin{aligned} Cross\ area &= length * width \\ \dot{m}_{air} &= defined\ by\ experiments \\ u_{air} &= \dot{m}_{air} / (cross\_area * \rho_{air}) \end{aligned}\right\} \qquad 7.4$$

The air velocity is assumed to be homogeneous for all the sub-elements. Therefore the air mass flow rate passing thorough each sub-element is calculated as below.

$$\left.\begin{aligned} Element_{\ cross\ area} &= \Delta z_k * \Delta z_i \\ \dot{m}\_air\_element &= Element_{\ cross\ area} * u_{air} * \rho_{air} \end{aligned}\right\} \qquad 7.5$$

Where ρ_{air} is the density of the air which is calculate for the each element based on the air parameters.

7.3.2. REFRIGERANT MASS FLOW RATE

The refrigerant mass flow rate is defined based on the experimental results of each test parameter. For the 3-row coil is assumed the total refrigerant mass flow is split equally on the 4 segments (inlets/outlets) and for the 2-row coil the mass flow rate is split into

the 2 segments. In Chapters 4, 5 and 6 the difference in mass flow rate and mass flux for both coil were explained.

7.3.3. CAPACITY RATE CALCULATIONS

The heat capacity rate it is dependent on the mass flow rates and the temperatures of the refrigerant and air passing through each individual sub-element. The capacity rate calculations are shown below.

$$\left.\begin{aligned} C_{refrigerant} &= \dot{m}_{ref} * C_{p,\,ref} \\ C_{p,\,ref} &= f\,(T, P) \\ C_{air} &= \dot{m}_{air} * C_{p,\,air} \\ C_{p,\,air} &= f\,(T, P) \end{aligned}\right\} \quad 7.6$$

For the NTU-ε method which has been used to calculate the heat transfer for air side in one sub-element the minimum and maximum capacity rates are required to complete the calculations. Two individual EES procedures were set to define the C_{min} and C_{max} for each sub-element. Below the C_{min} procedure is illustrated.

$$\left.\begin{aligned} &Procedure\ C_{minimum}\,(P_{air}, T_{air}, T_{ref}, P_{ref}, \dot{m}_{ref}, \dot{m}_{air}: C_{min}) \\ &If\ (C_{refrigerant} <= C_{air})\ then \\ &C_{min} = C_{refrigerant} \\ &else \\ &C_{min} = C_{air} \end{aligned}\right\} \quad 7.7$$

7.3.4. AIR SIDE HEAT TRANSFER COEFFICIENT

The air side heat transfer coefficient is calculated by using j-factor (Wang et al., 2001). The j factor is calculated as below.

$$j = 1.0691 {Re_{DC}}^{j4} \left(\frac{F_s}{Dc}\right)^{j5} \left(\frac{S_s}{S_h}\right)^{j5} N^{j7} \quad 7.8$$

For $Re_{DC} > 700$

The Reynolds number based on the tube collar diameter can be calculated as:

$$Re_{DC} = \frac{G_c D_c}{\mu_{air}} \; or \; Re_{DC} = \frac{\rho_{air} u_{air} D_c}{\mu_{air}} \qquad 7.9$$

The j-parameters 4 to 7 are calculated by using the following equations.

$$\left.\begin{aligned} j^4 &= -0.535 + 0.017\left(\frac{P_t}{P_l}\right) - 0.0107N \\ j^5 &= 0.4115 + 5.5756\sqrt{\frac{N}{Re_{DC}}}\, ln\frac{N}{Re_{DC}} + 24.2028\sqrt{\frac{N}{Re_{DC}}} \\ j^6 &= 0.2646 + 1.0491\left(\frac{S_s}{S_h}\right) ln\left(\frac{S_s}{S_h}\right) - 0.216\left(\frac{S_s}{S_h}\right)^3 \\ j^7 &= 0.3749 + 0.0046\sqrt{Re_{DC}}\, lnRe_{DC} - 0.0433\sqrt{Re_{DC}} \end{aligned}\right\} \qquad 7.10$$

Finally, the air side heat transfer coefficient is calculated as presents below.

$$a_{air,local} = \frac{j k_{air} Re_{DC} \left(Pr_{air}{}^{0.3}\right)}{Dc} \qquad 7.11$$

7.3.5. SURFACE AND FIN EFFICIENCY

By knowing the air side heat transfer coefficient the surface and fin efficiency can be calculated. The surface efficiency is calculated as showing below (Wang, 2010).

$$\eta_o = \left[1 - \frac{A_{fin}}{A_{ta}}(1 - n_{fin})\right] \qquad 7.12$$

The fin efficiency is presented by the Schmidt (1949) approximation and is illustrated below.

$$\left.\begin{aligned} n_{fin} &= \frac{\tanh(mr\varphi)}{mr\varphi} \\ \mathrm{m} &= \sqrt{\frac{2\, a_{air,local}}{\kappa_{fin}\delta_{fin}}} \\ \varphi &= \left(\frac{R_{eq}}{r} - 1\right)\left[1 + 0.35\ln\left(\frac{R_{eq}}{r}\right)\right] \\ \frac{R_{eq}}{r} &= 1.27\frac{X_M}{r}\left(\frac{X_L}{X_M} - 0.3\right)^{1/2} \end{aligned}\right\} \qquad 7.13$$

7.3.6. REFRIGERANT SIDE HEAT TRANSFER COEFFICIENT

The refrigerant heat transfer coefficient was calculated by using Pitla et al., (2002) correlation. This correlation it is take into account the mean Nusslet numbers that are calculated using the thermophysical properties for wall and bulk temperatures for each sub-element. Pitla et al defined this equation as below.

$$Nu_{mean} = \left(\frac{(Nu_{wall} + Nu_{bulk})}{2}\right)\left(\frac{K_{wall}}{K_{bulk}}\right) \tag{7.14}$$

Gnielinski (1976) correlation is used to calculate the respective Nusslet number for the individual grids.

$$Nu_{wall} = \frac{\frac{f_{wall}}{8}(Re_{wall}-1000)Pr}{12.7\sqrt{\frac{f_{wall}}{8}\left(Pr^{\frac{2}{3}}-1\right)}+1.07}$$

$$Nu_{bulk} = \frac{\frac{f_{bulk}}{8}(Re_{bulk}-1000)Pr}{12.7\sqrt{\frac{f_{bulk}}{8}\left(Pr^{\frac{2}{3}}-1\right)}+1.07} \tag{7.15}$$

The Reynolds number for wall and bulk temperature is shown below.

$$Re_{wall} = \frac{\rho_{wall} u_{ref,inlet} d_{hydarulic}}{\mu_{wall}}$$

$$Re_{bulk} = \frac{\rho_{bulk} u_{ref,average} d_{hydarulic}}{\mu_{bulk}} \tag{7.16}$$

To obtain the inlet and local mean refrigerant velocity the two equations below were used.

$$u_{ref,inlet} = \frac{\dot{m}_{ref}}{\rho_{wall}\pi\left(\frac{d_{in}}{2}\right)^2}$$

$$u_{ref,average} = \frac{\dot{m}_{ref}}{\rho_{bulk}\pi\left(\frac{d_{in}}{2}\right)^2} \tag{7.17}$$

As it clear from the correlations the wall temperature is used to calculate the inlet velocity at each sub-element and the bulk temperature to calculate the average refrigerant velocity at the finite section.

To calculate the Nusslet number for both wall and bulk temperatures the friction factor coefficient is required. For both cases the friction factor is calculated by using the same correlation which is a function of Reynolds number only. This correlation is applied for smooth surface condition with large Reynolds number range of Bergam et al., (2002):

$$3000 \leq \mathrm{Re} \leq 5 \times 10^{6} \qquad 7.18$$

The friction factor correlation has been developed by Petukhov (1970). The wall and bulk Reynolds number are inserted to the correlation to calculate the friction factor as below.

$$\left.\begin{aligned} f_{wall} &= \frac{1}{(0.79ln(Re_{wall})-1.64)^2} \\ f_{bulk} &= \frac{1}{(0.79ln(Re_{bulk})-1.64)^2} \end{aligned}\right\} \qquad 7.19$$

The friction factor for wall and bulk temperatures are inserted to solve Nu_{wall} and Nu_{bulk} respectively. The Prandtl number is defined by EES for the given refrigerant states. Once the mean Nusslet number has been obtained the refrigerant heat transfer coefficient can be calculated as below.

$$a_{ref,local} = \frac{Nu_{mean}}{d_{pipe,in}} k_{bulk} \qquad 7.20$$

7.3.7. WALL AND BULK TEMPERATURES

The first two loops of the model are used to calculate the actual values of wall and bulk temperature. For the first pipe first segment the system is assumed the wall and bulk temperature as illustrated on the following equations.

$$\left.\begin{aligned} T_{wall} &= \frac{(T_{ref,in} + T_{air,in})}{2} \\ T_{bulk} &= T_{ref,in} \end{aligned}\right\} \qquad 7.21$$

The actual wall temperature is a proportional of the air and refrigerant heat transfer coefficients, the refrigerant and air inlet temperatures at this specific sub-element and the fin and tube area. After all the above are know the actual wall temperature can be calculated as the following equation shows.

$$a_{air,local}A_{total,local}(T_{wall} - T_{air,in}) = a_{ref,local}A_{tube,local}(T_{ref,in} - T_{wall}) \quad 7.22$$

In case of the bulk temperature the model assumes that the bulk is equal to the refrigerant inlet temperature as shown in following.

$$T_{bulk,local} = T_{ref,in} \quad 7.23$$

To calculate the actual bulk temperature the refrigerant inlet and outlet temperatures for each sub-element are required. After the refrigerant temperature at the outlet of the grid is calculated the system is loop to calculate the actual bulk temperature as below.

$$T_{bulk,local} = \frac{(T_{i,j,k} + T_{i+1,j,k})}{2} \quad 7.24$$

7.3.8. THE OVERALL HEAT TRANSFER COEFFICIENT

One of the most essential part of the heat exchanger analysis is the determination of the overall heat transfer coefficient times the area which is known as UA value. The UA coefficient is a product of the total thermal resistance to the heat transfer between the refrigerant and air for the finned-tube air cooled heat exchanger. For the case of CO_2 gas cooler where the temperature and pressure is much higher comparing with the convectional refrigerants the analysis of the overall heat transfer coefficient is become very important. The UA can be calculated as following (Shah and Sekulic, 2003):

$$UA = \left(\frac{1}{a_{air,local}\eta_o A_{fin}} + R_{wall} + \frac{1}{a_{ref,local}A_{in,tube}}\right)^{-1} \quad 7.25$$

The thermal resistance of the fin surface area can be defined from the heat transfer coefficient of the air side and the surface fin efficiency as illustrated in Chapter 7.3.4

and 7.3.5 respectively. The fin area is taken into account the clean fin surface area without the area occupied by the pipe.

The R_{wall} is the total wall thermal resistance. For cylindrical tubular wall the thermal resistance can be defined as shown below.

$$R_{wall} = \frac{ln\frac{d_{pipe,out}}{d_{pipe,in}}}{2\pi k_{wall} L} \quad 7.26$$

The thermal resistance of the refrigerant side is defined by using the refrigerant side heat transfer coefficient and the tube heat transfer area. Both are specified for each individual sub-element. The refrigerant heat transfer coefficient calculation procedure is described in 7.3.6.

7.3.9. REFRIGERANT PRESSURE DROP

The momentum equation is used to calculate the refrigerant pressure drop across the finned-tube air cooled CO_2 heat exchanger.

$$\frac{1}{A_{in}}\left[(\dot{m}_r u_r)_{(i+1,j,k)} - (\dot{m}_r u_r)_{(i,j,k)}\right] = -\Delta P - \Delta P_f \quad 7.27$$

In general terms, the pressure drop increases as the mass flux increases and as the system pressure decreases. This is due to the higher density of the CO_2 when the system pressure is respectively higher. The pressure drop decreases if the density increases for the constant mass flux values.

Yoon et al (2003) measured the pressure drop for pure CO_2 and was found to be less than 1 kPa m^{-1}. Dang et al. (2007) reports the pressure drop will increase sharply when the oil concentration increases inside the system.

The momentum equation associated with the pipe of constant cross section due to the friction created by wall. This is calculated as shown below.

$$\Delta P_f = f\frac{{G_{ref}}^2 \Delta z_i}{2\rho_{ref} d_{pipe,in}} \quad 7.28$$

The f factor is the Fanning friction factor which is a proportional of the Reynolds number. The Fanning friction factor is calculated by using Blasius equation.

$$f = \frac{0.079}{Re_{ref}^{0.25}} \quad 7.29$$

The Reynolds number for the refrigerant flow is calculating as shown the following equation.

$$Re_{ref} = \frac{4m_{ref}}{\pi d_{pipe,in}\mu_{ref}} \quad 7.30$$

The viscosity and density were calculated based on the CO_2 thermodynamic properties for individual sub-elements. The mass flux is defined by the refrigerant mass flow rate and the pipe cross-section area.

$$G_{ref} = \frac{\dot{m}_{ref}}{A_{pipe,in}} \quad 7.31$$

The pressure drop calculated from above was used to calculate the pressure value entering to the next sub-element.

$$P_{ref,i+1,j,k} = P_{ref,i,j,k} - \Delta P_f \quad 7.32$$

7.3.10. ENERGY BALANCE EQUATION – REFRIGERANT OUTLET TEMPERATURE

The energy balance equation is used to define the refrigerant enthalpy outlet for each sub-element.

$$(\dot{m}_r h)_{(i+1,j,k)} - (\dot{m}_r h)_{(i,j,k)} = -(\pi d_o) q_{ref,flux}\, \Delta z_i \quad 7.33$$

The cross area and the length of the individual sub-element are taken into account. The heat transfer per square meter is calculated from the air side of the finned-tube air cooled CO_2 heat exchanger.

$$q_{ref,flux} = a_{air,local}\left(T_{wall,local} - T_{air,local}\right) \quad 7.34$$

The calculated enthalpy and pressure at the outlet of each sub-element can be used to define the refrigerant temperature outlet for this sub-element. Refrigerant temperature, pressure and enthalpy from the outlet of each sub-element can be used as input to the next one until the model completes the calculations for the whole heat exchanger.

$$T_{ref,i+1,j,k} = f(P_{ref,i+1,j,k}, h_{ref,i+1,j,k}) \quad 7.35$$

7.3.11. AIR SIDE HEAT TRANSFER

The air side heat transfer for the individual sub-elements is calculated by using the NTU-ε method. For each sub-element this is calculated as below.

$$Q_{air} = \varepsilon\, C_{min}(T_{ref(i,j,k)} - T_{air(i,j,k)}) \quad 7.36$$

The capacity rate, refrigerant and air temperature were calculated from previous sub-chapters. Ge and Cropper (2009) defined the equations to calculate the heat exchanger effectiveness. Those equations have been used in the model.

When $C_{max} = C_{hot}$ then:

$$\varepsilon = exp\left(-\gamma \frac{C_{max}}{C_{min}}\right)$$

$$\gamma = 1 - exp\left(-\frac{UA}{C_{max}}\right)$$

When $C_{min} = C_{hot}$ then:

$$\varepsilon = \frac{C_{max}}{C_{min}}\left(1 - exp\left(-\gamma \frac{C_{max}}{C_{min}}\right)\right)$$

$$\gamma = 1 - exp\left(-\frac{UA}{C_{min}}\right)$$

7.37

The effectiveness is calculated for individual sub-element as the air side heat transfer as well.

7.3.12. AIR OUTLET TEMPERATURE

The heat transfer equation in the discretised form is used to calculate the air temperature leaves each individual sub-element.

$$\left[\dot{m}_{air-i,j,k} cp_{air-i,j,k}\left(T_{air-i,j+1,k} - T_{air-i,j,k}\right)\right] = UA_{i,j,k}\left(T_{ref-i,j,k} - T_{air-i,j,k}\right) \quad 7.38$$

The air outlet of individual elements is calculated by taking into account the overall heat transfer coefficient and the temperature difference between the refrigerant flows inside the pipe for the calculated grid and the cold side of the air passing above the pipe. Also, the air heat extraction is used to balance the equation. For this case the heat transfer process taking place when the air extract heat from the pipe.

7.4. SOLVING ROUTINE

Refrigerant and air side equations are solved simultaneously using an iterative method for $i + 1$ and $j + 1$ respectively. Both refrigerant and air properties are obtained directly from the EES software for each sub-element.

The solving routine starts from refrigerant inlet to refrigerant outlet. The air side parameters for each sub-element are normally unknown initially will be assumed. Only the gas cooler air inlet properties are known which are entered to the simulation models. The rest of the air parameters such as temperature and properties of the gas cooler are calculated at the final model iteration.

The solution proceeds with the outlet of one sub-element as inlet for the next one with the same assumption for air temperature. The assumptions for the air temperature changed only when the pipe row changed.

The solving routing is used the "EES Duplicate command" to solve the conservation equations which are described above. The Duplicate command is equivalent to DO LOOP in Fortran and FOR LOOP in C. All the equations which are included in the Duplicate command are enclosed between the Duplicate and END command words. The "ARRAY" variable solution is used inside the Duplicate commands.

Solving routine is starting by using the Duplicate command to solve the sub-elements only in the first pipe – first row of the finned-tube air cooled CO_2 gas cooler. After the routine finished the Duplicate command is used to set the output of the last sub-element as the input of the next element. Then, two Duplicate commands are used to solve the rest of the pipes for the first pipe row which are 7 pipes (8 in total) for the 3-row and 15 pipes (16 in total) for the 2-row gas cooler heat exchanger. Each of the three Duplicate

commands is finished by using the END command to specify where the calculations need to be stopped.

The three Duplicate commands are written in order to allow the model to move in all three dimensions (3D) *i, j, k* of the gas cooler as explained before. The solving routing is continuing by using the three Duplicate commands as above to solve the pipes and sub-elements for the pipe row 2. For the 2-row gas cooler the solving routing is finished at this part. On the other hand, the three Duplicate commands are used once more to calculate the pipes and sub-elements of the pipe row number 3 for the 3-row finned-tube air cooled CO_2 gas cooler.

At the end of each pipe row the average, maximum and minimum air temperatures are calculated after the final iteration. Those included all the air parameters for each sub-element. The total gas cooler load is calculated at the end of each iteration and the iteration process continue till the loops are completed with the error value which has been specified at the beginning.

For the 3-row gas cooler the number of the simultaneously non-linear equations that the model solves is reach the 11,708, when the maximum for the EES professional version solves 12,000. This can be minimized by number of the parameters extracted by the imported procedures. The results are representing in Array form tables with 3D denotes. The x-axis (row) denotes the pipe row and pipe number and the y-axis (column) denotes the sub-element number.

7.5.MODEL VALIDATION

The models were validated using test results from the experimental test facility. The two finned-tube air cooled CO_2 gas coolers with different sizes and pipe arrangement were investigated experimentally in the existing refrigeration system briefly described in 7.2. More details can be found in Chapter 5.

The model is used to investigate the two different heat exchangers when the system runs in transcritical cycle with main fans speed of 50%, 60% and 70% of the total speed corresponding to 2000 l/s, 2400 l/s and 2800 l/s. The compressor speed was variable; the intermediate pressure was constant at 32 bar and the evaporating temperature -8 °C. The ICMT motorized valve which controlling the pressure at the gas cooler is explained in Chapter 5.

The discrete heat transfer model is used to predict the refrigerant temperature drop across each pipe segment, the pressure drop and the heat rejection under different test parameters. The local heat transfer coefficients for both air and refrigerant, UA, NU, ε and overall efficiency are calculated and presenting below.

The refrigerant temperature and pressure drop data collection procedure is explained in Chapter 5. The thermocouples are attached at the copper pipe wall and insulated to avoid any interference from the ambient. The pressure transmitters were connected with T-connection at the gas cooler header.

Table 7.2 Experimental test conditions used for model validation

Validation Test	**Coil Specification**	Tested Parameters				
		Air Parameters		**Refrigerant Parameters**		
		Fan Speed	$T_{air,in}$	$m_{ref,in}$	$T_{ref,in}$	$P_{ref,in}$
Val. 1	3-rows / 4 segments	50%	29.54°C	0.041 kg/s	94.93°C	76 bar
Val. 2	3-rows / 4 segments	50%	32.77°C	0.042 kg/s	105.54°C	85.14 bar
Val. 3	2-rows / 2 segments	50%	28.46°C	0.035 kg/s	88.11°C	75.37 bar
Val. 4	2-rows / 2 segments	50%	35.14°C	0.038 kg/s	100.85°C	87.27 bar

The experimental tests conditions were used to validate the model are illustrated in Table 7.2. The same conditions are used from Ge et al., (2015) to validate the model where the "TRNSYS" software was used.

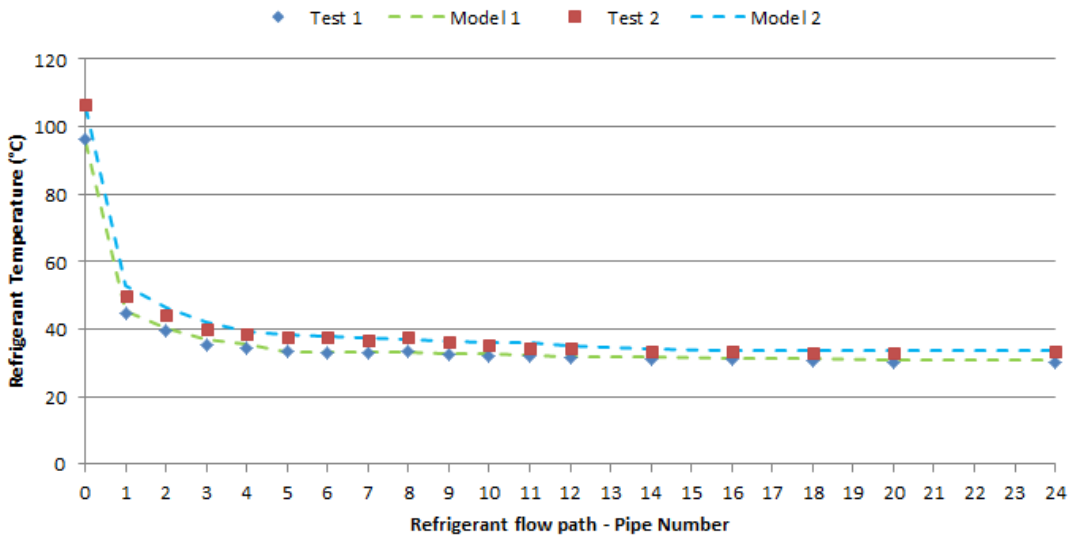

Figure 7.5 comparison between the experimental and predicted results for the temperature drop across the for the 3-row finned-tube CO_2 gas cooler

Figure 7.5 shows the comparison between the experimental and predicted results for the temperature drop across the for the 3-row finned-tube CO_2 gas cooler. Test 1 and 2 shows the experimental test data for Val. 1 and Val. 2 from the Table 7.2. Model 1 and 2 illustrates the results of the simulation model based on the same investigate parameters. The highest heat release found to be in the first two pipes of the pipe row 1. Overall, there is a very good agreement in results comparing the experimental and the model predicted data. The experimental data shows that the 53.41% and 11.72% of the temperature drop on the 1st and 2nd pipe respectively for the Val. 1. The simulation model predicts that the temperature drop 52.82% and 12.82% for the 1st and 2nd pipe respectively.

A thermal imaging camera was used to capture the temperature variation across each segment when the system was running. In Figure 7.6 the three out of the four pipe segments are clearly illustrated. It is clearly captured the highest temperature of the first pipe of each segment and the temperature drop when the refrigerant flows to the rest of the pipes. The temperature range on the right hand side of the Figure 7.6 is not based on the actual measurements due to the distance effect between the thermal camera and the heat source.

Due to the good agreement of the model and experimental results the heat rejection and approach temperature of the CO_2 gas cooler can be predicted accurately. Very similar trends can be found for all the test parameters of the 3-row gas cooler.

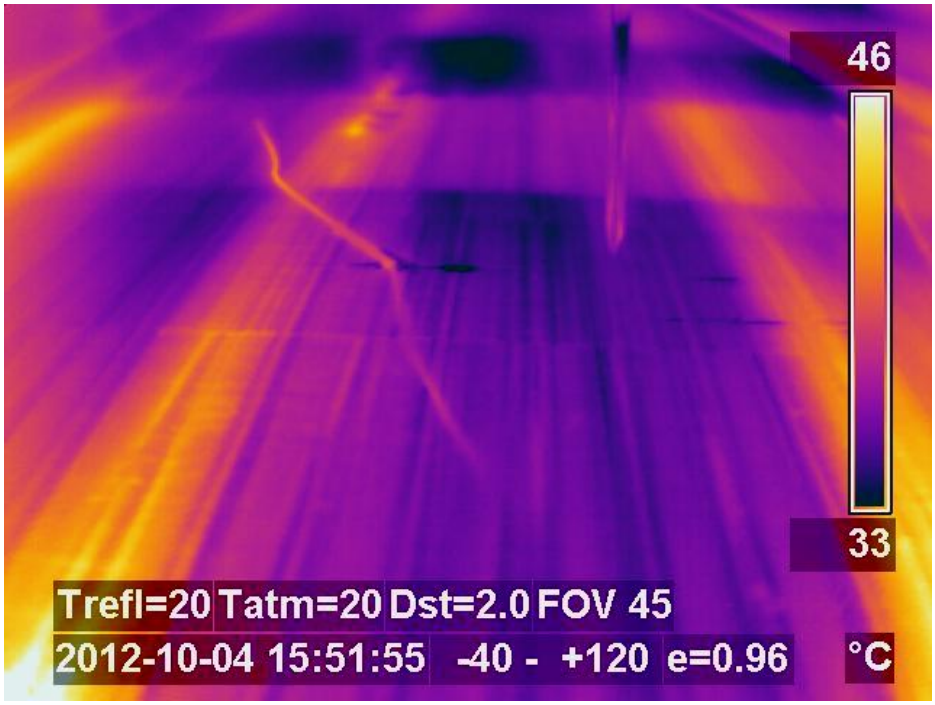

Figure 7.6 Thermal imaging capture

Figure 7.7 shows the comparison between the experimental and predicted results for the temperature drop across the for the 2-row finned-tube CO_2 gas cooler. Test 3 is showing the temperature drop for Val. 3 parameters. Model 3 line shows the predicted temperature drop for the same parameters. Both experimental and simulation tests results shows really good agreement.

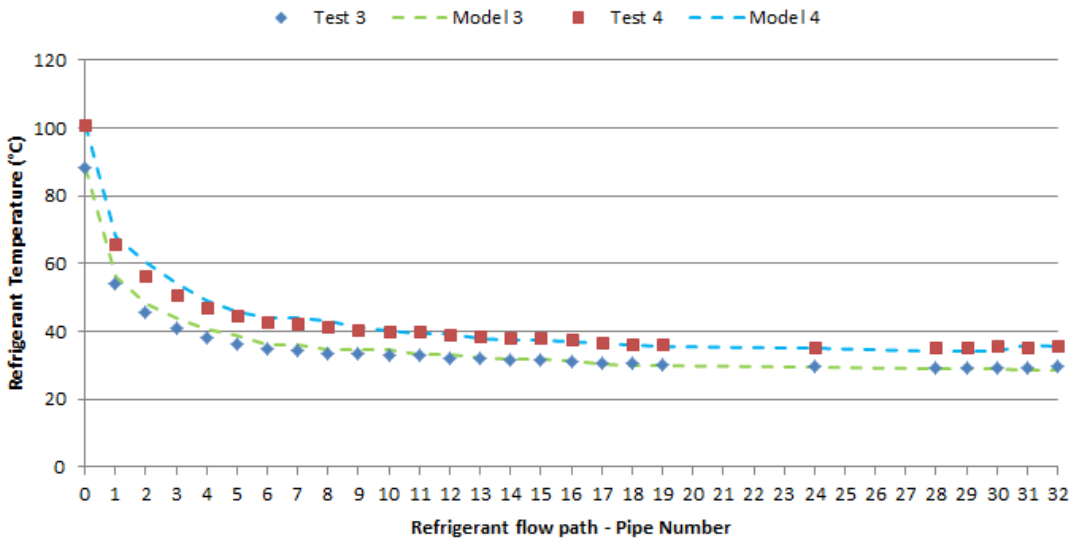

Figure 7.7 Comparison between the experimental and predicted results for the temperature drop across the for the 2-row finned-tube CO_2 gas cooler

Test 4 and Model 4 lines is the comparison of the experimental and predicted temperature profile across the heat exchanger for Val. 4 test parameters. As the 3-row heat exchanger it is seen from both simulation and test results that a sharp refrigerant temperature occurs on the first two pipes of each segment. This is due to the large difference between the air temperature passing through the pipe and the refrigerant temperature flow inside the pipe where the properties of CO_2 refrigerant is enhancing heat transfer in this local region.

The temperature discrepancies between simulation and test results for refrigerant temperature profile across the heat exchanger are mostly within ±2.2°C. Due to the fairly same refrigerant temperature outlet from both simulation and test results the simulation model can also accurately predict the finned-tube air cooled CO_2 gas cooler heat capacity and approach temperature.

As it mentioned in this chapter, the model can also predict the localised air and refrigerant side heat transfer coefficients, UA values and coil effectiveness. The fin and overall coil efficiency are also calculated by the model.

It is concluded that the simulation can fairly predicted the actual values recorded from the experimental tests and the model is therefore validated.

7.6.MODEL APPLICATION

The developed discrete heat transfer model is then replaced the simple gas cooler model which is represented in Chapter 4 to validate the experimental results for 2-rows and 3-rows heat exchangers based on the total COP of the system. The integrated model is used to compare and analyse the system results when it is run in transcritical cycle. The transition temperature is set to be at 26.8 °C as it was found from the experimental test analyses.

The total refrigerant mass flow rates, inlet refrigerant temperatures and pressures and air inlet (ambient conditions) parameters to the gas cooler which were obtained from the experimental results are imported to the first section of the simulation model. The first section of the model obtained the refrigerant and air outlet parameters from both 2-rows and 3-rows gas coolers. Those later used as an input to the second section of the model which starts from the ICMT suction line and finish at the discharge section of the compressors to complete the cycle. The refrigerant outlet parameters from section one

are also used to calculate the rate of the bypassed refrigerant (gas to liquid) on the liquid receiver level as explained in Chapter 4.

The intermediate and medium pressure levels of the system were kept constant for all the tests. The evaporating temperature for MT and AL was -8 °C and -10 °C respectively and both evaporator coils were used AKV expansion valves. The intermediate pressure was constant at 32 bar-atm and the average temperature after the ICMT valve was equal to -3°C.

The outputs from the "EES Procedures" written to the integrated model are reduced to the minimum level for the first section of the model. The outcomes were set to be the temperature and pressure for the refrigerant side only. This is to reduce the computation time. The COP for model predictions and experimental tests calculated with the following equation.

$$COP_{transcritical} = \frac{Q_{MT} + Q_{AL}}{W_{total} + W_{fan}} \qquad 7.39$$

More details can be found in Chapter 4 and 5. In order to take under consideration the effect of the different air volume flow rates passing through the condenser/gas cooler, the power consumption of the fan has been taken into account on the overall system COP as shown in Equations 7.39.

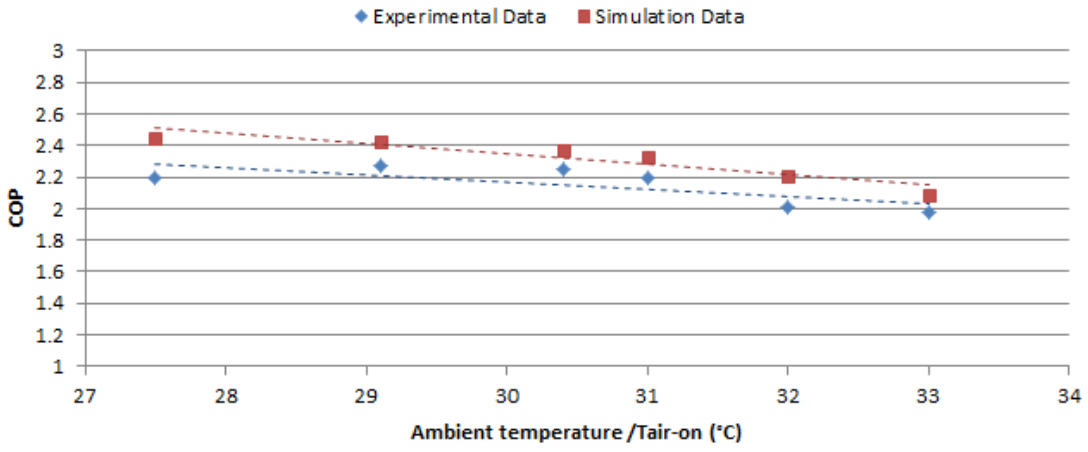

Figure 7.8 Variation of the COP for both experimental and simulation results

Figure 7.8 shows the variation of the COP for both experimental and simulation results for the 2-rows finned-tube air cooled CO_2 gas cooler when the main fan speed was set

to be at 70% of the total power. The maximum difference between simulation and experimental results for given test parameters was found to be slightly lower than 12%.

Very similar trends may be obtained for both 2-rows and 3-rows heat exchangers with 50% and 60% of main fan speed. Table 7.3 shows the comparison between simulation and experimental results for 2-rows and 3-rows gas coolers for specified values.

Table 7.3 Comparison between simulation and experimental results for 2-rows and 3-rows gas coolers for specified values

Parameters	Model COP	Experimental COP	Absolute Difference %
3-rows with 70% main fan speed at 31.4 °C ambient temperature	2.34	2.53	12.9
3-rows with 60% main fan speed at 30.9 °C ambient temperature	2.31	2.22	3.9
3-rows with 50% main fan speed at 32.8 °C ambient temperature	2.28	2.12	7.01
2-rows with 60% main fan speed at 29.5 °C ambient temperature	2.12	2.42	14.15
2-rows with 60% main fan speed at 35.2 °C ambient temperature	1.99	2.09	5.02
2-rows with 50% main fan speed at 33.7 °C ambient temperature	2.08	1.99	4.32

The experimental test results were used to validate the simulation model. The validation includes comparison between predicted parameters and the experimental results. The predicted COP of the system for both 3-rows and 2-rows gas cooler are separately installed and tested at the CO_2 booster refrigeration system have absolute difference of 5.40%. This indicates that the numerical model can predict the performance of refrigeration system quite accurately.

7.7. SUMMARY

When the CO_2 refrigerant cooled at supercritical pressures, the local heat transfer parameters are greatly dependent on local temperatures depending on the flow position. This is due to the unique thermophysical properties of CO_2 which are change drastically during the gas cooling process.

The discrete heat transfer model for the finned-tube air cooled CO_2 gas cooler has clearly explained in this chapter. This chapter has also described the validation of the model for both 3-rows and 2-rows heat exchanger based on the experimental test data. Finally, the model is used to integrate with the existing CO_2 system model. The outcomes of this were used to validate the system performance for both gas coolers. Both experimental and simulation model results showed a really good agreement.

Chapter 8 will presents the comparison of eight different supermarket refrigeration solutions based on cooling, energy and environmental performance for two different climate conditions.

8. THE SUPERMARKET CASE STUDIES

8.1.INTRODUCTION

Minimising the impact of climate change through energy use and reducing carbon footprint are the key environmental objectives over the last decades for the food retail industry. A number of solutions that safeguard food and protect the environment have been reported.

This chapter presents and discusses eight different combinations of system technologies and refrigerants which are referred as "cases". These include two CO_2 transcritical systems, two cascade systems which both high pressure (HP) and low pressure (LP) are supplied by CO_2, three cascade systems which the HP side feed by HFC refrigerant and the LP side by CO_2 and one system where the HP side is supplied by hydrocarbon (HC) refrigerant and the low side by CO_2. Energy and environmental performance of those eight different cases are presented. The initial investment cost is also briefly discusses.

The weather conditions of London – UK and Athens – Greece are used as boundary conditions on the models to calculate the annual energy and environmental performance. London is considerate as moderate climate where on the other hand is considering as a warm climate.

Models of the proposed eight solutions were implemented in EES software, which were based on the fundamental thermodynamic equations at steady state conditions.

8.2.OUTDOOR CONDITIONS

London was identified as moderate climate location and on the other hand Athens was considered as warm climate location in which implementing the aforesaid comparisons. Their different outdoor temperatures were obtained by using Weather Underground (TWC, 2016).

The downloaded weather file data are based on records every 20 mins for each location. Matlab software was used in order to calculate the yearly frequency (number per hours per year) for each ambient condition for both chosen locations. Later, Matlab was used for plotting the Box-and-Whisher (BWM) plots (Harbel and Abbas, 1998).

Figure 8.1 shows the monthly average ambient temperatures for Athens and London starting from July 2015 to June 2016. It is clear that all the year around Athens shows much higher ambient temperature comparing to London. Only on December 2015

Athens reached lower temperature comparing to London. As BWM plots shows this was an extreme condition.

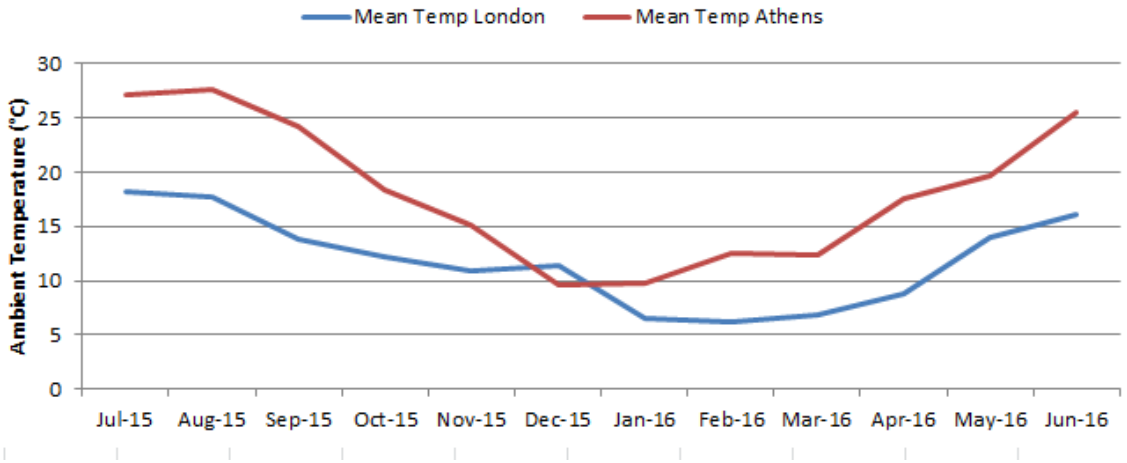

Figure 8.1 Monthly average ambient temperatures for Athens and London

Figure 8.2 and 8.3 present the monthly ambient temperature for Athens and London using the BWM plot. The red horizontal line in the boxes indicates the median while the outer limits of the boxes and whiskers show the 25th/75th and the 5th/95th percentiles respectively. The red-cross indicates an extreme outlier which occurred during each month. The blue line indicates the monthly average use based on hourly data.

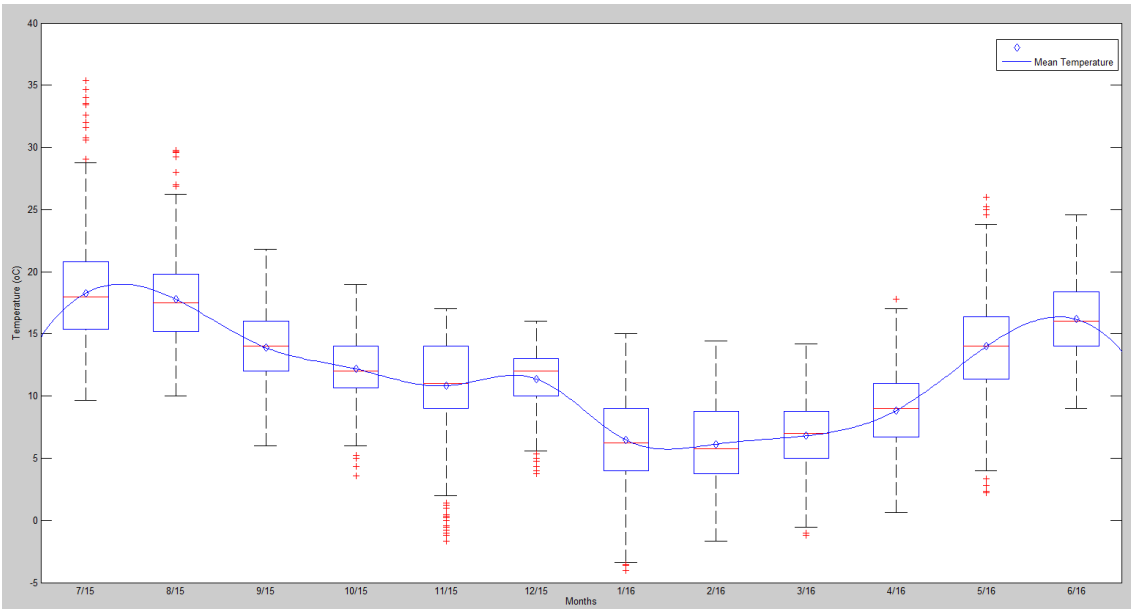

Figure 8.2 BWM plot for London weather data

It is clear from both graphs that the ambient temperature in Athens is much higher comparing with London. For Athens the higher frequency found to be at 15 °C and for London at 12 °C equal to 3.4% (297 hours/year) and 5.4% (478 hours/year) respectively.

According to the outdoor temperature was higher than 26.8 °C for about 15% of the time in Athens. In these conditions, the transcritical operation occurred for the cases where the CO_2 is used at the HP of the refrigeration system. This outcome points out the importance associated with choice of the suitable control strategy for the transition zone.

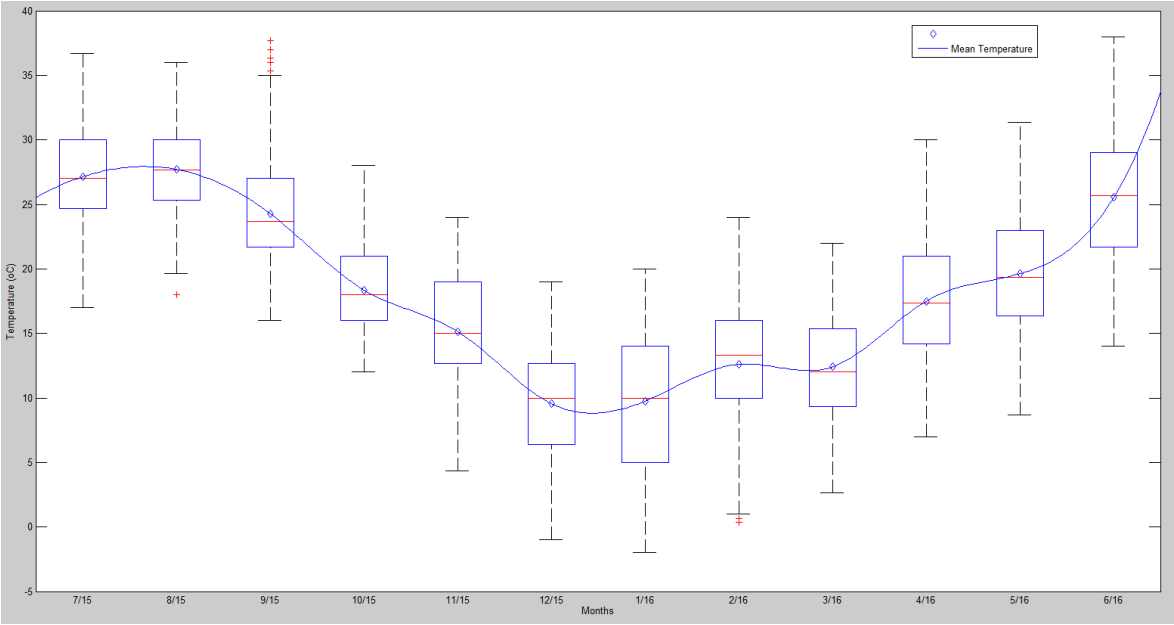

Figure 8.3 BWM plot for Athens weather data

The same control strategies have been used for all the systems which are comprises CO_2 (R744) at the high pressure side of the system. Those control strategies are estimated from the experimental results. Equations for pressure and temperature at the outlet of the condenser/gas cooler are estimated based on the data extracted from the experimental results. Many researchers in published work are using different control strategies to control the different CO_2 system arrangements (Gullo, et. al., 2016). These assumptions based on the theoretical work by using the optimisation solution in regards to COP.

Since the estimation of the control strategies on the high pressure side on the CO_2 cases is quite difficult the same control strategies which derived from the experimental results

are used for all the compared systems in this chapter. Those control strategies are proportional on the compressor discharge pressure settings, ICMT opening degree and condenser/gas cooler fan operation. Same procedure based on the control strategies for different CO_2 system arrangements have been reported from Singh (2016). The systems which are using HFC or HC at the high pressure side are controlled based on the Emerson Climate Technologies (2010).

8.3.CASE STUDIES

Table 8.1 illustrates the eight different supermarket refrigeration system cases were investigated in this chapter. Those are includes two "all-CO_2" refrigeration systems, two cascade refrigeration systems where CO_2 refrigerant is used in both HP and LP sides and four cascade cases where HFC and HC are used to feed the MT load and CO_2 for the LT load. More information for the CO_2 refrigeration system arrangements can be found in Chapter 3. For system comparison purposes "case 3" was considerate as reference case.

Table 8.1 Investigated case studies

Cases	MT or HP	LT or LP
1	Convectional Booster	
2	Improved Booster	
3	R134A	R744
4	R744 convectional cascade	
5	R744 improved cascade	
6	R404A	R744
7	R407A	R744
8	R290	R744

Case 1 and 2

Case 1 refers to a typical layout of a convectional booster CO_2 system or all-CO_2 system for supermarket application. All-CO_2 systems can operate in both subcritical and transcritical cycles depending on the ambient temperature. Unlike the cascade systems, the CO_2 refrigerant feed both MT and LT load cabinets inside the sales area. Two-stage compression is common used for the CO_2 booster systems. The refrigerant from the LT evaporator outlet is drawn into the low-stage compressor suction line. The discharge

from these compressor racks are mixed with the outlet of the MT evaporators at mixed point 1. The pressure at this point is equalised to avoid any refrigerant back-flow to the MT evaporators. Before the mixed refrigerant enters to the suction line of the high stage compressors is mixed with the gas by-passed refrigerant from the CO_2 liquid receiver at the mixed point 2. The gas by-passed from the ICM regulating valve is providing some inter-stage cooling enough to maintain the discharge pressure at the acceptable range at avoid any lubricant deterioration. The pressure at the mixing point 2 is equalised. The ICM by-pass valve is controlled the pressure drop at the acceptable level to avoid any back-flow.

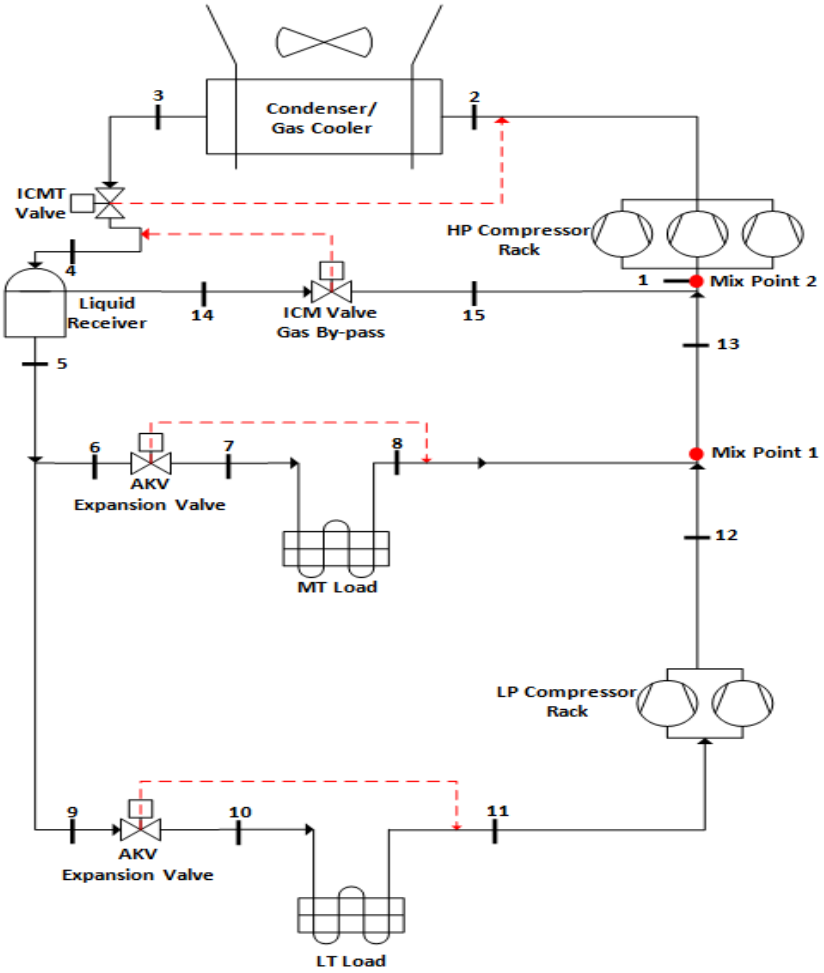

Figure 8.4 Convectional CO_2 booster system

Figure 8.4 shows the convectional CO_2 booster system for case 1. The red dashed lines in Fig. 8.4 represent the feedback communication for the individual components on the

system including the high pressure regulating valve (ICMT), the gas by-pass regulating valve (ICM) and the expansion valves for both MT and LT loads (AKV).

The mixed refrigerant enters to the suction line of the HP compressor rack and compressed at the inlet of the condenser/gas cooler. The pressure at that stage is controlled by the ICMT high pressure regulation valve and by employing variable fan speed control solution. The air cooled heat exchanger is act as a condenser at low outdoor temperatures and as gas cooler when the ambient temperature is high. In such a case the ingoing CO_2 undergoes a reduction in temperature with no phase change.

The refrigerant outlet from the C/GC enters at the suction line of the ICMT valve where the pressure dropped before the saturated refrigerant enters to liquid receiver. In this stage the ingoing CO_2 is isenthalpically expanded.

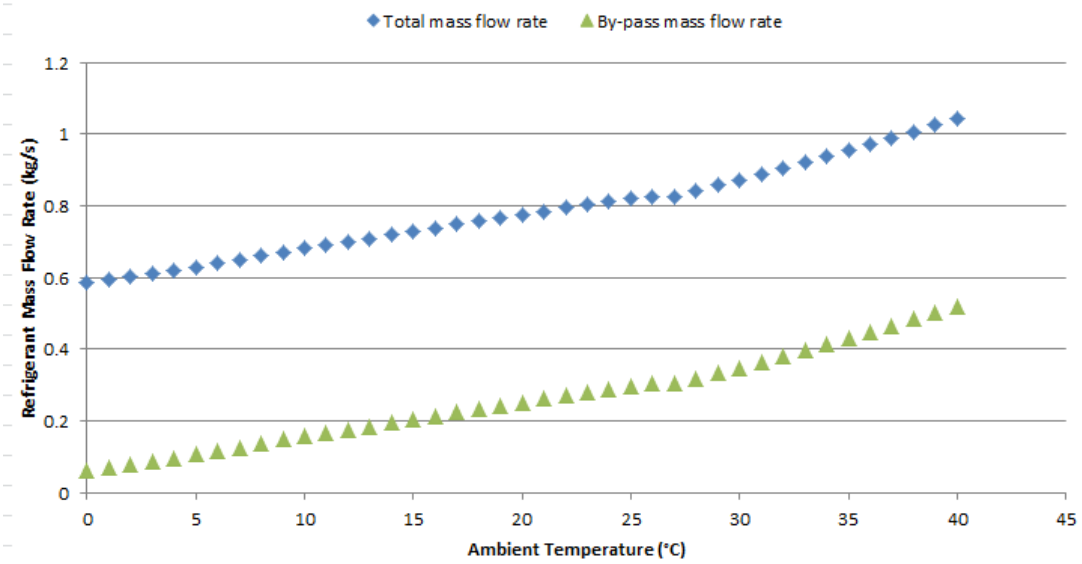

Figure 8.5 Total and bypass mass flow rate

The pressure at the liquid receiver controlled to be constant by employing the ICM flash gas by-pass valve. The liquid phase flows to feed the expansions valves of LT and MT loads. The gas phase is by passed to the suction line of the HP compressors through the ICM valve where the pressure is dropped.

The amount of the vapour which is produced at the discharge line of the ICMT regulating valve increases as the ambient temperature rises. This phenomenon leads to a higher amount of refrigerant which has to be passed and compressed through the HP compressor especially during the warm months. This has a proportional of the rise of the compressor power consumption and reduction of the system COP. In Fig. 8.5 the

rate of the by-passed refrigerant from the ICM and the total mass flow rate flows on the system are plotted against the ambient temperature. The average values for the mass flow rate by-passed from the ICM valve in respect to the total system mass flow rate for different outdoor conditions is represented in Table 8.2.

Table 8.2 Average values for the bypassed mass flow rates

Ambient Temperatures (°C)	Rate of refrigerant by-pass (%)
0 – 10	33.1
11 – 20	38.4
21 – 30	43.1
31 - 40	50.5

A solution to this problem is to install an additional compressor at the gas phase outlet of the CO_2 receiver. Therefore the mix point 2 is moved to the C/GC inlet. This means that the by-passed refrigerant is not mixed with the outlet of the MT and LT loads before entering to the HP compressor.

The by-passed refrigerant is compressed from higher pressure as it comes out from the receiver. Therefore, the pressure ratio is much lower at the additional compressor which means higher isentropic efficiency and less power consumption. This system is called "case 2".

Similar system is suggested by Sarkar and Agrawal (2010). For this work the performance optimization of different CO_2 systems including the parallel compression economization is discussed.

Figure 8.6 shows the CO_2 transcritical systems with the gas by-pass compressor solution. For the case 2 the same control strategy at the high pressure side is used in order to evaluate the system under the same conditions. The intermediate pressure was set to be constant at 35 bar.

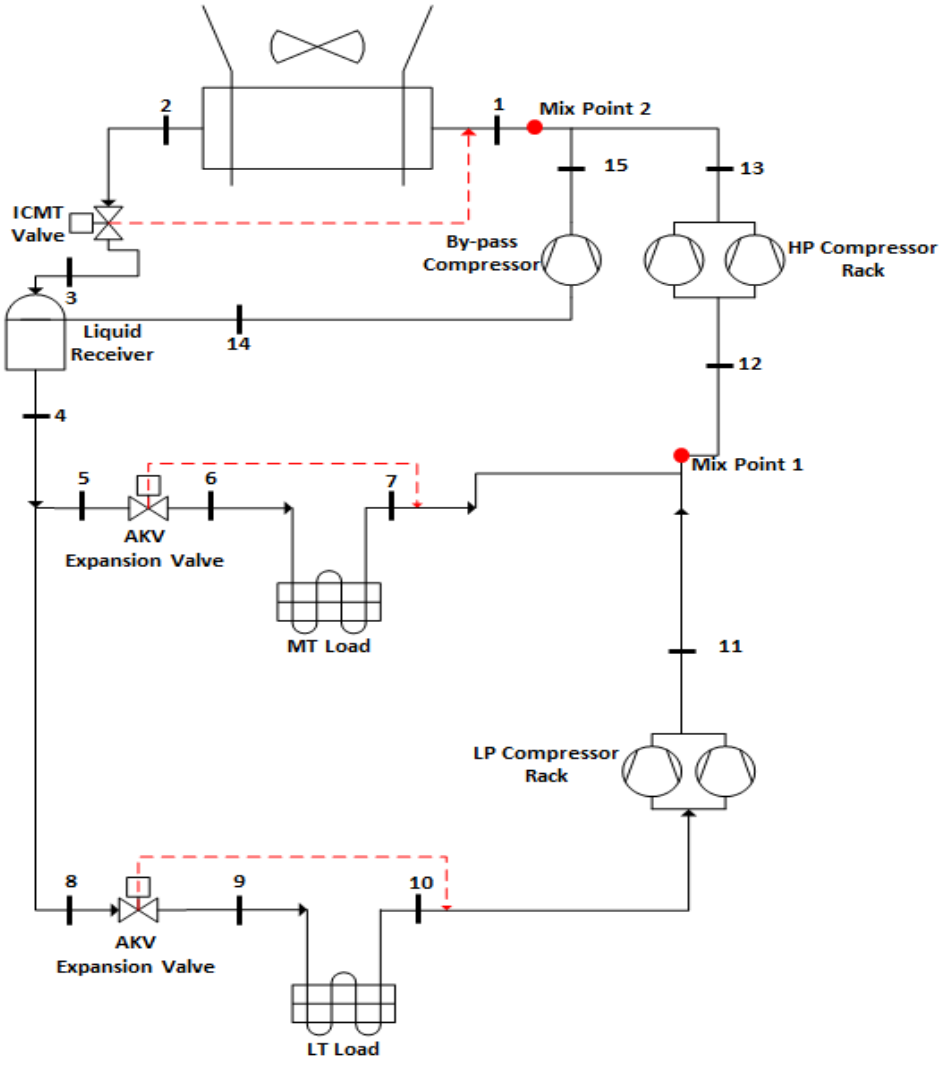

Figure 8.6 CO_2 booster system with bypass compressor

The main difference comparing with the convectional CO_2 booster system is the additional compressor installed at the intermediate pressure of the system as explained before. The two phase refrigerant enter to the receiver is split into gas and liquid by gravity. The liquid flows to feed both MT and LT expansion AKV valves and by the appropriate pressure drop reach the evaporating temperatures required to feed both load levels.

The gas phase CO_2 refrigerant at 35 bar entering to the by-pass compressor where compressed to the mixed point 2 before entering the C/GC. Different techniques have been reported based on the installation of ICM by-pass valve and gas by-pass compressor together where the system controlled by the ambient temperature. For low

outdoor conditions the gas by-pass flows back for the ICM valve and mix at mixed point 2 as in Figure 8.4. When the ambient condition is higher than the critical point of the CO_2 the ICM is shut and the gas by-pass is flowing to the gas by-pass compressor. In this solution, the capital cost is much higher comparing to case 1 and case 2 systems. In additional, the control strategies are become complex.

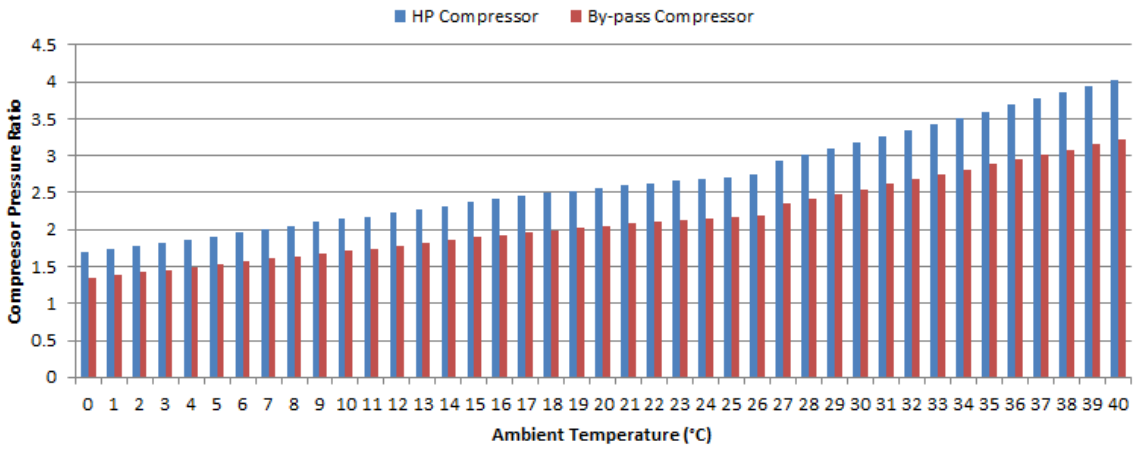

Figure 8.7 Pressure ratio across both HP and By-pass compressors

Figure 8.7 illustrates the pressure ratio across both HP and By-pass compressors. The pressure ratio is defined as the ratio between the discharges pressures divided by the suction pressure.

$$P_{ratio} = P_{discharge}/P_{suction} \qquad 8.1$$

It is clear from the graph that the difference between the pressure ratios is higher as the ambient condition is higher. The pressure ration is related to the isentropic efficiency of the compressor which means higher pressure ratio lower isentropic efficiency. The isentropic efficiency for both compressors is illustrated in Figure 8.8.

The isentropic efficiency for the by-pass compressor is higher as shown in graph as a proportional of the higher suction pressure. The higher isentropic efficiency gives less power consumption on the system overall and higher COP.

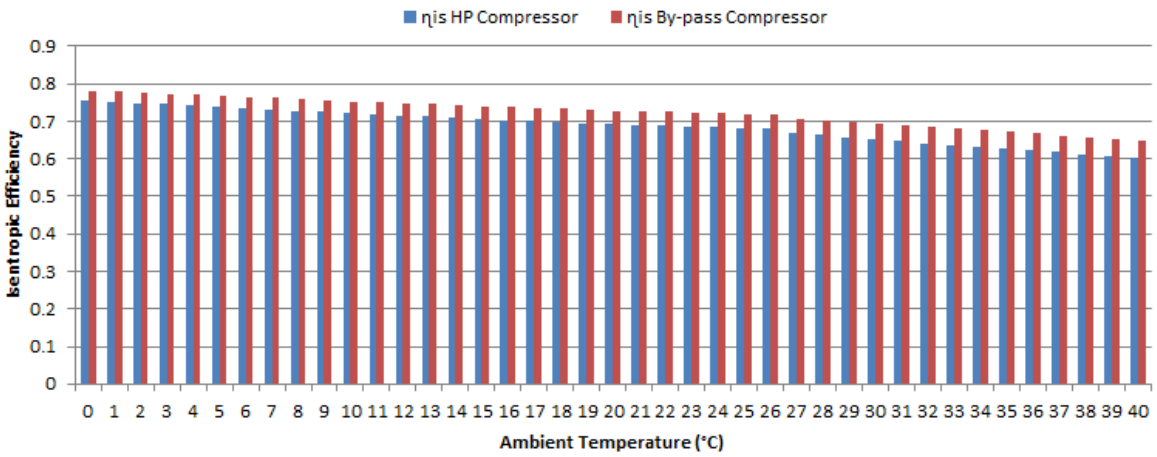

Figure 8.8 Isentropic efficiency for both compressors

Case 3

Figure 8.9 illustrates the cascade system solution which is referred as reference case for comparison purposes.

The cascade system consist of two circuits which called high temperature (HT) cascade and low temperature (LT) cascade which interact with each other by the cascade heat exchanger. In this particular case the HT circuit including the air cooled condenser, the two expansion valves, the MT and cascade load and the HT compressor rack. The fluid used to curry out the heat transfer process is the R134A. The low cascade system comprised from the cascade heat exchanger, the AKV expansion valve, the LT load and LT compressor rack. This circuit is operates by using R744. Therefore, the cascade heat exchanger operates as an evaporator for the HT circuit and as a condenser for the LT circuit.

By using R744 to feed the LT circuit of the cascade system and the appropriate temperature difference across the heat exchanger we make sure that the LT system is operates in subcritical mode all the time.

The cascade expansion valve is controlled by the temperature difference across the cascade heat exchanger and the R744 condensing temperature. More details for the cascade arrangements can be found in Chapter 3.

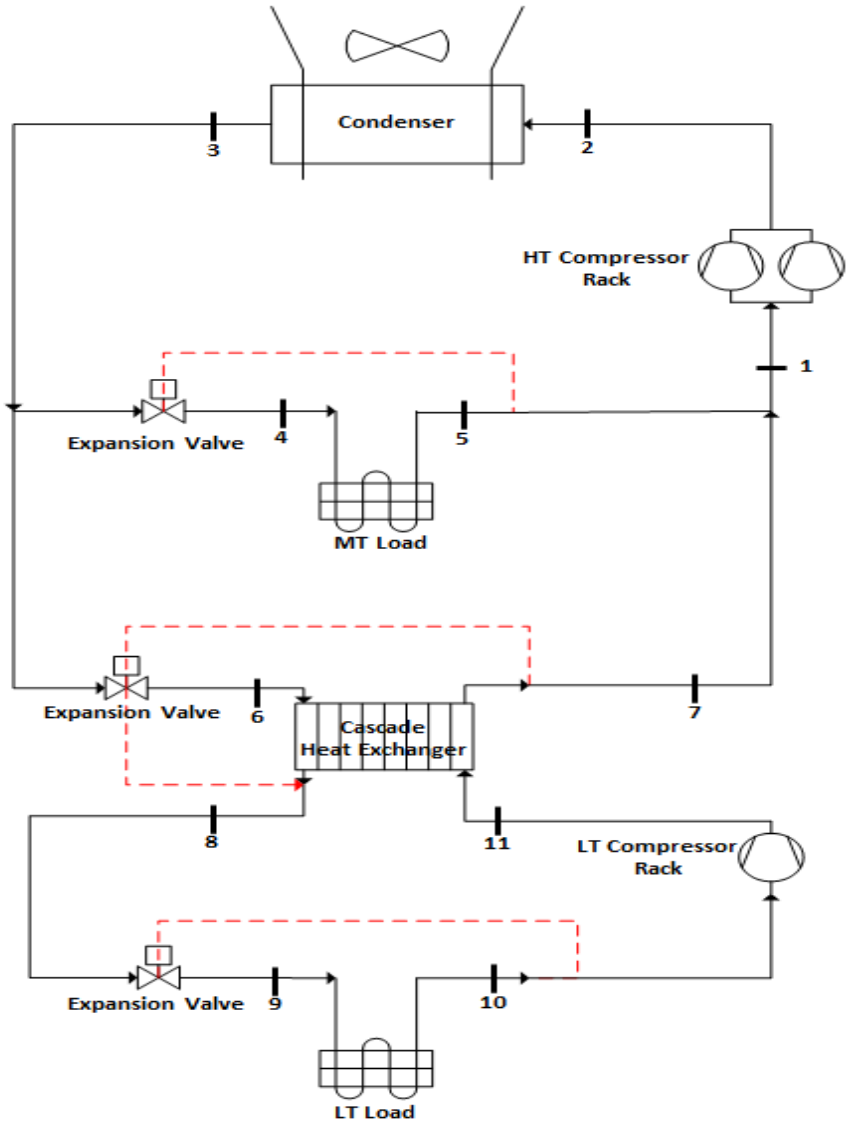

Figure 8.9 Cascade solution

Case 4 and 5

Cases 4 and 5 are representing a transcritical R744 system where the LT plant is a cascade from the HT plant. In simple words in this cascade system both MT and LT loads are feed with R744. The main advantage of this system is the continuously subcritical operation in the LT side and the lower environmental impacts coming from

the HT side comparing with cascade solutions where a HFC used to feed HT circuit. Figure 8.10 shows the case 4 system which is under investigation. This system is well known as cascade CO_2 system with flash gas by-pass.

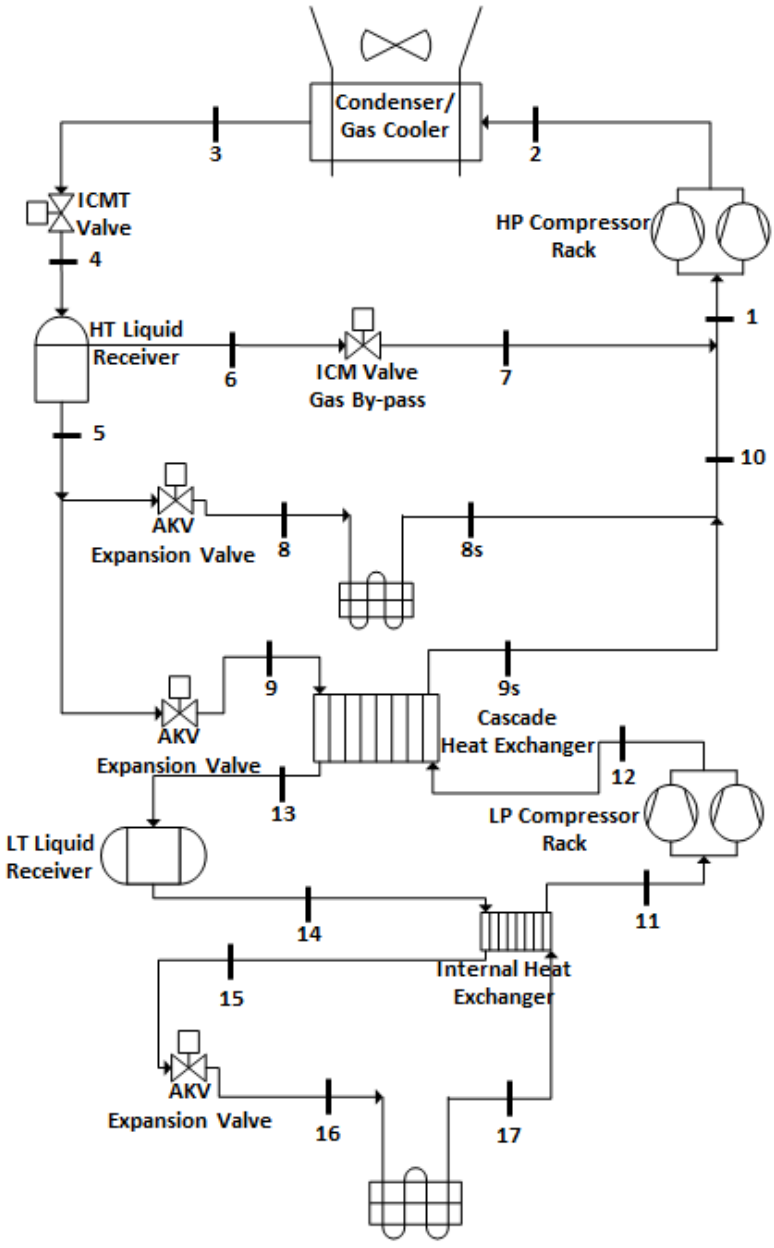

Figure 8.10 R744 cascade solution with gas bypass

The high stage section is similar to the booster system as described in cases 1 and 2. The difference is that the LT system is cascaded as an individual circuit with the HT system for heat rejection. The MT evaporators are divided into two groups: one provides refrigeration to the MT display cabinets and the other condenses the CO_2 gas for the LT systems. This solution has been implemented in a number of UK supermarkets (Campbell, 2009).

The disadvantage of this system is the same as discussed earlier in case 1. The gas by-passed outlet from the HT liquid receiver is passing through the ICM regulating valve where the pressure dropped and equalised with the outlet pressure of the MT and cascade heat exchanger. Therefore, the total refrigerant mass flow rate is compressed from low pressure to high pressure with very high compression ratio. As it is clear from before, the higher pressure ration between suction and discharge line the power consumption is increased and the COP is decreased. Also, the results from case 1 and 2 shows the gas by-pass from the ICM valve is increased as the ambient temperature is increased. For the summer months in Athens where the temperature is high the 43.1% of the total mass flow rate of the system is by-passed.

The system in case 5 is a proposed system where an additional by-pass compressor is replaced the ICM regulating valve. In simple words, the new proposed system is a combination of the improved CO_2 booster system and the CO_2 cascade system. The gas by-pass in point 6 is entering to the compressor suction line in high pressure equal to the HT receiver and compressed to mix with the discharge of the HP compressor before entering to the C/GC.

The control strategies at the pressure and temperature outlet of the C/GC were the same as cases 1 and 2 in order to compare the systems under the same reference point. Those control strategies as discussed earlier were derived from the experimental results which have been done for a range of ambient conditions and control strategies. The control strategies include, the C/GC fan speed, ICMT regulating valve settings, degree of subcooling and compressor speed variation.

Figure 8.11 shows the cascade CO_2 system with compressor flash gas by-pass. For such an installation the capital cost is increased due to the installation of the additional compressor and the pipeline from the discharge line to the inlet of the C/GC. The results of case 5 shows higher COP and lower annual power consumption comparing to original system of case 4.

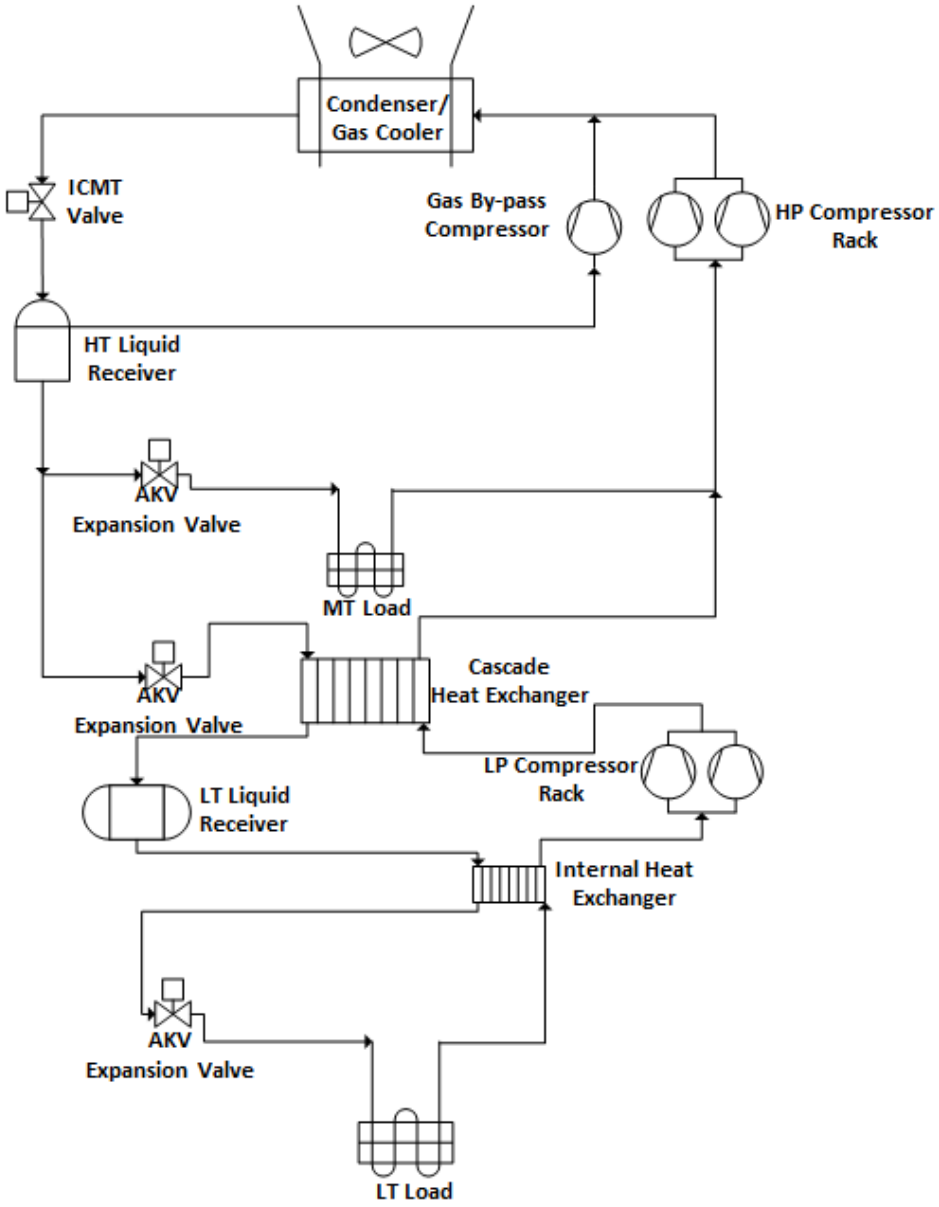

Figure 8.11 R744 cascade solution with gas bypass compressor

Case 6 and 7

The cases 6 and 7 are based in the same cascade system arrangement as in case 3. The difference between those is that case 3 is used R134A as fluid to curry out the heat transfer process where case 6 and 7 use R404A and R407A respectively. The low temperature side is operating by using R744 for all these systems.

Case 8

Case 8 is based in a different cascade refrigeration system with the difference that a natural refrigerant such as R290 is replaced the convectional HFC. The system arraignment is based on case 3 where the MT is feed by hydrocarbon (HC) refrigerant and LT with R744. The proposed system shows lower Total Equivalent Warming Impact (TEWI) due to very low GWP of 3 comparing with the HFC refrigerants.

8.4.INVESTMENT COST

In this chapter a briefly investigation of the initial capital and running costs for the given eight cases is discussed. Emerson (2010), present a simple relative investment cost structure for the refrigeration system installed in supermarket applications. Figure 8.12 shows the initial capital cost as reported by Emerson.

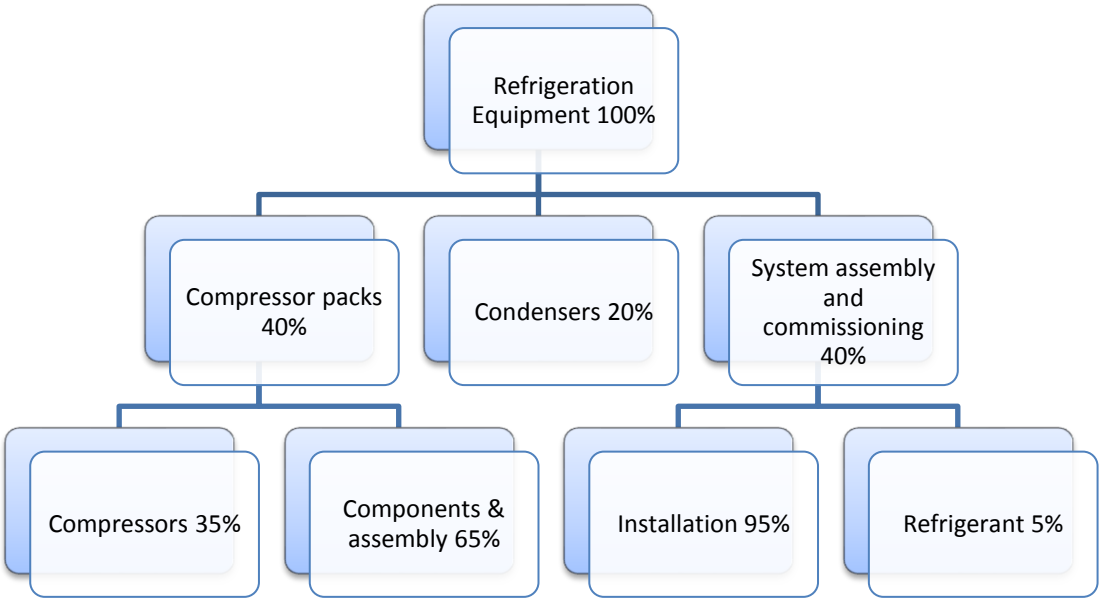

Figure 8.12 Simple relative investment cost structure

(Emerson, 2010)

The capital cost investigation of a CO_2 system has been reported by a number of researchers to be higher than that of an equivalent R404A system, which is the most common refrigerant in supermarket installations. Girotto (2004) reported an increase in capital cost of 20% for a transcritical CO_2 system compared to a R404A system. De Ono, (2008) also reported a 20% increase in costs for a CO_2 refrigeration system compared to an R404A system. Emerson (2010) compiled a report comparing the energy use, TEWI and investment costs for 14 different solutions commercial refrigeration systems. The CO_2 booster system had an investment cost 48% higher than that of a R404A system but the booster system reduced the TEWI by 42%.

All the above scenarios are reported in early stage of the CO_2 application when R744 was not widely used. This was limiting the choices of system component suppliers and installation companies. After 2010 the interest of R744 system increased and number of different companies invests in this research. It is worth to mention that on early of 2010 were only 2 companies in UK was doing the CO_2 training courses for the refrigeration technician staffs and after 2015 is more than 15 different courses across the UK.

It is well known that the CO_2 booster systems offering elimination of direct emissions comparing to HFCs installation. In additional, CO_2 refrigerant is not toxic and flammable. Also, the volume of CO_2 required to achieve the same cooling effect is much lower comparing with HFCs applications. This has reduction opportunities on the capital investment and running costs regarding the refrigerant need to be charged on the system. The refrigerant price of CO_2 is also much lower comparing to the convectional HFC systems.

On the other hand, R744 systems such as case 1-2-4-5 are operating in much higher pressures comparing with HFCs and HC systems. This requires the use components to be heavier and stand with higher pressure operations. Also, systems such the cases which named before need the additional installation of ICMT, ICM valves, liquid receiver, additional expansion valves for each evaporator cabinet and by-pass compressors for case 2 and 5.

The additional cost of those components and the complexity of the pipe arrangement made the R744 solutions more expensive in terms of capital costs.

For the cascade solution such case 3-4-5-6-7-8 the additional cascade heat exchanger is increasing the cost of the capital investment cost. Additional circuits, controls and heat exchangers are required.

The number of the controllers required for the systems use R744 only is much higher comparing to HFCs system due to the number of the additional equipment used to ensure the maximum system performance. The electrical panel on the CO_2 installations are more expensive as additional contactors and a larger panel is required due to the LP compressor rack controller and the additional controllers for the gas by-pass compressor or valve.

A number of PRV valves must be placed along the CO_2 system in order to avoid extremely high pressures and pipe or component fails. The cost of PRV is based on the system type and section and is an additional to the initial capital cost.

For the system cases where R744 and R290 are used a cost penalty associated with the extra safety precautions added to the capital cost.

More details for the advantages and disadvantages for the proposed eight cases can be found in Chapter 3.

8.5.SAFETY GROUP CLASSIFICATIONS

The classification of each refrigerant consists of two alphanumeric characters. Table 8.3 shows the safety group of each refrigerant used on the eight different cases. The capital letter corresponds to toxicity and the digit (number) to flammability. The numbers used on Table are from ASHRAE standard 34 (2007).

The GWP values for the investigated refrigerant are given on the same table. Those values used to carry out the direct emissions for each case. The values of GWP used to calculate the direct TEWI emissions are from IPCC (2007).

Table 8.3 Refrigerants safety group

Cases	Safety Group Classifications		GWP	
	MT	LT	MT	LT
1	A1		1	
2	A1		1	
3	A1	A1	1430	1
4	A1	A1	1	1
5	A1	A1	1	1
6	A1	A1	3922	1
7	A1	A1	2107	1
8	A3	A1	3	1

R744 and HFCs shows a safety group classification of A1 which means refrigerant which toxicity has not been identified at concentrations less than or equal to 400 ppm and there is no flame propagation risk. On the other hand, R290 is not toxic but very high flammable risk when the refrigerant reacts with ambient air fast. Based on that, system using R290 in sales area must be well designed and installed by experienced staff. This cause an additional cost on the capital investment as discussed earlier. Comparing the eight proposed cases in terms of refrigerant GWP, the cases 1-2-4-5 shows a very low value equal to 1. Also, case 8 where the natural refrigerant R290 replaced the HFCs on the HT circuit of the system has a very low number of 3. The higher GWP can be found on case 6 where the HT circuit side has a number equal to 3922. The analysis of those will present in following sub-chapter in terms of TEWI calculations.

8.6.SIMULATION MODELS

Refrigeration systems are crucial parts in retailed superstores to ensure proper merchandise and safety of the food products. Two temperature ranges are designed in a supermarket to store frozen (LT) and chilled food (MT) products. It is noted that the supermarket refrigeration systems contribute greatly to both direct greenhouse gas emissions due to refrigerant leakage and indirect greenhouse gas emissions by energy consumption. The calculations were based on the required refrigeration duties of a typical European supermarket as presented by Tassou et al. (2010), with total sales area of 1,400 m^2. The total refrigeration capacity is split into 100 kW and 30kW of MT and

LT respectively. Table 8.4 illustrates the common running models for the eight proposed cases. The values such as evaporating temperatures, superheat, condensing unit, fan power and cascade approach temperature in Table 8.5 were based on Emerson Climate Technologies (2010) published data.

Table 8.4 Common running models for the eight proposed cases

MT Load									
Cases	1	2	3	4	5	6	7	8	
Load	100	100	100	100	100	100	100	100	kW
Evaporating Temperature	-8	-8	-10	-8	-8	-10	-10	-10	°C
Superheat	10	10	10	10	10	10	10	10	K
Subcooling	2*	2*	2	2*	2*	2	2	2	K
Evaporator fans, lights, defrost	10.5	10.5	10.5	10.5	10.5	10.5	10.5	10.5	kW_{el}
Condenser/gas cooler fans	7.5	7.5	7.5	7.5	7.5	7.5	7.5	7.5	kW_{el}
* Subcritical operation only									

LT Load									
Cases	1	2	3	4	5	6	7	8	
Load	30	30	30	30	30	30	30	30	kW
Evaporating Temperature	-32	-32	-32	-32	-32	-32	-32	-32	°C
Superheat	10	10	10	10	10	10	10	10	K
Cascade Approach			5*	5*	5*	5*	5*	5*	K
Evaporator fans, lights, defrost	7	7	7	7	7	7	7	7	kW_{el}
* Cascade solutions only									

The MT evaporating temperature for cases 3-6-7-8 was set to -10 °C for the cascade systems where the HFCs and HC used as refrigerants. For cases where the MT is also feed with R744 the evaporating temperature set to -8 °C. The reason for this difference lies in better R744 performance during the vaporisation process than HFCs and HC (Girotto et al., 2004). The superheat for all the investigated cases set to 10K.

For cases1-2-4-5 where a liquid receiver is used as storage and gas-liquid separator the pressure set constant at 35 bar. The pressure at this section of the systems is called as an intermediate pressure as explained in Chapter 3. In real system applications the intermediate pressure is constant as a function of the gas by-pass valve settings, ICMT valve and additional condensing unit. The pressure drop was neglected and all the expansion valves of the proposed eight cases were treated as isenthalpic devices.

The control parameters at the high pressure of all the proposed systems were modelled based on the refrigerant which curry out the heat transfer process. For the cases where CO_2 is operate in HP circuit of the system this affect from the ambient conditions. Therefore, when the outdoor temperature is lower to 26.8°C the system is operates in subcritical cycle. The value of 26.8°C has been defined from the experimental results and the control strategies used to operate the condenser/gas cooler. The transition zones of the R744 systems in HP circuit were defined from the experimental results. The specific operating conditions for cases 1-2-4-5 are shown in Table 8.5.

Table 8.5 R744 operating zones

Transition Zones	Transition temperature range	Condenser/Gas Cooler Temperature outlet	Condenser/Gas Cooler Pressure outlet
a	$T_{\_amb}<0$	8°C	$P_{out}=f(T_{out}, \Delta T_{sub})$
b	$0<=T_{\_amb}<=10$	$T_{\_amb}+ \Delta T_{\_app}$	$P_{out}=f(T_{out}, \Delta T_{sub})$
c	$10<T_{\_amb}<26.8$	Derived from Exp. Results	Derived from Exp. Results
d	$T_{\_amb}=>26.8$	$T_{\_amb}+ \Delta T_{\_app\_GC}$	Derived from Exp. Results

Transition zone "*a*" referred to a subcritical condition where the condensing temperature was kept constant independently of the external temperature and kept to its minimum value of 8 °C. As a result of this, the energy consumption and COP were constant.

When the cases moved to transition zone "*b"* the condenser outlet temperature depended on the approach temperature between condenser and ambient air temperature which found to be equal to 10K. For both transition zones "*a"* and "*b"* the pressure at the condenser outlet is a function of the condensing temperature and the degree of subcooling which set to 2K. During the experimental results the ICMT regulating valve was controlled based on the degree of subcooling which set at the same value of 2K for the subcritical operation.

For the transition zone "*c*" referred to the transition zone from subcritical to transcritical operation. The temperature range was varied from 10 °C to 26.7 °C for this zone. Based on the experimental results two correlations have been derived to control the temperature and pressure at condenser outlet. The former is a function of the outdoor temperature and the pressure correlation is a function of the condenser outlet temperature.

$$T_{cond,\ zone\ "c"} = (-0.0144*(T_{amb}^2)) + (1.1264*T_{amb}) + 9.8272 \quad (8.2)$$

$$P_{condenser,\ zone\ "c"} = (0.0522*\ (T_{cond,\ zone\ "c"})^2) - (1.0178*\ T_{cond,\ zone\ "c"}) + 60.798 \quad (8.3)$$

$P_{condenser,\ zone\ "c"}$ in bar-atm.

Transition zone "*d*" is referred to the transcritical operation of the system where the pressure and temperature at the outlet of the gas cooler is independently. The gas cooler outlet temperature is a function of the ambient temperature and the approach temperature. The value of the approach temperature set to 3K which derived from the experimental results.

Based on the gas cooler outlet temperature a correlation has been created in order to calculate the outlet gas cooler pressure.

$$P_{gas\ cooler,\ zone\ "d"} = (2.3426*\ T_{GC,\ zone\ "d"}) + 11.541 \quad (8.4)$$

$P_{gas\ cooler,\ zone\ "d"}$ in bar-atm.

For cases 3-6-7-8 where HFCs and HC used as a refrigerant the control strategies for the condenser outlet conditions derived from Emerson Climate Technologies (2010). The transition zones were divided to two based on the ambient conditions and the minimum condensing temperature.

Table 8.6 HFCs and HC operating zones

Transition Zones	Transition temperature range	Condenser Temperature outlet	Condenser Pressure outlet
a	$T_{\_amb}$<=10	20°C	$P_{out}=f(T_{out}, \Delta T_{sub})$
b	$T_{\_amb}$>10	$T_{\_amb}+ \Delta T_{\_app}$	$P_{out}=f(T_{out}, \Delta T_{sub})$

The approach temperature for transition zone "*b*" was set to 10 K and the subcooling degree equal to 2 K for all the investigated cases. The pressure outlet of the condenser is a function of the outlet temperature and ΔT subcooling. The properties of all the refrigerants defined from EES library.

The isentropic efficiency of the compressor can be expressed as a function of the pressure ratio (R_p) across the compressors. Lee et al., (2006) equation used to the isentropic efficiency of the compressor for cases 1-2-4-5 as explained in Chapter 4.

The isentropic efficiency for case 3 is calculated by using BITZER software (Bitzer, 2016). The same software was used to calculate the isentropic efficiencies for cases 6-7. DORIN Innovation software (2016) was used to calculate the isentropic efficiencies for case 8.

8.7.TEWI CALCULATION

The environmental impact of a refrigeration system is measured by the direct and indirect carbon dioxide emissions from the operation of the refrigeration system. The direct carbon dioxide emissions are a result of refrigerant leakage from the system. The indirect emissions depend on the electrical power used by the system.

The TEWI (Total Equivalent Warming Impact) equation developed by the British Refrigeration Association (BRA, 2006) can be used to compare and assess the environmental impact of different refrigeration systems due to direct and indirect carbon dioxide emissions.

$$TEWI = TEWI_{direct} + TEWI_{indirect} \quad 8.5$$

$$TEWI_{direct} = GWP \cdot L \cdot n + GWP \cdot m \cdot (1\text{-}a) \quad 8.6$$

$$TEWI_{indirect} = E \cdot \beta \cdot n \quad 8.7$$

The values for GWP for all the refrigerants used in the eight investigated cased have been presented in Chapter 8.5. "L" is the annual leakage rate which set to 15% (UNEP, 2015). Where "n" is the operating lifetime of the refrigeration systems which set at 10 years for all proposed cases (UNEP, 2015, Emerson Climate Technologies 2010). "m" is the refrigerant charge amount in kilograms for each system. For system used R134A-R404A-R407A a refrigerant of $2kg \cdot kW\ Load$ was used (Emerson Climate Technologies 2010). For cases 1-2-4-5 where R744 used in HP circuit the refrigerant charge set to $1.2kg \cdot kW\ Load$ (Shilliday, 2012). For cases 3-6-7-8 where R744 used in LP circuit the refrigerant charge is $1kg \cdot kW\ Load$. For case 8 where R290 is used in HP circuit the refrigerant charge is $1.5kg \cdot kW\ Load$. The direct TEWI calculations take into account the recycling factor which set to be equal to 95% (UNEP, 2015, Emerson Climate Technologies 2010). The indirect TEWI calculations take into account the annual energy consumption (kWh/year) which calculated from the model. The indirect emission factor "β" for Athens is equal to 0.72 kg_{CO2}/kWh (International Energy Agency, 2013) and 0.53 kg_{CO2}/kWh for London (Carbon Trust 2011).

8.8.PERFOMANCE COMPARISON

Figure 8.13 illustrates the comparison in terms of COP among all the investigated cases. It is clear from the graph that the COP for cases 1 and 2 is higher when the ambient temperature is below 7 °C and for case 5 below 10 °C. For case 2 the system performed better until moves to transcritical operation and the performance drops drastically.

$$COP = \frac{Q_{MT} + Q_{LT}}{W_{com,HT} + W_{com,LT} + W_{MT,fans} + W_{LT,fans} + W_{\frac{C}{GC},fans}} \qquad 8.8$$

Equation 8.8 shows the cooling performance calculation for all the investigated cases including the cooling loads of MT and LT circuits and the electrical power consumption of HT and LT compressors and the fan power consumption including C/GC, LT and MT fans.

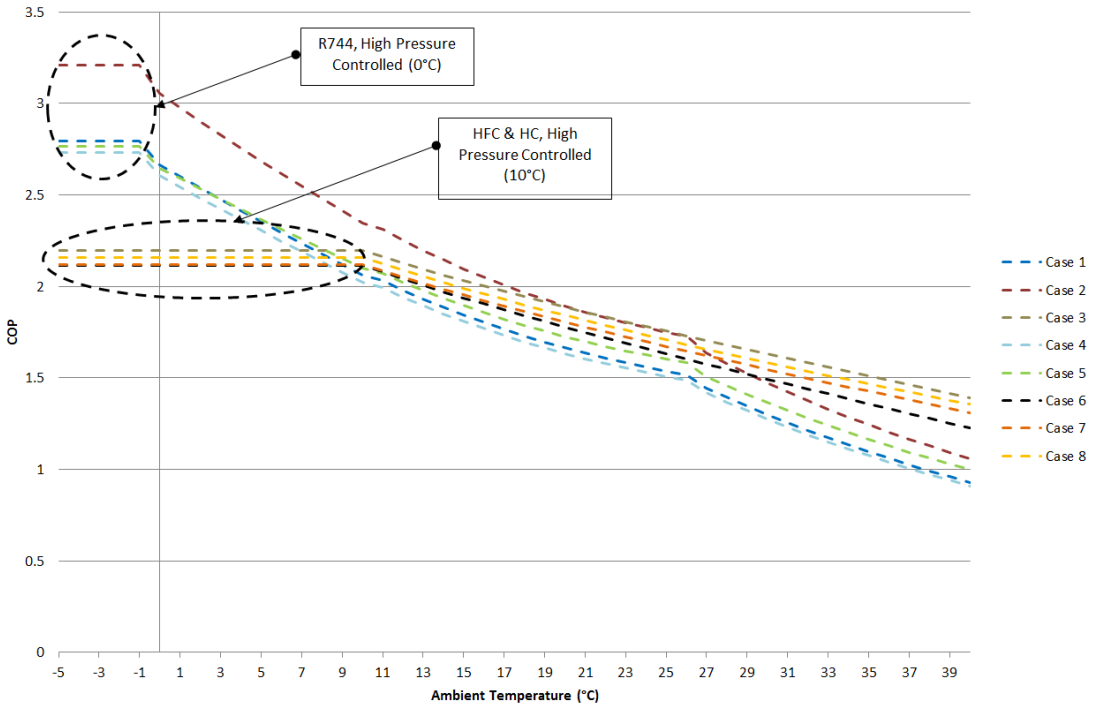

Figure 8.13 Comparison in terms of COP among all the investigated cases

The cases (3-6-7-8) where HFCs and HC were used in HP circuit show higher performance for ambient temperatures above 26.8 °C. Above this temperature the system with R744 in HP circuits operate in transcritical cycle where the energy consumption of the compressor increased and as a proportional to decrease the COP for those cases.

Comparing the improved system of case 2 with the reference case 3 the average COP difference is 36% when the ambient temperature is below 0 °C. Between 0 °C to 10 °C the case 2 has higher COP of 18%. As the ambient temperature increased the COP for case 2 is reduced rapidly. For ambient temperatures between 10 °C to 20 °C case 2 shows higher COP of 3%. Above this temperature range the COP of case 3 is become higher. For example case 2 shows higher COP of 20% for ambient temperatures between 30 °C to 40 °C. At those conditions the system for case 2 is operating in transcritical cycle. The quality of the refrigerant at the outlet of ICMT valve, the much higher by-pass refrigerant rate and the compressor power consumption made the case 2 less efficient at high ambient temperatures.

Case 4 and 5 are based on cascade systems where both HP and LP circuits are feed with R744. The difference between those systems is the additional by-pass compressor of case 5 which replaced the ICM by-pass valve of case 4. With this solution we try to achieve lower compressor power consumption and therefore higher COP. The additional by-pass compressor had a small compression ratio and higher isentropic efficiency leading to lower power consumption. It is clear from Fig. 8.3 that the difference of the COP values for those two cases is smaller at the very low ambient conditions and much higher in higher outdoor temperatures. For temperature range of 0 °C to 10 °C, 10 °C to 20 °C, 20 °C to 30 °C and 30 °C to 40 °C the average COP for case 5 increase for 2.8 %, 4.7 %, 6.20 % and 8.1 % respectively. The gas phase mass flow rate at the liquid receiver increased as the ambient temperature increased due to the enthalpy exits the condenser/gas cooler and the ICMT valve before the refrigerant enters to liquid receiver.

Table 8.7 demonstrates the comparison for cases 6-7-8 where HFCs and HC were used in HP circuit. The comparison is made with regards to reference case COP values.

Table 8.7 Comparison for cases 6-7-8 with reference case 3

Temperatures	Different in COP %		
	Case 6	Case 7	Case 8
0 °C to 10 °C	- 3.67	-3.52	-1.70
10 °C to 20 °C	-3.67	-3.52	-1.70
20 °C to 30 °C	-4.76	-3.98	-2.09
30 °C to 40 °C	-7.43	-4.86	-2.75

It is clear from the comparison table that case 8 shows the closest values to the reference case. Take into account the very low GWP of R290 which is equal to 3 (GWP of R134A: 1430) case 8 is a promising alternative for the cascade solutions.

To conclude, when the well-known booster system in case 1 compared with the improved solution of case 2 the power consumption is lower and the COP of system 2 is higher due to the additional by-pass compressor which replaced the ICM by-pass valve. Same idea has been applied on the cascade system of case 5. Case 5 show very lower

power consumption and much higher COP values comparing with the initial system design of case 4 especially in higher ambient conditions. Finally, the reference case of case 3 show higher COP for ambient temperatures higher than 26.8 °C.

8.9.ANNUAL ENERGY CONSUMPTION COMPARISON AMONG THE INVESTIGATED CASES

London

Figure 8.14 shows the total electrical energy consumption of the investigated cases based on the weather data of London (Heathrow).

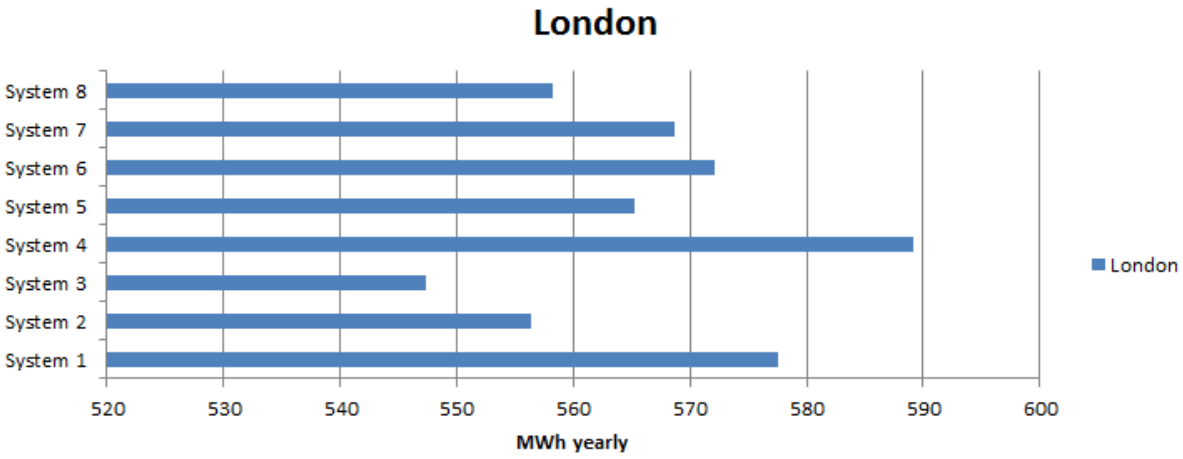

Figure 8.14 Total electrical energy consumption among the system for London

The case 3 shows lower power consumption comparing to other investigated systems. All-CO_2 systems shows higher energy consumption comparing to case 3 due to the higher ambient temperatures at London Heathrow and the higher number of hours of transcritical operation.

Table 8.8 shows the comparison of annual energy consumptions and the percentage difference in comparison with case 3.

Table 8.8 Annual energy consumptions (London)

1	2	3	4	5	6	7	8
Annual energy consumptions MWh							
577.54	556.33	547.37	589.08	565.17	572.16	568.74	558.20
Percentage Difference %							
+5.36	+1.62	-	+7.34	+3.20	+4.43	+3.83	+1.93

Cases 2 and 8 found to be closer to reference case 8 which showed the lower power consumption. The improved booster system of case 2 is showed great benefits in terms of power consumption by using the bypass compressor system. The power consumption is dropped drastically comparing to the original system of case 1.

In additional, we have to notice the great power consumption drop between cases 4 and 5 where the ICM regulating valve replaced by a bypass compressor.

Table 8.9 illustrates the annually running cost (electricity only) for the investigated cases. The values were calculated based on average electricity price of £0.144 per kWh (U-switch, 2016) of electricity in London Heathrow area.

The values below in Table included only the cost of annual electricity and not any service-maintenance cost of the investigated systems. In terms of maintenance the cascade systems in case 3-4-5-6-7-8 shows higher cost due to the complexity of the system.

Table 8.9 Annually running cost (electricity only) for London

1	2	3	4	5	6	7	8
Electricity Cost (£)							
83,166	80,112	78,823	84,828	81,385	82,391	81,899	80,382

Athens

Figure 8.15 shows the total electrical energy consumption of the investigated cases based on the weather data of Athens.

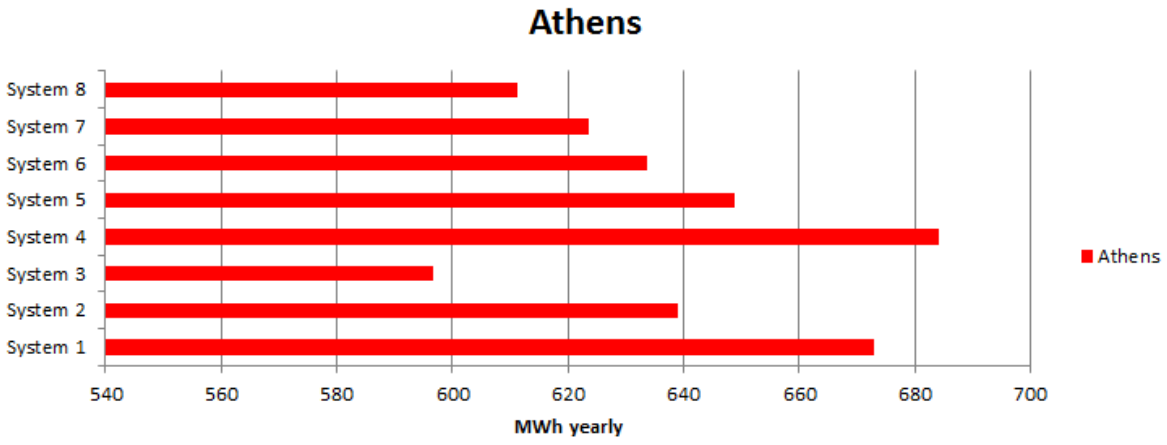

Figure 8.15 Total electrical energy consumption among the system for Athens

According to the outdoor temperature was higher than 26.8 °C for about 15% of the time in Athens. In these conditions, the transcritical operation occurred for the cases where the CO_2 is used at the HP of the refrigeration system. Due to this, the power consumed for cases 1-2-4-5 are much higher comparing to reference case 3.

Table 8.10 shows the comparison of annual energy consumptions and the percentage difference in comparison with case 3.

Table 8.10 Annual energy consumptions (Athens)

1	2	3	4	5	6	7	8
Annual energy consumptions MWh							
672.99	639.13	596.58	684.14	648.80	633.80	623.57	611.21
Percentage Difference %							
+12.03	+6.88	-	+14.06	+8.38	+6.03	+4.42	+2.42

Case 8 where the HC is used for the HP circuit shows the closest value to the reference case 3. In additional, all the cascade systems for case 6-7-8 found to be close to reference case 3 due to the lower pressure ratios comparing to the systems where R744 used in HP circuit.

Comparing cases 1-2 and 4-5 we can notice a very high energy reduction due to the additional bypass compressor which compressed with lower pressure ratio and higher isentropic efficiency from the intermediate pressure level to the high pressure level of the investigated systems.

Table 8.11 illustrates the annually running cost (electricity only) for the investigated cases. The values were calculated based on average electricity price of £0.156 per kWh (Helppost, 2016 - 1EUR = 0.86 GBP) of electricity in Athens area.

The values below in Table 8.11 included only the cost of annual electricity and not any service-maintenance cost of the investigated systems. In terms of maintenance the cascade systems in case 3-4-5-6-7-8 shows higher cost due to the complexity of the system.

Table 8.11 Annually running cost (electricity only) for Athens

1	2	3	4	5	6	7	8
Electricity Cost (£)							
104,987	99,067	93,067	106,726	101,214	98,862	97,278	95,349

Comparison between London and Athens

Figure 8.16 shows the power consumption for the eight investigated cases for London and Athens. It is clear that Athens showed much higher power consumption due to the ambient temperature as discussed above.

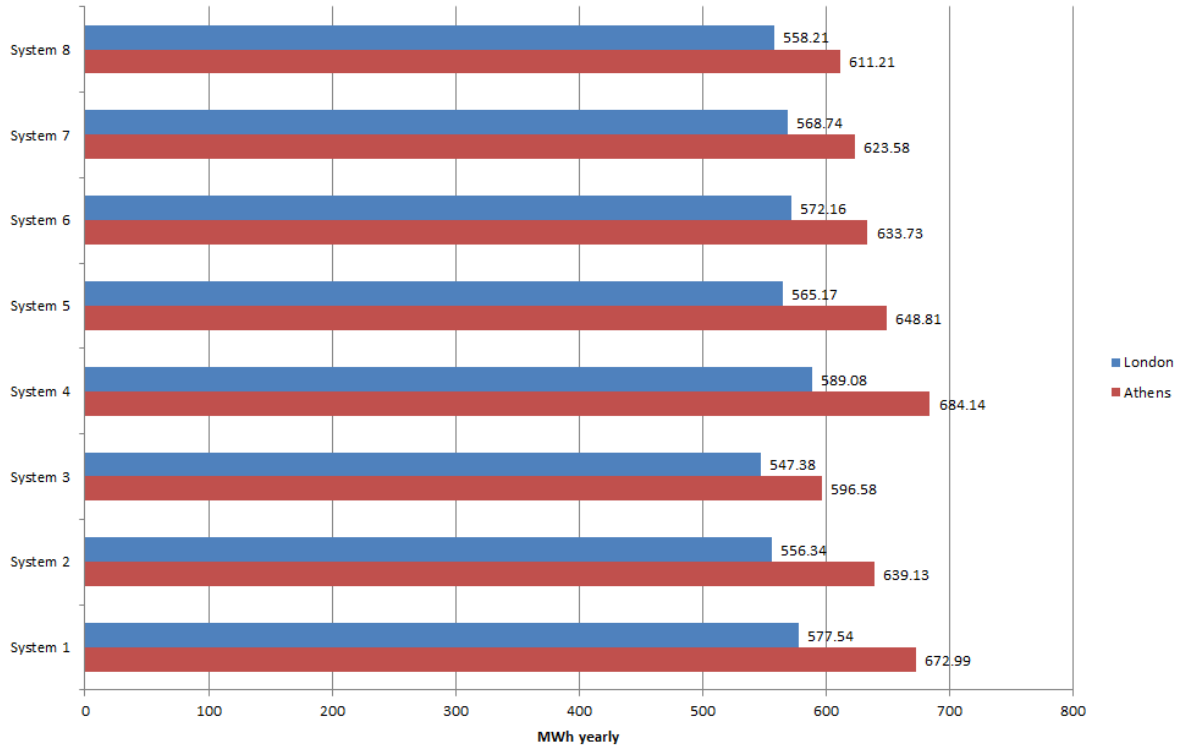

Figure 8.16 Electrical power consumption for the eight investigated cases for London and Athens

8.10. TEWI COMPARISON AMONG THE INVESTIGATED CASES

London

The values of TEWI of the investigated cases are illustrated in Fig. 8.17. The assumptions made for annual leakage and other values used to calculate the direct and indirect emissions are presented in Chapter 8.7.

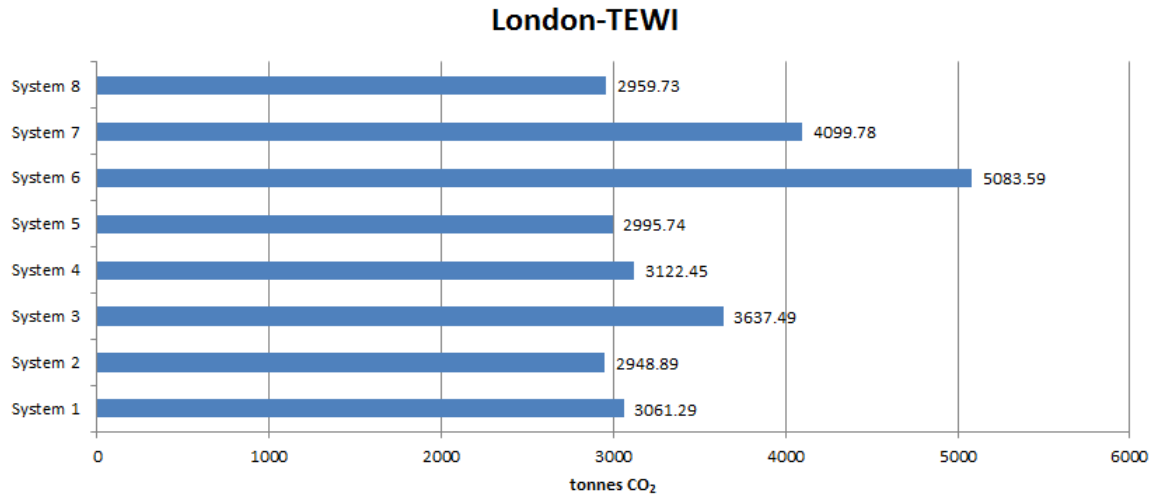

Figure 8.17 TEWI for London based on the eight on the investigated cases

The higher value it is found to be for case 6 where R404A is used in HP circuit of the system. The GWP number of R404A refrigerant is much higher compared with the other refrigerant solutions. Table 8.12 shows the percentage difference in terms of TEWI comparing with the reference case 3.

Table 8.12 Percentage difference in terms of TEWI for London

1	2	3	4	5	6	7	8
Percentage Difference %							
-17	-20	-	-15	-19	+33	+11	-20

The lowest TEWI achieved in case 8 where HC is used in HP side. However, the values of case 8 are really similar comparing to 2 and 5 where all CO_2 application is applied. The direct emissions for cases 1-2-4-5 are negligible but on the other hand the much higher indirect emissions due to the power consumptions are balanced the values.

Case 6 and 7 are the only two solutions which showed much higher TEWI values due to the higher GWP for the given refrigerants.

Comparing cases 1-2 and 4-5 the TEWI values are significantly reduced due to the less power consumption lead to lower indirect TEWI emissions. This power consumption reduction is proportional of the installation of the bypass compressor as discussed above.

Athens

The values of TEWI of the investigated cases are illustrated in Fig. 8.18 for the case of Athens. More information can be found in Chapter 8.7.

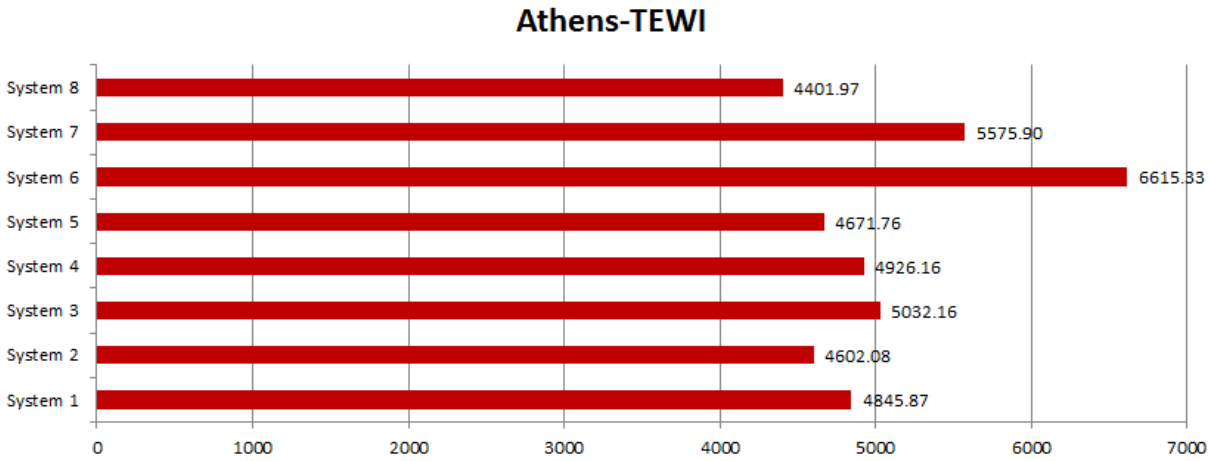

Figure 8.18 TEWI for Athens based on the eight on the investigated cases

For case of Athens the TEWI emissions comparing cases 1-4 with the reference case 3 are much closer due the very high power consumption of the system. The direct emissions are negligible but with much higher power consumptions values the results are close.

Table 8.13 shows the percentage difference in terms of TEWI comparing with the reference case 3 for case of Athens.

Table 8.13 Percentage difference in terms of TEWI for Athens

1	2	3	4	5	6	7	8
Percentage Difference %							
-3	-9	-	-2	-7	+27	+10	-13

The lower TEWI value found to be for case 8 where the HC is operates in HP circuit. Also, the GWP of HC is 3 and very lower comparing to HFCs. Figure 8.19 shows the difference between direct and direct emissions for the eight investigated cases in Athens.

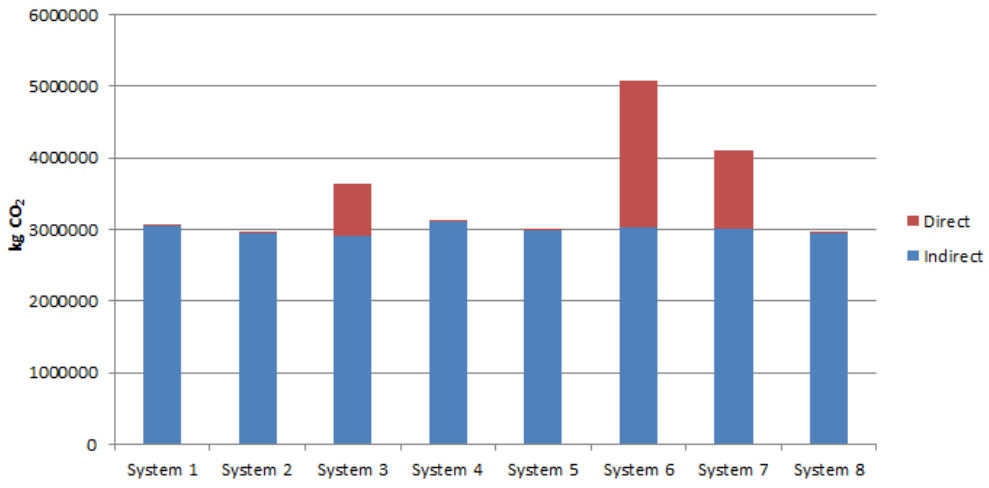

Figure 8.19 Direct and Indirect emissions for Athens

It is clear from the graph that the systems use a natural refrigerant such as R744 and R290 in HP circuit have negligible direct emissions. On the other hand those systems showing slightly higher power consumption. Figure 8.19 has similar trends for both of investigated locations of London and Athens. The direct emissions due to refrigerant leakage are similar for both investigated climate cases.

Comparison between London and Athens

Figure 8.20 shows the TEWI values for the eight investigated cases for London and Athens Due to the higher outdoor temperatures in Athens the power consumption from the refrigeration systems are increase dramatically. The pressure ratio is become higher and the isentropic efficiency of the compressor decreases. Due to this the power consumption and indirect TEWI emissions are higher for the case of Athens.

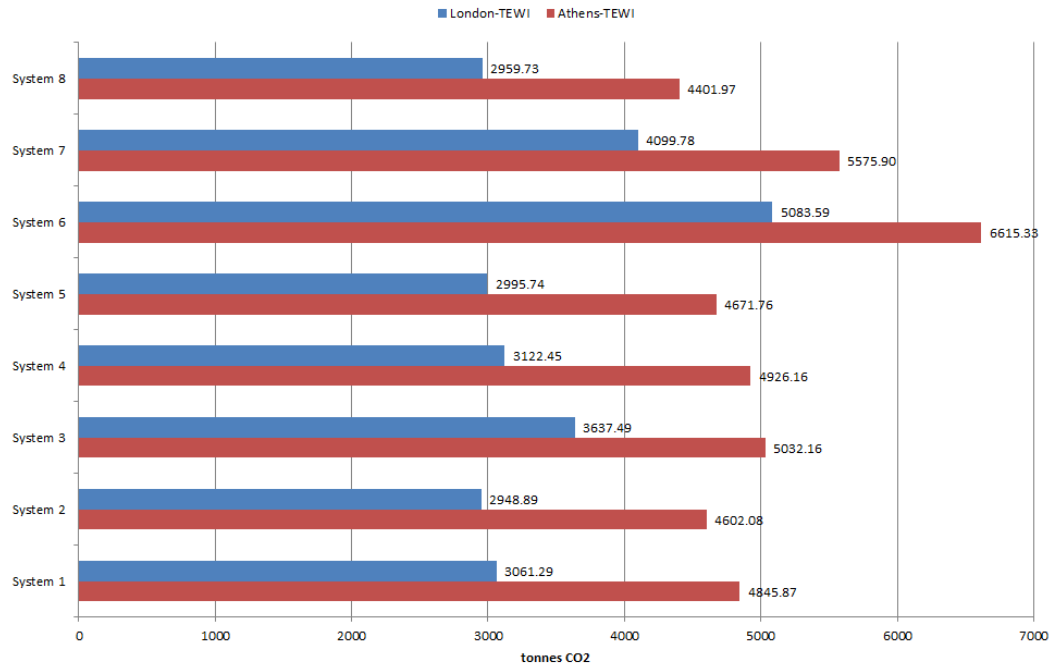

Figure 8.20 TEWI values for London and Athens

8.11. SUMMARY

In this chapter, comparative studies among eight different commercial refrigeration cases for supermarket installation have been performed. The comparative study based on the energy and environmental analyses of the eight investigated cases. The models of a typical European large supermarket represented by a MT and LT load of 100 kW and 30 kW respectively.

The evaluation has been based on the weather data files for London (Heathrow), UK and Athens, Greece. Those two cities were taken into account a warm and cold outdoor temperatures and the effect on the power consumption has been discussed.

Furthermore, the control strategies for case 1-2-4-5 where R744 is used in HP circuit were derived from the experimental results. Pressure and temperature correlations at the C/GC refrigerant outlet have been derived from the experimental results for the subcritical, transition and transcritical system operation. Those have been compared with literature data.

The eight investigated cases have been compared in terms of investment cost based on the system design, complexity, refrigerant price and component price. In additional, the safety aspects for each case have been discussed also.

Finally, cases 2 and 4 are improved all-CO_2 systems from already existing solutions. The additional benefit associated with the adoption of the bypass compressor has been described clearly above. This leads to lower power consumption of the system and lower indirect TEWI where the R744 systems are suffer comparing the HFCs. Cases 2-4-8 based on natural refrigerant solutions. Those are closest to the reference case 3 in terms of power consumption and the final values have nearly neglected difference in terms of power consumption and annual electricity cost. On the other hand cases 2-4-8 have much lower TEWI values compared with case 3. In terms of safety case 8 suffer due to the high flammability. Accelerated tax relief schemes for investments in climate-friendly and energy efficient technologies are available in UK. That makes case 2 and 4 very promising solution for new installation across the Europe.

9. CONCLUSIONS & RECOMMENDATIONS FOR FUTURE WORK

Refrigeration technology is an essential utility used in the food retail sector to ensure proper merchandising and safety of the food products by enabling the long-term storage for frozen foods and short-term storage for chilled foods. Two temperature levels are required in the food retail sector for frozen and chilled products -18°C to -35°C for frozen and -1°C to 7°C for chilled. Due to the huge amount of the refrigerant fluids used to cover the needs of food storage, the vapour compression refrigeration systems are responsible for a large amount of GHG emissions to the environment. The GHG emissions from refrigeration systems can be split into two main categories: direct and indirect emissions. The direct emissions are created by leakage of refrigerant with high GWP such as fluorocarbons including the HFC's. On the other hand, the indirect emissions produced from the energy required to operate the refrigeration systems.

The natural refrigerant CO_2 has been demonstrated to be a promising substitute in refrigeration systems for conventional HFC refrigerants such as R404A. The CO_2 solution into a supermarket application can significantly reduce the environmental direct impacts due to low GWP value. In additional, indirect emissions can be reduced from additional system arrangements and control strategies which allow the system to operate with lower energy consumption comparing to convectional CO_2 systems.

The research work involved the investigation and development of CO_2 refrigeration technologies for food retail refrigeration applications, which contributes to the overall aim of reducing this environmental impact by investigating the practicality, economic viability and environmental benefits achievable from the application of natural refrigerant CO_2, to large supermarket refrigeration systems.

The work can be detailed as follows:

- An extensive literature review of CO_2 refrigerant and comparisons with a number of other refrigerants based on the thermophysical properties. Refrigerant price and safety classification are presented also.
- The different types and designs of CO_2 refrigeration systems which fall into three categories: indirect, cascade and all-CO_2 transcritical systems have been discussed and presented clearly in terms of system components and operations. New system novelties which can be used to increase system performance and reduce power consumption have been discussed as well.

- The design and construction of CO_2 booster refrigeration test facility including high, intermediate and medium pressure levels.
- Design and build a condenser/gas cooler test rig in order to further examine the performance of CO_2 air cooled heat exchangers with different sizes and operating conditions and its integration with the booster CO_2 refrigeration system. Consequently, the condenser/gas cooler air on parameters, temperature and flow rate, can be well controlled to specified values.
- Experimental investigation based on controlling parameters in the high pressure level of the system.
- Computer simulation model for the existing CO_2 refrigeration system. Model validation against the experimental results and further system analysis based on the control parameters such a pressure and evaporation temperatures.
- Experimental investigations to determine the performance of different gas cooler coils over a range of sub-critical and transcritical operating conditions including a range of air flow velocities and refrigerant mass flow rates.
- Investigation of the effects of the different condenser/gas coolers designs and sizes on the overall system COP.
- Detailed modelling on the gas cooler performance for different deigns and sizes and its integration with the existing CO_2 model.
- Evaluation of the energy performance, environmental impacts and economic viability for eight different system cases for supermarket applications based on two different climate conditions of London and Athens. The control strategies for the systems use CO_2 refrigerant in high pressure circuit were derived from the experimental tests.
- Three out of the eight system arrangements are proposed systems. Two of these are improved systems comparing with the convectional booster system and CO_2 to CO_2 cascade with gas bypass. The third system is a natural refrigerant arrangement with HC feed the MT load and CO_2 the LT load.

9.1.CONCLUSIONS

1.

The choice of a suitable refrigerant in supermarket applications should be taking into consideration a number of factors which are divided into three main groups: practical – environmental – financial. The first group include the performance and energy efficiency of the individual systems based on the thermodynamic and heat transfer properties of the refrigerant used. The second group including the physical, chemical and physiological properties of the refrigerant which is describe the environmental impact of the refrigerant. System design, operation and maintenance cost are describing from the financial point of view. One approaching gaining the last two decades is the use of natural refrigerants such as ammonia, HC and carbon dioxide. The high toxicity of the ammonia and the size restrictions of the HC systems create the carbon dioxide as a strong competitor for the centralized supermarket systems. The unique thermos-physical properties of CO_2 lead to deliver higher rates of evaporative heat transfer as a proportional of the gas/liquid density. Furthermore, the boiling heat transfer coefficient of the CO_2 is twice higher comparing with other fluorocarbons fluids. The very low viscosity increases the heat transfer without effect on the pressure losses. In the early stage of the CO_2 condenser-evaporator design, the refrigerant flow path can be extensive than other refrigerants. By using the advantage of favourable pressure-temperature relationship allows designing the system with higher mass flux values and increases the internal coefficient. In general:

- ✓ CO_2 provide good heat transfer in heat exchangers and allows the selection of smaller system components comparing with HFCs.
- ✓ The pressure ratio and suction-gas specific volume of the CO_2 systems are lower comparing with HFCs. This allows the designer to choose smaller size compressors and suction pipe diameters for the same given conditions.
- ✓ The selection of the smaller system components and pipe diameters lead to a significant reduction in the refrigerant charge per required load comparing to HFCs.

2.

CO_2 refrigeration applications have also disadvantages comparing to the convectional HFCs systems. As a main disadvantage of a CO_2 refrigeration system can be defined the much higher operating pressure. This can be overcome by using smaller and stronger components to withstand with higher pressures. The available components on the market and the controller quality have been significantly improved over the last years which allow controlling the system more efficiently and safely.

Another disadvantage of the CO_2 refrigeration system is the power consumption and cooling performance for warm climate conditions. Different system designs and solutions were presented in order to overcome this system disadvantage.

3.

The experimental test facilities were designed and built in order to facilitate the experimental programme plan for this work. Those involved a CO_2 transcritical system consists of the gas cooler/condenser, an ICMT motorized valve which act as an expansion valve of the system, ICM gas bypass valve, liquid receiver, a CO_2 accumulator and two semi-hermetic compressors. A medium temperature direct expansion open vertical multi-deck refrigerated display was used for the investigations and the tests were carried out at controlled conditions in an environmental chamber. An additional CO_2/brine load has been installed on the system in order to balance the capacity of the compressor. The system is divided into three pressure sections, high, intermedium and medium.

The main system controller enables stable control of the condenser/gas cooler pressure, compressor speed, degree of sub-cooling, intermediate pressure and MT evaporating pressure and temperature.

To examine extensively the performance of CO_2 condenser/gas coolers with different sizes and operating conditions, a test unit has been purposely built. The variation of the air flow rate and air-inlet temperature can be controlled by adjustable air fan speed and air heaters respectively. The controlled air-inlet temperature enabled to simulate the

subcritical, transition and transcritical operating zones without effect from the ambient temperatures.

4.

A number of tests were carried out to investigate the performance of the condenser /gas cooler based on different designs and sizes. Three different heat exchangers were purposely built. The analysis firstly based on the performance of the air cooled heat exchanger each self under different test conditions. Heat rejection (Q), approach temperature (AT), pressure drop (ΔP) and temperature drop (ΔP) are mainly concerned for the first analysis.

The performance of the air cooled heat exchanger reduced as the air-on temperature increased. As the temperature arises the heat transfer rate in the coil is reduced due to the fact that the thermophysical properties such as density, viscosity and specific heat became dependent with the temperature and pressure of the fluid. The pressure drop of the CO_2 refrigerant found to be reduced with increasing condenser/gas cooler pressure due to density reduction. In additional, the pressure drop found to be affected by the mass flow rate of the refrigerant and pipe length.

The test results show that the system discharge pressure is controlled at an optimal value based on the gas cooler outlet temperature when the system is in transcritical cycle and specified subcooling when it is in subcritical cycle. Considering the close relationship between the gas cooler/condenser air-on and the heat exchanger exit CO_2 temperatures, the measured discharge pressure increases almost linearly with the air-on temperature. Subsequently, the system discharge pressure control can function alongside the air-on temperature. The switching point from a subcritical to transcritical operation is at 26.8 °C and 72.77 Bar.

5.

The second stage analyses of the experimental test results are taking into account the effect of the condenser /gas cooler design and sizes on the system COP. The three different air cooled heat exchangers were tested based on the same conditions and the

cooling performance of the system was calculated based on the outlet refrigerant conditions.

The higher air-on temperature found to increase the compression pressure ratio and decrease the compressor isentropic efficiency, thus leading to higher compressor power consumption.

This lead to lower COP values for higher ambient conditions and when the system runs in transcritical operation.

When a larger size gas cooler/condenser is utilised in the system, at a constant air-on temperature, the controlled discharge pressure will be reduced due to the smaller approach temperature or lower CO_2 temperature at the heat exchanger exit. The approach temperatures at the gas cooler outlet are influenced by the air-on temperature, gas cooler fan speed, compressor controller and ICMT motorized valve opening.

For the higher air-on temperatures, the approach temperature founds to drops dramatically. Moreover, the approach temperature for 70% of the main fan speed (2800l/s) is smaller compared to the 60% fan speed (2400 l/s) due to an enhanced air side heat transfer. Therefore, the heat exchanger outlet temperature or approach temperature can be controlled by modulating the heat exchanger fan speed or air flow rate.

However, the approach temperature may be reduced and controlled by increasing the heat exchanger air flow rate or fan speed, although in such scenarios the fan power consumption and air side pressure drop will simultaneously increase. An increased fan power consumption could conversely affect the overall system COP such that an optimal fan speed could be designed and selected.

The cooling capacity is higher for the 3-row gas cooler/condenser due to its lower approach temperature at the gas cooler/condenser outlet while the compressor power consumption is slightly reduced for the system with a larger gas cooler/condenser. This leads to a higher COP for the 3-row CO_2 coil system and different fan speeds. In addition, the COP for both circumstances decreases at higher air-on temperatures. A higher COP was found at the 60% main fan speed, corresponding to 2400 l/s of air passing through the coil, and contributes to the lower power consumption of the fan when compared to 70% of fixed fan speed.

6.

Engineering Equations Solver (EES) modelling was employed to investigate the overall system performance for the initial system design without take into consideration a different coil designs and fan speed. A simple thermodynamic equations based on the refrigerant to air approach temperature were used for the condenser/gas cooler operations. The model was validated against the initial experimental results by using the three row heat exchanger. The validated model was used to explore the effect of intermediate pressures and evaporating temperatures on the overall system COP.

The COP of the given refrigeration system found be reduced with higher intermediate pressures at the liquid receiver. This is a proportional of the enthalpy entering to the expansions valve for both MT and AL loads.

Also, the COP found to be reduced with higher evaporating temperature due to the refrigeration effect at the inlet to evaporator and superheat degree at the outlet of the evaporator coil. The evaporating temperature range was specified by the product temperature at the MT display cabinet which were monitored during the experimental tests.

7.

A detailed EES model based on the gas cooler operation was employed to investigate the effect of the pipe arrangement and coil size under various air flow rates and air-inlet conditions. The detailed models created based on the gas cooler sizes and designs which previously have been investigated. Due to the limitation of the EES (12,000 simultaneous non-linear equations), the gas cooler was modelled by divided each circuit in 16 segments.

The maximum difference for the temperature variation across the gas cooler was found to be 2.2 °C which considered acceptable considering the uncertainty of the experimental results.

The validated gas cooler model was used to integrate with the initial CO_2 system model in order to investigate and validate the experimental results based on the COP for

different coil design and control parameters. The maximum difference was found to be 14% with mean difference of 7% which considered acceptable considering the model complexity and experimental results uncertainty.

8.

Eight different combinations of system technologies and refrigerants which are referred as "cases" were presented and discussed. These include two CO_2 transcritical systems, two cascade systems which both high pressure (HP) and low pressure (LP) are supplied by CO_2, three cascade systems which the HP side feed by HFC refrigerant and the LP side by CO_2 and one system where the HP side is supplied by hydrocarbon (HC) refrigerant and the low side by CO_2.

The models were used to calculate the energy and environmental performance of the investigated cases under two different climate conditions for London and Athens. The investment cost is also briefly discussed.

Models of the proposed eight solutions were implemented in EES software, which were based on the fundamental thermodynamic equations at steady state conditions.

Cases 1 and 2 are referred to a convectional CO_2 booster system with gas bypass and an improved CO_2 booster system with gas bypass compressor solution respectively. Case 2 shows on average 13% higher COP comparing with convectional booster system due to the power consumption reduction by using an additional compressor on the bypass side. The bypass compressor shows 3.5% to 7.5% higher isentropic efficiency due the lower pressure ratio across the compressor.

Cases 4 and 5 are referred to a convectional CO_2 cascade system with gas bypass and an improved CO_2 cascade system with gas bypass compressor respectively. The system for case 5 shows 1.3% to 9.1% COP improvement for ambient conditions of 0 °C and 40 °C. This is due to the power consumption reduction due the higher efficiency of the bypass compressor applied in case 5.

The control strategies for cased 1-2-4-5 where the CO_2 is used to operate in high pressure circuit were derived from the experimental results. These included the pressure and temperature of the refrigerant outlet from the condenser/gas cooler.

All the investigated cases where compared with the cascade solution of case 3 in terms of COP, annual power consumption and TEWI. In terms of annual power consumption for case of London, cases 2-4-8 shows very similar values with the reference case. For the ambient conditions of Athens, case 8 shows very similar annual consumption to the reference case 3. Furthermore, case 2 and 5 shows great improvement comparing to the convectional systems 1 and 4.

For case of London cases 1-2-4-5-8 shows much lower TEWI values comparing to reference case 3 due to the lower GWP of the CO_2 and HC. For case 2 and 8 the TEWI was reduced for 20% comparing to case 3.

For case of Athens the TEWI values are closest to the reference case due to the high power consumption of the natural refrigerant systems. For case 2 and 8 the TEWI reduced 9% and 13% respectively compared to case 3.

9.2. RECCOMENDATIONS FOR FUTURE WORK

Due to time limitations, the modifications on the existing CO_2 refrigeration test rig were limited. Additional modifications such the installation of IHX, parallel bypass compressor and sub-cooler solution at the outlet of condenser/gas cooler will be useful in providing a wider range of experimental data which can be used to validate a new developed model. It is therefore recommended further tests by modifying the test facility in order to explore different system techniques and the effects on the system COP.

It will be useful for further investigation the use of water cooled condenser which will be replace the existing air cooled condenser/gas cooler. The comparison between water and air cooled heat exchanger will provide a more clear idea for heat exchangers design and size. In case of a real supermarket application the use of water cooled condenser can be minimize the overall size and noise from the fans. On the other hand, the initial investment cost will be much higher because the additional water system to cool down the hot refrigerant inlet to condenser. The payback period can be reduced by using this water for use inside the supermarket. In such a case, the CO_2 system will work in subcritical cycle all the time which means higher COP and reasonable power consumption compared with the HFCs system.

It is important to investigate different system solutions by enable a heat recovery solution. The high temperature of the CO_2 transcritical system and the favourable heat rejection characteristics of the CO_2 refrigerant can be used efficiently when hot water required for sanitary or space heating purposes. Also, the cooling produced after the ICMT valve and inside the liquid receiver due to the pressure drop can be used for cold water capture for space cooling purposes. Again in this case, the capital cost it will be higher comparing to the convectional system but the payback period must be carefully calculated.

A data collection based on cooling performance of the system and annual power consumption from different supermarket system solutions will provide a better and clear idea how the system perform. Data from real supermarket fields will be used to validate model and explore different system potentials. The effect of the outdoor conditions on the system power consumption and cooling performance can be clearly identified.

Over the last five years, more and more companies/manufactures are getting involved with CO_2 components and control systems research and development. The interest for CO_2 systems has extremely extensive the range of the CO_2 products and prices. Therefore, the CO_2 systems are not considered as expensive solutions comparing to convectional HFCs. A proper cost breakdown analysis will help to identify the difference between CO_2 systems and HFCs in terms of initial investment and payback period. This cost analysis will help the clients to choose the best option based on their requirements.

The cascade R290/CO_2 system shows really promising results comparing to reference case of R134A/CO_2. Due to the high flammability risk of R290, safety aspects should be taken into account. Those must be specified the pipeline construction inside the sales area and customer safety in case of system failure or pipe burst. Additional safety methods must be clearly specified.

References

Arthur, B. (2011) Marks and Spencer's PLAN A and experience with alternative refrigerants, Atmosphere Europe 2011 Conference Brussels. Available at: http://www.atmo.org/media.presentation.php?id=82 (accessed: 28/10/15)

ASHRAE 15, 2013. Safety Standards For Refrigeration Systems. www.ashrae.org ISSN 1041-2336

ASHRAE Standard 34, 2007, Designation and Safety Classification of Refrigerants, ISSN 1041-2336.

ASHRAE, 2010, ASHRAE Refrigeration Handbook, ISBN 978-1-933742-82-3, Atlanta, www.ashrae.org

ASHRAE, 2014. Refrigeration Handbook. ISBN 978-1-936504-72-5, Atlanta, www.ashrae.org

Bansal P., 2012. A review – Status of CO_2 as a low temperature refrigerant: Fundamental and R&D opportunities. Applied Thermal Engineering 41 18-29

Bergam T., Lavine A., Incopera F. and Dewitt, (2002). Fundamentals of Heat and Mass Transfer 7th Edition. John Wiley and Sons, New York, 2002

Better Buildings, 2015. Case Study: Transcritical Carbon Dioxide Supermarket Refrigeration Systems. Prepared for Office of Energy Efficiency and Renewable Energy U.S. Department of Energy

BITZER software 2016, version 6.5.0.1610. Available from: https://www.bitzer.de/websoftware/ (accessed: 10/08/16)

Bobbo, S., M. Scattolini, R. Camporese, L. Fedele. 2006, Solubility of CO_2 in some commercial POE oil. Proceedings of 7th IIR Conference

BRA (2006) Guideline Methods of Calculating TEWI, Issue 2. British Refrigeration Association, Reading, Berks, UK, 36 pgs.

BS EN 287-1:2011, Qualification test of welders. Fusion welding. Steels.

BS EN 378-1:2008+A2:2012, Refrigerating systems and heat pumps — Safety and environmental requirements, Part 1: Basic requirements, definitions, classification and selection criteria, ISBN 978 0 580 76022 8

Campbell, 2007. Carbon Dioxide for Supermarkets. The institute of refrigeration. Available from: www.ior.org.uk 11 pgs.

Campbell, A., 2009. Working with CO_2 supermarkets. Available from: http:// www.atmosphere2009.com/speakers.presentations.php (Accessed 14/01/2013).

Carbon Trust (2011) Carbon Trust Conversion factors: Energy and carbon conversions 2011 update, Available at: http://www.carbontrust.com (Accessed 10/08/16).

CCA, 2008. Climate Change Act 2008 – Chapter 27 – Part 1: Carbon target and budgeting. Available from: www.legislation.gov.uk 108 pgs

CCC, 2010. The fourth carbon budget, reducing emissions through the 2020s, 376 pgs, available from: http://www.theccc.org.uk (accessed 16/11/2015).

Chang YS, Kim MS., 2007 Modelling and performance simulation of a gas cooler for CO_2 heat pump system. HVAC&R Research 2007 ; 13: 445-456.

Chen, Y., & Gu, J. (2005). The Optimum High Pressure for CO_2 Transcritical Refrigeration Systems with Internal Heat Exchangers. International Journal of Refrigeration, 28(8), 1238-1249.

Cheng, L., Ribatski, G., Moreno-Quiben, J., Thome, J.R., 2008. New prediction methods for CO_2 evaporation inside tubes: Part I - A two-phase flow pattern map and a flow pattern based phenomenological model for two-phase flow frictional pressure drops. Int. J. Heat and Mass Transfer 51, 111-124.

Conde M. Engineering, 2011. Thermo-physical properties of brines, Zurich, Switzerland, 9 pgs. Available at: http://www.mrc-eng.com/Downloads/Brine%20Properties.pdf. (Accessed: 28/10/15)

Cowan, D., Chaer, I., Maidment, G., 2010. Reducing refrigerant emissions and leakage – An overview and feedback from two EU projects. Proc. Sustainable Refrigeration and Heat Pump Conference, Stockholm, Sweden, ISBN 978-2-913149-81-6, 16 pgs.

Danfoss, 2010. Cascade HC/HFC – CO_2 system, How to control the system. Application guide. Available: www..com

Danfoss, 2010b, Transcritical CO_2 booster system. Available from www.danfoss.com/CO_2 (accessed 12/11/14)

Danfoss, 2012, 1 and 2 stage Transcritical CO_2 systems. How to control the system. Available from www.danfoss.com/CO_2 (accessed 12/11/14)

Dang, C., Iino, K., Fukuoka, K., Hihara, E., 2007. Effect of lubricating oil on cooling heat transfer of supercritical carbon dioxide. International Journal of Refrigeration 30, 724 – 731.

Dopazo A, Fernandez-Seara J, Sieres J, Uhia F., 2009, Theoretical analysis of a CO_2 - NH_3 cascade refrigeration system for cooling applications at low temperature. Applied Thermal Engineering 2009;29:1577-1573

DORIN Innovation software (2016), Available from: http://www.dorin.com/en/Software/ (accessed: 10/08/16)

EES, 2014. Engineering Equation Solver, version 9.810, www.fChart.com

EFCTC (2013). European Fluorocarbons Technical Committee EFCTC Accident Database – Last update: December 2013. Available from: www.flurocarbons.org 11 pgs. (accessed: 28/10/15)

EIA, 2014. Chilling Facts VI: Closing the door on the HFCs. Environmental Investigation Agency. Available from: www.eia-international.org 24pgs

Emerson Climate Technologies, 2010. Refrigerant Choices for Commercial Refrigeration. Finding the Right Balance. Available from: http://www.emersonclimate.com (accessed 28/10/2015).

Emerson, 2015. Commercial CO_2 Refrigeration Systems. Guide for Subcritical and Transcritical CO_2 Applications. 44 pgs. Available: http://www.emersonclimate.com (accessed 15/10/15)

EN 10216-1: 2014 Seamless steel tubes for pressure purposes. Technical delivery conditions. Non-alloy steel tubes with specified room temperature properties.

EN 10305-1: 2010 Steel tubes for precision applications. Seamless cold drawn tubes. Technical delivery conditions.

EPA, 2010, US EPA: Transitioning to low GWP alternatives in commercial refrigeration. Fact sheet, October 2010

EPEE, 2014. The new F-GAS Regulation. European Partnership for Energy and the Environment, Promoting energy efficiency and responsible refrigerant management. Published September 2014. Available on: http://www.epeeglobal.org/refrigerants/f-gas-regulation/ (accessed 16/11/15)

EU, REGULATION (EU) No 517/2014 OF THE EUROPEAN PARLIAMENT AND OF THE COUNCIL of 16 April 2014 on fluorinated greenhouse gases and repealing Regulation (EC) No 842/2006, 36 pgs.

Finckh O, Schrey R and Wozny M. 2011, Energy and efficiency comparison between standardized HFC and CO_2 transcritical systems for supermarket applications. 23rd Int. Congr. of Refrig., Prague

Funder-Kristensen, T., Wilkins, R., Vonsild, A. L. (2012). New Components for Natural Refrigerants.Proceedings, 10th IIR Gustav Lorentzen Conference, Delft. The Netherlands.

Ge Y.T., S.A. Tassou, 2009. Control optimisation of CO_2 cycles for medium temperature retail food refrigeration systems, International Journal of Refrigeration 32 1376-1388

Ge Y.T., S.A. Tassou, 2011. Thermodynamic analysis of transcritical CO_2 booster refrigeration systems in supermarket, Energy Conversion and Management 52 1868-1875

Ge Y.T., Tassou S.A., Santosa ID. and Tsamos K.M. (2015). Design optimisation of CO_2 gas cooler/condenser in a refrigeration system. Applied Energy 160, 973-981

Ge, Y.T, and Tassou, S.A., 2011b. Performance evaluation and optimal design of supermarket refrigeration systems with supermarket model “SuperSim”. Part II: Model applications. International Journal of Refrigeration 34,540-549

GEA BOCK Compressors 2009, Product information (12 pages), Available from: http://www.bock.de/en/home.html, (accessed 03/04/2014) - Online published on: 09/06/2009

Girotto S. 2007, Carbon dioxide in supermarket refrigeration, Pres. at CO_2 Food – climate friendly refrigeration in supermarkets, Berlin

Girotto, S., Minetto, S. and Neksa, P. (2004). Commercial refrigeration system using CO_2 as the refrigerant. International Journal of Refrigeration, 27. 717-723.

Girotto, S., Minetto, S., & Nåksa, P. 2003. Commercial Refrigeration System with CO_2 as Refrigerant Experimental Results. Paper presented at the 21st IIR International Congress of Refrigeration, Washington, D.C., USA.

Gnielinski V. (1976). New equation for heat and mass transfer in turbulent pipe and channel flow. Int. Chemical Enginnering 16, 359-68

GTZ Proklima, 2008. Natural refrigerants. GTZ GmbH, Eschborn, Germany, 208 pgs.

Gullo P., Elmegaard B., Cortella G., 2016. Energy and performance assessment of R744 booster supermarket refrigeration systems operating in warm climates. International Journal of Refrigeration 64, 61 - 79

Hafner, A. , Neska, P. , 2014. System configurations for supermarkets in warm climates applying R-744 refrigeration technologies. Case studies for selected cities. International Special Issue 2014 - United Nations Environment Programme, International Institute of Refrigeration, Centro Studi Galileo, Associazione dei Tecnici del Freddo, European Energy Centre, Casale M.to, Italy.

Harbel J.S. and Abbas M., 1998. Development of graphical indices for viewing building energy data: Part 1. Journal Solar Energy Engineering 120, 156 - 161

Helppost, 2016 Available on: http://www.helppost.gr/dei/ypologismos-reuma-katanalosi/ (accessed: 16/08/2016)

Hinde D, Zha S, Lan L., 2009, Carbon dioxide in North American supermarket. ASHRAE journal 2009; 18-24.

Hu B., Li Y., Cao F., Xing Z., 2015. Extremum seeking control of COP optimization for air-source transcritical CO_2 heat pump water heater system. Applied Energy 147 , 361–372.

Hwang Y, Jin DDH, Radermacher R, Hutchins JW., 2005 Performance measurement of CO_2 heat exchangers. ASHRAE Transactions 2005; 306–316.

Incropera F.P., DeWitt D.P., Introduction to Heat Transfer, third edition, John Wiley and Sons, New York, 1996

International Energy Agency, 2015. CO_2 Emissions from fuels combustion highlights. 152 pgs. Available from: https://www.iea.org (Accessed: 10/08/2016).

IOR, 2009. Environmental, cost and legal aspects of refrigerant leakage, Refrigerant Emissions and Leakage ZERO Project. Available on http://www.REAL Zero.org.uk/

IOR-BRA-CT, 2010. Refrigeration Road Map. 58 pgs. Available on: www.carbontrust.co.uk, (accessed 10/10/2013).

IPCC, 2007. Fourth Assessment Report, Climate Change. Available on: http://www.ipcc.ch/pdf/assessment-report/ar4/syr/ar4_syr_cover.pdf (accessed: 08/08/2016)

ISO 5149 , 2013. Refrigerating Systems and heat pumps – Safety and environmental requirements. Part 2: Design, construction, testing, marking and documentation. ISO/FDIS 5149-2

ISO, 2012. Refrigerated Display cabinets. Part 2: Classification, requirements and test conditions. BS EN ISO 23953-2:2005+A1:2012. 96 pgs

ISO, 2012. Refrigerated Display cabinets. Part 2: Classification, requirements and test conditions. BS EN ISO 23953-2:2015. 100 pgs

Kauf, F. (1998). Determination of the Optimum High Pressure for Transcritical CO_2-Refrigeration Cycles. International Journal of Thermal Science, 38(4), 325-330.

Kim M.H., Pettersen J., Bullard C.W., 2004, Fundamental process and system design issues in CO_2 vapour compression systems. Progress in Energy and Combustion Science 30 119–174

Lee TS, Liu CH, Chen TW. Thermodynamic analysis of optimal condensing temperature of cascade refrigeration systems. International Journal of Refrigeration 2006; 29 : 1100-1108

Lee TS, Liu CH, Chen TW., 2006, Thermodynamic analysis of optimal condensing temperature of cascade refrigeration systems. International Journal of Refrigeration 2006; 29: 1100-1108

Leslie, N., Sweetser, R., Zimron, O. and Stovall, T., 2009. "Recovered Energy Generation Using an Organic Rankine Cycle System" ASHRAE Transactions Vol. 115 Part 1, Atlanta

Liao S. , Zhao T. , 2002. Measurements of heat transfer coefficients from supercritical carbon dioxide flowing in horizontal mini/meso channels. J. Heat Transfer. 124: 413-20

Lorentzen G., 1993. Revival of carbon dioxide as a refrigerant. International Journal of Refrigeration. 17(7):292-301

Ma Y., Liu Z., Tian H., 2013. A review of transcritical carbon dioxide heat pump ands refrigeration cycle. Energy 55, 156-172

Madsen, 2010. Transcritical CO_2 Refrigeration with heat reclaim. Available from: www.danfoss.com 10 pgs.

MarketandMarket, 2015. Transcritical CO_2 Market – Global Forecast to 2020. Available from: www.marketsandmarkets.com (accessed 06/11/15). Publish date: September 2015. Main report brochure. 26 pgs.

Messineo Antonio, 2012. R744-R717 Cascade Refrigeration System: Performance Evaluation compared with a HFC Two-Stage System. Energy Procedia 14, 56-65

Mikhailov, A. 2011, CO_2 Secondary Coolant Systems: Energy Efficiency and Control Strategies Considerations, presented at the 23rd IIR International Congress of Refrigeration, Prague, Czech Republic.

Milnes, J. (2011) Tesco suffers second CO_2 blast. Available at: http://www.racplus.com/news/tesco-suffers-second-CO_2-blast/8609639.article (accessed: 10/02/15)

Ming Ma, Jianlin Yu, Xiao Wang (2014). Performance evaluation and optimal configuration analysis of a CO_2/NH_3 cascade refrigeration system with falling film evaporator–condenser. Energy Conversion and Management 79, 224–231

Moreno-Quiben, J., and Thome, J.R., 2007a. Flow pattern based two-phase frictional pressure drop model for horizontal tubes: Part I - Diabatic and adiabatic experimental study. Int. J. Heat and Fluid Flow 28, 1049-1059

Moreno-Quiben, J., and Thome, J.R., 2007b. Flow pattern based two-phase frictional pressure drop model for horizontal tubes: Part II - New phenomenological model. Int. J. Heat and Fluid Flow 28, 1060-1072.

MTP, 2008. BNCR36: Direct emission of refrigerant gases. Market Transformation Programme, available from: http://efficient-products.defra.gov.uk/cms/productstrategies/ subsector/commercial-refrigeration (accessed 05/12/2012).

NAO, 2007. The climate change levy and climate change agreements. National Audit Office. Available from: www.nao.org.uk 48 pgs

Navarro, E., Granryd, E., Urchueguia, J.F., Corberan, J.M., 2007. A phenomenological model for analyzing reciprocating compressors. Int. J. Refrigeration 30, 1254-1265.

Nekså P, Rekstad H, Zakeri GR and Schiefloe PA. 1998, CO_2–heat pump water heater: characteristics, system design and experimental results, Int. J. Refrig.,Vol. 21, n°3, pp. 172-179

Nekså P, Walnum H and Hafner A. 2010, CO_2-a refrigerant from the past with prospects of being one of the main refrigerants in the future, Proc IIR 9th Gustav Lorentzen Conf, Sydney

Pearson, 2014. CO_2 as a Refrigerant, International Institute of Refrigeration. ISBN: 978-2-36215-006-7. 126 pgs.

Pettersen J. , 2004. Flow vaporization of CO_2 in microchannel tubes. Experimental Thermal and Science, Volume 28, Issue 2-3, Pages 111 - 121

Pettersen J. 2002, Refrigerant R-744 fundamentals. VDA Alternate Refrigerant Winter Meeting, Saalfelden, Austria.

Petukhov, B. S., in T. F. Irvine and J. P. Hartnett, Eds., Advances in Heat Transfer, Vol. 6, Academic Press, New York, 1970.

Pitla S.S., Groll E.A. and Ramadhyani S., (2002). International Journal of Refrigeration 25, 887-895

Rezayan Omid, Ali Behbahaninia, 2011. Thermoeconomic optimization and exergy analysis of CO_2/NH_3 cascade refrigeration systems. Energy 36, 885-895

Rhiemeier, J.M., Harnisch, J., Ters, C., Kauffeld, M., Leisewitz, A., 2009. Comparative assessment of the climate relevance of supermarket refrigeration systems and equipment. Federal Environment Agency, 270 pgs, available from: www.umweltbundesamt.de.

Rogstam J., Tamilarasan L., and Sawalha S. (2010). "Field Measurement and Comparison of Supermarket Refrigeration Systems". IIR Sustainable Refrigeration and Heat Pump Conference, Stockholm, Sweden.

Rohatgi, N.D. 2010, Stability of candidate lubricants for CO_2 refrigeration. ASHRAE Research Project RP-1409

Rolfsmann L. 1999, Plant design considerations for cascade systems using CO_2, 20th Int. Congr. of Refrig., IIR, Sydney

Sanz-Kock C., Rodrigo Llopis, Daniel Sanchez, Ramon Cabello, Enrique Torrella, (2014), Experimental evaluation of a R134a/CO_2 cascade refrigeration plant, Applied Thermal Engineering 73 41-50

Sarkar J. and Agrawal N., 2010. Performance optimization of transcritical CO_2 cycle with parallel compression economization. International Journal of Thermal Sciences 49, 838 - 843

Sarkar J., Bhattacharyya S., Gopal R.M., 2004. Optimization of a transcritical CO_2 heat pump cycle for simultaneous cooling and heating applications. International Journal of Refrigeration 27,830-838.

Sawalha, S. (2008) 'Theoretical evaluation of trans-critical CO_2 systems in supermarket refrigeration. Part I: Modelling, simulation and optimization of two system solutions', International Journal of Refrigeration, 31 (3) pp. 516-524.

Sawalha, S. (2012). Investigation of heat recovery in CO_2 transcritical solution for supermarket refrigeration. International journal of refrigeration 36 (1), 145-156.

Schmidt Th. E. (1949), Heat Transfer Calculations for Extended Surfaces. Refrig. Eng., pp. 351-357

Shah R. K., and Sekulic D. P. (2003). Fundamentals of heat exchanger design. John Wiley and Sons (New Jersey – 2003)

Shah R., Sekulic D., 2003, Fundamentals of heat exchanger design. ISBN 0-471-32171-0

Shecco, 2013, New GUIDE on NH_3/CO_2 Secondary Refrigeration Systems. Published: 21/02/2013. Available on: www.shecco.com/articles. (accessed 28/10/15)

Shecco, 2014. Guide 2014: Natural Refrigerants continued growth & innovation in Europe. Available from: www.shecco.com 195 pgs.

Shilliday J.A., 2012. Investigation and optimisation of commercial refrigeration cycles using the natural refrigerant CO_2. PhD Thesis – Brunel University, Available from: http://bura.brunel.ac.uk/handle/2438/7454 (Accessed: 10/10/2013).

Silva, A., Almeida, E. and Bandarra Filho, E.P. (2010) "Energy Efficiency Comparison of the CO_2 Cascade and the R404A and R22 Conventional System for Supermarkets", 9th IIR Gustav Lorentzen Conference 2010, Sydney, Australia

Singh S., Purohit N. and Dasgusta M.S., 2016. Comparative study of cycle modification strategies for transcritical CO_2 refrigeration cycle for warm climates. Case Studies in Thermal Engineering 7, 78 – 91

SKM Enviros - Sinclair Knight Merz, 2011, Examination of the Global Warming Potential of Refrigeration in the Food Chain, 65 pgs.

Son CH, Park SJ. An experimental study on heat transfer and pressure drop characteristics of carbon dioxide during gas cooling process in a horizontal tube. International Journal of Refrigeration 2006; 29:539–546.

Srinivas SP, Groll EA, Ramadhyani S., 2002 New correlation to predict the heat transfer coefficient during in-tube cooling of turbulent supercritical CO_2. International Journal of Refrigeration 2002; 25 : 887–895.

Srinivasan, K., Sheahen, P. and Sarathy, C.S.P. (2010) 'Optimum thermodynamic conditions for upper pressure limits of transcritical carbon dioxide refrigeration cycle', International Journal of Refrigeration, 33 (7) pp. 1395-1401.

Tao YB, He YL, Tao WQ., 2010, Exergetic analysis of transcritical CO_2 residential air conditioning system based on experimental data. Applied Energy 2010; 87 : 3065–3072

Tassou A, Lewis J, Ge YT, Hasawey A and Chaer I. 2010, A review of emerging technologies for food refrigeration applications, Applied Thermal Eng., Vol. 30, pp. 263-276

Tassou SA. 2007, Potential for Solar Energy in Food Manufacturing, Distribution and Retail, Report to DEFRA, AC045, 2007; 25 pgs.

Tsamos K.M., Ge Y.T., Santosa I.D.M.C., Tassou S.A. Experimental investigation of gas cooler/condenser designs and effects on a CO_2 booster system, Applied Energy. doi:10.1016/j.apenergy.2016.03.004

TWC, 2016. The Weather Company, LLC - Weather Underground. Available on: https://www.wunderground.com/ (accessed 04/07/16)

UK NIR 2014, UK Greenhouse Gas Inventory, 1990 to 2012, Annual Report for Submission under the Framework Convention on Climate Change, Department of Energy and Climate Change, ISBN: 978-0-9573549-4-4, Issue 1

UNEP, 2010, Report of the refrigeration, air conditioning and heat pumps technical options committee, 2010 Assessment. 243 pgs.

UNEP, 2014, Report of the refrigeration, air conditioning and heat pumps technical options committee, 243 pgs.

U-switch, 2016 Available on: https://www.uswitch.com/gas-electricity/consumptions/new (accessed: 16/08/2016)

Wallace, 2013. Supermarket for future – Natural Refrigeration and Heat Recovery. 51 pgs.

Walravens, F. and Hailes, J. (2010) Chilling Facts II. The supermarket refrigeration scandal continues Available at: http://chillingfacts.org.uk/uploads/chillingfacts2.pdf (accessed: 28/10/15)

Wang C.C. (1999)., Investigation of wavy fin and tube heat exchangers: A contribution to databank. Experimental Heat Transfer: A journal of thermal energy generation, transport, storage and conversion. 12:1, 73-89.

Wang C.C., Wei S. L. and Wen J. S., (2001) A comparative study of compact enhanced fin-tube-tube heat exchangers. International Journal of Heat and Mass Transfer 44, 3565-3573

Yoon JI, Choi KH, Son CH, Yi WB, Ha SJ, Jeon MJ., 2014, Performance characteristics of the R404a indirect refrigeration system using CO_2 as a secondary refrigerant. International journal of Engineering Sciences & Research Technology, October 2014: ISSN:2277- 9655: 459-473,

Yoon, S.H., Kim, J.H., Hwang, Y.W., Kim, M.S., 2003. Heat transfer and pressure drop characteristic during the in-tube cooling process of carbon dioxide in the supercritical region. International Journal of Refrigeration 26, 857 – 864.

Qureshi, B.A., Zubair, S.M., 2013. Mechanical sub-cooling vapor compression systems: current status and future directions. Int. J. Refrigeration 36 (8), 2097–2110.

Llopis, R., Cabello, R., Sánchez, D., Torrella, E., 2015. Energy improvement of CO_2 transcritical refrigeration cycles using dedicated mechanical subcooling. Int. J. Refrigeration 55, 129– 141

Minetto, S., Girotto, S., Salvatore, M., Rossetti, A., Marinetti, S., 2014. Recent installations of CO_2 supermarket refrigeration system for warm climates: data from field. In: Proceedings of the 3rd IIR International Conference on Sustainability and Cold Chain, London, United Kingdom.

Appendix A:

SPECIFIC REFRIGERANT CHARGE VALUES AND PERCENTAGE OF REFRIGERANT LEAKAGE

The specific refrigerant charge by the refrigerant type are illustrated in table A-1 below.

Sector	Specific refrigerant charge by refrigerant type (kg/kw)			
	HC	HFC/HCFC	R717	R744
Domestic	0.20 – 0.40	0.70 – 1.2	-	-
Retail				
✓ Central Supermarkets	0.15 – 0.35	**2.0 – 5.0**	0.09 – 0.21	1.0 – 2.5
✓ Integral units	0.25 – 0.60	0.60 – 1.5	-	0.30 – 0.75
✓ Split/condensing units	-	0.40 – 0.70	-	0.20 – 0.35
Stationary Air-Conditioning				
✓ Unitary/split	0.10 – 0.15	0.25 – 0.70	-	0.15 – 0.35
✓ Chillers	0.13 – 0.15	0.27 – 0.35	0.04 – 0.25	-
✓ Heat Pumps	0.08 – 0.11	0.19 – 0.53	-	0.10 – 0.25

Source: MTP, 2008

The reported annual leakage rates for particular refrigeration system applications in the UK are shown in Table A-2.

Sector	Annual leakage rates (% of charge per annum)			
	Johnson (1998)	March (1999)	Haydock (2003)	ETSU (1997)
Domestic	1 %	1 %	0.3 – 0.7 %	2.5 %
Retail Refrigeration	9 – 23 %			
✓ Central Supermarket		10 – 25 %	10 – 20 %	8 %
✓ Integral units		1 %	3 – 5 %	2.5 %
✓ Split/condensing units		10 – 20 %	8 – 15 %	15 %
Air conditioning	12 – 20 %			
✓ Unitary/Split		10 – 20 %	8 – 20 %	
✓ Chillers	15 – 22 %	3 – 20 %	3 – 5 %	4 %
✓ Heat pumps		3 – 20 %	3 – 5 %	4 %

Source: MTP, 2008

Appendix B:

EXPOSURE TO CARBON DIOXIDE

The effects of carbon dioxide exposure are described in Table B-1.

Carbon dioxide level in air (ppm v/v)	Equivalent mass (g/m3)	Comments
388 ppm	0.7	Atmospheric level
5,000 ppm	9	NIOSH time-weighted exposure limit (8 hours)
25,000 ppm	45	Short of breath, hyperventilation
30,000 ppm	54	NIOSH short term exposure limit (10 minutes)
40,000 ppm	72	NIOSH IDLH
50,000 ppm	90	Laboured breathing, sweating, increased pulse rate, numbness in fingertips (narcosis)
75,000 ppm	135	Headaches, dizziness, restlessness, breathlessness, increased heart rate and blood pressure, visual distortion,
100,000 ppm	180	Impaired hearing, nausea, vomiting, loss of consciousness

Source: Pearson, 2014

The following Table A-2 is a list of selected concentration levels of CO_2 and expected effects on the human health.

PPM	Effects on health
350	Normal value in the atmosphere
1000	Recommended not to be exceeded for human comfort
5000	Concentration to which one may be repeatedly exposed for 8 hours per day 40 hours per week without adverse effect.
30000	100% increase in breathing rate after short time exposure
50000	Maximum level for which one could escape within 30 minutes without any escape-impairing symptoms or any irreversible health effects.
10000	Few mins of exposure produces unconsciousness
200000	Death accidents have been reported
300000	Quickly results in an unconsciousness and convulsions

Source: GTZ Proklima, 2008

Appendix C:

HT COMPRESSOR

CO_2 Performance data — 50 Hz

Type			Cooling capacity $\dot{Q}_0$ [W] / Power consumption P_e [kW] — Evaporating temperature °C							
	t_c °C		15	10	5	0	-5	-10	-15	-20
			SUBCRITICAL							
RKX26/31-2 CO2 T	10	Q					20350	16600	13300	10400
		P					4,45	4,45	4,35	4,15
	15	Q				22450	18500	15000	11900	9150
		P				4,85	4,90	4,85	4,70	4,50
	20	Q			24000	20000	16400	13200	10300	7800
		P			5,25	5,35	5,35	5,25	5,10	4,80
	25	Q		24550	20650	17100	13950	11100	8550	6300
		P		5,70	5,80	5,80	5,75	5,65	5,45	5,10
	30	Q		19850	16600	13650	11000	8650	6550	4650
		P		6,25	6,30	6,30	6,20	6,05	5,75	5,40
	t_{ga} °C		TRANSCRITICAL							
RKX26/31-2 CO2 T	30	p_{V2}	75	75	75	75	75	75	75	75
		Q	24600	20900	17500	14400	11600	9050	6750	4750
		P	6,45	6,55	6,55	6,50	6,40	6,20	5,90	5,55
	35	p_{V2}	85	85	85	90	90	90	85	
		Q	22000	18600	15450	13300	10450	7900	5550	
		P	7,20	7,20	7,15	7,30	7,10	6,80	6,25	
	40	p_{V2}	100	100	100	100	105	95		
		Q	21100	17550	14400	11500	8900	6350		
		P	8,30	8,20	8,00	7,80	7,65	6,95		
	45	p_{V2}	110	110	115	115	110	95		
		Q	18450	15300	12750	10000	7450	4050		
		P	9,00	8,80	8,80	8,45	7,85	6,95		
	50	p_{V2}	125	125	130	125	110			
		Q	16900	13900	11650	8800	5700			
		P	10,00	9,70	9,55	8,85	7,85			

Subcritical performance data 50 Hz
Relative to 10 K suction gas superheat without liquid subcooling

Transcritical performance data 50 Hz
Relative to 10 K suction gas superheat

The performance data are indicated at a high pressure level, which is close to a optimal high pressure level.
Optimal high pressure is thereby related to an ideal cyclic process.

t_c = Condensing temperature
t_{ga} = Gas cooler outlet temperature
p_{V2} = Pressure at the compressor outlet [bar]

Optimal high pressure is outside of the operating limits.
Performance data are indicated at maximal possible high pressure.

Type	Number of cylinders	Swept volume 50 / 60 Hz	Electrical data ③ Voltage ①	Max. working current ②	Max. power consumption ②	Starting current (rotor locked)	Weight	Connections ⑤ Discharge line DV	Suction line SV	Oil charge
		m³/h		A Δ / Y	kW	A Δ / Y	kg	mm	mm	Ltr.
RKX26/31-4 CO2 T	6	2,70 / 3,30	④	14,3 / 8,2	5	107 / 62	68	Max. 12	Max. 12	1,0
RKX26/31-2 CO2 T	6	5,40 / 6,50	④	40 / 23	10,6	235 / 136	73	Max. 12	Max. 12	1,0

Source: GEA BOCK Compressors 2009

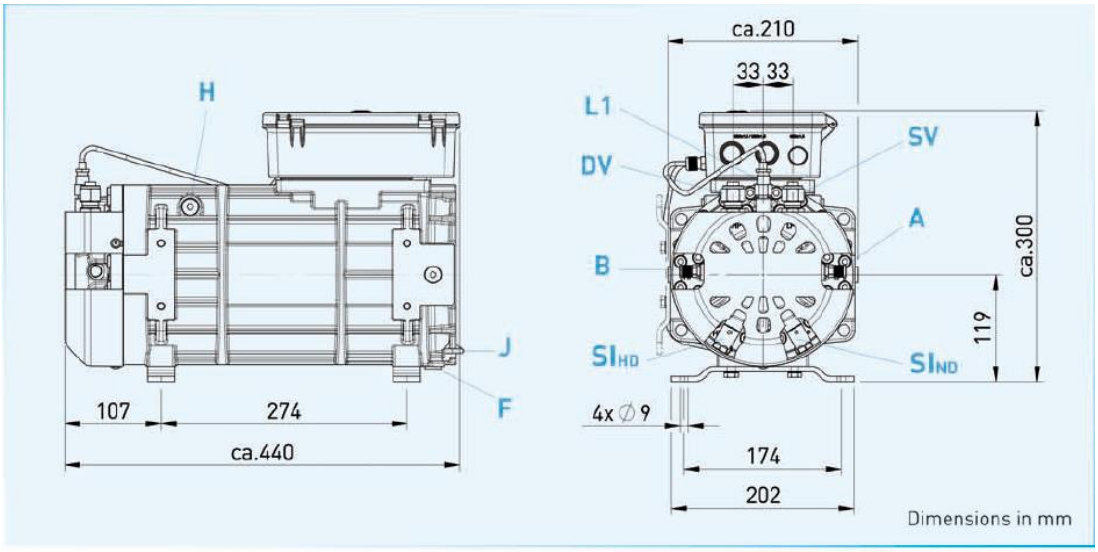

Connections		RKX CO2 T
SV DV	Suction line Discharge line	Please refer to technical data
A	Connection suction side, not lockable	1/8" NPTF
B	Connection discharge side, not lockable	1/8" NPTF
f	Oil drain	G 1/4"
H	Oil charge plug	G 1/4"
j	Oil sump heater	Ø 15 mm
L1	Thermal protection thermostat	1/8" NPTF
SI	Safety valve HD Safety valve ND	M 12 x 1 M 10 x 1

Source: GEA BOCK Compressors 2009

Appendix D:

RUNNING INFORMATION

The oil system is shown in Figure D-1.

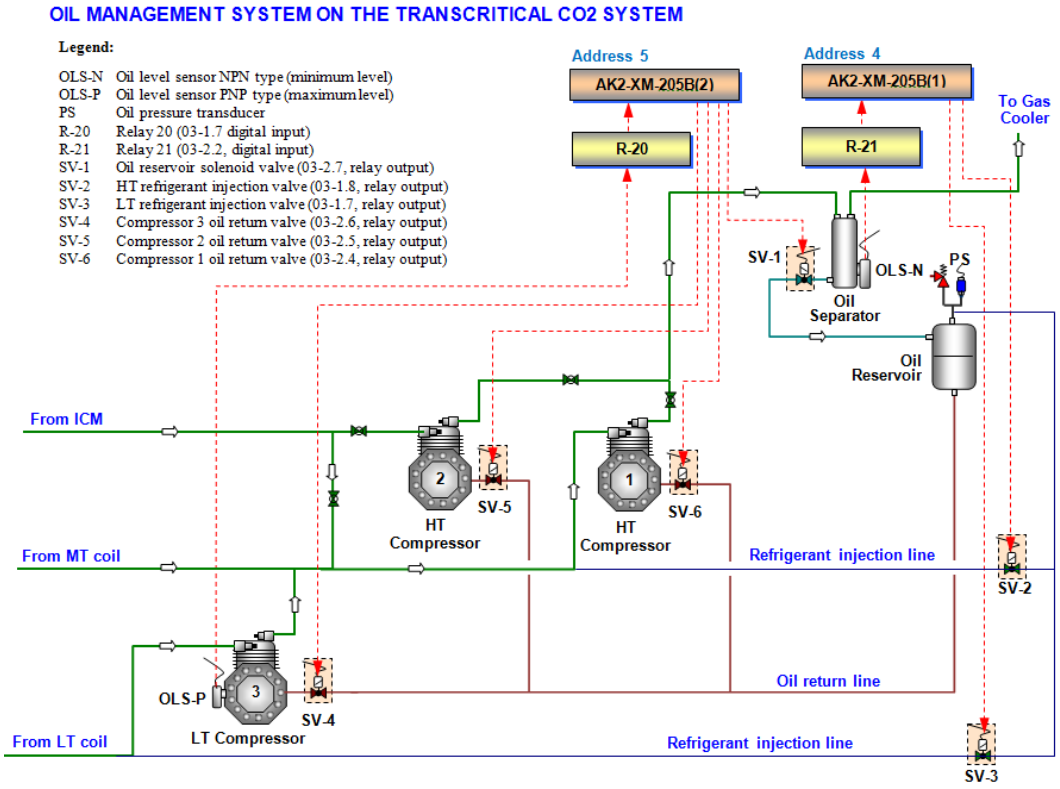

Observation on the oil management system of the Transcritical CO_2 System:

Originally the oil management system of the transcritical CO_2 booster system was as shown in the previous figure. Unfortunately after we sent a suggestion for not using copper tube particularly on the HT circuit, Space Engineering (the contractor who worked on the test rig before) disconnected the oil return line to the HT compressors (Compressor 1 and 2). At that time they said they had obtained a confirmation that the HT compressors did not require oil return line.

Then we took over the rig from Space Engineering. I could run the system continuously with full speed by doing a small changing on the controller. However the performance of the system was very bad, because of the discharge temperature of HT compressor was very high (reached 130oC) and the superheat of the HT compressor and LT compressor were also very high (25 to 35 K). I ran the system for about 15 hours, I

noticed the oil level of the HT compressor was on its low level but the oil level on the oil reservoir increase significantly. It meant that the oil separator was working properly and oil trapped in there then stored to the oil reservoir. Oil level of the LT compressor was still on a correct level.

Based on that fact I managed to find out the causes. I found valve SV-1 and SV-3 (see previous figure) were always open when the system was running. Therefore there was high temperature refrigerant injection from HT pressure level to the suction of the LT Compressor (compressor-3) when the system running. The hot refrigerant injection increased the suction line temperature, superheat and HT compressor discharge temperature.

Then I reset up all the controllers and fixed the components addresses in the main controller. All components had correct addresses and seemed to be working properly as well as the valves of the oil management system. From that time the valve SV-1 and SV-3 would open when there was enough oil in the oil separator or LT compressor oil level indicated low level. Most of the time, both valves would close when the system was running.

I charged the oil to the HT compressor manually and ran the system again with new setting on the controller. The system could perform well. I checked the oil level of the compressor regularly, because the compressors without oil return line. Unfortunately after 2 hours running the oil level of the HT compressor reach its low level again. It took shorter time than when the system was working with hot refrigerant injection circuit. To make sure the time required to run out the oil in the HT compressor, I did recharge the compressor oil and did another test. It took quite the same time to get the low oil level. Note: oil level of the LT compressor still on its correct level.

Defines:

- With hot refrigerant injection circuit open; no oil return line, oil of HT compressor would be run out in 15 hours
- No refrigerant injection; no oil return line, HT compressor oil ran out in 2 hours (test conditions as shown in the following figure)

A fixed permanent charging point was used to charge the CO_2 system. The CO_2 cylinder used to charge the system are shows below.

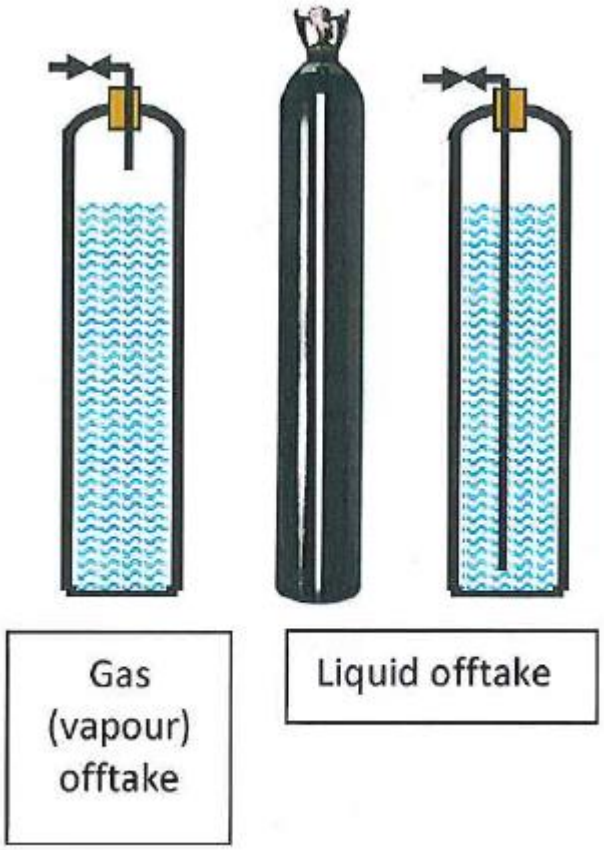

Source: CoolConcern, 2015

1) Charge from gas until the system reach 10 bar pressure

2) Then charge from liquid until the sight glasses at the receiver full

Appropriate charging equipment was used to connect the cylinder and the charging point which located at the top of the receiver. Before charging the system vacuumed for more than 10 hours. All the valves were opened before the vacuum process. In additional magnets were used to keep open the AKV valves.

An additional condensing unit was used to keep the pressure down during the charging procedure. The condensing unit installed at the top of the roof and the evaporating coil was installed inside the CO_2 liquid receiver. The expansion valve was installed before the liquid receiver.

① A04 versions equipped with KP17WB. FSA kit and power cord
② Pre-mounted LP/HP tubes for easy connection of pressure switch
③ Easy accessible valves
④ High efficient condenser
⑤ Low noise level
⑥ Optimum airflow due to Danfoss designed fan cowl
⑦ Compact design and extented application envelope
⑧ Base rails designed for easy installation

Source: Danfoss, 2010

Problems found during the charging or operation:

- During the charging process the pressure found to be increased rapidly when the condensing unit was off.

✓ Actions:

Check the pressure switch of the condensing unit.
Replace the compressor for higher capacity.
Check the delay settings of the compressor delay

- High pressure during first run.

✓ Actions:

Check the valves.
Check the mass flow meter
Run the system by using the by-pass valves

- Unbalanced operation.

✓ Actions:

Check the settings at the gas cooler inlet conditions
Check recirculation fans
Check air heaters
Check both loads of the system (MT and AL)

- Compressor fault.

✓ Actions:

Check oil level – condition
Check power supply
Check the power inverter

- Main Controller error.

✓ Actions:

Check system power supply
Read and understand the error
Contact with Danfoss specialist

Appendix E:

MAIN FAN POWER CONSUMPTION MEASUREMENTS

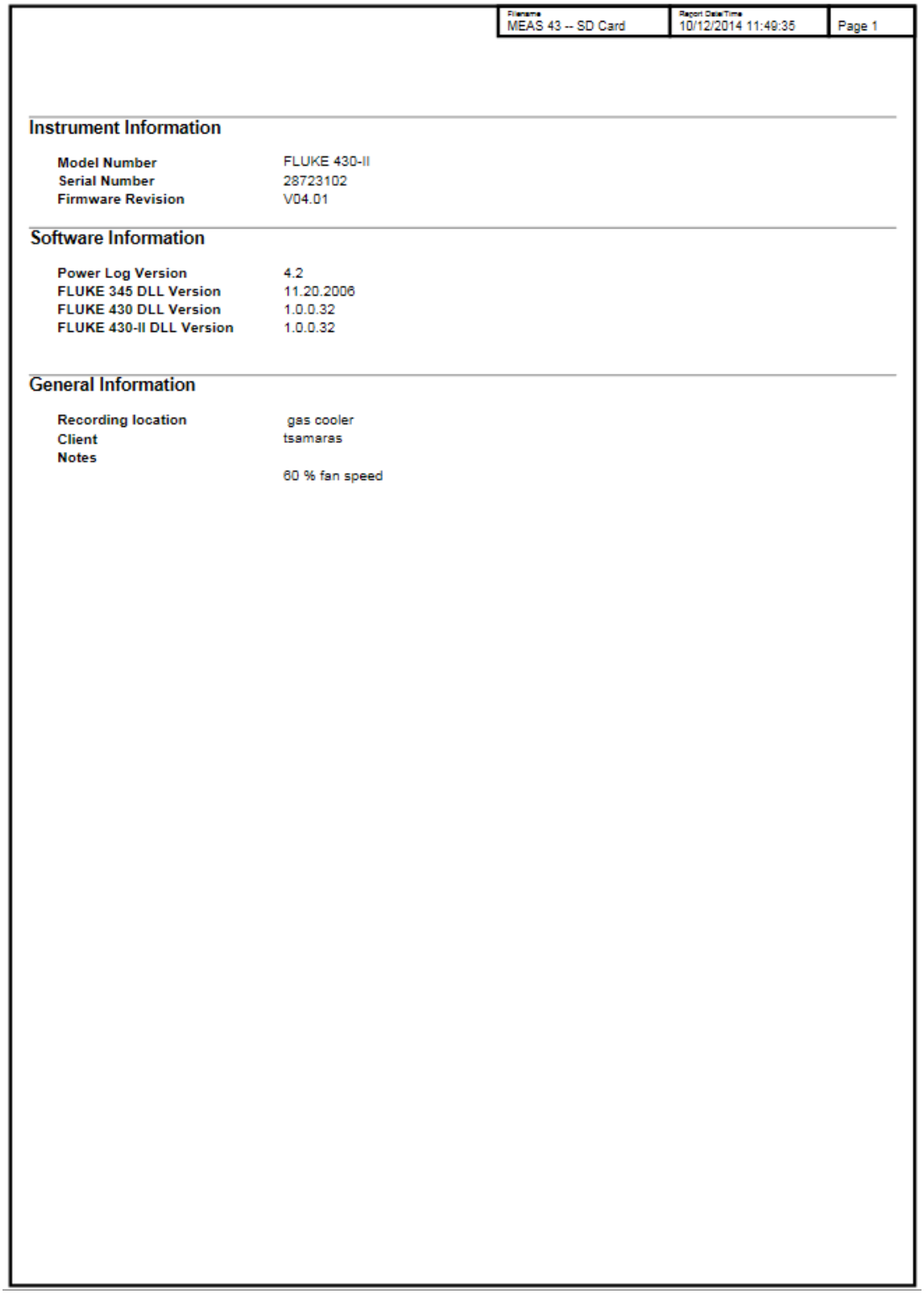

Filename	Report Date/Time	
MEAS 43 -- SD Card	10/12/2014 11:49:35	Page 1

Instrument Information

Model Number	FLUKE 430-II
Serial Number	28723102
Firmware Revision	V04.01

Software Information

Power Log Version	4.2
FLUKE 345 DLL Version	11.20.2006
FLUKE 430 DLL Version	1.0.0.32
FLUKE 430-II DLL Version	1.0.0.32

General Information

Recording location	gas cooler
Client	tsamaras
Notes	
	60 % fan speed

Measurement Summary

Measurement topology	Wye mode
Application mode	Power & Energy
First recording	10/12/2014 11:06:53
Last recording	10/12/2014 11:40:03
Recording interval	0h 0m 10s 0msec
Nominal Voltage	440 V
Nominal Current	300 A
Nominal Frequency	60 Hz
File start time	10/12/2014 11:06:53
File end time	10/12/2014 11:40:03
Duration	0d 0h 33m 10s 0msec
Number of events	0
Events downloaded	No
Number of screens	9
Screens downloaded	No
Power measurement method	Unified
Cable type	Copper
Harmonic scale	%H1
THD mode	THD 40
CosPhi / DPF mode	DPF

Recording Summary

RMS recordings	200
DC recordings	0
Frequency recordings	0
Unbalance recordings	0
Harmonic recordings	0
Power harmonic recordings	0
Power recordings	200
Power unbalance recordings	0
Energy recordings	200
Energy losses recordings	0
Flicker recordings	0
Mains signaling recordings	0

Events Summary

Dips	0
Swells	0
Transients	0
Interruptions	0
Voltage profiles	0
Rapid voltage changes	0
Screens	0
Waveforms	0
Intervals without measurements	0
Inrush current graphics	0
Wave events	0
RMS events	0

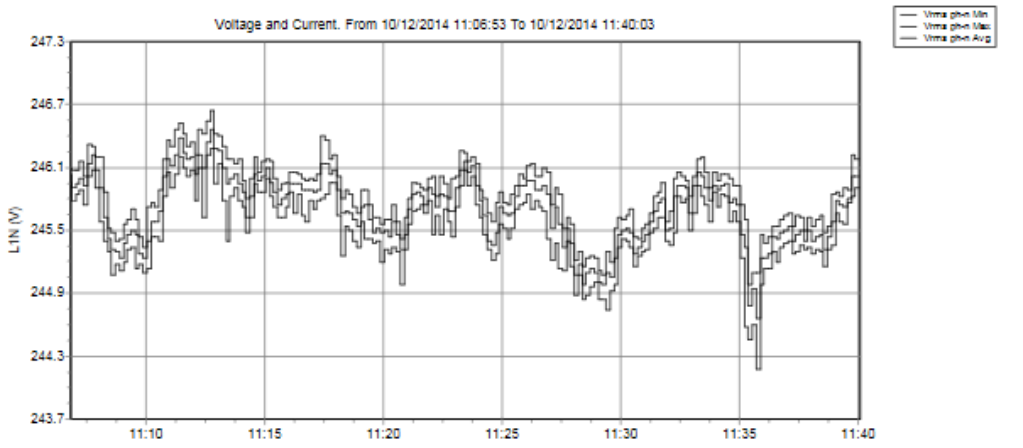
Voltage and Current. From 10/12/2014 11:06:53 To 10/12/2014 11:40:03
Vrms ph-n Min
Vrms ph-n Max
Vrms ph-n Avg
L1N (V)
247.3
246.7
246.1
245.5
244.9
244.3
243.7
11:10
11:15
11:20
11:25
11:30
11:35
11:40

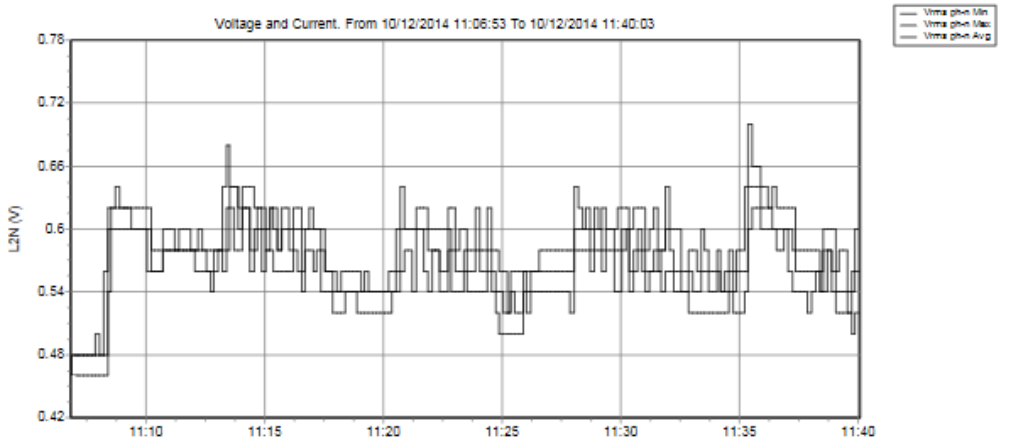
Voltage and Current. From 10/12/2014 11:06:53 To 10/12/2014 11:40:03
Vrms ph-n Min
Vrms ph-n Max
Vrms ph-n Avg
L2N (V)
0.78
0.72
0.66
0.6
0.54
0.48
0.42
11:10
11:15
11:20
11:25
11:30
11:35
11:40

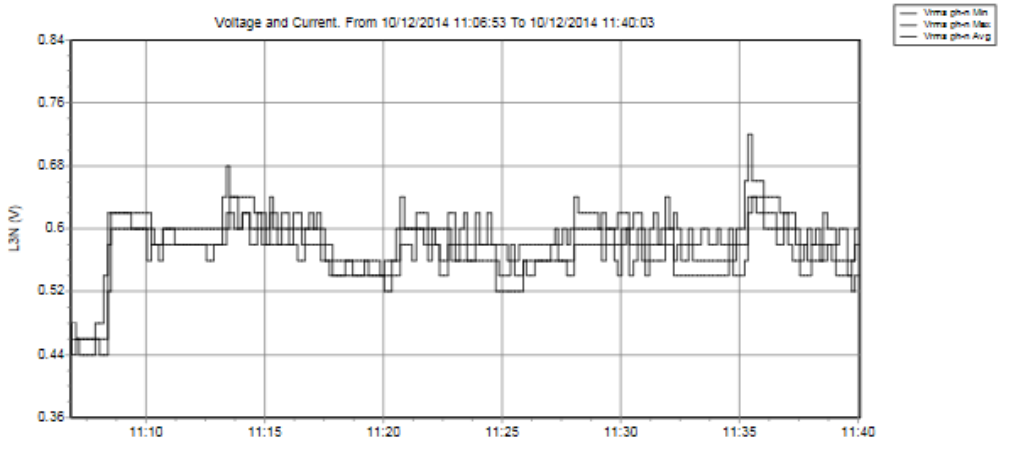
Voltage and Current. From 10/12/2014 11:06:53 To 10/12/2014 11:40:03
Vrms ph-n Min
Vrms ph-n Max
Vrms ph-n Avg
L3N (V)
0.84
0.76
0.68
0.6
0.52
0.44
0.36
11:10
11:15
11:20
11:25
11:30
11:35
11:40

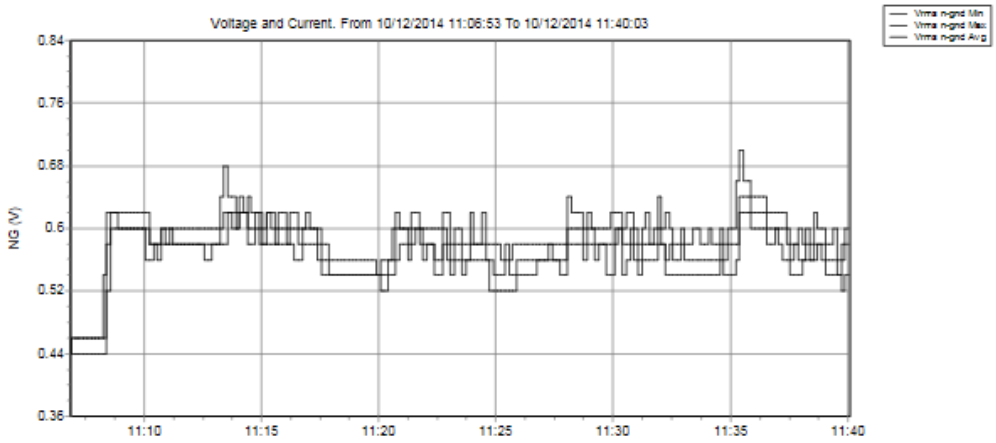
Voltage and Current. From 10/12/2014 11:06:53 To 10/12/2014 11:40:03
Vrms n-gnd Min
Vrms n-gnd Max
Vrms n-gnd Avg
NG (V)
0.84
0.76
0.68
0.6
0.52
0.44
0.36
11:10
11:15
11:20
11:25
11:30
11:35
11:40

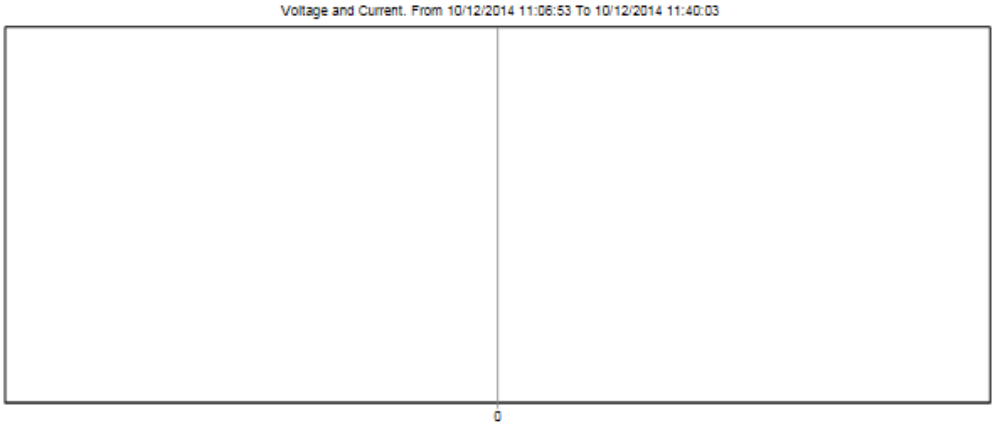
Voltage and Current. From 10/12/2014 11:06:53 To 10/12/2014 11:40:03
0

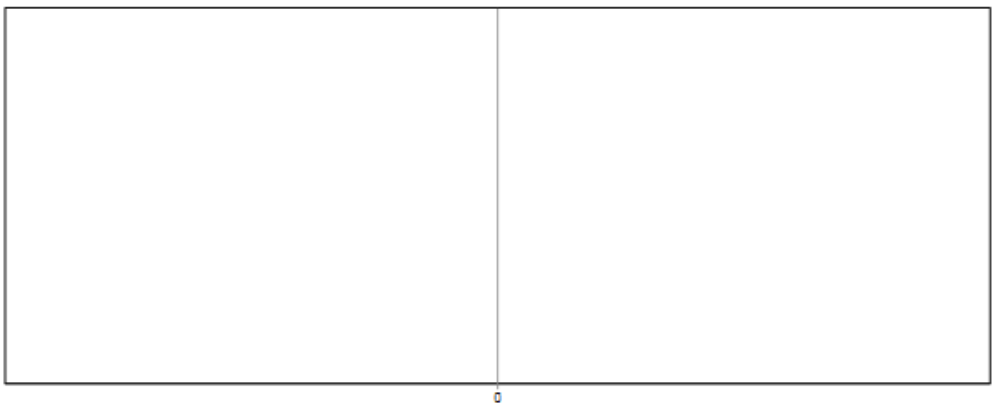
Voltage and Current. From 10/12/2014 11:06:53 To 10/12/2014 11:40:03
0

Voltage and Current. From 10/12/2014 11:06:53 To 10/12/2014 11:40:03

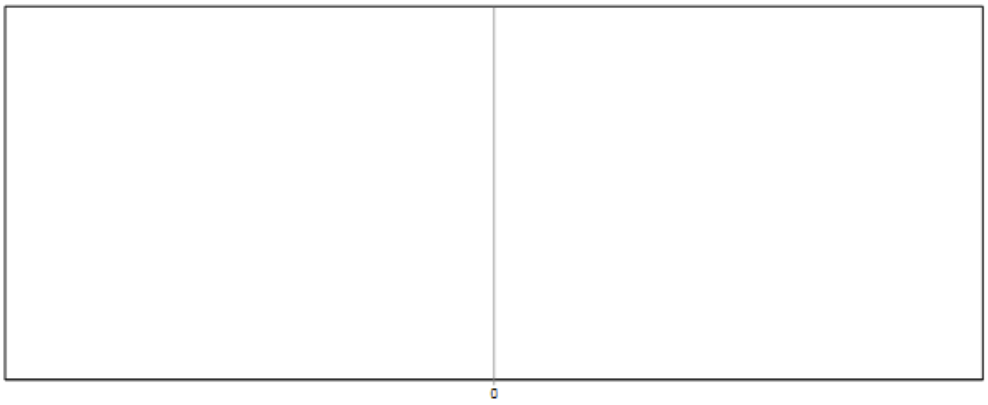

Voltage and Current. From 10/12/2014 11:06:53 To 10/12/2014 11:40:03

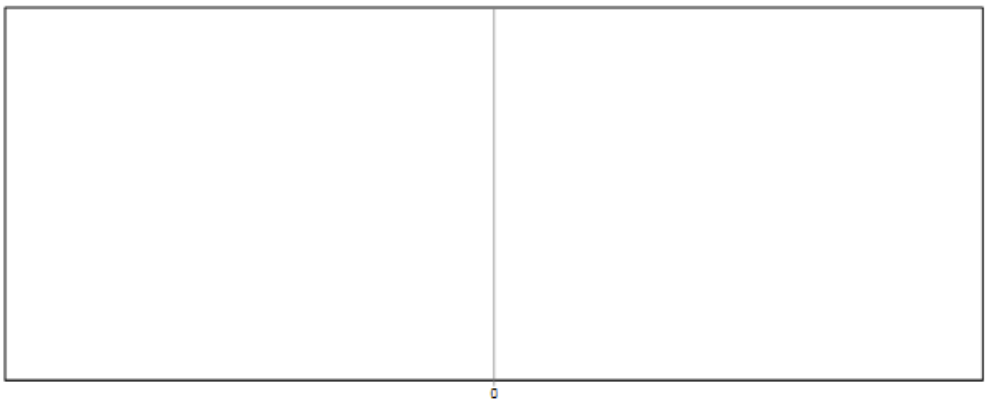

Power. From 10/12/2014 11:06:53 To 10/12/2014 11:40:03

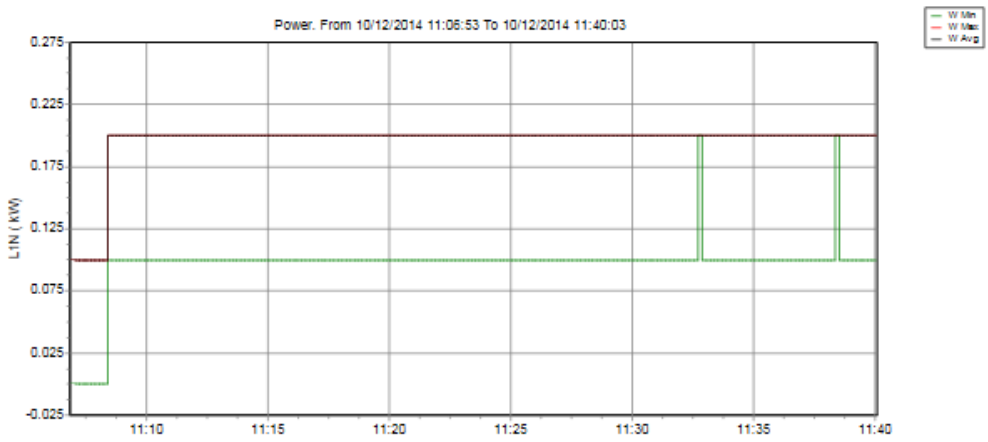

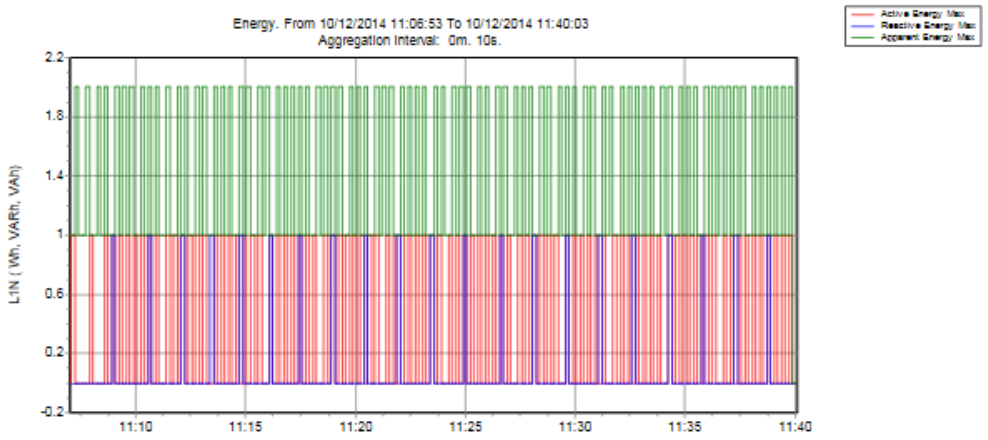
Energy. From 10/12/2014 11:06:53 To 10/12/2014 11:40:03
Aggregation Interval: 0m. 10s.
Active Energy Max
Reactive Energy Max
Apparent Energy Max
L1N (Wh, VARh, VAh)
2.2
1.8
1.4
1
0.6
0.2
-0.2
11:10
11:15
11:20
11:25
11:30
11:35
11:40

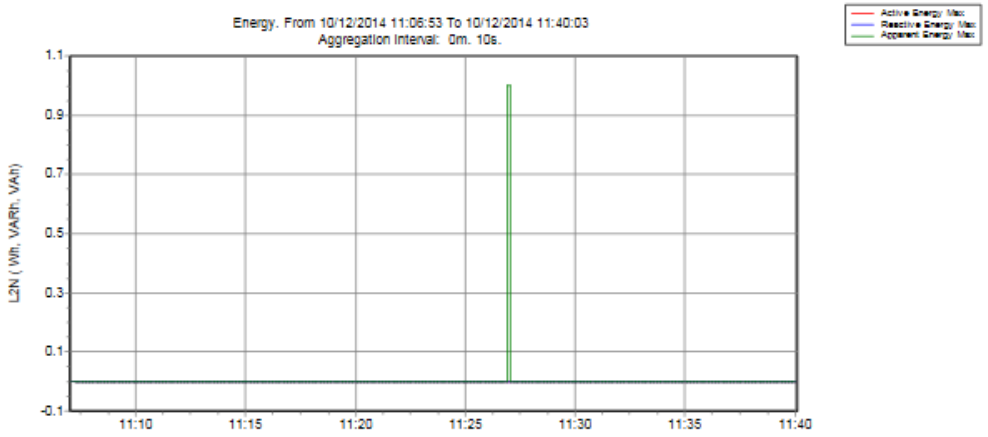
Energy. From 10/12/2014 11:06:53 To 10/12/2014 11:40:03
Aggregation Interval: 0m. 10s.
Active Energy Max
Reactive Energy Max
Apparent Energy Max
L2N (Wh, VARh, VAh)
1.1
0.9
0.7
0.5
0.3
0.1
-0.1
11:10
11:15
11:20
11:25
11:30
11:35
11:40


Energy. From 10/12/2014 11:06:53 To 10/12/2014 11:40:03
Aggregation Interval: 0m. 10s.
Active Energy Max
Reactive Energy Max
Apparent Energy Max
L3N (Wh, VARh, VAh)
1.2
0.8
0.4
0
-0.4
-0.8
11:10
11:15
11:20
11:25
11:30
11:35
11:40

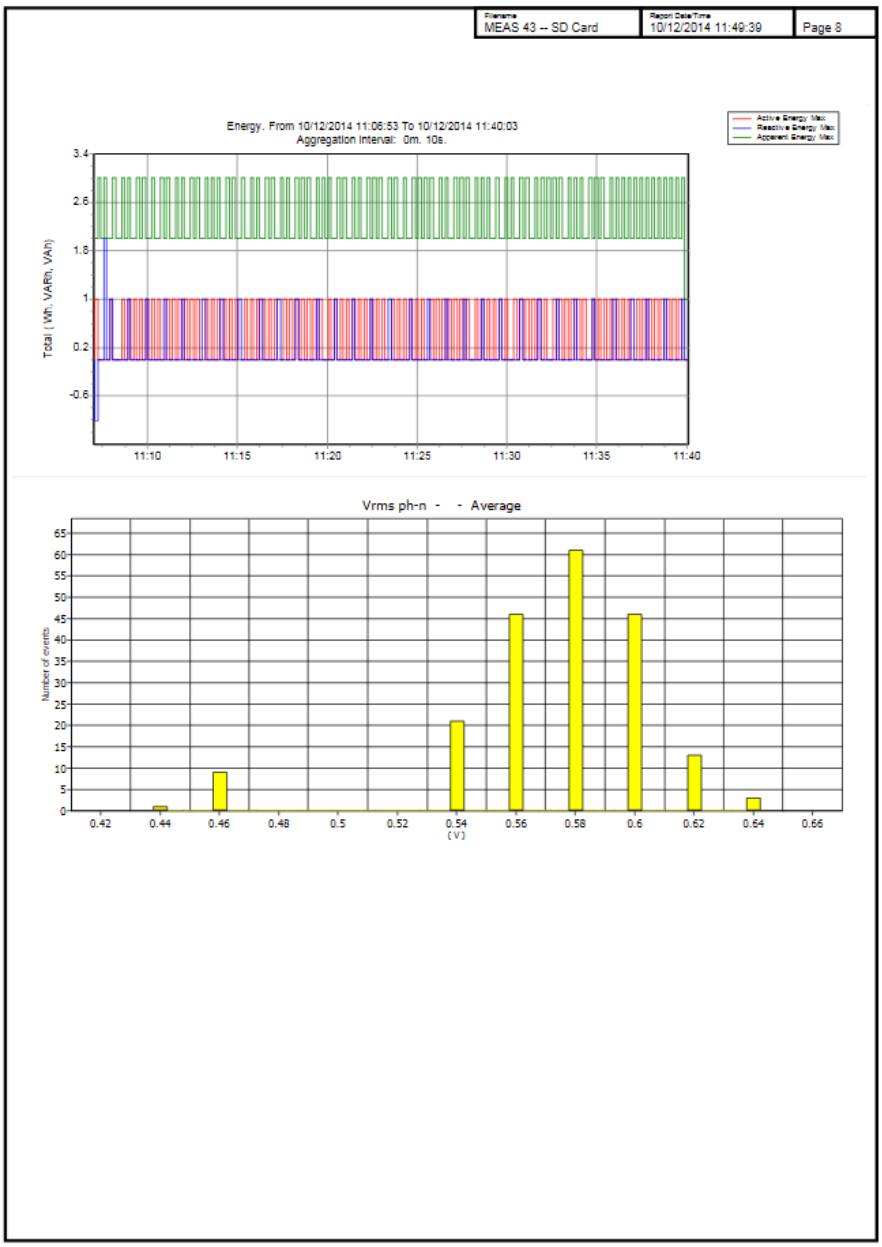
Filename
MEAS 43 -- SD Card
Report Date/Time
10/12/2014 11:49:39
Page 8
Energy. From 10/12/2014 11:06:53 To 10/12/2014 11:40:03
Aggregation Interval: 0m. 10s.
Active Energy Max
Reactive Energy Max
Apparent Energy Max
Total (Wh, VARh, VAh)
3.4
2.6
1.8
1
0.2
-0.6
11:10
11:15
11:20
11:25
11:30
11:35
11:40
Vrms ph-n - - Average
Number of events
65
60
55
50
45
40
35
30
25
20
15
10
5
0
0.42
0.44
0.46
0.48
0.5
0.52
0.54
0.56
0.58
0.6
0.62
0.64
0.66
(V)

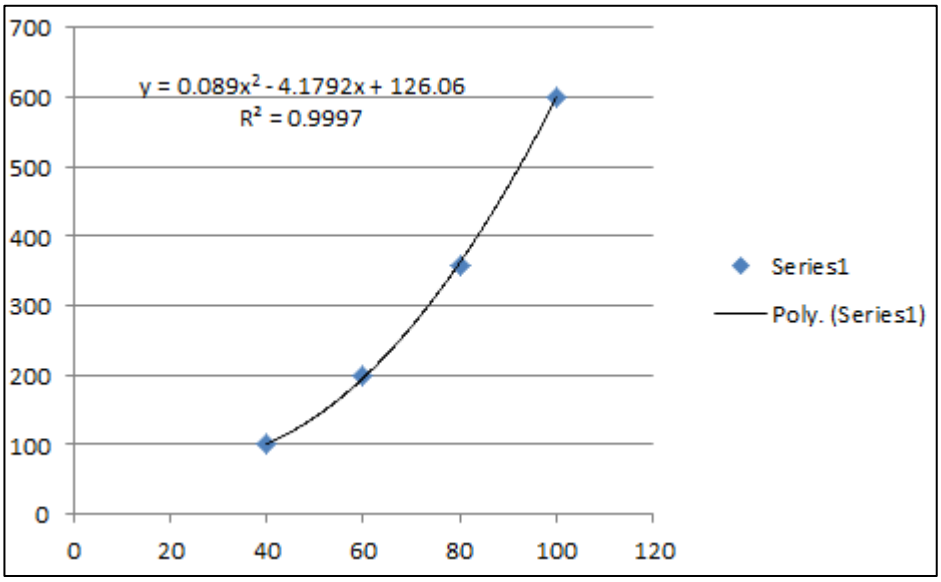
y = 0.089x² - 4.1792x + 126.06
R² = 0.9997
700
600
500
400
300
200
100
0
0
20
40
60
80
100
120
Series1
Poly. (Series1)

Appendix F:

COOLING CAPACITIES OF ADDITIONAL AIR COOLER

Capacity Calculations

Conservation of energy

Example of the calculation (70% Fan – 100% Compressor– 80.8 bar G/C pressure)

The equations resulting from the energy balance are summarized as:

$$\dot{Q}_{evap} = \dot{Q}_{evap,a} = \dot{Q}_{evap,ref}$$

$$\dot{Q}_{evap} = \dot{m}_{ref}\left(\dot{h}_{ref,in} - \dot{h}_{ref,out}\right) = \dot{m}_{air}\left(\dot{h}_{air,in} - \dot{h}_{air,out}\right)$$

Heat extraction rate calculated from air side:

$$\dot{Q}_{evap,air} = \underbrace{\rho \cdot v \cdot A_{coil}}_{\dot{m}_{air}} \left(\dot{h}_{air,in} - \dot{h}_{air,out}\right)$$

Coil area: 0.198 m^2

Density of air: 1.248 kg/m^3

Velocity: 2.26 m/s (TSI)

$$\dot{\boldsymbol{Q}}_{\boldsymbol{evap,air}} = \mathbf{0.5584}\ (\mathbf{283.37} - \mathbf{277.96}) = \mathbf{3.02}\ \boldsymbol{kW}$$

Heat extraction rate calculated from refrigerant side:

$\dot{m}_{ref}$: 39.59 kg/h = 0.010998 kg/s

$$\dot{\boldsymbol{Q}}_{\boldsymbol{evap,ref}} = \mathbf{0.010998}\ (\mathbf{-52.02} - (\mathbf{-327}) = \mathbf{3.02}\ \boldsymbol{kW}$$

Thermodynamic properties defined by using EES**.**

Test Conditions		Condenser/Gas Cooler Data										Air Cooler	
Comp speed	**Fan speed**	**Pref_in Bar-g**	**Tair_ON °C**	**Tref_in °C**	**Ambient C**	**Pref_out Bar-g**	**Tair_OFF °C**	**Tref_out °C**	**T_Subcool K**	**Q_HX kW**	**Approach Temp K**	**Qevap,ref kW**	**Qevap,air kW**
100%	50%	69.55	22.03	82.67	16.04	68.47	31.10	27.41	1.61	10.8	5.38	**3.07**	**3.00**
100%	50%	72.67	23.89	84.12	17.41	71.61	33.14	29.05	1.53	10.7	5.16	**2.98**	**2.99**
100%	50%	74.54	25.43	87.03	18.26	73.47	34.58	29.68	N/A	10.7	4.25	**3.13**	**3.10**
100%	50%	75.49	25.85	86.71	19.38	74.51	34.46	29.93	N/A	10.1	4.08	**3.01**	**3.08**
100%	50%	77.23	26.72	83.89	18.96	76.17	35.85	30.95	N/A	10.7	4.23	**3.12**	**-**
100%	50%	78.11	28.10	86.70	20.09	77.13	36.36	31.31	N/A	9.6	3.21	**2.78**	**2.82**
100%	50%	82.64	30.79	91.56	22.59	81.73	39.19	33.74	N/A	9.7	2.95	**2.70**	**2.53**
100%	50%	84.00	32.02	91.00	24.08	83.05	40.22	34.92	N/A	9.4	2.90	**-**	**-**
100%	50%	84.09	32.71	94.58	23.93	83.23	40.39	35.40	N/A	8.8	2.69	**2.96**	**2.80**

Test Conditions		Condenser/Gas Cooler Data										Air Cooler	
Comp speed	Fan speed	Pref_in Bar-g	Tair_ON °C	Tref_in °C	Ambient C	Pref_out Bar-g	Tair_OFF °C	Tref_out °C	T_Subcool K	Q_HX kW	Approach Temp K	Qevap,ref kW	Qevap,air kW
100%	60%	68.0	21.1	77.2	14.7	66.9	28.6	26.9	1.2	10.9	5.8	**3.33**	**3.50**
100%	60%	68.3	21.7	79.1	16.0	67.1	29.0	27.0	1.2	10.8	5.3	**3.26**	**3.41**
100%	60%	69.4	22.7	77.4	13.6	68.3	29.9	27.9	1.0	10.6	5.2	**3.25**	**3.30**
100%	60%	71.8	24.4	83.4	17.6	70.7	31.6	28.6	1.8	10.3	4.2	**3.16**	**3.24**
100%	60%	73.8	25.6	84.7	18.4	72.7	32.8	29.2	1.7	10.1	3.6	**3.05**	**3.09**
100%	60%	75.4	26.6	87.0	18.9	74.4	33.7	30.0	N/A	10.0	3.4	**2.94**	**3.09**
100%	60%	78.4	28.5	92.1	21.3	77.4	35.7	31.7	N/A	10.1	3.2	**2.96**	**2.93**

Test Conditions		Condenser/Gas Cooler Data										Air Cooler	
Comp speed	**Fan speed**	**Pref_in Bar-g**	**Tair_ON °C**	**Tref_in °C**	**Ambient C**	**Pref_out Bar-g**	**Tair_OFF °C**	**Tref_out °C**	**T_Subcool K**	**Q_HX kW**	**Approach temp K**	**Qevap,ref kW**	**Qevap,air kW**
100%	70%	68.65	21.56	76.94	15.41	67.60	28.30	26.64	1.82	11.26	5.08	**3.37**	**3.48**
100%	70%	69.93	22.99	81.92	16.71	68.89	29.69	27.63	1.63	11.14	4.63	**3.39**	**3.23**
100%	70%	70.30	23.07	81.77	16.60	69.28	29.81	27.60	1.88	11.20	4.53	**3.39**	**3.40**
100%	70%	71.25	24.08	83.31	18.22	70.21	30.70	28.00	2.06	10.97	3.92	**3.17**	**3.42**
100%	70%	71.77	24.92	85.74	18.36	70.78	31.20	28.24	2.09	10.39	3.32	**3.11**	**-**
100%	70%	80.76	28.92	91.01	22.66	79.86	35.73	31.10	N/A	11.11	2.18	**3.02**	**3.02**
100%	70%	82.61	30.87	93.18	23.47	81.76	37.30	32.82	N/A	10.45	1.95	**2.66**	**2.74**
100%	70%	83.51	31.93	94.83	23.77	82.64	37.97	33.41	N/A	9.78	1.48	**2.70**	**2.82**

Air Side Measurements

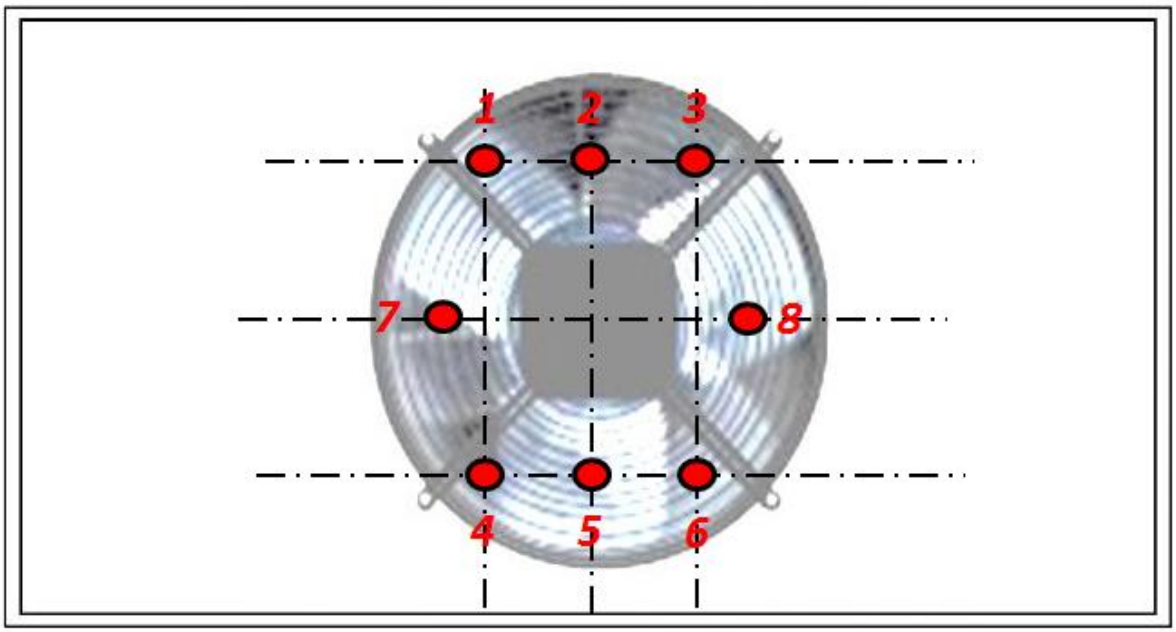

Points							
1				5			
Vel	T	H	Dew point	Vel	T	H	Dew point
m/s	deg C	%rh	deg C	m/s	deg C	%rh	deg C
10.6	**2.7**	71.6	-1.7	11.13	1.7	73.7	-2.2
11.2	**6.5**	56.1	-1.4	11.2	2.3	66.8	-2.9
2				6			
Vel	T	H	Dew point	Vel	T	H	Dew point
m/s	deg C	%rh	deg C	m/s	deg C	%rh	deg C
10.3	**3.55**	70.2	-1.1	13.2	0.3	80.7	-2.3
9.8	**5.7**	56.5	-1.9	13.5	1.1	76.2	-2.3
3				7			
Vel	T	H	Dew point	Vel	T	H	Dew point
m/s	deg C	%rh	deg C	m/s	deg C	%rh	deg C
12.7	5.7	64.8	-0.3	10.6	1.9	75.2	-1.7
10.8	6.4	55.6	-1.5	13.4	4.7	71.3	-0.02
				12.1	3.8	73.5	-0.4
4				8			
Vel	T	H	Dew point	Vel	T	H	Dew point
m/s	deg C	%rh	deg C	m/s	deg C	%rh	deg C
13.2	6.1	64.9	0.025	12.7	4.5	69.9	-0.4
13.8	7.4	59.1	0.06	13.3	4	68.0	-1.2
				13.5	3.4	66.5	-1.9

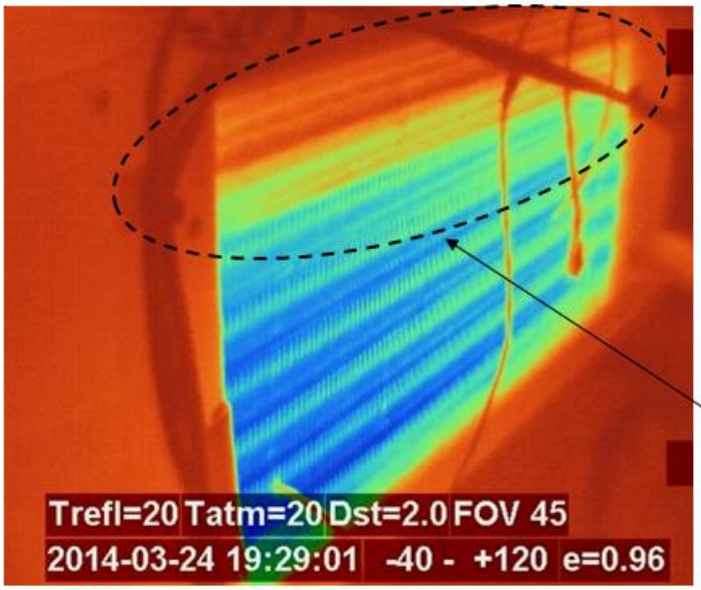

Note:

Refrigerant inlet is at the bottom of the coil and the exit is at the top.

Higher Temperature

(Top half)

Appendix G:

INTERMIDIATE PRESSURE

The liquid receiver acts as a stock of liquid refrigerant for the evaporators. However, the receiver should be sized to hold the full system charge during service work.

*** In this system the receiver is not only storage but also separator (gas/liquid).**

Type	Total Volume	Weight
Custom Build	40 kg.	36,7 kg

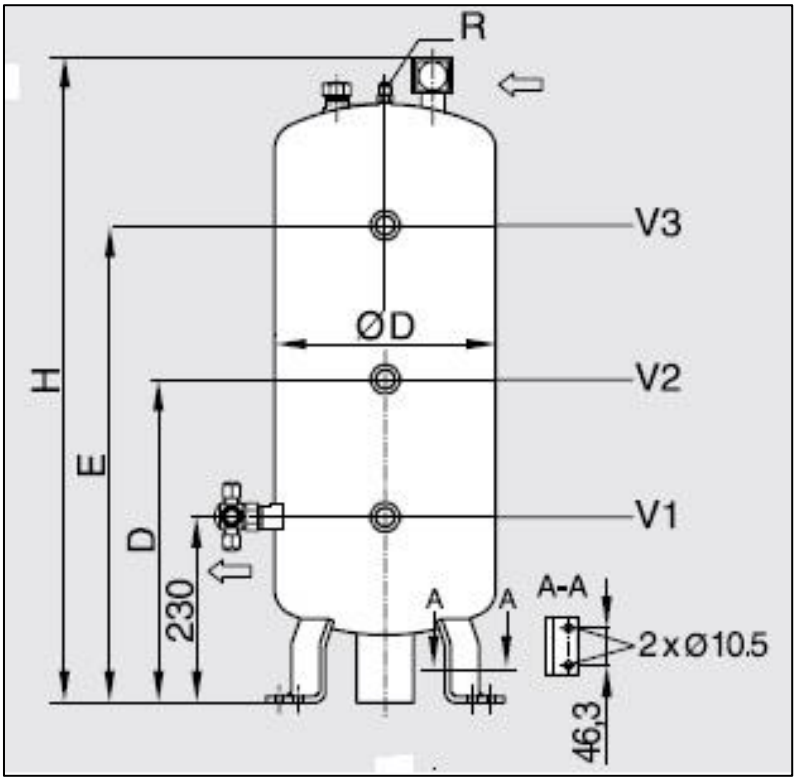

Control Strategy

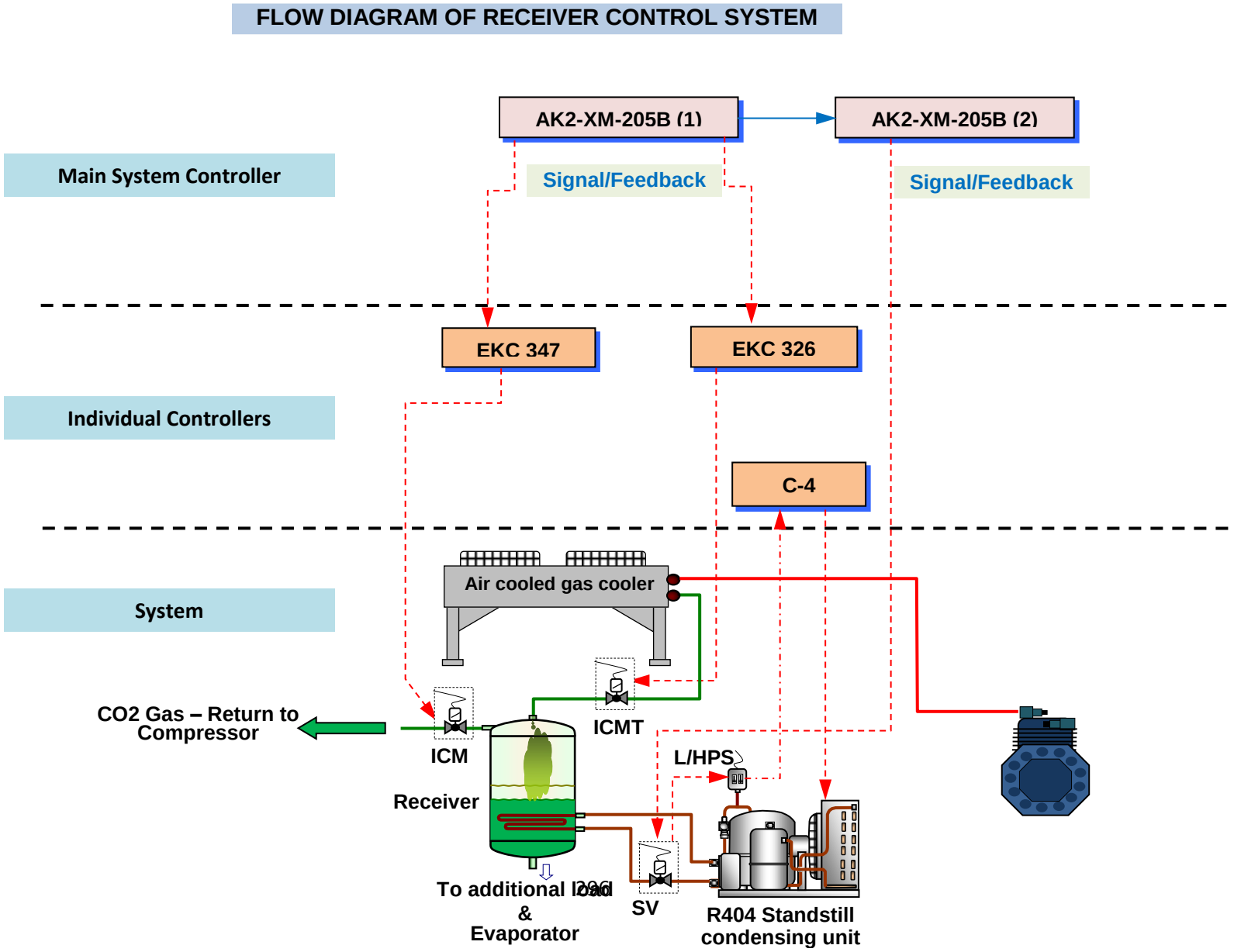

Individual Controllers

- Danfoss EKC 326 (A): CO_2 Gas Pressure Regulator – ICMT valve
- Danfoss EKC 347: Liquid Level Controller – ICM valve

Main System Controllers

- **Danfoss AK-SC255**

Parameters

EKC 326: In order to control the receiver pressure an ETS valve is required.

The ETS valve has been not installed in our system. In this case we cannot control the receiver pressure by adjust the EKC controller.

EKC 347: The EKC 347 is a PI liquid level controller that can be used to regulate the refrigerant level in receiver (not pressure). A signal transmitter constantly measures the refrigerant level in the receiver and the controller receiver the signal.

The EKC controller required the installation of ICM motorized modulating valve with ICAD motor actuator, Type AKV pulse width modulating expansion valve and soleinoid valve for ON/OFF control.

Pressure inside the receiver

The pressure inside the receiver is a proportional of ICM - ICMT valves and EKC 347 - EKC 326 controller settings respectively. As is mentioned before, the ETS valve has been not installed in our system. This has a proportional that the pressure inside the receiver cannot by adjust/controlled by regulating the ICM and ICMT valves.

Based on the above, we have to find other way(s) to adjust the pressure inside the cylinder. Moreover the pressure inside the receiver must be keeping lower than the system maximum operating pressures. The maximum working pressures are showing below:

- ✓ Receiver: 55 bar
- ✓ Handle Valves: 55 bar
- ✓ Relief (safety) valve: 46 bar

Test Procedure

The alternative method to increase the pressure inside the receiver is showing below,

- Increase the volume of the liquid refrigerant inside the cylinder (% of liquid and % gas)
- Decrease the set point of the additional load from -5 oC to -7oC
- Change the settings of the condensing unit from 31 bar to 35 and 37 bar respectively
- Decrease the temperature inside the chamber room (effect to RH %)
- Set max and min superheat settings of the coil 15 and 10 respectively.

By increasing the volume of the liquid refrigerant inside the receiver we increase the pressure as well. First step is to increase the percentage of the volume from 62% to 70% and change the condensing unit setting from 31bar to 35bar. Second step is to increase the percentage of the volume to 75% and adjust the condensing unit to 37bar. The results of the above changes illustrate in the next page,

Steps	Settings	Pressure in the Receiver
0	Volume: 62% Condensing unit: 31 bar	31 bar
1	Volume: 70% Condensing unit: 35 bar	38 bar
2	Volume: 75% Condensing unit: 37 bar	42 bar

This is the maximum that we can achieve as the relief valve open at 46bar.

Test 1.1 – Receiver Pressure 38.1 Bar

Test procedure is illustrated below,

- Increase the volume of the liquid refrigerant inside the cylinder from 62% to 70%
- Decrease the set point of the additional load from -5 oC to -7oC
- Change the settings of the condensing unit from 31 bar to 35 bar
- Decrease the temperature inside the chamber room (effect to RH %)
- Set max and min superheat settings of the coil 15 and 10 respectively.

Summarized Results

- Compressor Suction Temperature T13: 2.9 °C
- Compressor Discharge Temperature – Gas Cooler inlet T14: 105.5 °C
- Gas Cooler Temperature outlet T6: 31.7 °C
- Receiver Inlet Temperature T25: 3.5 °C
- Receiver Outlet Temperature T16: -5.3 °C
- Evaporator Inlet Temperature T18: -2.4 °C
- Evaporator Outlet Temperature T19: 1.9 °C
- Receiver Pressure (*before AKV valve* - closest pressure transmitter before evaporator inlet) PT8: 38.1 bar (absolute)
- Evaporator Outlet Pressure PT9: 32.6 bar (absolute)
- Evaporator Air Inlet Temperature: 6.86 °C
- Evaporator Air Outlet (Bottom) Temperature: 2.58 °C

Evaporator Air Outlet (Top) Temperature: 3.65 °C

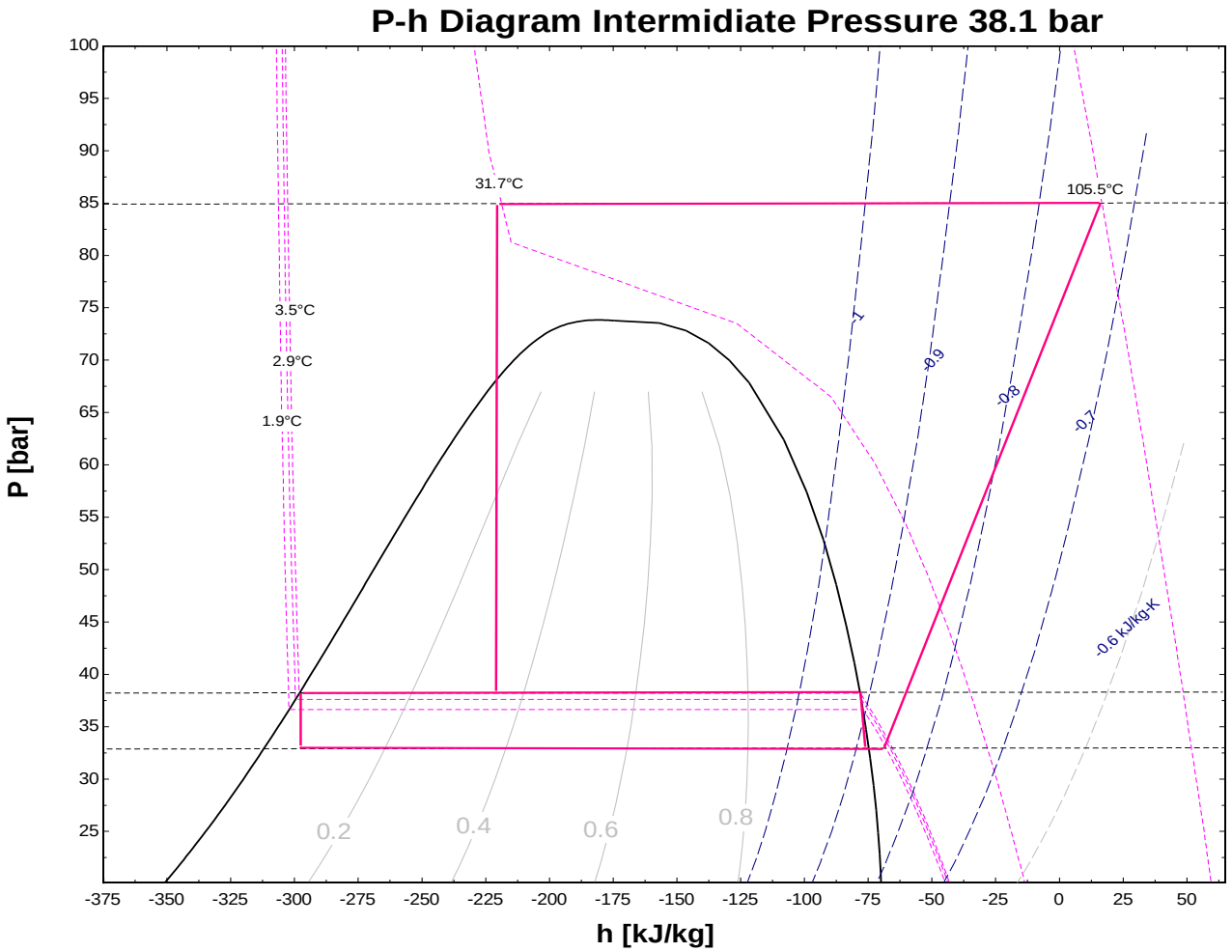
P-h Diagram Intermidiate Pressure 38.1 bar
P [bar]
h [kJ/kg]
31.7°C
105.5°C
3.5°C
2.9°C
1.9°C
-1
-0.9
-0.8
-0.7
-0.6 kJ/kg-K
0.2
0.4
0.6
0.8

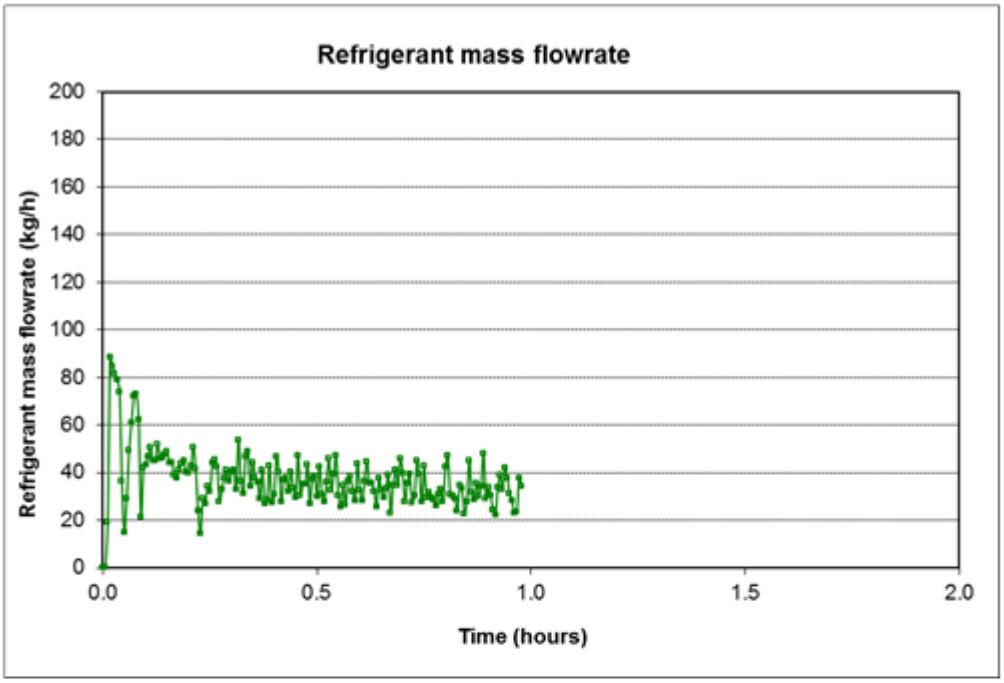

**Refrigerant mass flow rate average: 37.3 kg/h

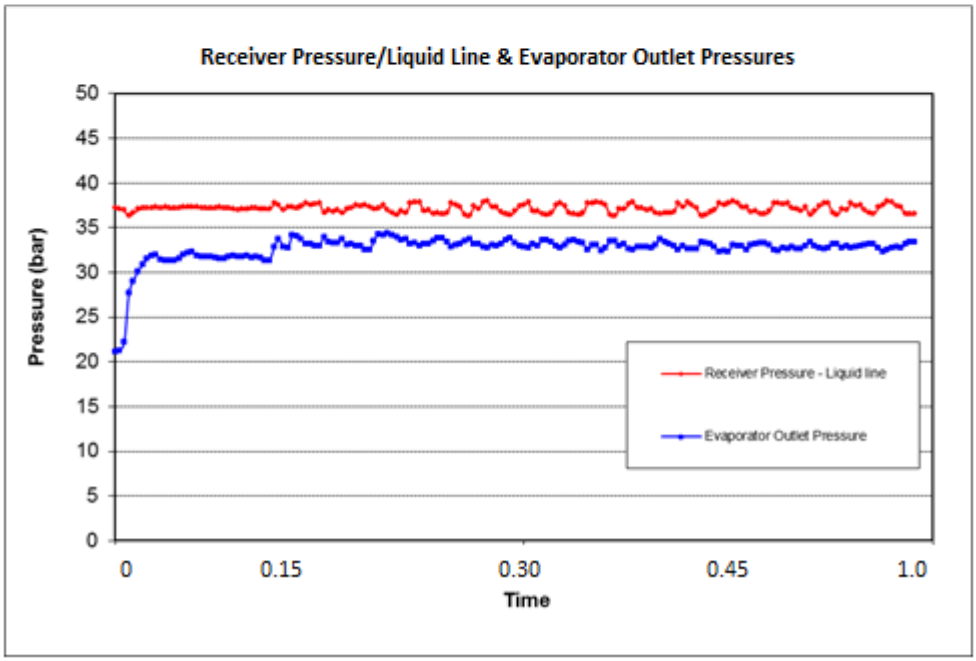

Test 1.2 – Receiver Pressure 41.8 Bar

Test procedure is illustrated below,

- Increase the volume of the liquid refrigerant inside the cylinder from 70% to 75%
- Decrease the set point of the additional load from -5 oC to -7oC
- Change the settings of the condensing unit from 35 bar to 37 bar
- Decrease the temperature inside the chamber room (effect to RH %)
- Set max and min superheat settings of the coil 15 and 10 respectively.

Summarized Results

- Compressor Suction Temperature T13: -1.2 °C
- Compressor Discharge Temperature – Gas Cooler inlet T14: 74.6 °C
- Gas Cooler Temperature outlet T6: 32.9 °C
- Receiver Inlet Temperature T25: 6.9 °C
- Receiver Outlet Temperature T16: -2.8 °C
- Evaporator Inlet Temperature T18: -1.1 °C
- Evaporator Outlet Temperature T19: 1.1 °C
- Receiver Pressure (*before AKV valve* - closest pressure transmitter before evaporator inlet) PT8: 41.8 bar (absolute)
- Evaporator Outlet Pressure PT9: 33.9 bar (absolute)
- Evaporator Air Inlet Temperature: 6.13 °C
- Evaporator Air Outlet (Bottom) Temperature: 2.01 °C
- Evaporator Air Outlet (Top) Temperature: 2.93 °C

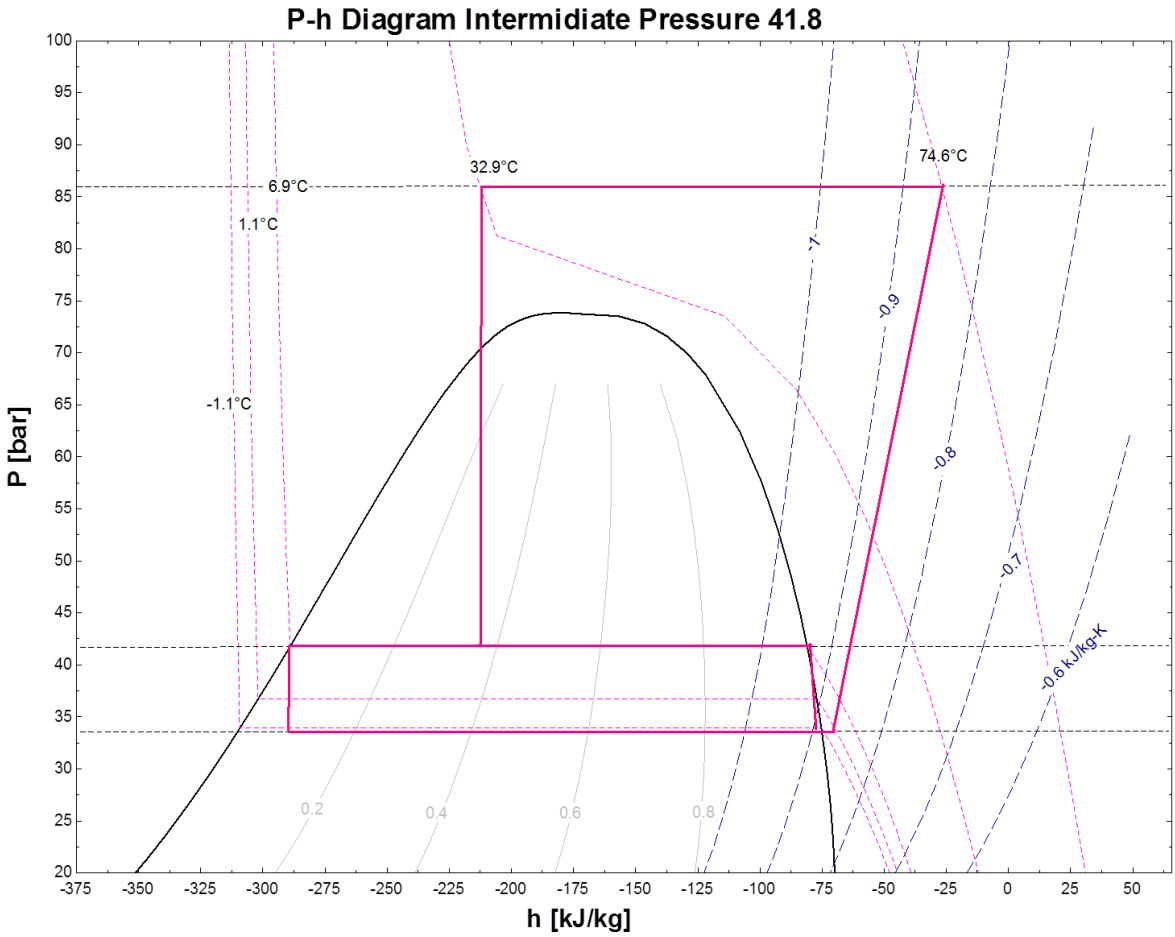
P-h Diagram Intermidiate Pressure 41.8
P [bar]
h [kJ/kg]
32.9°C
74.6°C
6.9°C
1.1°C
-1.1°C
-1
-0.9
-0.8
-0.7
-0.6 kJ/kg-K
0.2
0.4
0.6
0.8

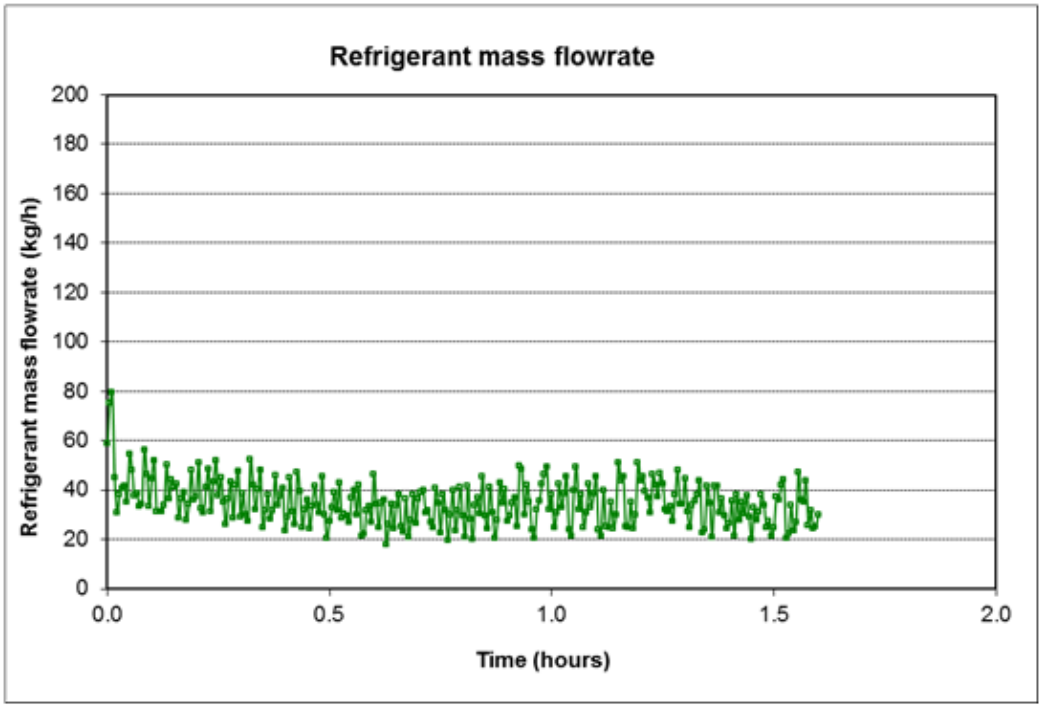

**Refrigerant mass flow rate average: 34.87 kg/h

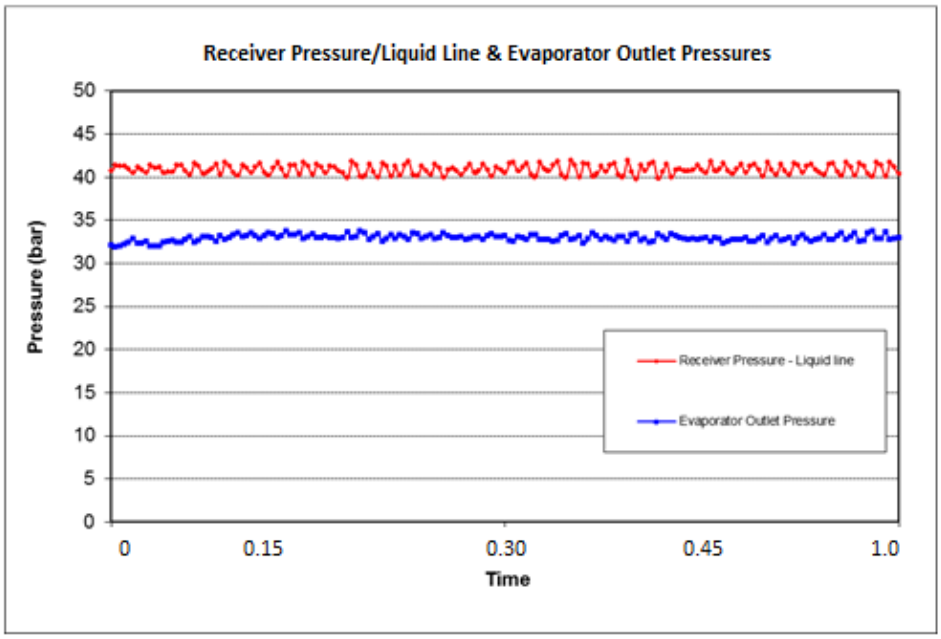

Appendix I:

CO_2 COURSE CERTIFICATION

This is to certify that

Konstantinos M. Tsamos

Attended & successfully passed the course:

BRA CO_2 Short Course

in retail refrigeration service & maintenance

Certificate No. CCL/355

Issued by:

Cool Concerns Ltd
20th October 2015

Alan Snelling
Alan Snelling MInstR
Training Centre Manager

coolconcerns
Training | Consultancy | Technical Support

Unit 5 Duddage Business Park, Brockeridge Road, Twyning Tewkesbury GL20 6BY
01684 290333 hello@coolconcerns.co.uk www.coolconcerns.co.uk